



UNIVERSITÀ DEGLI STUDI DI CAGLIARI

Dipartimento di Matematica e Informatica  
Dottorato di Ricerca in Matematica e Calcolo Scientifico  
XXIII ciclo

# Band Structure in Photonic Crystals

## Analytical and Numerical Methods

**Advisors:**

Prof. Cornelis van der Mee  
Prof. Sebastiano Seatzu

**PhD Student:**

Pietro Contu

Academic Year 2010-2011



## Acknowledgements

This PhD thesis is the fruit of three years of hard study and I would like to seize the opportunity to acknowledge various people who have played a significant role in concluding the thesis. Particular acknowledgments concern my advisors, Prof. C. van der Mee and Prof. S. Seatzu, who have devoted a lot of time in improving my basic preparation, changing my way of relating to mathematical and numerical problems and introducing me to the area of Photonic Crystals. Further, working with them I have appreciated their human qualities. Next, I wish to thank the Applied Mathematics Group of the University of Cagliari. In particular, I thank Professor G. Rodriguez, Francesco Demontis and Antonio Aricò for their availability shown in all circumstances and the interest shown in the arguments discussed in this work. Special thanks go to Paolo Pintus, a PhD student at the Scuola Superiore Sant'Anna in Pisa (Italy) whose master thesis on photonic crystals has been very important for me to start this thesis. I also acknowledge Prof. T. Aktosun of the University of Texas at Arlington who helped me studying some topics on Photonic Crystals in a very accurate way. Finally, I thank various family members for having been close to me during the past three years, especially my mother, my sister Marianna and my brother-in-law Giancarlo.



# Contents

<b>Acknowledgements</b>	<b>i</b>
<b>1 Introduction</b>	<b>1</b>
1.1 General Remarks . . . . .	1
1.2 Physical properties and applications . . . . .	3
1.3 Physical and mathematical model . . . . .	5
<b>2 One-Dimensional Photonic Crystals</b>	<b>9</b>
2.1 Floquet's Theorem . . . . .	11
2.2 Green's Function Analysis . . . . .	13
2.3 Analysis of the Hill Discriminant . . . . .	16
2.4 Conversion to Quasimomentum . . . . .	28
2.5 Direct Scattering Theory . . . . .	33
2.5.1 Direct Scattering for the Periodic Problem . . . . .	33
2.5.2 Jost Solutions and Scattering Coefficients . . . . .	35
2.6 Evaluation of the Impurity Period Map . . . . .	43
<b>3 Inverse Problem for 1D Photonic Crystals</b>	<b>49</b>
3.1 Reviewing various inverse problems . . . . .	50
3.2 Conversion to Travel Time . . . . .	53
3.3 Reconstructing the refractive index . . . . .	57
3.4 Recovery of a piecewise constant media . . . . .	64
3.4.1 Two-Layer photonic crystal . . . . .	66
3.4.2 General case . . . . .	69
3.4.3 Recovery from the Hill discriminant . . . . .	73
<b>4 Two-Dimensional Photonic Crystals</b>	<b>79</b>
4.1 nD crystals and Brillouin zones . . . . .	81
4.2 TM and TE eigenvalue problems . . . . .	87
4.3 Separation of variable method . . . . .	90

4.4	Prevailing Numerical Methods . . . . .	105
4.4.1	Time Domain Methods . . . . .	105
4.4.2	Frequency Domain Methods . . . . .	107
4.5	Periodic Finite Element Method . . . . .	113
4.5.1	1D Case . . . . .	115
4.6	Periodic Finite Difference Method . . . . .	118
4.6.1	1D Case . . . . .	119
4.6.2	2D Case: TM Modes . . . . .	122
4.6.3	1D and 2D Cases: TE Modes . . . . .	125
4.6.4	Nonrectangular lattices . . . . .	128
<b>5</b>	<b>Numerical Results</b>	<b>133</b>
5.1	1D spectrum . . . . .	134
5.2	TM spectrum in rectangular lattices . . . . .	136
5.3	TE spectrum in rectangular lattices . . . . .	138
5.4	Nonrectangular lattice . . . . .	142
5.4.1	TM and TE spectra . . . . .	143
5.5	Conclusions . . . . .	144
	<b>Appendices</b>	<b>146</b>
	<b>A Extreme values of Hill's discriminant</b>	<b>147</b>
	<b>B Circulant Matrices</b>	<b>151</b>
	<b>Bibliography</b>	<b>153</b>

# Chapter 1

## Introduction

### 1.1 General Remarks

Pure photonic crystals are periodic nano-structures in which light cannot travel at certain frequency intervals (photonic band gaps), but does travel and is scattered at other frequencies. This phenomenon is due to the periodic variation of the crystal's electric permittivity  $\varepsilon(\mathbf{r})$  or, equivalently, to the periodic variation of the refraction index<sup>1</sup>  $n(\mathbf{r})$  [1, 2].

Photonic crystals are said to be one-dimensional ( $1D$ ) if the electric permittivity varies and is periodic in only one spatial variable,  $z$ , and does not depend on  $x$  and  $y$ . They are said to be two-dimensional ( $2D$ ) if the electric permittivity depends on two spatial variables,  $x$  and  $y$ , and not on the third,  $z$ , and does not change upon translation by integer linear combinations of two linearly independent vectors in the  $xy$ -plane. They are said to be three-dimensional ( $3D$ ), if the electric permittivity does not upon translation by integer linear combinations of three linearly independent vectors. These periodic structures can also be seen in nature like in the frustules of some unicellular algae [3] or on the surface of butterfly wings [4].

One of the most important properties of such crystals is the emergence of localized defect modes in the band gap frequency region, when a disorder (impurity) is introduced to their periodic dielectric structure. Introducing a different material or changing the crystal period in a bounded region allows us to insert a monochromatic frequency into the photonic band gaps.

A fundamental problem in this field is the design of a photonic crystal

---

<sup>1</sup>Refraction index and electric permittivity are related by  $n(\mathbf{r}) = \sqrt{\varepsilon(\mathbf{r})\mu(\mathbf{r})/\varepsilon_0\mu_0}$ , where  $\mu$  is the magnetic permeability of the medium, whereas  $\varepsilon_0$  and  $\mu_0$  are the electric permittivity and magnetic permeability of vacuum, respectively.

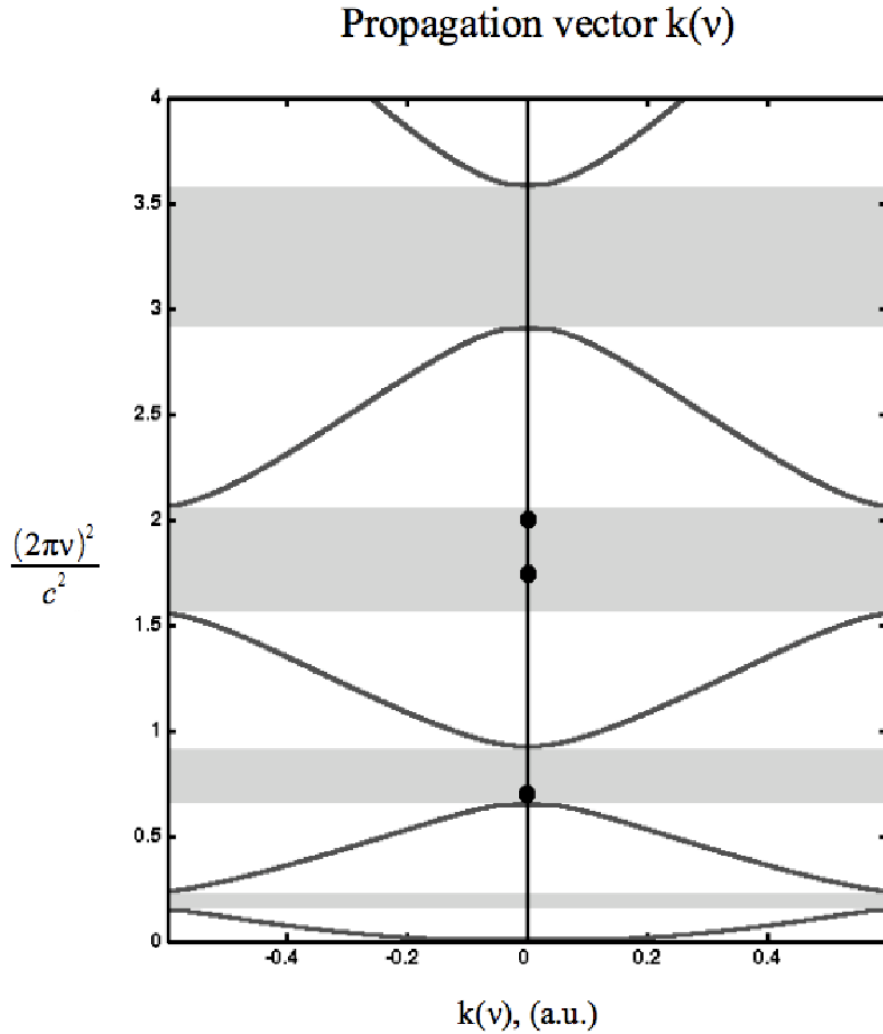


**Figure 1.1:** Band gap structure of a one-dimensional photonic crystal. In the horizontal axis we have the propagation vector  $k(\nu)$ , while in the vertical axis we consider  $(2\pi\nu/c)^2$  where  $\nu$  is the wave frequency and  $c$  is the light speed. In this picture we have plotted the relation between energy (for e.m. waves Energy  $\sim \nu^2$ ) and propagation vector  $\mathbf{k}$ . Band gaps are plotted in light grey while black dots represent allowed energy levels introduced by an impurity. The axis units are arbitrary (a.u. = arbitrary unit).

with specified properties. Photonic crystal design formally is a type of mathematical inverse problem: given the allowed frequencies and the photonic path at each allowed frequency we want to identify is the corresponding re-

fractive index as a function of the location in the crystal. A successful design method for photonic crystals will have a big impact in computer circuitry as well in the photonic devices for optical fibers [5]. The replacement of the electric current with a photonic flow will enable us to build future optical integrated circuits that are much faster, use much less energy, and dissipate much less heat. Photonic crystal design is an excellent tool in the development of algorithms for the optimization of boundaries and edges in the Level Set Method [6, 7].

## 1.2 Physical properties and applications

The main aspect of a photonic crystal is the periodic variation of its refractive index. Such a periodic structure affects the motion of photons in a similar way as a periodic potential affects the motion of electrons in a semiconductor crystal.

The frequency intervals in which electromagnetic wave propagation is forbidden are called *Photonic band-gaps* or in short PBGs. This physical phenomenon is based on constructively and destructively interfering diffraction<sup>2</sup> of electromagnetic waves. At each interface where the refractive index changes, light is reflected and transmitted. If all scattered waves interfere destructively, we have a photonic band-gap.

Since the basic phenomenon of the band gap structure is diffraction, the periodicity of the refractive index  $n(\mathbf{r})$  has to have the same length-scale as half the wavelength. For a photonic crystal operating in the visible spectrum,<sup>3</sup> it means that the period  $p$  will be in the interval from  $200\text{ nm}$  to  $350\text{ nm}$ , ( $1\text{ nm} = 10^{-9}\text{ m}$ ).

Replacing the material in a bounded region by a different material or changing the size of a single period while keeping the same material, we can “create” a (discrete) energy level or equivalently an allowed frequency into a

---

<sup>2</sup>From Joannopoulos et al. 2006 [1]: “Diffraction is a confusing word because it refers to phenomena in two very different limits. In the limit where the wavelength  $\lambda$  is small relative to the structure, it refers to deviations from geometric optics due to the fact that  $\lambda > 0$  [...]. In the context of scattering from periodic structures, on the other hand, it refers to unusual reflected/refracted waves that arise because  $\lambda < \infty$ , and especially in the case where  $\lambda/2$  is comparable to or smaller than the periodicity. Here, we are using it in the latter sense, specifically for the phenomenon of multiple reflected/refracted waves [...],” also called Bragg-diffraction [8].

<sup>3</sup>The wavelength of visible light is greater the  $400\text{ nm}$  (violet) and less then  $700\text{ nm}$  (red).

band gap (black dots in figure 1.1). In general we call *impurity* or *defect* this deviation from a perfect periodic lattice. A stationary wave is associated with the state introduced. This wave is constrained within the impurity region and cannot propagate in the rest of the material.

The band structure is also the reason of some unusual properties as diffractive reflection and refraction, supercollimation<sup>4</sup> and the superprism effect [1].

When an incident plane wave strikes an interface of a homogeneous material, both a reflected and a refracted plane wave are generated and their directions are determined by Snell's law. In a photonic crystal the wavelength  $\lambda$  is comparable to the lattice period and we may have a finite number of additional reflected and/or refracted waves (Bragg-diffraction). Then we can have not only a specularly reflected wave but, depending on the frequency, several reflected waves with different angles. Refracted waves might be multiple too and their directions may depend on the dispersion curve of the band structure. In some cases the rays will be refracted on the same side of the normal upon entering the material, contrary to what is usually observed. This particular phenomenon is called *negative refraction* and is typical of left-handed materials<sup>5</sup>.

Supercollimation and superprism effects are two different aspects of the same phenomenon. Supercollimation consists of a luminous cone collimating inside photonic crystals, unlike what occurs in a homogeneous medium, while the superprism effect induces an enormous change in refracted angle at a small change in the incident frequency. A prism made up of a photonic crystal would have a dispersion capability that is about 500 times stronger than that of a prism made of a conventional material [10]. Both of these phenomena are generated by the complex dispersion relation between the propagation vector  $\mathbf{k}$  and the angular frequency  $\omega$ .

So far we have considered properties of the crystal that are independent of the electric field amplitude. If the intensity of the wave is not so small, several non linear phenomena may occur. The most interesting are: second and third harmonics generation (SHG [11] and THG [12]), optical parametric amplification (OPA), optical rectification, white-light supercontinuum generation (WLSCG), and the Kerr effect.

---

<sup>4</sup>Supercollimation is also called negative diffraction. In this case, the term diffraction refers to deviations from geometric optics. To avoid misunderstanding we use the word supercollimation to refer to this effect.

<sup>5</sup>A left-handed material is a material whose permeability and permittivity are simultaneously negative. Left-handed materials have a negative refractive index, so Snell's Law is still valid but it is reversed. The term "left-handed material" was coined by a prediction of Russian theorist V.G.Veselago in 1968 [9].

Let us consider them in more detail. Illuminating a crystal, e.g. Potassium Dihydrogen Phosphate (KDP), by light of frequency  $\nu$  we are able to generate light with double or triple frequency (SHG [11] or THG [12]), whereas using a Beta Barium Borate crystal (BBO) the signal input is amplified in the presence of a higher-frequency wave (OPA).

An important property, commonly used for spectroscopic purposes, is white-light supercontinuum generation. A quasi-static electric field or an optical spectrum which covers all of the visible range are produced using narrow light pulses (a few tenths of a nanometer or less). Finally, the Kerr effect is a change in the refractive index of a material in response to an electric field ( $n = n(|\mathbf{E}|)$ ). It was discovered by John Kerr in 1877 [13].

Considering the band gap structure, it allows us to design resonant cavities [5, 14, 15], waveguides [5, 14, 15] and optical fibers [16]. Introducing impurities we can either confine light (resonant cavity) or create preferred pathways in order to guide it (waveguide).

Photonic crystals can also be used to design next generation optical fibers. Standard optical fibers rely on light being guided by the physical law known as *total internal reflection* (TIR) or *index guiding*. In order to achieve TIR in these fibers, which consist of two different dielectric materials, it is required that the refractive index of the core exceeds that of the surrounding media or cladding. In photonic crystal fibers light is constrained to propagate along PBGs, while the core can be a different medium with a smaller refractive index. These fibers have properties that differ from those of standard fibers: they allow bending by larger angles and light dissipation is negligible. Either advance is very important to telecommunication, because of the reduced need of using amplifiers.

Two other important applications are multiplexing, de-multiplexing and switching. Using negative refraction, supercollimation and the superprism effect, an optical de-multiplexer has been designed by a research group at the Georgia Institute of Technology [17], while the Kerr effect permits to design basic components of integrated optics like optical transistors [18].

The narrow size of these crystals makes the fabrication cumbersome and complex. For this purpose many different methods have been introduced. The most important are: micro-machining and growth using semiconductor processing techniques and holographic exposure of photoresist [5].

## 1.3 Physical and mathematical model

In order to study the propagation of light in a photonic crystal, we must turn to Maxwell's equations, since we are dealing with a nanostructure where the

refractive index is a periodic function whose period  $p$  has the same order of magnitude of the wavelength of the incident electromagnetic radiation.

Let us now state Maxwell's equations [19] in the form

$$\nabla \times \mathbf{H}(\mathbf{r}, t) = \frac{\partial \mathbf{D}(\mathbf{r}, t)}{\partial t} + \mathbf{J}(\mathbf{r}, t), \quad (1.3.1)$$

$$\nabla \times \mathbf{E}(\mathbf{r}, t) = -\frac{\partial \mathbf{B}(\mathbf{r}, t)}{\partial t}, \quad (1.3.2)$$

$$\nabla \cdot (\mathbf{D}(\mathbf{r}, t)) = \rho(\mathbf{r}, t), \quad (1.3.3)$$

$$\nabla \cdot (\mathbf{B}(\mathbf{r}, t)) = 0, \quad (1.3.4)$$

where:

- $\mathbf{E}(\mathbf{r}, t)$  e  $\mathbf{H}(\mathbf{r}, t)$  are the electric and magnetic fields, respectively;
- $\mathbf{D}(\mathbf{r}, t)$  e  $\mathbf{B}(\mathbf{r}, t)$  are the displacement and magnetic induction fields, respectively;
- $\rho(\mathbf{r}, t)$  e  $\mathbf{J}(\mathbf{r}, t)$  are the electric density and current, respectively.

Certain assumptions should be taken into account to cast Maxwell's equations into the photonic crystal framework:

- 1) constitutive relations:<sup>6</sup>

$$\mathbf{P}(\mathbf{r}, t) = \mathbf{f}_1(\mathbf{E}(\mathbf{r}, t)) \quad \text{and} \quad \mathbf{M}(\mathbf{r}, t) = \mathbf{f}_2(\mathbf{B}(\mathbf{r}, t));$$

- 2) photonic crystals are linear and isotropic materials<sup>1</sup>:

$$\mathbf{D}(\mathbf{r}, t) = \varepsilon_0 \varepsilon(\mathbf{r}) \mathbf{E}(\mathbf{r}, t), \quad \mathbf{B}(\mathbf{r}, t) = \mu_0 \mu(\mathbf{r}) \mathbf{H}(\mathbf{r}, t); \quad (1.3.5)$$

- 3) photonic crystals are magnetically homogeneous:  $\mu(\mathbf{r}) = \mu \simeq 1$ ;
- 4) losses can be neglected:  $\varepsilon(\mathbf{r}) : \mathbb{R}^3 \rightarrow \mathbb{R}$ , i.e.,  $\varepsilon(\mathbf{r})$  is real-valued;
- 5) photonic crystals are mixed dielectric media without free charges and current densities:  $\rho(\mathbf{r}, t) = 0$ ,  $\mathbf{J}(\mathbf{r}, t) = 0$ ;
- 6) we look for harmonic modes:

$$\mathbf{H}(\mathbf{r}, t) = \mathbf{H}(\mathbf{r}) e^{i\omega t}, \quad \mathbf{E}(\mathbf{r}, t) = \mathbf{E}(\mathbf{r}) e^{i\omega t}. \quad (1.3.6)$$

---

<sup>6</sup>  $\mathbf{P}(\mathbf{r}, t)$  and  $\mathbf{M}(\mathbf{r}, t)$  are the electric and magnetic polarization vectors, respectively.

Consequently, Maxwell's equations given in (1.3.1)-(1.3.4) become:

$$\nabla \times \mathbf{H}(\mathbf{r}) = -i\omega\varepsilon_0\varepsilon(\mathbf{r})\mathbf{E}(\mathbf{r}), \quad (1.3.7)$$

$$\nabla \times \mathbf{E}(\mathbf{r}) = i\omega\mu_0\mathbf{H}(\mathbf{r}), \quad (1.3.8)$$

$$\nabla \cdot (\varepsilon(\mathbf{r})\mathbf{E}(\mathbf{r})) = 0, \quad (1.3.9)$$

$$\nabla \cdot (\mathbf{H}(\mathbf{r})) = 0, \quad (1.3.10)$$

which can be decoupled into **two equivalent selfadjoint eigenvalue problems**:

$$\begin{cases} \nabla \times \left( \frac{1}{\varepsilon(\mathbf{r})} \nabla \times \mathbf{H}(\mathbf{r}) \right) = \eta \mathbf{H}(\mathbf{r}) \\ \nabla \cdot [\mathbf{H}(\mathbf{r})] = 0 \end{cases}, \quad (1.3.11)$$

$$\begin{cases} \nabla \times (\nabla \times \mathbf{E}(\mathbf{r})) = \eta \varepsilon(\mathbf{r}) \mathbf{E}(\mathbf{r}) \\ \nabla \cdot [\varepsilon(\mathbf{r}) \mathbf{E}(\mathbf{r})] = 0 \end{cases}, \quad (1.3.12)$$

where

$$\eta \stackrel{\text{def}}{=} \omega^2/c^2 = \omega^2\varepsilon_0\mu_0$$

is the spectral parameter.

The subject of this PhD thesis is the mathematical and numerical study of one-dimensional and two-dimensional pure photonic crystals (PC), i.e., crystals without impurities. In Chapter 2 we will study one-dimensional photonic crystals in an analytical way based on the Hill discriminant formalism. In Chapter 3 we will still be dealing with one-dimensional PC, trying to solve an inversion problem useful in the PC design. Basically we will try to find how a 1D PC looks like if its band spectrum is given. After trying to extend the Hill discriminant formalism to 2D photonic crystals with rectangular lattices, we will focus on the numerical study of 2D PC spectra in Chapter 4, proposing two numerical methods. The first one proposed is a finite element scheme based on the choice of periodic test functions and the second one is a finite difference scheme, where the periodicity conditions are incorporated in formulating a linear system of minimal order. Numerical results will be given in Chapter 5.



# Chapter 2

## One-Dimensional Photonic Crystals

In this chapter, we focus on a one-dimensional photonic crystal and consider TEM modes, i.e., polarized light propagating along the periodic direction (Fig. 2.1). Then it is straightforward to see that the electric eigenvalue problem (1.3.12) is described by the Helmholtz equation<sup>1</sup>

$$-\psi''(\eta, x) = \eta n^2(x)\psi(\eta, x), \quad (2.0.1)$$

where  $x \in \mathbb{R}$ ,  $\eta \stackrel{\text{def}}{=} \omega^2/c^2$  is the spectral parameter, the prime denotes differentiation with respect to  $x$ , the refractive index  $n(x) = \sqrt{\varepsilon(x)}$  is a periodic function with period  $p > 0$ , i.e.,  $n(x+p) = n(x)$ ,  $x \in \mathbb{R}$ , and  $\psi(\eta, x)$  is the polarized component of the electric field. Indeed, the electric field points along the  $z$  axis and depends only on the  $x$ -variable (direction of propagation):

$$\mathbf{E}(\mathbf{r}) = \begin{pmatrix} 0 \\ 0 \\ E_z(x) \end{pmatrix}.$$

As a result,

$$\begin{aligned} \left[ \nabla \times (\nabla \times \mathbf{E}(\mathbf{r})) \right]_s &= \epsilon_{slm} \partial_l \epsilon_{mnh} \partial_h E_k = (\delta_{sh} \delta_{lk} - \delta_{sk} \delta_{lh}) \partial_l \partial_h E_k \\ &= \partial_k \partial_s E_k - \partial_h \partial_h E_s, \end{aligned}$$

where  $\epsilon_{slm}$  are the components of the Levi-Civita tensor which satisfy the relation  $\epsilon_{slm} \epsilon_{mnh} = \delta_{sh} \delta_{lk} - \delta_{sk} \delta_{lh}$ . Since we are dealing with TEM modes,

---

<sup>1</sup>In the above configuration the divergence condition turns out to be automatically satisfied.

we have

$$\nabla \times (\nabla \times \mathbf{E}(\mathbf{r})) = \begin{pmatrix} 0 \\ 0 \\ -E_z''(x) \end{pmatrix}.$$

Thus the eigenvalue problem for TEM modes in a 1D periodic medium

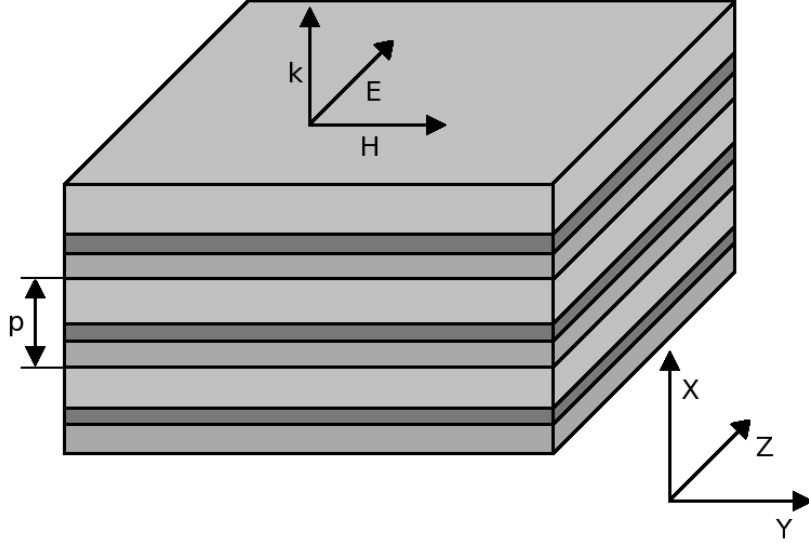


**Figure 2.1:** In a pure 1D photonic crystal the dielectric medium is periodic only in one direction (x-axis). Polarized light propagates along the x-axis, while the magnetic field  $\mathbf{H}$  and the electric field  $\mathbf{E}$  are directed along the y- and z-axes, respectively, and depend only on the x-variable (TEM modes).

reduces to the differential equation (2.1.1) with suitable boundary conditions.

In Sections 2.1 and 2.2 we adapt the Floquet theory usually developed for Schrödinger equations with periodic potentials [20, 21, 22] to the Helmholtz equation (2.1.1) with periodic refractive index. In particular, we prove the existence of band spectrum and indicate an algorithm to determine it. In Section 2.3 we introduce the conformal mapping  $k = k(\eta)$  from  $\eta$  to the quasimomentum variable  $k$  to facilitate the derivation of analyticity properties. We then go on, in Sections 2.5 and 2.6, to allow the refractive index to have impurities. As for the periodicity plus impurity Schrödinger equations [23, 24], we introduce Jost solutions and scattering coefficients and derive their continuity and analyticity properties in the quasimomentum variable  $k$ . For impurities confined to finitely many periods, we develop a method to compute the period map of these periods from appropriate scattering data.

## 2.1 Floquet's Theorem

Let us give the theoretical background needed to derive Floquet's theorem ([22, Ch. XXI] and [21, 20]). Consider the Helmholtz equation

$$-\psi''(\eta, x) = \eta n(x)^2 \psi(\eta, x), \quad (2.1.1)$$

where  $x \in \mathbb{R}$ , the prime denotes differentiation with respect to  $x$ ,  $\eta \in \mathbb{C}$  is a spectral parameter representing squared energy when real, and  $n(x+p) = n(x)$ ,  $x \in \mathbb{R}$ . Here  $n$  is assumed to be piecewise continuous and positive.

There exist unique linearly independent solutions  $\theta(\eta, x)$  and  $\varphi(\eta, x)$  of Eq. (2.1.1) satisfying the initial conditions

$$\theta(\eta, 0) = 1, \quad \theta'(\eta, 0) = 0, \quad (2.1.2a)$$

$$\varphi(\eta, 0) = 0, \quad \varphi'(\eta, 0) = 1. \quad (2.1.2b)$$

Now assume  $\psi(\eta, x) \not\equiv 0$  is a solution of Eq. (2.1.1) satisfying

$$\psi(\eta, p) = \tau \psi(\eta, 0), \quad (2.1.3a)$$

$$\psi'(\eta, p) = \tau \psi'(\eta, 0), \quad (2.1.3b)$$

for some constant  $0 \neq \tau \in \mathbb{C}$ . Then a nontrivial linear combination

$$c_1 \theta(\eta, x) + c_2 \varphi(\eta, x)$$

satisfies the boundary conditions (2.1.3) if and only if the linear system

$$\begin{pmatrix} \tau - \theta(\eta, p) & -\varphi(\eta, p) \\ -\theta'(\eta, p) & \tau - \varphi'(\eta, p) \end{pmatrix} \begin{pmatrix} c_1 \\ c_2 \end{pmatrix} = \begin{pmatrix} 0 \\ 0 \end{pmatrix}$$

has a nontrivial solution. This is the case if and only if the system determinant

$$\tau^2 - [\theta(\eta, p) + \varphi'(\eta, p)]\tau + 1 \quad (2.1.4)$$

vanishes. Here we have used the  $x$ -independence of the Wronskian, which equals 1 for  $x = 0$  and hence for any  $x \in \mathbb{R}$ . Introducing the *Hill discriminant*

$$\Delta(\eta) = \theta(\eta, p) + \varphi'(\eta, p), \quad (2.1.5)$$

this is the case if and only if

$$\Delta(\eta) = \tau + \tau^{-1}. \quad (2.1.6)$$

Solutions of Eq. (2.1.1) under the boundary conditions (2.1.3) can be extended in a natural way to  $C^1$ -solutions of Eq. (2.1.1) on the whole real axis. These extended solutions satisfy

$$\psi(x+p) = \tau \psi(x), \quad x \in \mathbb{R}.$$

When nontrivial, such solutions are unbounded as  $x \rightarrow +\infty$  if  $|\tau| > 1$  and as  $x \rightarrow -\infty$  if  $|\tau| < 1$ . Thus boundedness of such nontrivial solutions requires that  $|\tau| = 1$ . Then it is easily verified that for  $|\tau| = 1$

$$\int_0^p |\psi'(\eta, x)|^2 dx = \eta \int_0^p n(x)^2 |\psi(\eta, x)|^2 dx. \quad (2.1.7)$$

Let us now introduce the *travel time variable*

$$y(x) = \int_0^x n(\hat{x}) d\hat{x}, \quad q = \int_0^p n(\hat{x}) d\hat{x}, \quad (2.1.8)$$

which yields a 1, 1-correspondence  $x \mapsto y$  from  $\mathbb{R}$  onto itself which converts periodic functions of  $x$  of period  $p$  into periodic functions of  $y$  of period  $q$ . Let  $\alpha \in \mathbb{C}$  be a constant such that  $e^{i\alpha q} = \tau$ . Then the natural extension of a solution of Eq. (2.1.1) to the real axis has the *Bloch representation*

$$\psi(\eta, x) = e^{i\alpha y(x)} \phi(\eta, x),$$

where  $\phi(\eta, x)$  is periodic with period  $p$ . This is easily verified by checking the periodicity of  $e^{-i\alpha y(x)} \psi(\eta, x)$ .

**Theorem 2.1.1 (Floquet)** *If the roots  $\tau_1$  and  $\tau_2$  of the quadratic polynomial (2.1.4) are distinct, then Eq. (2.1.1) has two linearly independent solutions of the type*

$$e^{i\alpha y(x)} \chi_1(x) \quad \text{and} \quad e^{-i\alpha y(x)} \chi_2(x),$$

where  $\chi_1(x)$  and  $\chi_2(x)$  are periodic with period  $p$ . If  $\tau_1 = \tau_2$ , then Eq. (2.1.1) has a nontrivial periodic solution ( $\tau_1 = \tau_2 = 1$ ) or a nontrivial antiperiodic solution ( $\tau_1 = \tau_2 = -1$ ). Let  $\chi(x)$  denote such a solution and let  $\phi(x)$  be another solution linearly independent of  $\chi(x)$ . Then there exists a constant  $\vartheta$  such that  $\phi(x+p) = \tau_1 \phi(x) + \vartheta \chi(x)$ , while  $\vartheta = 0$  occurs if and only if

$$\theta(\eta, p) = \varphi'(\eta, p) = \pm 1 \quad \text{and} \quad \varphi(\eta, p) = \theta'(\eta, p) = 0.$$

Further, the solutions of Eq. (2.1.1) are all bounded if and only if

- (a) either  $\theta(\eta, p) + \varphi'(\eta, p)$  belongs to  $(-2, 2)$ ,
- (b) or  $\theta(\eta, p) = \varphi'(\eta, p) = \pm 1$  and  $\varphi(\eta, p) = \theta'(\eta, p) = 0$ .

**Proof.** If  $\tau_1 = \tau_2 = \pm 1$ , there is a nontrivial solution  $\phi_1^*(x)$  such that  $\phi_1^*(x+p) = \tau_1 \phi_1^*(x)$ . Then, obviously,  $\phi_1^*(x)$  is periodic if  $\tau_1 = \tau_2 = 1$  and antiperiodic if  $\tau_1 = \tau_2 = -1$ . If  $\varphi(\eta, p) \neq 0$ , we choose

$$\begin{aligned}\phi_1^*(x) &= \varphi(\eta, p)\theta(\eta, x) + [\tau_1 - \theta(\eta, p)]\varphi(\eta, x), \\ \phi_2^*(x) &= \varphi(\eta, x).\end{aligned}$$

Then  $\theta(\eta, p) + \varphi'(\eta, p) = 2\tau_1$  implies  $\phi_2^*(x+p) = \tau_1 \phi_2^*(x) + \phi_1^*(x)$ . If  $\varphi(\eta, p) = 0$ , we take  $\phi_1^*(x) = \varphi(\eta, x)$  and  $\phi_2^*(x) = \theta(\eta, x)$ . Then the Wronskian relation and  $\varphi(\eta, p) = 0$  imply  $\theta(\eta, p) = \varphi'(\eta, p) = \tau_1$ , leading to  $\phi_1^*(x+p) = \varphi'(\eta, p)\varphi(\eta, x) = \tau_1\varphi(\eta, x)$  and  $\phi_2^*(x+p) = \tau_1\phi_2^*(x) + \theta'(\eta, p)\phi_1^*(x)$ .

■

## 2.2 Green's Function Analysis

Let us now solve Eq. (2.1.1) by Green's function analysis, where  $n(x)$  is a positive piecewise continuous function with period  $p$ . For  $\tau \in \mathbb{C}$  with  $|\tau| = 1$  we consider the selfadjoint boundary conditions (2.1.3). Let us assume that  $\eta$  is not an eigenvalue of the differential equation (2.1.1) with boundary conditions (2.1.3). Let  $\phi_1(\eta, x)$  and  $\phi_2(\eta, x)$  stand for nontrivial solutions of (2.1.3) such that

$$\phi_1(\eta, p) = \tau\phi_1(\eta, 0), \quad \phi_2'(\eta, p) = \tau\phi_2'(\eta, 0).$$

Then their (constant) Wronskian  $w$  is nonzero. We choose  $\phi_1(\eta, x)$  and  $\phi_2(\eta, x)$  as real functions under periodic ( $\tau = 1$ ) and antiperiodic ( $\tau = -1$ ) boundary conditions.

Let us solve the differential equation

$$-\psi''(\eta, x) = \eta n(x)^2 \psi(\eta, x) + n(x)^2 f(x) \quad (2.2.1)$$

under the boundary conditions (2.1.3). Here  $f(x)$  is an arbitrary continuous function. Following the method of variation of parameters, we write

$$\psi(\eta, x) = c_1(x)\phi_1(\eta, x) + c_2(x)\phi_2(\eta, x)$$

and arrive at the linear system

$$\begin{pmatrix} \phi_1(\eta, x) & \phi_2(\eta, x) \\ \phi_1'(\eta, x) & \phi_2'(\eta, x) \end{pmatrix} \begin{pmatrix} c_1(x) \\ c_2(x) \end{pmatrix} = \begin{pmatrix} 0 \\ -n(x)^2 f(x) \end{pmatrix},$$

where the system determinant equals  $w$ . Then

$$\begin{aligned}\begin{pmatrix} c_1(x) \\ c_2(x) \end{pmatrix} &= \frac{1}{w} \begin{pmatrix} \phi_2'(\eta, x) & -\phi_2(\eta, x) \\ -\phi_1'(\eta, x) & \phi_1(\eta, x) \end{pmatrix} \begin{pmatrix} 0 \\ -n(x)^2 f(x) \end{pmatrix} \\ &= \frac{n(x)^2 f(x)}{w} \begin{pmatrix} \phi_2(\eta, x) \\ -\phi_1(\eta, x) \end{pmatrix}.\end{aligned}$$

Thus there exist constants  $c_1$  and  $c_2$  such that

$$\begin{aligned} \psi(\eta, x) &= c_1\phi_1(\eta, x) + c_2\phi_2(\eta, x) \\ &+ \frac{\phi_1(\eta, x)}{w} \int_0^x \phi_2(\eta, y)n(y)^2 f(y) dy - \frac{\phi_2(\eta, x)}{w} \int_0^x \phi_1(\eta, y)n(y)^2 f(y) dy. \end{aligned} \quad (2.2.2)$$

Differentiating (2.2.2) with respect to  $x$  we get

$$\begin{aligned} \psi'(\eta, x) &= c_1\phi_1'(\eta, x) + c_2\phi_2'(\eta, x) \\ &+ \frac{\phi_1'(\eta, x)}{w} \int_0^x \phi_2(\eta, y)n(y)^2 f(y) dy - \frac{\phi_2'(\eta, x)}{w} \int_0^x \phi_1(\eta, y)n(y)^2 f(y) dy. \end{aligned} \quad (2.2.3)$$

Substituting (2.1.3a) and using  $\phi_1(\eta, p) = \tau\phi_1(\eta, 0)$  in (2.2.2) we obtain

$$\begin{aligned} \tau c_2\phi_2(\eta, 0) &= c_2\phi_2(\eta, p) + \frac{\phi_1(\eta, p)}{w} \int_0^p \phi_2(\eta, y)n(y)^2 f(y) dy \\ &- \frac{\phi_2(\eta, p)}{w} \int_0^p \phi_1(\eta, y)n(y)^2 f(y) dy. \end{aligned}$$

Substituting (2.1.3b) and using  $\phi_2'(\eta, p) = \tau\phi_2'(\eta, 0)$  in (2.2.3) we get

$$\begin{aligned} \tau c_1\phi_1'(\eta, 0) &= c_1\phi_1'(\eta, p) + \frac{\phi_1'(\eta, p)}{w} \int_0^p \phi_2(\eta, y)n(y)^2 f(y) dy \\ &- \frac{\phi_2'(\eta, p)}{w} \int_0^p \phi_1(\eta, y)n(y)^2 f(y) dy. \end{aligned}$$

We now compute the constants  $c_1$  and  $c_2$  and substitute the resulting expressions in (2.2.2). We finally obtain

$$\psi(\eta, x) = \int_0^p \mathcal{G}(x, y; \eta)n(y)^2 f(y) dy, \quad (2.2.4)$$

where

$$\begin{aligned} \mathcal{G}(x, y; \eta) &= \frac{\phi_1'(\eta, p)\phi_1(\eta, x)\phi_2(\eta, y) - \phi_2'(\eta, p)\phi_1(\eta, x)\phi_1(\eta, y)}{w[\tau\phi_1'(\eta, 0) - \phi_1'(\eta, p)]} \\ &+ \frac{\phi_1(\eta, p)\phi_2(\eta, x)\phi_2(\eta, y) - \phi_2(\eta, p)\phi_2(\eta, x)\phi_1(\eta, y)}{w[\tau\phi_2(\eta, 0) - \phi_2(\eta, p)]} \end{aligned} \quad (2.2.5a)$$

for  $0 \leq x \leq y \leq p$  and

$$\begin{aligned} \mathcal{G}(x, y; \eta) &= \frac{\tau\phi_1'(\eta, 0)\phi_1(\eta, x)\phi_2(\eta, y) - \phi_2'(\eta, p)\phi_1(\eta, x)\phi_1(\eta, y)}{w[\tau\phi_1'(\eta, 0) - \phi_1'(\eta, p)]} \\ &+ \frac{\phi_1(\eta, p)\phi_2(\eta, x)\phi_2(\eta, y) - \tau\phi_2(\eta, 0)\phi_2(\eta, x)\phi_1(\eta, y)}{w[\tau\phi_2(\eta, 0) - \phi_2(\eta, p)]}. \end{aligned} \quad (2.2.5b)$$

for  $0 \leq y \leq x \leq p$ .

Since  $\mathcal{G}(x, y; \eta)n(y)^2$  is the hermitian integral kernel of an integral operator that is the inverse of a selfadjoint operator on  $L^2[(0, p); n(x)^2 dx]$ , we have [25, 26]

$$\mathcal{G}(x, y; \eta) = \overline{\mathcal{G}(y, x; \eta)}. \quad (2.2.6)$$

The Green's function is real-valued if  $\tau = \pm 1$ .

Let us now differentiate  $\mathcal{G}(x, y; \eta)$  with respect to  $x$ . We get

$$\begin{aligned} \frac{\partial \mathcal{G}}{\partial x} &= \frac{\phi'_1(\eta, p)\phi'_1(\eta, x)\phi_2(\eta, y) - \phi'_2(\eta, p)\phi'_1(\eta, x)\phi_1(\eta, y)}{w[\tau\phi'_1(\eta, 0) - \phi'_1(\eta, p)]} \\ &+ \frac{\phi_1(\eta, p)\phi'_2(\eta, x)\phi_2(\eta, y) - \phi_2(\eta, p)\phi'_2(\eta, x)\phi_1(\eta, y)}{w[\tau\phi_2(\eta, 0) - \phi_2(\eta, p)]} \end{aligned} \quad (2.2.7a)$$

for  $0 \leq x < y \leq p$  and

$$\begin{aligned} \frac{\partial \mathcal{G}}{\partial x} &= \frac{\tau\phi'_1(\eta, 0)\phi'_1(\eta, x)\phi_2(\eta, y) - \phi'_2(\eta, p)\phi'_1(\eta, x)\phi_1(\eta, y)}{w[\tau\phi'_1(\eta, 0) - \phi'_1(\eta, p)]} \\ &+ \frac{\phi_1(\eta, p)\phi'_2(\eta, x)\phi_2(\eta, y) - \tau\phi_2(\eta, 0)\phi'_2(\eta, x)\phi_1(\eta, y)}{w[\tau\phi_2(\eta, 0) - \phi_2(\eta, p)]}. \end{aligned} \quad (2.2.7b)$$

for  $0 \leq y < x \leq p$ . Then

$$\frac{\partial \mathcal{G}}{\partial x}(x, x^+; \eta) - \frac{\partial \mathcal{G}}{\partial x}(x, x^-; \eta) = \frac{\phi_1(\eta, x)\phi'_2(\eta, x) - \phi'_1(\eta, x)\phi_2(\eta, x)}{w} = 1. \quad (2.2.8)$$

**Theorem 2.2.1** *The eigenvalues of Eq. (2.1.1) under the boundary conditions (2.1.2) form a sequence of real numbers which tends to  $+\infty$ . For  $\tau \neq \pm 1$  these eigenvalues are simple, while for  $\tau = \pm 1$  they have multiplicity one or two. The zero eigenvalue can only occur if the corresponding eigenfunction is constant and the boundary conditions are periodic.*

**Proof.** For a noneigenvalue  $\eta_0 \in \mathbb{R}$  we write Eq. (2.1.1) with boundary conditions (2.1.3) as the equivalent integral equation

$$\psi(\eta, x) - (\eta - \eta_0) \int_0^p \mathcal{G}(x, y; \eta_0)n(y)^2\psi(\eta, y) dy = \int_0^p \mathcal{G}(x, y; \eta_0)n(y)^2 f(y) dy. \quad (2.2.9)$$

Then the integral kernel  $\mathcal{G}(x, y; \eta)$  has the form

$$\mathcal{G}(x, y; \eta) = \sum_j \frac{\varphi_j(x)\overline{\varphi_j(y)}}{\eta^{(j)} - \eta},$$

where  $\{\varphi_j\}$  is an orthonormal basis of  $L^2((0, p); n(x)^2 dx)$  consisting of eigenfunctions corresponding to the (real) eigenvalues  $\{\eta^{(j)}\}$ . The summation is finite for degenerate kernels and infinite for nondegenerate kernels. Since  $\mathcal{G}(x, y; \eta)$  cannot be  $C^1$  in  $(x, y)$  [because this would contradict (2.2.8)], the summation and hence the number of eigenvalues must be infinite. Further, from (2.1.7) it follows that the eigenvalues  $\eta^{(j)}$  are nonnegative and can only coincide with zero if the eigenfunction is constant and hence the boundary conditions are periodic. Thus there exist two infinite sequences, one of eigenvalues

$$0 \leq \eta_0 \leq \eta_1 \leq \eta_2 \leq \eta_3 \leq \dots, \quad \eta_n \rightarrow +\infty,$$

under periodic boundary conditions and the other of eigenvalues

$$0 < \mu_1 \leq \mu_2 \leq \mu_3 \leq \dots, \quad \mu_n \rightarrow +\infty,$$

under antiperiodic boundary conditions. For  $\tau \neq \pm 1$  there also exists an infinite sequence of eigenvalues

$$0 < \eta_1^{(\tau)} \leq \eta_2^{(\tau)} \leq \eta_3^{(\tau)} \leq \dots, \quad \eta_n^{(\tau)} \rightarrow +\infty,$$

under the boundary conditions (2.1.3). The multiplicity of an eigenvalue is at most 2, because the differential equation (2.1.1) has order 2. For  $\tau \neq \pm 1$  the multiplicity is always one, because the eigenvalues  $\eta$  follow from (2.1.6) and the differential equation (2.1.1) has both a  $\tau$ -periodic and a  $\tau^{-1}$ -periodic solution.

It is clear from (2.1.6) that

$$\Delta(\eta_n) = 2, \quad \Delta(\mu_n) = -2, \quad \Delta(\eta_n^{(\tau)}) = \tau + \tau^{-1},$$

which completes the proof. ■

## 2.3 Analysis of the Hill Discriminant

In this section we analyze the entire function  $\Delta(\eta)$  defined by (2.1.5). We prove it to be entire of order  $\frac{1}{2}$  and prove Theorem 2.2.1 in a different way. We derive some additional properties of the eigenvalues which lead to the band structure. Our arguments are inspired by those presented by Titchmarsh [22] and Eastham [20] for Hill's equation.

Let us first compile some definitions involving entire functions [27]. An entire function  $f(z)$  is said to be of *finite order* if there exist positive constants  $a, r_0$  such that

$$|f(z)| \leq e^{|z|^a}, \quad |z| \geq r_0.$$

Then the infimum of all such positive constants  $a$  is called the order,  $\rho(f)$ , of  $f(z)$ . In fact,

$$\rho(f) = \lim_{r \rightarrow +\infty} \sup \frac{\log \log \max_{|z|=r} |f(z)|}{\log r}.$$

The entire functions of order zero are exactly the polynomials. It is well known ([28], Lemma 1.4.1) that entire functions of noninteger order have infinitely many zeros and that the order  $\rho$  is the infimum of all positive numbers  $\sigma$  for which the series

$$\sum_{j=1}^{\infty} \frac{1}{|a_j|^\sigma}$$

converges. Here  $\{a_j\}_{j=1}^{\infty}$  are the zeros of  $f(z)$ , multiplicities taken into account. Moreover, entire functions of order  $\rho \in (0, 1)$  satisfy the Hadamard factorization theorem

$$f(z) = \frac{1}{m!} f^{(m)}(0) z^m \prod_{j=1}^{\infty} \left(1 - \frac{z}{a_j}\right),$$

where  $m$  is the order of zero as a zero of  $f(z)$ . Applying the Hadamard factorization theorem to the entire functions  $\cos(\sqrt{z})$  and  $\sin(\sqrt{z})/\sqrt{z}$  of order  $1/2$ , we get the well known infinite product representations of the cosine and sine functions [27].

Put  $\omega = \sqrt{\eta}$ . Let  $C(\omega, x, x_0)$  and  $S(\omega, x, x_0)$  be the solutions of the differential equation

$$-\psi''(\eta, x) = \eta n(x)^2 \psi(\eta, x) \quad (2.3.1)$$

under the initial conditions

$$\begin{aligned} C(\omega, x_0, x_0) &= 1, & C'(\omega, x_0, x_0) &= 0, \\ S(\omega, x_0, x_0) &= 0, & S'(\omega, x_0, x_0) &= 1. \end{aligned}$$

Then the functions  $C(\omega, x, x_0)$  and  $S(\omega, x, x_0)$  satisfy the integral equations

$$C(\omega, x, x_0) = 1 - \omega^2 \int_{x_0}^x (x - \hat{x}) n(\hat{x})^2 C(\omega, \hat{x}, x_0) d\hat{x}, \quad (2.3.2a)$$

$$S(\omega, x, x_0) = x - x_0 - \omega^2 \int_{x_0}^x (x - \hat{x}) n(\hat{x})^2 S(\omega, \hat{x}, x_0) d\hat{x}. \quad (2.3.2b)$$

Letting  $n_+$  be the maximum of  $n(x)$ , we easily see that

$$|C(\omega, x, x_0)| \leq \cosh(n_+ |\omega| (x - x_0)), \quad |S(\omega, x, x_0)| \leq \frac{\sinh(n_+ |\omega| (x - x_0))}{n_+ |\omega|}, \quad (2.3.3)$$

because, for  $x \geq x_0$ ,  $|C(\omega, x, x_0)|$  and  $|S(\omega, x, x_0)|$  are dominated by the solutions of the respective integral equations:

$$\overline{C}(|\omega|, x, x_0) = 1 + |\omega|^2 \int_{x_0}^x (x - \hat{x}) n_+^2 \overline{C}(|\omega|, \hat{x}, x_0) d\hat{x}, \quad (2.3.4a)$$

$$\overline{S}(|\omega|, x, x_0) = x - x_0 + |\omega|^2 \int_{x_0}^x (x - \hat{x}) n_+^2 \overline{S}(|\omega|, \hat{x}, x_0) d\hat{x}. \quad (2.3.4b)$$

On the imaginary  $\omega$ -axis (for  $\omega = i\phi$ ) we get the more precise estimates

$$\cosh(\phi n_-(x - x_0)) \leq C(\omega, x, x_0) \leq \cosh(\phi n_+(x - x_0)), \quad (2.3.5a)$$

$$\frac{\sinh(\phi n_-(x - x_0))}{\phi n_-} \leq S(\omega, x, x_0) \leq \frac{\sinh(\phi n_+(x - x_0))}{\phi n_+}, \quad (2.3.5b)$$

where  $n_-$  is the positive minimum of  $n(x)$  and the second inequality holds only for  $\phi(x - x_0) \geq 0$  (and for  $\phi(x - x_0) \leq 0$  with its direction reversed). Since the iteration of Eqs. (2.3.2) leads to a series of functions that are continuous in  $(x, x_0) \in \mathbb{R}^2$  and analytic in  $\omega \in \mathbb{C}$  and converge uniformly in  $(x, x_0, \omega)$  on bounded subsets of  $\mathbb{R}^2 \times \mathbb{C}$ , their sums  $C(\omega, x, x_0)$  and  $S(\omega, x, x_0)$  are continuous in  $(x, x_0) \in \mathbb{R}^2$  and analytic in  $\omega \in \mathbb{C}$ . Thus for each  $(x, x_0) \in \mathbb{R}^2$  the functions  $C(\omega, x, x_0)$  and  $S(\omega, x, x_0)$  are entire functions of  $\omega$  of exact order 1 and therefore entire functions of  $\eta$  of exact order  $\frac{1}{2}$ . Thus  $C(\omega, x, x_0)$  and  $S(\omega, x, x_0)$  have infinitely many zeros  $\eta$  (cf. [28, Sec. I.10]).

Let us now estimate the  $x$ -derivatives of  $C(\omega, x, x_0)$  and  $S(\omega, x, x_0)$ . In analogy with (2.3.2) we derive by differentiation

$$\frac{\partial C(\omega, x, x_0)}{\partial x} = -\omega^2 \int_{x_0}^x n(\hat{x})^2 C(\omega, \hat{x}, x_0) d\hat{x}, \quad (2.3.6a)$$

$$\frac{\partial S(\omega, x, x_0)}{\partial x} = 1 - \omega^2 \int_{x_0}^x n(\hat{x})^2 S(\omega, \hat{x}, x_0) d\hat{x}. \quad (2.3.6b)$$

Using (2.3.4) we thus get

$$\left| \frac{\partial C(\omega, x, x_0)}{\partial x} \right| \leq n_+ |\omega| \sinh(n_+ |\omega| (x - x_0)), \quad (2.3.7a)$$

$$\left| \frac{\partial S(\omega, x, x_0)}{\partial x} \right| \leq \cosh(n_+ |\omega| (x - x_0)). \quad (2.3.7b)$$

On the imaginary  $\omega$ -axis (for  $\omega = i\phi$ ) we get the more precise estimates

$$n_- \phi \sinh(\phi n_-(x - x_0)) \leq \frac{\partial C(\omega, x, x_0)}{\partial x} \leq n_+ \phi \sinh(\phi n_+(x - x_0)), \quad (2.3.8a)$$

$$\cosh(\phi n_-(x - x_0)) \leq \frac{\partial S(\omega, x, x_0)}{\partial x} \leq \cosh(\phi n_+(x - x_0)), \quad (2.3.8b)$$

where  $n_-$  is the positive minimum of  $n(x)$  and the first inequality holds only for  $\phi(x - x_0) \geq 0$  (and for  $\phi(x - x_0) \leq 0$  with its direction reversed).

From the above it is clear that

$$\theta(\eta, x) = C(\omega, x, 0), \quad \varphi(\eta, x) = S(\omega, x, 0),$$

where  $\omega = \sqrt{\eta}$ . Hence  $\theta(\eta, x)$ ,  $\varphi(\eta, x)$ ,  $\theta'(\eta, x)$  and  $\varphi'(\eta, x)$  are entire functions in  $\eta$  of exact order  $1/2$  for each  $x \in \mathbb{R}$ . Thus

$$\Delta(\eta) = \theta(\eta, p) + \varphi'(\eta, p)$$

is an entire function in  $\eta$  of order  $\leq 1/2$ .

To prove that  $\Delta(\eta)$  is an entire function of  $\eta$  of exact order  $\frac{1}{2}$ , we need to show the existence of a positive constant  $M$  such that  $|\Delta(\eta)|e^{-M\sqrt{|\eta|}}$  is bounded for  $\eta \in \mathbb{C}$  and  $|\Delta(\eta)|e^{-m\sqrt{|\eta|}} \rightarrow +\infty$  as  $\eta \rightarrow -\infty$  for any  $m \in (0, M)$ . Indeed, put

$$\eta^\# = \min_{x \in \mathbb{R}} \frac{-1}{n(x)^2}.$$

Then Eq. (2.1.1) is converted into the equation

$$-\psi''(\eta, x) + [-\eta^\# n(x)^2] \psi(\eta, x) = (\eta - \eta^\#) n(x)^2 \psi(\eta, x), \quad (2.3.9)$$

where  $Q^\#(x) = -\eta^\# n(x)^2 \geq 1$  for each  $x \in \mathbb{R}$  and  $Q^\#(x)$  is periodic with period  $p$ . Then it's straightforward to see that

$$\theta(\eta, x) = C(\omega^\#, x, 0) + \int_0^x S(\omega^\#, x, \hat{x}) Q^\#(\hat{x}) \theta(\eta, \hat{x}) d\hat{x}, \quad (2.3.10a)$$

$$\varphi(\eta, x) = S(\omega^\#, x, 0) + \int_0^x S(\omega^\#, x, \hat{x}) Q^\#(\hat{x}) \varphi(\eta, \hat{x}) d\hat{x}, \quad (2.3.10b)$$

where  $[\omega^\#]^2 = \eta - \eta^\#$ . For  $\eta < \eta^\#$  we write  $\omega^\# = i\phi^\#$  with  $\phi^\# \in \mathbb{R}$ . Then we have the lower bounds

$$\begin{aligned} \theta(\eta, x) &\geq \cosh \left( x \sqrt{1 + [\phi^\# n_-]^2} \right), \\ \varphi(\eta, x) &\geq \frac{\sinh \left( x \sqrt{1 + [\phi^\# n_-]^2} \right)}{\sqrt{1 + [\phi^\# n_-]^2}}. \end{aligned}$$

We thus easily see that  $\Delta(\eta)$  is an entire function of  $\eta$  of order at least (and hence equal to)  $\frac{1}{2}$ . As a result,  $2 + \Delta(\eta)$  and  $2 - \Delta(\eta)$  both have infinitely many zeros (cf. [28, Sec. I.10]).

**Theorem 2.3.1 (Oscillation theorem)** *There exist two monotonically increasing infinite sequences of real numbers  $\{\eta_n\}_{n=0}^\infty$  and  $\{\mu_n\}_{n=1}^\infty$  such that Eq. (2.1.1) has a solution of period  $p$  if and only if  $\eta = \eta_n$  ( $n = 0, 1, 2, \dots$ ) and a solution of primitive period  $2p$  if and only if  $\eta = \mu_n$  ( $n = 1, 2, 3, \dots$ ). These sequences satisfy the inequalities*

$$\eta_0 < \mu_1 \leq \mu_2 < \eta_1 \leq \eta_2 < \mu_3 \leq \mu_4 < \eta_3 \leq \eta_4 < \dots \quad (2.3.11)$$

and the relations

$$\lim_{n \rightarrow \infty} \eta_n = +\infty, \quad \lim_{n \rightarrow \infty} \mu_n = +\infty. \quad (2.3.12)$$

The solutions are all bounded for  $\eta$  in the intervals

$$(\eta_0, \mu_1), \quad (\mu_2, \eta_1), \quad (\eta_2, \mu_3), \quad (\mu_4, \eta_3), \dots \quad (2.3.13)$$

For  $\eta$  at the endpoints of these intervals (and always for  $\eta = \eta_0$ ) there exist unbounded solutions. The solutions are all bounded for  $\eta = \eta_{2n+1}$  or  $\eta = \eta_{2n+2}$  if and only if  $\eta_{2n+1} = \eta_{2n+2}$  and they are all bounded for  $\eta = \mu_{2n+1}$  or  $\eta = \mu_{2n+2}$  if and only if  $\mu_{2n+1} = \mu_{2n+2}$ . The numbers  $\eta_n$  are the zeros of  $\Delta(\eta) = 2$  and the numbers  $\mu_n$  are the zeros of  $\Delta(\eta) = -2$ .

We call  $\eta_n$  the *characteristic values of the first kind* and  $\mu_n$  the *characteristic values of the second kind*. The intervals in (2.3.13) are called *energy bands*. We consider an endpoint as belonging to a band if for that value of  $\eta$  all solutions of Eq. (2.1.1) are bounded. The gaps between the energy bands are called *band gaps*, one of which is the zero-th band gap  $(-\infty, 0]$ . The bands are numbered consecutively  $1, 2, 3, \dots$  and may line up. The band gaps are numbered consecutively  $0, 1, 2, \dots$  and may be empty.

**Proof.** 1. *If (2.1.1) has a nontrivial bounded solution, then  $\eta \in \mathbb{R}$ . Indeed, if  $\eta \in \mathbb{C} \setminus \mathbb{R}$ , then all nontrivial solutions of Eq. (2.1.1) are unbounded. Indeed, let  $\eta = \mu + i\nu$  with  $\mu, \nu \in \mathbb{R}$  and  $\nu \neq 0$  and let  $\phi = u + iv$  be a solution of Eq. (2.1.1) of the type*

$$\phi(x) = e^{i\alpha y(x)} \chi(x) = u + iv,$$

where  $u, v$  are real functions,  $\alpha \in \mathbb{R}$  and  $q(x)$  is periodic with period  $p$ . Then

$$\begin{aligned} -u'' + Q(x)u &= n(x)^2[\mu u - \nu v], \\ -v'' + Q(x)v &= n(x)^2[\nu u + \mu v]. \end{aligned}$$

Multiplying the second equation by  $u$  and the first by  $v$  and subtracting we get

$$u''v - uv'' = \nu n(x)^2(u^2 + v^2).$$

Upon integrating we get

$$u'v - uv' = \nu \int_0^x n(t)^2[u(t)^2 + v(t)^2] dt + \text{const.}$$

Since  $\chi(x)$  is  $C^1$ , the left-hand side is bounded. Thus

$$+\infty > \int_0^\infty n(t)^2[u(t)^2 + v(t)^2] dt = \lim_{m \rightarrow \infty} \int_0^{mp} n(t)^2|\chi(t)|^2 dt,$$

which is a contradiction due to the periodicity of  $n(x)\chi(x)$ . Thus if  $\eta$  is not real, then all nontrivial solutions of Eq. (2.1.1) are unbounded.

**2.** We have  $\Delta(0) = 2$ . Moreover,  $\theta(\eta, x) \rightarrow +\infty$  as  $x \rightarrow +\infty$  whenever  $\eta < 0$ . Indeed, for  $\eta = 0$ , Eq. (2.1.1) has the constant solution which obviously is periodic with period  $p$ . Thus

$$\Delta(0) = 2. \tag{2.3.14}$$

We will now show that  $\theta(\eta, x) \rightarrow +\infty$  as  $x \rightarrow +\infty$  whenever  $\eta < 0$ . Indeed, writing Eq. (2.1.1) in the form

$$\theta''(\eta, x) = (Q(x) - \eta n(x)^2)\theta(\eta, x),$$

we see that  $\theta(\eta, x) > 0$  for small positive  $x$ , because of  $\theta(\eta, 0) = 1$ ,  $\theta'(\eta, 0)$  and  $\theta''(\eta, 0) > 0$ . Using that  $\theta'(\eta, 0) = 0$ , for each  $\varepsilon > 0$  we have

$$\theta'(\eta, \varepsilon)^2 = 2 \int_0^\varepsilon [Q(x) - \eta n(x)^2]\theta(\eta, x)\theta'(\eta, x) dx. \tag{2.3.15}$$

Thus if  $\varepsilon > 0$  is the smallest positive zero of  $\theta'(\eta, x)$ , then (2.3.15) leads to a contradiction. Therefore,  $\theta'(\eta, x) > 0$  for each  $x > 0$ . The positivity of the second derivative for  $x > 0$  then implies that  $\theta(\eta, x) \rightarrow +\infty$  as  $x \rightarrow +\infty$ , as claimed.

**3.** We have  $\Delta'(\eta) \neq 0$  whenever  $\Delta(\eta) \in (-2, 2)$ . Indeed, put

$$\begin{aligned} z_1(\eta, x) &= \frac{\partial}{\partial \eta} \theta(\eta, x), & z_2(\eta, x) &= \frac{\partial}{\partial \eta} \varphi(\eta, x), \\ z'_1(\eta, x) &= \frac{\partial}{\partial \eta} \theta'(\eta, x), & z'_2(\eta, x) &= \frac{\partial}{\partial \eta} \varphi'(\eta, x). \end{aligned}$$

Let us differentiate Eq. (2.1.1) with respect to  $\eta$ . We get

$$\begin{aligned} -z''_1(\eta, x) + Q(x)z_1(\eta, x) &= n(x)^2[\eta z_1(\eta, x) + \theta(\eta, x)], \\ -z''_2(\eta, x) + Q(x)z_2(\eta, x) &= n(x)^2[\eta z_2(\eta, x) + \varphi(\eta, x)]. \end{aligned}$$

Using the method of variation of parameters we obtain

$$z_1(\eta, x) = \theta(\eta, x) \int_0^x n(t)^2 \varphi(\eta, t) \theta(\eta, t) dt - \varphi(\eta, x) \int_0^x n(t)^2 \theta(\eta, t)^2 dt, \quad (2.3.16a)$$

$$z_1'(\eta, x) = \theta'(\eta, x) \int_0^x n(t)^2 \varphi(\eta, t) \theta(\eta, t) dt - \varphi'(\eta, x) \int_0^x n(t)^2 \theta(\eta, t)^2 dt, \quad (2.3.16b)$$

$$z_2(\eta, x) = \theta(\eta, x) \int_0^x n(t)^2 \varphi(\eta, t)^2 dt - \varphi(\eta, x) \int_0^x n(t)^2 \theta(\eta, t) \varphi(\eta, t) dt, \quad (2.3.16c)$$

$$z_2'(\eta, x) = \theta'(\eta, x) \int_0^x n(t)^2 \varphi(\eta, t)^2 dt - \varphi'(\eta, x) \int_0^x n(t)^2 \theta(\eta, t) \varphi(\eta, t) dt. \quad (2.3.16d)$$

Thus (2.3.16) imply

$$\begin{aligned} \Delta'(\eta) &= z_1(\eta, p) + z_2'(\eta, p) \\ &= [\theta(\eta, p) - \varphi'(\eta, p)] \int_0^p n(t)^2 \theta(\eta, t) \varphi(\eta, t) dt \\ &\quad - \varphi(\eta, p) \int_0^p n(t)^2 \theta(\eta, t)^2 dt + \theta'(\eta, p) \int_0^p n(t)^2 \varphi(\eta, t)^2 dt. \end{aligned} \quad (2.3.17)$$

Multiplying (2.3.17) by  $4\varphi(\eta, p)$  and rearranging terms we get

$$\begin{aligned} 4\varphi(\eta, p)\Delta'(\eta) &= - \int_0^p n(t)^2 \{[\theta(\eta, p) - \varphi'(\eta, p)]\varphi(\eta, t) - 2\varphi(\eta, p)\theta(\eta, t)\}^2 dt \\ &= -[4 - \Delta(\eta)^2] \int_0^p n(t)^2 \varphi(\eta, t)^2 dt, \end{aligned} \quad (2.3.18)$$

where we have used that

$$\begin{aligned} \Delta(\eta)^2 - 4 &= [\theta(\eta, p) + \varphi'(\eta, p)]^2 - 4[\theta(\eta, p)\varphi'(\eta, p) - \theta'(\eta, p)\varphi(\eta, p)] \\ &= [\theta(\eta, p) - \varphi'(\eta, p)]^2 + 4\theta'(\eta, p)\varphi(\eta, p). \end{aligned}$$

Now suppose that  $\Delta(\eta) \in (-2, 2)$ . Then (2.3.18) implies  $\varphi(\eta, p)\Delta'(\eta) < 0$ , in particular  $\Delta'(\eta) \neq 0$ .

4.  $\Delta'(\eta) = 0$  at the endpoints of the energy bands if and only if  $\theta'(\eta, p) = \varphi(\eta, p) = 0$ . Indeed, if  $\theta'(\eta, p) = \varphi(\eta, p) = 0$ , then, by Floquet's theorem,  $\theta(\eta, p) = \varphi'(\eta, p)$ . By (2.3.17) we then get  $\Delta'(\eta) = 0$ . Conversely, if  $\Delta'(\eta) = 0$  and  $\Delta(\eta) = \pm 2$ , then the first integrand in (2.3.18) vanishes identically. The linear independence of  $\theta(\eta, x)$  and  $\varphi(\eta, x)$  implies  $\theta(\eta, p) = \varphi'(\eta, p)$  and  $\varphi(\eta, p) = 0$ . By (2.3.17), we get  $\theta'(\eta, p) = 0$ .

5. If  $\Delta(\eta) = \pm 2$  and  $\Delta'(\eta) = 0$ , then  $[\pm \Delta''(\eta)] < 0$ . Indeed, let  $\Delta(\eta) = 2$  and  $\Delta'(\eta) = 0$ . Differentiating (2.3.17) with respect to  $\eta$  we get

$$\begin{aligned} \Delta''(\eta) &= [z_1(\eta, p) - z_2'(\eta, p)] \int_0^p n(x)^2 \theta(\eta, x) \varphi'(\eta, x) \\ &\quad - z_2(\eta, p) \int_0^p n(x)^2 \theta(\eta, x)^2 dx + z_1'(\eta, p) \int_0^p n(x)^2 \varphi(\eta, x)^2 dx, \end{aligned}$$

where we have used part 4 of the proof to cancel out the terms proportional to the vanishing quantities  $\theta(\eta, p) - \varphi'(\eta, p)$ ,  $\varphi(\eta, p)$ , and  $\theta'(\eta, p)$ . Substituting (2.3.16) we get in abbreviated form

$$\begin{aligned} \Delta''(\eta) &= (\theta\beta - \varphi\alpha - \theta'\gamma + \varphi'\beta)\beta - (\theta\gamma - \varphi\beta)\alpha + (\theta'\beta - \varphi'\alpha)\gamma \\ &= -(\theta + \varphi')\beta^2 = -\Delta(\alpha\gamma - \beta^2), \end{aligned}$$

where  $\alpha = \int_0^p n^2 \theta^2$ ,  $\beta = \int_0^p n^2 \theta \varphi$ ,  $\gamma = \int_0^p n^2 \varphi^2$ , and the arguments  $(\eta, p)$  have not been written in  $\theta$ ,  $\theta'$ ,  $\varphi$ , and  $\varphi'$ . Hence,

$$\Delta''(\eta) = 2 \left[ \int_0^p n^2 \theta \varphi \right]^2 - 2 \left[ \int_0^p n^2 \theta^2 \right] \left[ \int_0^p n^2 \varphi^2 \right] < 0,$$

where the equality sign cannot occur because of the linear independence of  $\theta(\eta, x)$  and  $\varphi(\eta, x)$ . If  $\Delta(\eta) = -2$  and  $\Delta'(\eta) = 0$ , then a similar argument gives  $\Delta''(\eta) > 0$ .

6. We have  $\Delta'(0) < 0$ . Indeed,  $\Delta(0) = 2$  and  $\Delta(\eta) > 2$  for  $\eta < 0$ . By the above, we cannot have  $\Delta'(0) = 0$ , because it would imply  $\Delta''(0) < 0$  and hence a local maximum in  $\eta = 0$ , which is not the case. Hence,  $\Delta'(0) \neq 0$ . Since the mean value theorem implies the existence of negative  $\eta$  where  $\Delta'(\eta) < 0$  (because  $\Delta(\eta) \rightarrow +\infty$  as  $\eta \rightarrow -\infty$ ), we must have  $\Delta'(0) < 0$ .

7. The infinitude of the number of periodic and antiperiodic eigenvalues follows directly from the fact that  $\Delta(\eta) - 2$  and  $\Delta(\eta) + 2$  are entire functions of order  $\frac{1}{2}$ . ■

In Appendix B we have proved that  $\Delta(\eta)$  has only one extreme value in each nonempty band gap. At each empty band gap the Hill discriminant has either a maximum (if  $\Delta(\eta) = 2$ ) or a minimum (if  $\Delta(\eta) = -2$ ). For the Schrödinger equation with periodic potential this result was proved before by Kramers [29]. In Appendix B we have applied his methods to generalize the result to the periodic Helmholtz-Schrödinger equation.

According to the Hadamard Factorization Theorem [28, Theorem I.3] valid for entire functions of order  $\frac{1}{2}$ , we have the representation

$$2 - \Delta(\eta) = -\Delta'(0)\eta \prod_{j=1}^{\infty} \left( 1 - \frac{\eta}{\eta_j} \right), \quad (2.3.19)$$

$$2 + \Delta(\eta) = 4 \prod_{j=1}^{\infty} \left(1 - \frac{\eta}{\mu_j}\right), \quad (2.3.20)$$

where we have used (2.3.14) and  $\Delta'(0) < 0$ . According to [28, Theorem I.3] we have

$$\sum_{j=1}^{\infty} \left( \frac{1}{|\eta_j|^s} + \frac{1}{|\mu_j|^s} \right) < \infty, \quad s > \frac{1}{2},$$

which implies the absolute convergence of the infinite products in (2.3.19) and (2.3.20). It is easily verified that the unknown constant  $\Delta'(0)$  can be evaluated from the infinite product (2.3.20) as follows:

$$\Delta'(0) = -4 \sum_{j=1}^{\infty} \frac{1}{\mu_j}.$$

**Example 2.3.2** Let us consider the example  $n(x) \equiv 1$ . Then

$$\theta(\eta, x) = \cos(x\sqrt{\eta}), \quad \varphi(\eta, x) = \frac{\sin(x\sqrt{\eta})}{\sqrt{\eta}},$$

so that

$$\Delta(\eta) = 2 \cos(p\sqrt{\eta}). \quad (2.3.21)$$

Then the zeros  $\{\eta_n\}_{n=0}^{\infty}$  of  $\Delta(\eta) = 2$  and  $\{\mu_n\}_{n=1}^{\infty}$  of  $\Delta(\eta) = -2$  are given by

$$\eta_n = \begin{cases} \left(\frac{n\pi}{p}\right)^2, & n \text{ even,} \\ \left(\frac{(n+1)\pi}{p}\right)^2, & n \text{ odd,} \end{cases} \quad \mu_n = \begin{cases} \left(\frac{(n-1)\pi}{p}\right)^2, & n \text{ even,} \\ \left(\frac{n\pi}{p}\right)^2, & n \text{ odd.} \end{cases}$$

Thus (the interiors of) the bands are

$$\left( \left[ \frac{(k-1)\pi}{p} \right]^2, \left[ \frac{k\pi}{p} \right]^2 \right), \quad k = 1, 2, 3, \dots,$$

while the band gaps are empty. Moreover

$$2 - \Delta(\eta) = 4 \sin^2\left(\frac{1}{2}np\sqrt{\eta}\right) = (np)^2 \eta \prod_{j=1}^{\infty} \left(1 - \frac{(np)^2 \eta}{4j^2 \pi^2}\right)^2,$$

$$2 + \Delta(\eta) = 4 \cos^2\left(\frac{1}{2}np\sqrt{\eta}\right) = \prod_{j=1}^{\infty} \left(1 - \frac{(np)^2 \eta}{(2j-1)^2 \pi^2}\right)^2.$$

This is in perfect agreement with the periodic eigenvalues

$$\mu_1 = 0, \quad \mu_{2k} = \mu_{2k+1} = \left( \frac{2k\pi}{np} \right)^2,$$

where  $k = 1, 2, 3, \dots$ , and with the antiperiodic eigenvalues

$$\bar{\mu}_k = \left( \frac{(2k-1)\pi}{np} \right)^2, \quad k = 1, 2, 3, \dots$$

Also,

$$\begin{aligned} \Delta'(0) &= -8 \sum_{k=1}^{\infty} \left( \frac{np}{(2k-1)\pi} \right)^2 = -\frac{8(np)^2}{\pi^2} \sum_{k=1}^{\infty} \frac{1}{(2k-1)^2} \\ &= -\frac{8(np)^2}{\pi^2} \frac{\pi^2}{8} = -(np)^2 = \left[ \frac{\partial}{\partial \eta} 2 \cos(np\sqrt{\eta}) \right]_{\eta=0}. \end{aligned}$$

**Example 2.3.3** Now consider the more general example where  $n(x) = n_j$  for  $b_{j-1} < x < b_j$  ( $0 = b_0 < b_1 < \dots < b_n = p$  and  $a_j = b_j - b_{j-1}$  for  $j = 1, \dots, m$ ). Then any solution  $\psi(\eta, x)$  of (2.1.1) on  $(b_{j-1}, b_j)$  satisfies

$$\psi(\eta, x) = c_{1j} \cos(n_j \sqrt{\eta} (x - b_{j-1})) + c_{2j} \frac{\sin(n_j \sqrt{\eta} (x - b_{j-1}))}{n_j \sqrt{\eta}}, \quad (2.3.22a)$$

$$\psi'(\eta, x) = -n_j \sqrt{\eta} c_{1j} \sin(n_j \sqrt{\eta} (x - b_{j-1})) + c_{2j} \cos(n_j \sqrt{\eta} (x - b_{j-1})), \quad (2.3.22b)$$

where  $j = 1, \dots, m$ . The requirement that  $\psi(\eta, x)$  is  $C^1$  at the points  $b_1, \dots, b_{m-1}$  leads to the identities

$$\begin{pmatrix} c_{1j} \\ c_{2j} \end{pmatrix} = A_{j-1}(\eta) \begin{pmatrix} c_{1,j-1} \\ c_{2,j-1} \end{pmatrix},$$

where

$$A_{j-1}(\eta) = \begin{pmatrix} \cos(n_{j-1} a_{j-1} \sqrt{\eta}) & \frac{\sin(n_{j-1} a_{j-1} \sqrt{\eta})}{n_{j-1} \sqrt{\eta}} \\ -n_{j-1} \sqrt{\eta} \sin(n_{j-1} a_{j-1} \sqrt{\eta}) & \cos(n_{j-1} a_{j-1} \sqrt{\eta}) \end{pmatrix}.$$

Thus

$$\begin{pmatrix} c_{1m} \\ c_{2m} \end{pmatrix} = A_{m-1}(\eta) \dots A_2(\eta) A_1(\eta) \begin{pmatrix} c_{11} \\ c_{21} \end{pmatrix}.$$

On the other hand,

$$\begin{pmatrix} \psi(\eta, p) \\ \psi'(\eta, p) \end{pmatrix} = A_m(\eta) \begin{pmatrix} c_{1m} \\ c_{2m} \end{pmatrix}.$$

Consequently, we have derived an expression for the *period map*  $M(\eta)$  as follows:

$$\begin{pmatrix} \psi(\eta, p) \\ \psi'(\eta, p) \end{pmatrix} = \underbrace{A_m(\eta)A_{m-1}(\eta) \dots A_2(\eta)A_1(\eta)}_{\stackrel{\text{def}}{=}M(\eta)} \begin{pmatrix} \psi(\eta, 0) \\ \psi'(\eta, 0) \end{pmatrix},$$

implying that

$$\begin{pmatrix} \theta(\eta, p) & \varphi(\eta, p) \\ \theta'(\eta, p) & \varphi'(\eta, p) \end{pmatrix} = M(\eta) \begin{pmatrix} \theta(\eta, 0) & \varphi(\eta, 0) \\ \theta'(\eta, 0) & \varphi'(\eta, 0) \end{pmatrix} = M(\eta). \quad (2.3.23)$$

Hence

$$\Delta(\eta) = \theta(\eta, p) + \varphi'(\eta, p) = \text{Tr } M(\eta), \quad (2.3.24)$$

where  $\text{Tr}$  stands for the matrix trace. For  $m = 2$  we get (see left-hand side of Fig. 2.2)

$$\begin{aligned} \Delta(\eta) &= 2 [\cos(n_2 a_2 \sqrt{\eta}) \cos(n_1 a_1 \sqrt{\eta}) \\ &\quad - \frac{1}{2} \left( \frac{n_1}{n_2} + \frac{n_2}{n_1} \right) \sin(n_2 a_2 \sqrt{\eta}) \sin(n_1 a_1 \sqrt{\eta})]. \end{aligned} \quad (2.3.25)$$

For  $m = 3$  we get (see right-hand side of Fig. 2.2)

$$\begin{aligned} \Delta(\eta) &= 2 [\cos(n_3 a_3 \sqrt{\eta}) \cos(n_2 a_2 \sqrt{\eta}) \cos(n_1 a_1 \sqrt{\eta}) \\ &\quad - \frac{1}{2} \left( \frac{n_1}{n_2} + \frac{n_2}{n_1} \right) \cos(n_3 a_3 \sqrt{\eta}) \sin(n_2 a_2 \sqrt{\eta}) \sin(n_1 a_1 \sqrt{\eta}) \\ &\quad - \frac{1}{2} \left( \frac{n_1}{n_3} + \frac{n_3}{n_1} \right) \sin(n_3 a_3 \sqrt{\eta}) \cos(n_2 a_2 \sqrt{\eta}) \sin(n_1 a_1 \sqrt{\eta}) \\ &\quad - \frac{1}{2} \left( \frac{n_2}{n_3} + \frac{n_3}{n_2} \right) \sin(n_3 a_3 \sqrt{\eta}) \sin(n_2 a_2 \sqrt{\eta}) \cos(n_1 a_1 \sqrt{\eta})]. \end{aligned}$$

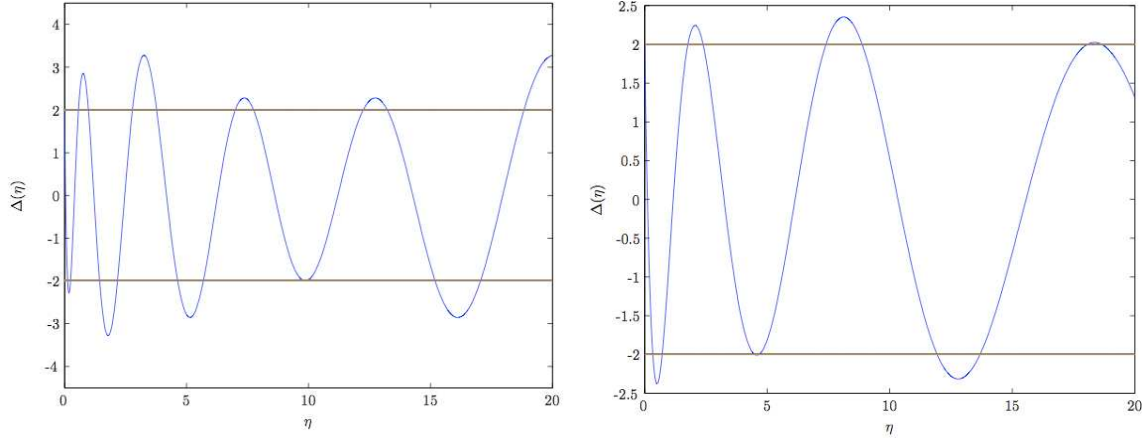


**Figure 2.2:** Graphs of  $\Delta(\eta)$  as a function of  $\eta$  for the example with  $m = 2$ ,  $n_1 = 3$ ,  $n_2 = 1$ ,  $a_1 = 2$ ,  $a_2 = 1$  (left hand-side of the figure) and for the example with  $m = 3$ ,  $n_1 = 2$ ,  $n_2 = 1$ ,  $n_3 = 1.8$ ,  $a_1 = 1$ ,  $a_2 = 1.5$  and  $a_3 = 0.5$  (right hand-side of the figure).

For  $m = 4$  we get (see Fig. 2.3)

$$\begin{aligned}
\Delta(\eta) = & 2 [\cos(n_4 a_4 \sqrt{\eta}) \cos(n_3 a_3 \sqrt{\eta}) \cos(n_2 a_2 \sqrt{\eta}) \cos(n_1 a_1 \sqrt{\eta}) \\
& - \frac{1}{2} \left( \frac{n_1}{n_2} + \frac{n_2}{n_1} \right) \cos(n_4 a_4 \sqrt{\eta}) \cos(n_3 a_3 \sqrt{\eta}) \sin(n_2 a_2 \sqrt{\eta}) \sin(n_1 a_1 \sqrt{\eta}) \\
& - \frac{1}{2} \left( \frac{n_1}{n_3} + \frac{n_3}{n_1} \right) \cos(n_4 a_4 \sqrt{\eta}) \sin(n_3 a_3 \sqrt{\eta}) \cos(n_2 a_2 \sqrt{\eta}) \sin(n_1 a_1 \sqrt{\eta}) \\
& - \frac{1}{2} \left( \frac{n_2}{n_3} + \frac{n_3}{n_2} \right) \cos(n_4 a_4 \sqrt{\eta}) \sin(n_3 a_3 \sqrt{\eta}) \sin(n_2 a_2 \sqrt{\eta}) \cos(n_1 a_1 \sqrt{\eta}) \\
& - \frac{1}{2} \left( \frac{n_3}{n_4} + \frac{n_4}{n_3} \right) \sin(n_4 a_4 \sqrt{\eta}) \sin(n_3 a_3 \sqrt{\eta}) \cos(n_2 a_2 \sqrt{\eta}) \cos(n_1 a_1 \sqrt{\eta}) \\
& - \frac{1}{2} \left( \frac{n_2}{n_4} + \frac{n_4}{n_2} \right) \sin(n_4 a_4 \sqrt{\eta}) \cos(n_3 a_3 \sqrt{\eta}) \sin(n_2 a_2 \sqrt{\eta}) \cos(n_1 a_1 \sqrt{\eta}) \\
& - \frac{1}{2} \left( \frac{n_1}{n_4} + \frac{n_4}{n_1} \right) \sin(n_4 a_4 \sqrt{\eta}) \cos(n_3 a_3 \sqrt{\eta}) \cos(n_2 a_2 \sqrt{\eta}) \sin(n_1 a_1 \sqrt{\eta}) \\
& + \frac{1}{2} \left( \frac{n_1 n_3}{n_2 n_4} + \frac{n_2 n_4}{n_1 n_3} \right) \sin(n_4 a_4 \sqrt{\eta}) \sin(n_3 a_3 \sqrt{\eta}) \sin(n_2 a_2 \sqrt{\eta}) \sin(n_1 a_1 \sqrt{\eta}) ] .
\end{aligned}$$

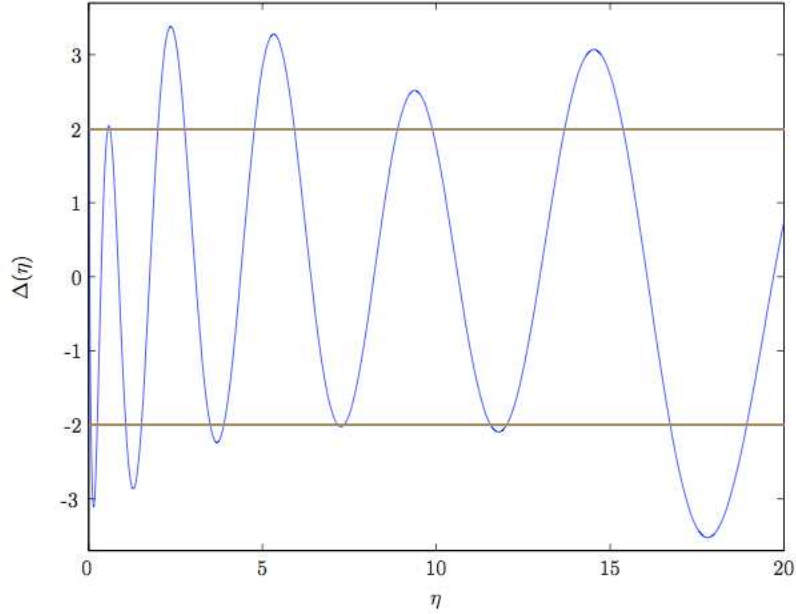


**Figure 2.3:** Graph of  $\Delta(\eta)$  as a function of  $\eta$  for the example with  $m = 4$ ,  $n_1 = 0.8$ ,  $n_2 = 0.5$ ,  $n_3 = 1.5$ ,  $n_4 = 2$ ,  $a_1 = 0.5$ ,  $a_2 = 1.2$ ,  $a_3 = 1$  and  $a_4 = 1.5$ .

## 2.4 Conversion to Quasimomentum

In the usual scattering theory of the Schrödinger equation on the line [30, 31]

$$-\psi''(k, x) + Q(x)\psi(k, x) = k^2\psi(k, x),$$

the continuous spectrum of the Hamiltonian  $H = -(d^2/dx^2) + Q$  coincides with  $\eta = k^2 \in [0, \infty)$  if  $Q$  is a real function such that  $(1 + |x|)Q(x)$  belongs to  $L^1(\mathbb{R})$ , where it is customary to convert from the energy variable  $\eta$  (in the complex plane cut along  $[0, \infty)$ ) to the wavenumber  $k$ , where  $\eta = k^2$ . Two Riemann surfaces can be introduced, one in the energy variable  $\eta$  and the other in the wavenumber  $k$ . The Riemann surface  $\Lambda$  in the energy variable consists of two copies of the complex plane cut along  $[0, \infty)$ , one being the physical sheet, corresponding to the upper half complex  $k$ -plane, and the other the unphysical sheet, corresponding to the lower half complex  $k$ -plane, glued together by attaching the upper side of the cut in the physical sheet to the lower side of the cut in the unphysical sheet and the lower side of the cut in the physical sheet to the upper side of the cut in the unphysical sheet.

We then define the wavenumber<sup>2</sup>

$$k(\eta) = \pm i\sqrt{-\eta}$$

in such a way that the physical  $\eta$ -sheet corresponds to the upper half  $k$ -plane and the unphysical  $\eta$ -sheet to the lower half  $k$ -plane. The Riemann surface  $\mathbb{K}$  in the  $k$ -variable then is the complex  $k$ -plane cut along the real line. Obviously, the Riemann surfaces  $\Lambda$  and  $\mathbb{K}$  are in 1, 1-correspondence.

Let us first summarize what we have proved regarding the behavior of the Hill discriminant  $\Delta(\eta)$ :

- (a) It decreases monotonically from  $+\infty$  to  $+2$  as  $\eta$  increases from  $-\infty$  to  $\eta_0$ .
- (b) It decreases monotonically from  $+2$  to  $-2$  as  $\eta$  increases from  $\eta_{2k}$  to  $\mu_{2k+1}$  ( $k = 0, 1, \dots$ ) along the odd numbered bands.
- (c) It increases monotonically from  $-2$  to  $+2$  as  $\eta$  increases from  $\eta_{2k-1}$  to  $\mu_{2k}$  ( $k = 1, 2, \dots$ ) along the even numbered bands.

In the band gaps the behavior of  $\Delta(\eta)$  is as follows:

- (a) It decreases monotonically from  $+\infty$  to  $+2$  as  $\eta$  increases from  $-\infty$  to  $\eta_0$  (zero-th band gap).
- (b) It has a single extreme value  $\eta = \zeta_l$  in each nonempty band gap.
- (c) The coalescence points of two bands with empty intermediate band gap are extreme values.

Then  $\Delta(\eta)$  is real whenever  $\eta \in \mathbb{R}$  or  $\eta$  belongs to any of the curves  $\Gamma_l$  which intersect the real line at  $\zeta_l$  at a right angle, has  $\{\eta \in \mathbb{C} : \operatorname{Re} \eta = \pi^2 l^2\}$  as its vertical asymptotes, are mirror symmetric with respect to the real line, and do not intersect each other, where  $l = 1, 2, 3, \dots$ . Put  $\Gamma_l^\pm = \Gamma_l \cap \{\eta \in \mathbb{C} : (\pm \operatorname{Re} \eta) \geq 0\}$ . The real lines and the curves  $\Gamma_l$  divide the physical and physical sheets of  $\Lambda$  in sections on which the transformation  $\eta \mapsto k$  to quasimomentum will be performed separately as indicated in Table 2.4.

In general [32, 33], define the *quasimomentum*  $k(\eta)$  in such a way that

$$\Delta(\eta) = 2 \cos(qk(\eta)), \quad \sqrt{\Delta(\eta)^2 - 4} = -2i \sin(qk(\eta)), \quad \frac{dk}{d\eta} = -\frac{\Delta'(\eta)}{2q \sin(qk)}.$$

---

<sup>2</sup>Thus if  $\eta = \rho e^{i\theta}$  with  $0 \leq \theta < 2\pi$ , then  $k(\eta) = \sqrt{\rho} e^{i\theta/2}$  on the physical sheet and  $k(\eta) = \sqrt{\rho} e^{i(\theta-2\pi)/2}$  on the unphysical sheet.

**Table 2.1:** Closed regions  $\Omega_j^+$  in the physical  $\eta$ -sheet along with their boundaries, followed by their images in the upper half  $k$ -plane. The left column contains the regions and the right column their boundaries. The upper part of each entry regards the  $\eta$ -plane and the lower part the  $k$ -plane. Here  $\varepsilon_j = \frac{1}{q} \operatorname{arcsinh}(\frac{1}{2} \sqrt{\Delta(\zeta_j)^2 - 4})$ , where  $j = 1, 2, 3, \dots$

$\Omega_{1+}$	$(-\infty, \eta_0] \cup s_1^+ \cup [\mu_1, \zeta_1] \cup \Gamma_1^+$
$[0, \pi] \times i\mathbb{R}^+$	$(i\infty, i0] \cup [0, \pi] \cup [\pi, \pi + i\varepsilon_1]$ $\cup [\pi + i\varepsilon_1, \pi + i\infty)$
$\Omega_{2+}$	$\Gamma_1^+ \cup [\zeta_1, \mu_2] \cup s_2^+ \cup [\eta_1, \zeta_2] \cup \Gamma_2^+$
$[\pi, 2\pi] \times i\mathbb{R}^+$	$(\pi + i\infty, \pi + i\varepsilon_1] \cup [\pi + i\varepsilon_1, \pi]$ $\cup [\pi, 2\pi] \cup [2\pi, 2\pi + i\varepsilon_2]$ $\cup [2\pi + i\varepsilon_2, 2\pi + i\infty)$
$\Omega_{2k,+}$	$\Gamma_{2k-1}^+ \cup [\zeta_{2k-1}, \mu_{2k}] \cup s_{2k}^+ \cup [\eta_{2k-1}, \zeta_{2k}] \cup \Gamma_{2k}^+$
$[(2k-1)\pi, 2k\pi] \times i\mathbb{R}^+$	$((2k-1)\pi + i\infty, (2k-1)\pi + i\varepsilon_{2k-1}]$ $\cup [(2k-1)\pi + i\varepsilon_{2k-1}, (2k-1)\pi]$ $\cup [(2k-1)\pi, 2k\pi] \cup [2k\pi, 2k\pi + i\varepsilon_{2k}]$ $\cup [2k\pi + i\varepsilon_{2k}, 2k\pi + i\infty)$
$\Omega_{2k+1,+}$	$\Gamma_{2k}^+ \cup [\zeta_{2k}, \eta_{2k}] \cup s_{2k+1}^+ \cup [\mu_{2k+1}, \zeta_{2k+1}] \cup \Gamma_{2k+1}^+$
$[2k\pi, (2k+1)\pi] \times i\mathbb{R}^+$	$(2k\pi + i\infty, 2k\pi + i\varepsilon_{2k}] \cup [2k\pi + i\varepsilon_{2k}, 2k\pi]$ $\cup [2k\pi, (2k+1)\pi]$ $\cup [(2k+1)\pi, (2k+1)\pi + i\varepsilon_{2k+1}]$ $\cup [(2k+1)\pi + i\varepsilon_{2k+1}, (2k+1)\pi + i\infty)$

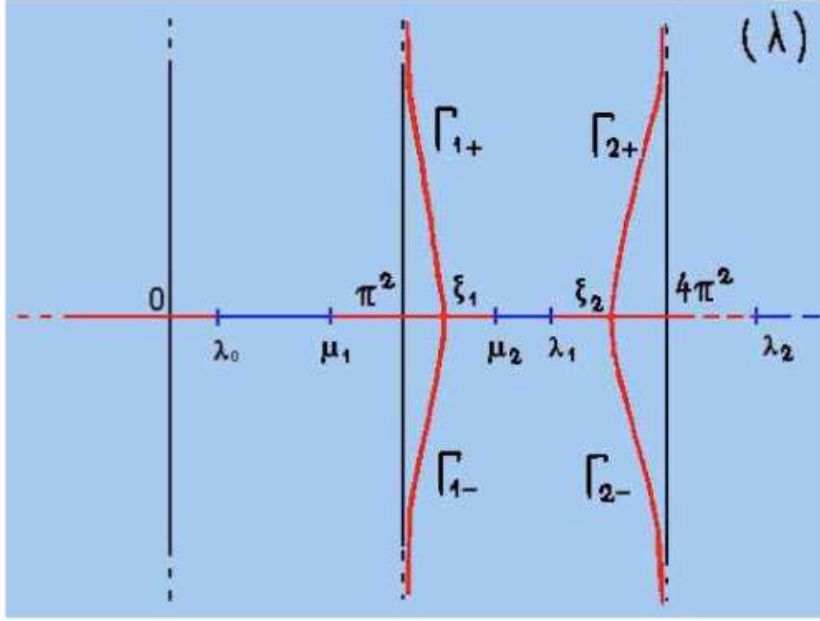


**Figure 2.4:** This figure shows in red the zones where  $\Delta(\eta)$  is real in the  $\Lambda$ -plane. The stability intervals are depicted in blue.

Moreover, define the eigenvalues

$$\tau_{1,2}(\eta) = \begin{cases} e^{\pm i q k(\eta)}, & \text{physical sheet,} \\ e^{\mp i q k(\eta)}, & \text{unphysical sheet,} \end{cases} \quad (2.4.1)$$

where  $|\tau_1| < 1$  and  $|\tau_2| > 1$  whenever  $\Delta(\eta) \notin [-2, 2]$ . Since different points in the complex plane have the same sines, cosines, and squares, some care is needed when defining  $k(\eta)$ . Let us denote the upper side of the  $k$ -th band by  $s_k^+$  and the lower side of the  $k$ -th band by  $s_k^-$ , where  $k = 1, 2, 3, \dots$ . Let us subdivide the complex  $\eta$ -plane cut along the bands as follows, performing the subdivision separately for the physical  $\eta$ -sheet and the nonphysical  $\eta$ -sheet. Then we define<sup>3</sup> for  $\eta \in (-\infty, \eta_0)$

$$k(\eta) = \begin{cases} \frac{i}{q} \operatorname{arcsinh}\left(\frac{1}{2} \sqrt{\Delta(\eta)^2 - 4}\right), & \text{physical sheet,} \\ \frac{-i}{q} \operatorname{arcsinh}\left(\frac{1}{2} \sqrt{\Delta(\eta)^2 - 4}\right), & \text{unphysical sheet,} \end{cases}$$

where the square root is positive. We now engage in successive analytic continuations of  $k(\eta)$  in the physical  $\eta$ -sheet to  $\Omega_1^+$ , then to  $\Omega_2^+$ , then to  $\Omega_3^+$ ,

<sup>3</sup>If  $\sinh(z) = w$ , then  $z = \operatorname{arcsinh}(w) = \log(w + \sqrt{w^2 + 1})$ . We define either function as a 1, 1-correspondence between  $\mathbb{R}$  and itself.

**Table 2.2:** Conversion from the energy variable  $\eta$  to the quasimomentum variable  $k$ .

	physical sheet	unphysical sheet
upper half-plane	first quadrant	third quadrant
lower half-plane	second quadrant	fourth quadrant

etc., thus mapping the intersection of the physical  $\eta$ -sheet and the upper half  $\eta$ -plane onto the first  $k$ -quadrant in a 1, 1 manner. Similarly, the intersection of the physical  $\eta$ -sheet and the lower half  $\eta$ -plane is mapped onto the second  $k$ -quadrant in a 1, 1 manner. Next, the intersection of the unphysical  $\eta$ -sheet and the upper half  $\eta$ -plane is mapped onto the third  $k$ -quadrant in a 1, 1 manner and the intersection of the unphysical  $\eta$ -sheet and the lower half  $\eta$ -plane onto the fourth  $k$ -quadrant in a 1, 1 manner. As a result, we obtain the symmetry relation

$$k(\eta)_{\text{unphysical}} = \overline{k(\bar{\eta})_{\text{physical}}}.$$

Let us work out the introduction of the  $k$ -variable for  $n(x) \equiv 1$ . Then  $\Delta(\eta)$  is given by (2.3.21). As a result,  $q = p$  and

$$\Delta'(\eta) = \frac{-p \sin(p\sqrt{\eta})}{2\sqrt{\eta}}, \text{ implying } \zeta_k = \left(\frac{k\pi}{p}\right)^2, \quad k = 1, 2, 3, \dots$$

Then  $\Delta(\eta)$  is real-valued if and only if  $\text{Re } \eta = \eta_k$  for some  $k = 1, 2, 3, \dots$ <sup>4</sup> For  $\eta \in (-\infty, 0)$  (where  $\eta_0 = 0$ ) we now have

$$k(\eta) = \begin{cases} +i\sqrt{-\eta}, & \text{physical sheet,} \\ -i\sqrt{-\eta}, & \text{unphysical sheet,} \end{cases}$$

where the square root is positive. The net result is  $k(\eta)$  as for the usual Schrödinger equation on the line.

For later use we let  $\tau_1(\eta)$  and  $\tau_2(\eta)$  be the roots of the quadratic Hill polynomial equation (2.1.4) such that  $|\tau_1(\eta)| < 1$  and  $|\tau_2(\eta)| > 1$  whenever

<sup>4</sup>This follows from (2.3.21) using the equality  $\cos(\sigma + i\tau) = \cos \sigma \cosh \tau - i \sin \sigma \sinh \tau$ .

$\Delta(\eta) \notin [-2, 2]$ . We then have

$$\tau_1(\eta) = \begin{cases} \frac{1}{2}[\Delta(\eta) - \sqrt{\Delta(\eta)^2 - 4}], & \Delta(\eta) > 2, \\ \frac{1}{2}[\Delta(\eta) + \sqrt{\Delta(\eta)^2 - 4}], & \Delta(\eta) < -2, \end{cases} \quad (2.4.2a)$$

$$\tau_2(\eta) = \begin{cases} \frac{1}{2}[\Delta(\eta) + \sqrt{\Delta(\eta)^2 - 4}], & \Delta(\eta) > 2, \\ \frac{1}{2}[\Delta(\eta) - \sqrt{\Delta(\eta)^2 - 4}], & \Delta(\eta) < -2, \end{cases} \quad (2.4.2b)$$

where the square root is positive. For  $\Delta(\eta) \notin [-2, 2]$ ,  $\tau_1(\eta)$  and  $\tau_2(\eta)$  are defined by analytic continuation. For  $\Delta(\eta) \in (-2, 2)$  we distinguish between limiting values as  $\eta$  approaches the band from above and from below. For  $\Delta(\eta) \notin [-2, 2]$  and  $\eta \notin \mathbb{R}$ ,  $\tau_1(\eta)$  and  $\eta$  have imaginary parts of opposite sign and  $\tau_2(\eta)$  and  $\eta$  have imaginary parts of the same sign, where  $\tau_1(\eta)$  and  $\tau_2(\eta)$  have product 1 and sum  $\Delta(\eta)$ .

## 2.5 Direct Scattering Theory

In this section we study the direct scattering theory of (2.1.1), where  $n(x)$  has a periodic component and a component describing the effect of impurities.

### 2.5.1 Direct Scattering for the Periodic Problem

Equation (2.1.1) has one linearly independent solution  $\psi_1(\eta, x)$  in  $L^2(\mathbb{R}^+)$  and one linearly independent solution  $\psi_2(\eta, x)$  in  $L^2(\mathbb{R}^-)$ . These solutions are called *Floquet solutions*. Thus for each  $\eta \in \mathbb{C}$  there exist unique *Weyl coefficients*  $m_1(\eta)$  and  $m_2(\eta)$  such that

$$\psi_1(\eta, x) = \theta(\eta, x) + m_1(\eta)\varphi(\eta, x), \quad (2.5.1a)$$

$$\psi_2(\eta, x) = \theta(\eta, x) + m_2(\eta)\varphi(\eta, x). \quad (2.5.1b)$$

If  $\Delta(\eta) \notin [-2, 2]$ , then (2.1.4) has a solution  $\tau_1$  with  $|\tau_1| < 1$  and a solution  $\tau_2$  with  $|\tau_2| > 1$ . Therefore,

$$\begin{pmatrix} \tau_{1,2}(\eta) - \theta(\eta, p) & -\varphi(\eta, p) \\ -\theta'(\eta, p) & \tau_{1,2}(\eta) - \varphi'(\eta, p) \end{pmatrix} \begin{pmatrix} 1 \\ m_{1,2}(\eta) \end{pmatrix} = \begin{pmatrix} 0 \\ 0 \end{pmatrix}. \quad (2.5.2)$$

Thus the Weyl coefficients satisfy

$$m_{1,2}(\eta) = \frac{\tau_{1,2}(\eta) - \theta(\eta, p)}{\varphi(\eta, p)}. \quad (2.5.3)$$

The Floquet solutions have the Bloch representation

$$\psi_{1,2}(k, x) = e^{\pm iky(x)} \chi_{1,2}(k, x), \quad (2.5.4)$$

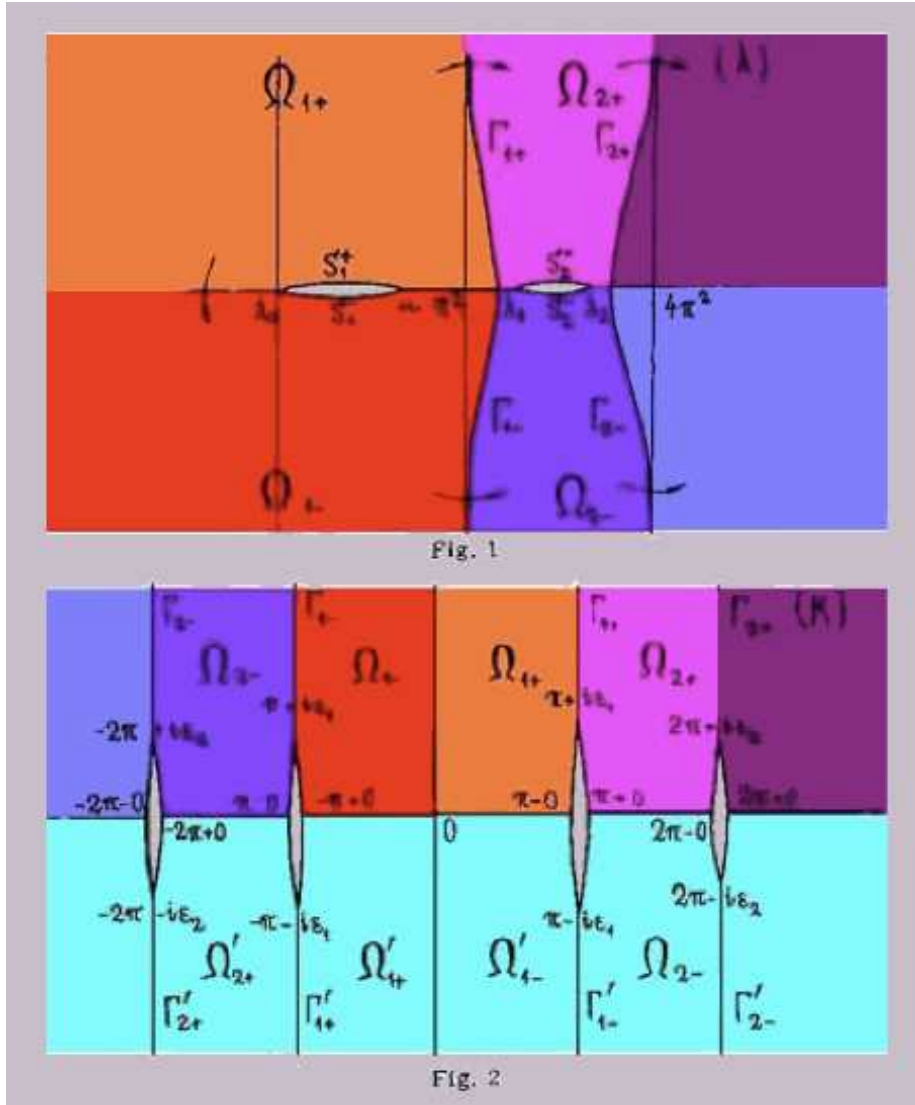


**Figure 2.5:** This figure shows the correspondence between the physical plane  $\Lambda$  and the halfplane  $\mathbb{K}$  with  $Imk > 0$ .

where  $\chi_{1,2}(k, x + p) \equiv \chi_{1,2}(k, x)$  are periodic. Because the quasimomenta  $\pm k \in \mathbb{R}$  correspond to  $\eta$  in the limit to a band from above and below, we have the symmetry relations

$$\psi_{1,2}(k, x) = \begin{cases} \overline{\psi_{1,2}(-\bar{k}, x)}, \\ \psi_{2,1}(-k, x), \quad k \in \mathbb{R}. \end{cases} \quad (2.5.5)$$

We also get for the Wronskian

$$\begin{aligned} w(k) &\stackrel{\text{def}}{=} W[\psi_1(k, \cdot), \psi_2(k, \cdot)] = W[\theta(\eta, \cdot) + m_1(\eta)\varphi(\eta, \cdot), \theta(k, \cdot) + m_2(\eta)\varphi(k, \cdot)] \\ &= \{m_2(\eta) - m_1(\eta)\} W[\theta(\eta, \cdot), \varphi(\eta, \cdot)] \\ &= m_2(\eta) - m_1(\eta) = \frac{-2i \sin(qk)}{\varphi(\eta, p)}. \end{aligned}$$

With the help of the inversion and conjugation symmetries (2.5.5) we get

$$w(k) = W[\psi_1(k, \cdot), \psi_2(k, \cdot)] = \begin{cases} W[\psi_2(-k, \cdot), \psi_1(-k, \cdot)] = -w(-k), & k \in \mathbb{R}, \\ W[\psi_1(-\bar{k}, \cdot), \psi_2(-\bar{k}, \cdot)] = w(-\bar{k}). \end{cases} \quad (2.5.6)$$

The Wronskian  $w(k)$  can only be zero for those  $k \in \mathbb{R}$  that correspond to the endpoints of the bands, i.e., for  $k = m\pi$  for some  $m \in \mathbb{Z}$ . Following the praxis of the scattering theory of the Schrödinger equation on the line [30, 31, 34], we say that the *generic case* occurs in  $k = m\pi$  if  $w(m\pi) \neq 0$ , and that the *exceptional case* occurs in  $k = m\pi$  if  $w(m\pi) = 0$ . In the generic case the two Floquet solutions are linearly independent, whereas in the exceptional case they are linearly dependent. For  $n(x) \equiv 1$  we have  $\psi_{1,2}(k, x) = e^{\pm ikx}$  and  $w(k) = -2ik$ ; hence the generic case occurs in  $k = m\pi$  for  $0 \neq m \in \mathbb{Z}$  and the exceptional case occurs in  $k = 0$ .

Since the (simple) zeros of  $\varphi(p, \eta)$  can only occur at points of the bands, the Weyl coefficients  $m_{1,2}(\eta)$  are analytic in  $\eta$  outside the bands. As a result,<sup>5</sup>  $\psi_{1,2}(k, x)$  are continuous functions in  $k$  in the closed upper half-plane and analytic functions in  $k$  in the open upper half-plane.

## 2.5.2 Jost Solutions and Scattering Coefficients

We now add impurities by studying the generalized Helmholtz equation (2.1.1), where

$$n(x)^2 = n_0(x)^2[1 + \varepsilon(x)],$$

$n_0(x)$  is a real piecewise continuous periodic function of period  $p$ ,  $\varepsilon(x)$  is piecewise continuous, vanishes as  $x \rightarrow \pm\infty$ , and has the lower bound  $\inf\{\varepsilon(x) : x \in \mathbb{R}\} > -1$ , and  $\int_{-\infty}^{\infty} (1 + |x|)|\varepsilon(x)| < \infty$ . We introduce the Hill discriminant  $\Delta(\eta)$  and the quasimomentum  $k(\eta)$  as pertaining to the corresponding periodic problem

$$-\psi''(\eta, x) = \eta n_0(x)^2 \psi(\eta, x).$$

---

<sup>5</sup>From now on, we take  $\eta$  in the physical sheet and hence  $k$  in the upper half-plane.

We now define the *Jost solutions* of Eq. (2.1.1) as those solutions that satisfy the asymptotic relations

$$f_1(k, x) = \psi_1(k, x)[1 + o(1)], \quad x \rightarrow +\infty, \quad (2.5.7a)$$

$$f_2(k, x) = \psi_2(k, x)[1 + o(1)], \quad x \rightarrow -\infty. \quad (2.5.7b)$$

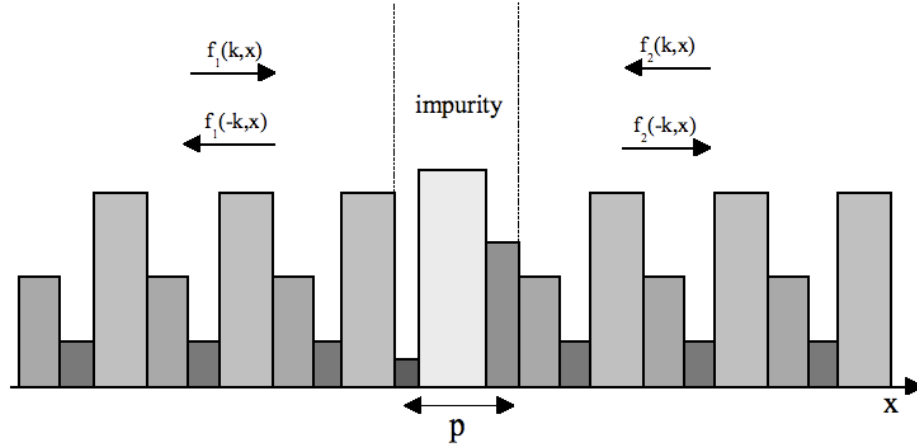


**Figure 2.6:** Example of a periodic structure with period  $p$  having a localized impurity due to the presence of materials with different refractive index. The impurity generates scattering phenomena (Jost functions). The refractive index profile along the  $x$ -direction is drawn.

Using the method of variation of parameters (or by direct substitution in the differential equation) we easily prove the following

**Lemma 2.5.1** *Let  $g(x)$  be a bounded measurable function. Then the unique solutions of the inhomogeneous differential equation*

$$-\psi''(\eta, x) = \eta n_0(x)^2 \psi(\eta, x) + g(x) \quad (2.5.8)$$

satisfying  $\psi(k, x) = \psi_{1,2}(k, x)[1 + o(1)]$  as  $x \rightarrow \pm\infty$  is given by

$$\psi(\eta, x) = \psi_1(k, x) + \int_x^\infty \frac{\psi_2(k, x)\psi_1(k, t) - \psi_1(k, x)\psi_2(k, t)}{w(k)} g(t) dt, \quad (2.5.9a)$$

$$\psi(\eta, x) = \psi_2(k, x) - \int_{-\infty}^x \frac{\psi_2(k, x)\psi_1(k, t) - \psi_1(k, x)\psi_2(k, t)}{w(k)} g(t) dt, \quad (2.5.9b)$$

respectively. Here  $w(k) = W[\psi_1(k, \cdot); \psi_2(k, \cdot)]$ .

**Proof.** Let us write the solution in the form

$$\psi(k, x) = c_1(x)\psi_1(k, x) + c_2(x)\psi_2(k, x),$$

where

$$\begin{pmatrix} \psi_1(k, x) & \psi_2(k, x) \\ \psi_1'(k, x) & \psi_2'(k, x) \end{pmatrix} \begin{pmatrix} c_1'(x) \\ c_2'(x) \end{pmatrix} = \begin{pmatrix} 0 \\ -g(x) \end{pmatrix}.$$

Then

$$\begin{aligned} c_1(x) &= c_1 + \frac{1}{w(k)} \int_{-\infty}^x \psi_2(k, t)g(t) dt, \\ c_2(x) &= c_2 + \frac{1}{w(k)} \int_x^{\infty} \psi_1(k, t)g(t) dt. \end{aligned}$$

Therefore,

$$\begin{aligned} \psi(k, x) &= \left[ c_1 + \frac{1}{w(k)} \int_{-\infty}^x \psi_2(k, t)g(t) dt \right] \psi_1(k, x) \\ &\quad + \left[ c_2 + \frac{1}{w(k)} \int_x^{\infty} \psi_1(k, t)g(t) dt \right] \psi_2(k, x). \end{aligned}$$

To obtain the solution asymptotically equivalent to  $\psi_1(k, x)$  as  $x \rightarrow +\infty$ , we take  $c_2 = 0$  to cancel out any contribution proportional to  $\psi_2(k, x)$  and get

$$\begin{aligned} &\left[ \underbrace{c_1 + \frac{1}{w(k)} \int_{-\infty}^{\infty} \psi_2(k, t)g(t) dt}_{=1} \right] \psi_1(k, x) \\ &- \frac{1}{w(k)} \int_x^{\infty} \psi_2(k, t)g(t) dt \psi_1(k, x) + \frac{1}{w(k)} \int_x^{\infty} \psi_1(k, t)g(t) dt \psi_2(k, x), \end{aligned}$$

yielding (2.5.9a). Analogously, to obtain the solution asymptotically equivalent to  $\psi_2(k, x)$  as  $x \rightarrow -\infty$ , we take  $c_1 = 0$  to cancel out any contribution proportional to  $\psi_1(k, x)$  and get

$$\begin{aligned} &\left[ \underbrace{c_2 + \frac{1}{w(k)} \int_{-\infty}^{\infty} \psi_1(k, t)g(t) dt}_{=1} \right] \psi_2(k, x) \\ &+ \frac{1}{w(k)} \int_{-\infty}^x \psi_2(k, t)g(t) dt \psi_1(k, x) - \frac{1}{w(k)} \int_{-\infty}^x \psi_1(k, t)g(t) dt \psi_2(k, x), \end{aligned}$$

yielding (2.5.9b). ■

Applying Lemma 2.5.1 for  $g = \eta n_0^2 \varepsilon f_{1,2}(k, \cdot)$  we get

$$f_1(k, x) = \psi_1(k, x) + \int_x^\infty A(k; x, t) [\eta n_0(t)^2 \varepsilon(t)] f_1(k, t) dt, \quad (2.5.10a)$$

$$f_2(k, x) = \psi_2(k, x) - \int_{-\infty}^x A(k; x, t) [\eta n_0(t)^2 \varepsilon(t)] f_2(k, t) dt, \quad (2.5.10b)$$

where

$$A(k; x, t) = \frac{\psi_2(k, x)\psi_1(k, t) - \psi_1(k, x)\psi_2(k, t)}{w(k)}. \quad (2.5.11)$$

As a result of the symmetry relations of the Floquet solutions, we have the inversion and conjugation symmetries

$$f_{1,2}(k, x) = \begin{cases} \overline{f_{1,2}(-\bar{k}, x)} \\ f_{2,1}(-k, x), \end{cases} \quad k \in \mathbb{R}. \quad (2.5.12)$$

We also have the asymptotic relations

$$f_1(k, x) = a_1(k)\psi_1(k, x) + b_1(k)\psi_2(k, x) + o(1), \quad x \rightarrow -\infty, \quad (2.5.13a)$$

$$f_2(k, x) = b_2(k)\psi_1(k, x) + a_2(k)\psi_2(k, x) + o(1), \quad x \rightarrow +\infty, \quad (2.5.13b)$$

where

$$\begin{aligned} a_1(k) &= 1 - w(k)^{-1}I_{21}(k), & b_1(k) &= w(k)^{-1}I_{11}(k), \\ b_2(k) &= w(k)^{-1}I_{22}(k), & a_2(k) &= 1 - w(k)^{-1}I_{12}(k), \end{aligned}$$

and

$$I_{jl}(k) = \int_{-\infty}^{\infty} [\eta n_0(t)^2 \varepsilon(t)] \psi_j(k, t) f_l(k, t) dt.$$

For the Wronskians we find with the help of the inversion symmetry (2.5.5)

$$\begin{aligned} W[f_1(k, \cdot), f_2(k, \cdot)] &= W[\psi_1, b_2\psi_1 + a_2\psi_2] = a_2(k)w(k), \\ &= W[a_1\psi_1 + b_1\psi_2, \psi_2] = a_1(k)w(k), \end{aligned}$$

so that

$$a(k) \stackrel{\text{def}}{=} a_1(k) = a_2(k), \quad k \in \mathbb{C} \setminus \mathbb{R},$$

where the relation extends to its boundary value as  $k$  approaches the real line from above and below. Using the conjugation symmetry (2.5.5) we obtain

$$\overline{w(-\bar{k})a(-\bar{k})} = W[\overline{f_1(-\bar{k}, \cdot)}, \overline{f_2(-\bar{k}, \cdot)}] = W[f_1(k, \cdot), f_2(k, \cdot)] = w(k)a(k),$$

so that

$$\overline{a(-\bar{k})} = a(k), \quad k \in \mathbb{C} \setminus \mathbb{R}, \quad (2.5.14)$$

where the relation extends to its boundary value as  $k$  approaches the real line from above and below. Observe that  $w(k)a(k)$  is continuous in  $k \in \overline{\mathbb{C}^+}$ . As yet, we do not get relations involving  $b_1(k)$  and  $b_2(k)$  for nonreal  $k$ .

Let us now look for relations for  $k \in \mathbb{R}$ . For  $k \in \mathbb{R}$  we have

$$\begin{aligned} & W[f_1(k, \cdot), f_1(-k, \cdot)] \\ &= \begin{cases} W[\psi_1(k, \cdot), \psi_1(-k, \cdot)] = W[\psi_1(k, \cdot), \psi_2(k, \cdot)] = w(k), \\ W[a_1(k)\psi_1(k, \cdot) + b_1(k)\psi_2(k, \cdot), a_1(-k)\psi_1(-k, \cdot) + b_1(-k)\psi_2(-k, \cdot)] \\ = W[a_1(k)\psi_1(k, \cdot) + b_1(k)\psi_2(k, \cdot), a_1(-k)\psi_2(k, \cdot) + b_1(-k)\psi_1(k, \cdot)] \\ = \{a_1(k)a_1(-k) - b_1(k)b_1(-k)\}w(k), \end{cases} \end{aligned}$$

so that

$$a_1(k)a_1(-k) - b_1(k)b_1(-k) = 1, \quad k \in \mathbb{R}.$$

Similarly, for  $k \in \mathbb{R}$  we have

$$\begin{aligned} & W[f_2(k, \cdot), f_2(-k, \cdot)] \\ &= \begin{cases} W[\psi_2(k, \cdot), \psi_2(-k, \cdot)] = W[\psi_2(k, \cdot), \psi_1(k, \cdot)] = -w(k), \\ W[a_2(k)\psi_2(k, \cdot) + b_2(k)\psi_1(k, \cdot), a_2(-k)\psi_2(-k, \cdot) + b_2(-k)\psi_1(-k, \cdot)] \\ = W[a_2(k)\psi_2(k, \cdot) + b_2(k)\psi_1(k, \cdot), a_2(-k)\psi_1(k, \cdot) + b_2(-k)\psi_2(k, \cdot)] \\ = -\{a_2(k)a_2(-k) - b_2(k)b_2(-k)\}w(k), \end{cases} \end{aligned}$$

so that

$$a_2(k)a_2(-k) - b_2(k)b_2(-k) = 1, \quad k \in \mathbb{R}.$$

Analogously, for  $k \in \mathbb{R}$  we have

$$\begin{aligned} & W[f_1(k, \cdot), f_2(-k, \cdot)] \\ &= \begin{cases} W[\psi_1(k, \cdot), a_2(-k)\psi_2(-k, \cdot) + b_2(-k)\psi_1(-k, \cdot)] \\ W[\psi_1(k, \cdot), a_2(-k)\psi_1(k, \cdot) + b_2(-k)\psi_2(k, \cdot)] = b_2(-k)w(k), \\ W[a_1(k)\psi_1(k, \cdot) + b_1(k)\psi_2(k, \cdot), \psi_2(-k, \cdot)] \\ = W[a_1(k)\psi_1(k, \cdot) + b_1(k)\psi_2(k, \cdot), \psi_1(k, \cdot)] = -b_1(k)w(k), \end{cases} \end{aligned}$$

so that

$$b_2(-k) = -b_1(k), \quad k \in \mathbb{R}.$$

For  $k \in \mathbb{R}$  we now write  $b(k) \stackrel{\text{def}}{=} b_1(k) = -b_2(-k)$ . We do not define  $b(k)$  off the real line. Using (2.5.12) and (2.5.6) for  $k \in \mathbb{R}$  we get for  $k \in \mathbb{R}$

$$\overline{b(-k)w(-k)} = -W[\overline{f_1(-k, x)}, \overline{f_2(-k, x)}] = b(-k)w(-k),$$

which yields

$$b(-k) = \overline{b(k)}, \quad k \in \mathbb{R}. \quad (2.5.15)$$

Observe that  $w(k)b(k)$  is continuous in  $k \in \mathbb{R}$ .<sup>6</sup>

Let us consider coefficients  $d_{ij}(k)$  ( $i, j = 1, 2$ ) such that

$$f_1(-k, x) = d_{11}(k)f_1(k, x) + d_{12}(k)f_2(k, x), \quad (2.5.16a)$$

$$f_2(-k, x) = d_{21}(k)f_1(k, x) + d_{22}(k)f_2(k, x). \quad (2.5.16b)$$

Writing asymptotic expressions  $x \rightarrow \pm\infty$  we get

$$\begin{aligned} \psi_1(-k, x) &= d_{11}(k)\psi_1(k, x) + d_{12}(k)[-b(-k)\psi_1(k, x) + a(k)\psi_2(k, x)], \\ a(-k)\psi_1(-k, x) + b(-k)\psi_2(-k, x) &= d_{11}(k)[a(k)\psi_1(k, x) + b(k)\psi_2(k, x)] \\ &\quad + d_{12}(k)\psi_2(k, x), \\ -b(k)\psi_1(-k, x) + a(-k)\psi_2(-k, x) &= d_{21}(k)\psi_1(k, x) \\ &\quad + d_{22}(k)[-b(-k)\psi_1(k, x) + a(k)\psi_2(k, x)], \\ \psi_2(-k, x) &= d_{21}(k)[a(k)\psi_1(k, x) + b(k)\psi_2(k, x)] + d_{22}(k)\psi_2(k, x). \end{aligned}$$

Using that  $\psi_{1,2}(-k, x) = \psi_{2,1}(k, x)$  and using the linear independence of the Floquet solutions to equate coefficients of  $\psi_1(k, x)$  and  $\psi_2(k, x)$  we get

$$\begin{aligned} 0 &= d_{11}(k) - d_{12}(k)b(-k), & 1 &= d_{12}(k)a(k), \\ b(-k) &= d_{11}(k)a(k), & a(-k) &= d_{11}(k)b(k) + d_{12}(k), \\ a(-k) &= d_{21}(k) - d_{22}(k)b(-k), & -b(k) &= d_{22}(k)a(k), \\ 1 &= d_{21}(k)a(k), & 0 &= d_{21}(k)b(k) + d_{22}(k). \end{aligned}$$

Therefore,

$$\begin{pmatrix} d_{11}(k) & d_{12}(k) \\ d_{21}(k) & d_{22}(k) \end{pmatrix} = \frac{1}{a(k)} \begin{pmatrix} b(-k) & 1 \\ 1 & -b(k) \end{pmatrix}, \quad k \in \mathbb{R}.$$

We now define the *transmission coefficient*  $T(k)$ , the *reflection coefficient from the right*  $R(k)$ , and the *reflection coefficient from the left*  $L(k)$  by

$$\begin{cases} T(k) = d_{12}(k) = d_{21}(k) = \frac{1}{a(k)}, \\ R(k) = -d_{11}(k) = -\frac{b(-k)}{a(k)}, & L(k) = -d_{22}(k) = \frac{b(k)}{a(k)}, \end{cases} \quad (2.5.17)$$

where  $k \in \mathbb{R}$ . Then (2.5.14) and (2.5.15) imply that the *scattering matrix*

$$S(k) = \begin{pmatrix} T(k) & R(k) \\ L(k) & T(k) \end{pmatrix}, \quad k \in \mathbb{R}, \quad (2.5.18)$$

---

<sup>6</sup>Since  $w(k)$  may vanish at certain  $k = m\pi$ , we cannot be sure if  $a(k)$  and  $b(k)$  are continuous in  $k$  at these points in  $\overline{\mathbb{C}^+}$ .

is unitary. Obviously, the scattering matrix is continuous in  $k \in \mathbb{R} \setminus \{l\pi : l \in \mathbb{Z}\}$ .<sup>7</sup> All of this leads to the Riemann-Hilbert problem

$$\begin{pmatrix} f_1(-k, x) \\ f_2(-k, x) \end{pmatrix} = JS(k)J \begin{pmatrix} f_2(k, x) \\ f_1(k, x) \end{pmatrix}, \quad k \in \mathbb{R}, \quad (2.5.19)$$

where  $J = \text{diag}(1, -1)$ . From (2.5.14), (2.5.15), and (2.5.17) we get for  $k \in \mathbb{R}$

$$T(-k) = \overline{T(k)}, \quad R(-k) = \overline{R(k)}, \quad L(-k) = \overline{L(k)}. \quad (2.5.20)$$

We also get for  $k \in \mathbb{R}$

$$\begin{aligned} \begin{pmatrix} f_1(-k, x) \\ f_2(-k, x) \end{pmatrix} &= JS(k)J \begin{pmatrix} f_2(k, x) \\ f_1(k, x) \end{pmatrix} = JS(k)J \begin{pmatrix} 0 & 1 \\ 1 & 0 \end{pmatrix} \begin{pmatrix} f_1(k, x) \\ f_2(k, x) \end{pmatrix} \\ &= JS(k)J \begin{pmatrix} 0 & 1 \\ 1 & 0 \end{pmatrix} JS(-k)J \begin{pmatrix} f_2(-k, x) \\ f_1(-k, x) \end{pmatrix} \\ &= JS(k)J \begin{pmatrix} 0 & 1 \\ 1 & 0 \end{pmatrix} JS(-k)J \begin{pmatrix} 0 & 1 \\ 1 & 0 \end{pmatrix} \begin{pmatrix} f_1(-k, x) \\ f_2(-k, x) \end{pmatrix}, \end{aligned}$$

so that

$$\begin{aligned} S(k)^{-1} &= J \begin{pmatrix} 0 & 1 \\ 1 & 0 \end{pmatrix} JS(-k)J \begin{pmatrix} 0 & 1 \\ 1 & 0 \end{pmatrix} J \\ &= \begin{pmatrix} T(-k) & L(-k) \\ R(-k) & T(-k) \end{pmatrix} = \begin{pmatrix} \overline{T(k)} & \overline{L(k)} \\ \overline{R(k)} & \overline{T(k)} \end{pmatrix} = S(k)^\dagger, \end{aligned}$$

where the dagger denotes the conjugate transpose and  $J = \text{diag}(1, -1)$ . Consequently,  $S(k)$  is a unitary matrix for  $k \in \mathbb{R}$ . In combination with (2.5.17) we get for  $k \in \mathbb{R}$  the crucial relation

$$|a(k)|^2 - |b(k)|^2 = 1, \quad k \in \mathbb{R}, \quad (2.5.21)$$

which implies that  $a(k) \neq 0$  for  $k \in \mathbb{R}$ . This crucial relation (2.5.21) also implies that  $f_1(k, x)$  and  $f_2(k, x)$  are linearly independent whenever  $\psi_1(k, x)$  and  $\psi_2(k, x)$  are linearly independent, i.e., whenever  $k$  is not an integer multiple  $m\pi$  of  $\pi$  (i.e., whenever  $\eta$  is not the endpoint of a band) and whenever the generic case occurs at  $m\pi$ . The linear independence of the two Floquet solutions is described by Floquet's Theorem 2.1.1 in an alternative way.

In the case of the Schrödinger equation on the line it is well-known how to recover  $S(k)$  [and hence  $a(k)$  and  $b(k)$ ] uniquely from one reflection coefficient and the finitely many, necessarily positive imaginary and simple, poles of the transmission coefficient [31]. This procedure can in principle be generalized

---

<sup>7</sup> $S(k)$  is continuous in  $k = m\pi$  if the generic case occurs in  $k = m\pi$ .

using a result by Firsova [35] on the asymptotics of the poles of  $T(k)$  in the band gaps (derived if  $n(x) \equiv 1$ ). If  $n(x) \equiv 1$ ,  $\varepsilon(x) \equiv 0$ , we have infinitely many such poles (unless there are only finitely many band gaps).

Let us now compute the relevant scattering data in an elementary case.

**Example 2.5.2** Let the periodic part of the Helmholtz equation be as in Example 2.3.2 (i.e.,  $n(x) \equiv 1$ ) and let  $n(x) = 1 + \varepsilon$  for  $x \in (0, p)$ , where  $\varepsilon > -1$  is a nonzero constant. Working in the  $k$ -image of the physical sheet (i.e., taking  $\text{Im } k \geq 0$  with  $\eta = k^2$ ), the Floquet solutions are given by

$$\psi_1(k, x) = e^{ikx}, \quad \psi_2(k, x) = e^{-ikx},$$

while  $m_1(\eta) = ik$ ,  $m_2(\eta) = -ik$ , and  $w(k) = -2ik$ . Then the general solution for  $x \in (0, p)$  is given by

$$\psi(k, x) = d_1 \cos(kx\sqrt{1+\varepsilon}) + d_2 \frac{\sin(kx\sqrt{1+\varepsilon})}{k\sqrt{1+\varepsilon}}.$$

In order to allow  $\psi(k, x)$  to coincide with either Jost solution  $f_{1,2}(k, x)$ , we have the contingency relations

$$\begin{aligned} f_1(k, p) &= \psi_1(k, p), & f_2'(k, p) &= \psi_1'(k, p), \\ f_2(k, 0) &= \psi_2(k, 0), & f_1'(k, 0) &= \psi_2'(k, 0). \end{aligned}$$

Then for  $j = 1, 2$  we have

$$f_j(k, x) = d_1^{(j)} \cos(kx\sqrt{1+\varepsilon}) + d_2^{(j)} \frac{\sin(kx\sqrt{1+\varepsilon})}{k\sqrt{1+\varepsilon}},$$

where  $d_1^{(2)} = \psi_2(k, 0) = 1$ ,  $d_2^{(2)} = \psi_2'(k, 0) = -ik$ , and

$$\begin{pmatrix} \cos(kp\sqrt{1+\varepsilon}) & \frac{\sin(kp\sqrt{1+\varepsilon})}{k\sqrt{1+\varepsilon}} \\ -k\sqrt{1+\varepsilon} \sin(kp\sqrt{1+\varepsilon}) & \cos(kp\sqrt{1+\varepsilon}) \end{pmatrix} \begin{pmatrix} d_1^{(1)} \\ d_2^{(1)} \end{pmatrix} = e^{ikp} \begin{pmatrix} 1 \\ ik \end{pmatrix}.$$

Therefore, for  $x \in (0, p)$  we have the Jost solutions

$$\begin{aligned} f_1(k, x) &= e^{ikp} \left[ \cos(k(p-x)\sqrt{1+\varepsilon}) - i \frac{\sin(k(p-x)\sqrt{1+\varepsilon})}{\sqrt{1+\varepsilon}} \right], \\ f_2(k, x) &= \cos(kx\sqrt{1+\varepsilon}) - i \frac{\sin(kx\sqrt{1+\varepsilon})}{\sqrt{1+\varepsilon}}. \end{aligned}$$

Now (2.5.13) yields for  $k \in \mathbb{R}$

$$\begin{aligned} \begin{pmatrix} f_1(k, 0) \\ f_1'(k, 0) \end{pmatrix} &= \begin{pmatrix} \psi_1(k, 0) & \psi_2(k, 0) \\ \psi_1'(k, 0) & \psi_2'(k, 0) \end{pmatrix} \begin{pmatrix} a(k) \\ b(k) \end{pmatrix}, \\ \begin{pmatrix} f_2(k, p) \\ f_2'(k, p) \end{pmatrix} &= \begin{pmatrix} \psi_1(k, p) & \psi_2(k, p) \\ \psi_1'(k, p) & \psi_2'(k, p) \end{pmatrix} \begin{pmatrix} -\overline{b(k)} \\ a(k) \end{pmatrix}. \end{aligned}$$

Consequently,

$$\begin{aligned} a(k) &= e^{ikp} \left[ \cos(kp\sqrt{1+\varepsilon}) - i\zeta_+(\varepsilon) \sin(kp\sqrt{1+\varepsilon}) \right], \\ b(k) &= e^{ikp} \left[ i\zeta_-(\varepsilon) \sin(kp\sqrt{1+\varepsilon}) \right], \end{aligned}$$

where

$$\zeta_{\pm}(\varepsilon) = \frac{1}{2} \left[ \sqrt{1+\varepsilon} \pm \frac{1}{\sqrt{1+\varepsilon}} \right].$$

## 2.6 Evaluation of the Impurity Period Map

In this section we indicate how the period map of the periodic plus impurity problem can be recovered from the scattering coefficients  $a(k)$  and  $b(k)$ . We shall work it out for the piecewise constant case of Example 2.3.3, but the reduction can be applied in general.

Let the impurity be concentrated in the period  $(0, p]$  and let us refer to the rest of the crystal by the term *bulk*. Assuming the period  $(0, p]$  and the bulk to be piecewise constant, we define

$$n(x)\sqrt{[1+\varepsilon(x)]} = \begin{cases} \tilde{n}_j, & \tilde{b}_{j-1} < x \leq \tilde{b}_j, \quad j = 1, \dots, l, \\ n(x), & x \notin [0, p], \end{cases}$$

where  $0 = \tilde{b}_0 < \tilde{b}_1 < \dots < \tilde{b}_l = p$  and  $n(x)$  is as in the Example 2.3.3.

Now let us define  $M_i(\eta)$  as the matrix  $M(\eta)$  of Example 2.3.3, but with  $n_j$  replaced by  $\tilde{n}_j$  ( $j = 1, \dots, l$ ).<sup>8</sup> Then outside the interval  $[0, p]$  the Jost solutions can be expressed in the Floquet solutions as follows [cf. (2.5.13)]:

$$\begin{aligned} f_1(k, x) &= \begin{cases} \psi_1(k, x), & x \geq p, \\ a(k)\psi_1(k, x) + b(k)\psi_2(k, x), & x \leq 0, \end{cases} \\ f_2(k, x) &= \begin{cases} -\overline{b(k)}\psi_1(k, x) + a(k)\psi_2(k, x), & x \geq p, \\ \psi_2(k, x), & x \leq 0. \end{cases} \end{aligned}$$

---

<sup>8</sup>We could just consider any periodic and periodic-plus-impurity problem, because we only need to work with the period maps  $M(\eta)$  and  $M_i(\eta)$ .

Putting

$$W(k, x) \stackrel{\text{def}}{=} \begin{pmatrix} \psi_1(k, x) & \psi_2(k, x) \\ \psi'_1(k, x) & \psi'_2(k, x) \end{pmatrix}, \quad (2.6.1)$$

we obtain

$$\begin{aligned} W(k, 0) \begin{pmatrix} a(k) \\ b(k) \end{pmatrix} &= \begin{pmatrix} f_1(k, 0) \\ f'_1(k, 0) \end{pmatrix} = M_i(\eta)^{-1} \begin{pmatrix} f_1(k, p) \\ f'_1(k, p) \end{pmatrix} \\ &= M_i(\eta)^{-1} \begin{pmatrix} \psi_1(k, p) \\ \psi'_1(k, p) \end{pmatrix} = M_i(\eta)^{-1} M(\eta) \begin{pmatrix} \psi_1(k, 0) \\ \psi'_1(k, 0) \end{pmatrix} \end{aligned}$$

and

$$\begin{aligned} W(k, 0) \begin{pmatrix} -\overline{b(k)} \\ a(k) \end{pmatrix} &= M(\eta)^{-1} W(k, p) \begin{pmatrix} -\overline{b(k)} \\ a(k) \end{pmatrix} = M(\eta)^{-1} \begin{pmatrix} f_2(k, p) \\ f'_2(k, p) \end{pmatrix} \\ &= M(\eta)^{-1} M_i(\eta) \begin{pmatrix} f_2(k, 0) \\ f'_2(k, 0) \end{pmatrix} = M(\eta)^{-1} M_i(\eta) \begin{pmatrix} \psi_2(k, 0) \\ \psi'_2(k, 0) \end{pmatrix}. \end{aligned}$$

As a result of  $w(k) = m_2(\eta) - m_1(\eta)$ ,  $\psi_1(k, 0) = \psi_2(k, 0) = 1$ ,  $\psi'_1(k, 0) = m_1(\eta)$ , and  $\psi'_2(k, 0) = m_2(\eta)$  we get

$$\begin{pmatrix} a(k) \\ b(k) \end{pmatrix} = \frac{1}{w(k)} \begin{pmatrix} m_2(\eta) & -1 \\ -m_1(\eta) & 1 \end{pmatrix} M_i(\eta)^{-1} M(\eta) \begin{pmatrix} 1 \\ m_1(\eta) \end{pmatrix}, \quad (2.6.2a)$$

$$\begin{pmatrix} -\overline{b(k)} \\ a(k) \end{pmatrix} = \frac{1}{w(k)} \begin{pmatrix} m_2(\eta) & -1 \\ -m_1(\eta) & 1 \end{pmatrix} M_i(\eta) M(\eta)^{-1} \begin{pmatrix} 1 \\ m_2(\eta) \end{pmatrix}. \quad (2.6.2b)$$

Equations (2.6.2) allow one to compute the period map  $M_i(\eta)$  of the periodic plus impurity problem if the impurity is concentrated in one period, the periodic data are known, and  $a(k)$  and  $b(k)$  are known. The latter scattering data can easily be compute from one reflection coefficient and the transmission coefficient by using (2.5.17) and (2.5.21).

More generally, let the impurity be concentrated in  $[-Mp, Np]$ , where  $M$  is a nonnegative integer and  $N$  a positive integer. Then  $f_1(k, x) = \psi_1(k, x)$  for  $x \geq Np$  and  $f_2(k, x) = \psi_2(k, x)$  for  $x \leq -Mp$ . Now let  $M_{i+}(\eta)$  be the period map of the periodic plus impurity problem for computing solutions at  $x = Np$  from those at  $x = 0$ , and let  $M_{i-}(\eta)$  be the period map of the periodic plus impurity problem to compute solutions at  $x = 0$  from those at  $x = -Mp$ . Then

$$\begin{aligned} W(k, 0) \begin{pmatrix} a(k) \\ b(k) \end{pmatrix} &= \begin{pmatrix} f_1(k, 0) \\ f'_1(k, 0) \end{pmatrix} = M_{i+}(\eta)^{-1} \begin{pmatrix} f_1(k, Np) \\ f'_1(k, Np) \end{pmatrix} \\ &= M_{i+}(\eta)^{-1} \begin{pmatrix} \psi_1(k, Np) \\ \psi'_1(k, Np) \end{pmatrix} = M_{i+}(\eta)^{-1} M(\eta)^N \begin{pmatrix} \psi_1(k, 0) \\ \psi'_1(k, 0) \end{pmatrix} \end{aligned}$$

and

$$\begin{aligned}
W(k, 0) \begin{pmatrix} -\overline{b(k)} \\ a(k) \end{pmatrix} &= M(\eta)^{-N} W(k, Np) \begin{pmatrix} -\overline{b(k)} \\ a(k) \end{pmatrix} = M(\eta)^{-N} \begin{pmatrix} f_2(k, Np) \\ f_2'(k, Np) \end{pmatrix} \\
&= M(\eta)^{-N} M_{i+}(\eta) M_{i-}(\eta) \begin{pmatrix} f_2(k, -Mp) \\ f_2'(k, -Mp) \end{pmatrix} \\
&= M(\eta)^{-N} M_{i+}(\eta) M_{i-}(\eta) \begin{pmatrix} \psi_2(k, -Mp) \\ \psi_2'(k, -Mp) \end{pmatrix} \\
&= M(\eta)^{-N} M_{i+}(\eta) M_{i-}(\eta) M(\eta)^{-M} \begin{pmatrix} \psi_2(k, 0) \\ \psi_2'(k, 0) \end{pmatrix}.
\end{aligned}$$

Instead of (2.6.2) we now get

$$\begin{pmatrix} a(k) \\ b(k) \end{pmatrix} = \frac{1}{w(k)} \begin{pmatrix} m_2(\eta) & -1 \\ -m_1(\eta) & 1 \end{pmatrix} M_{i+}(\eta)^{-1} M(\eta)^N \begin{pmatrix} 1 \\ m_1(\eta) \end{pmatrix}, \quad (2.6.3a)$$

$$\begin{pmatrix} -\overline{b(k)} \\ a(k) \end{pmatrix} = \frac{1}{w(k)} \begin{pmatrix} m_2(\eta) & -1 \\ -m_1(\eta) & 1 \end{pmatrix} M(\eta)^{-N} M_{i+}(\eta) M_{i-}(\eta) M(\eta)^{-M} \begin{pmatrix} 1 \\ m_2(\eta) \end{pmatrix}. \quad (2.6.3b)$$

Equations (2.6.3) allow one to compute the period maps  $M_{i+}(\eta)$  and  $M_{i-}(\eta)$  of the periodic plus impurity problem if the impurity is concentrated in finitely many (known) periods, the periodic data are known, and  $a(k)$  and  $b(k)$  are known. The latter scattering data can easily be compute from one reflection coefficient and the transmission coefficient by using (2.5.17) and (2.5.21).

Let us write  $N(\eta) = M_i(\eta)^{-1} M(\eta)$  as in (2.6.2a). Then

$$\begin{aligned}
a(\eta) &= \frac{1}{w(\eta)} \left( [m_2(\eta) + m_1(\eta)] \frac{1}{2} [N_{11}(\eta) - N_{22}(\eta)] - N_{21}(\eta) \right. \\
&\quad \left. + m_2(\eta) m_1(\eta) N_{12}(\eta) + [m_2(\eta) - m_1(\eta)] \frac{1}{2} [N_{11}(\eta) + N_{22}(\eta)] \right). \quad (2.6.4)
\end{aligned}$$

Now for  $\Delta(\eta) \notin [-2, 2]$  we have

$$\begin{aligned}
w(\eta) &= m_2(\eta) - m_1(\eta) = \frac{\tau_2(\eta) - \tau_1(\eta)}{\varphi(\eta, p)}, \\
m_2(\eta) + m_1(\eta) &= \frac{\Delta(\eta) - 2\theta(\eta, p)}{\varphi(\eta, p)} = \frac{\varphi'(\eta, p) - \theta(\eta, p)}{\varphi(\eta, p)}, \\
m_2(\eta) m_1(\eta) &= \frac{\tau_2(\eta) \tau_1(\eta) - [\tau_2(\eta) + \tau_1(\eta)] \theta(\eta, p) + \theta(\eta, p)^2}{\varphi(\eta, p)^2} \\
&= \frac{1 - [\theta(\eta, p) + \varphi'(\eta, p)] \theta(\eta, p) + \theta(\eta, p)^2}{\varphi(\eta, p)^2} = -\frac{\theta'(\eta, p)}{\varphi(\eta, p)}.
\end{aligned}$$

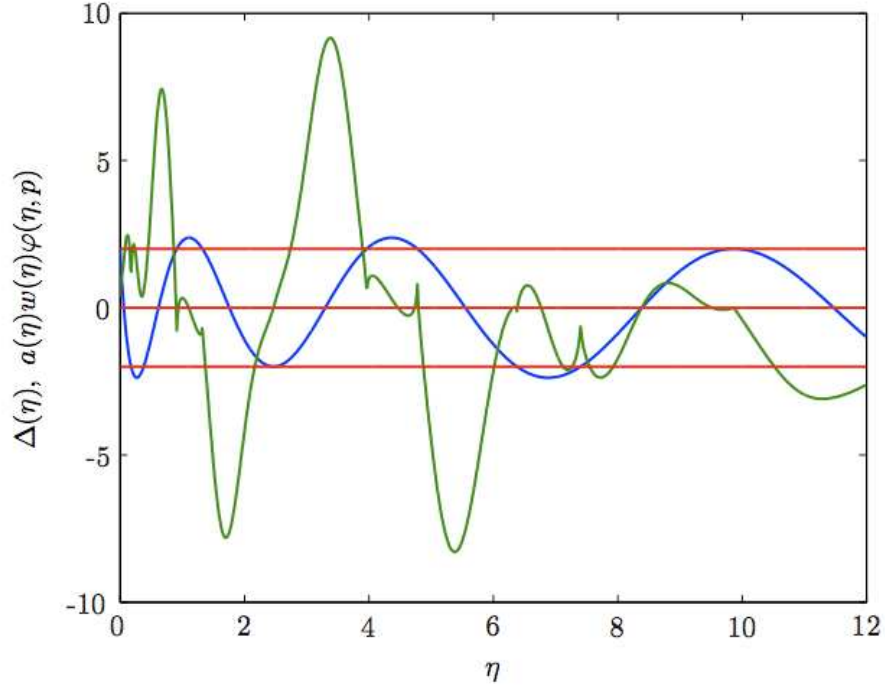


**Figure 2.7:** In this figure the function  $\Delta(\eta)$  is drawn in blue, whereas  $a(\eta)w(\eta)\varphi(\eta, p)$  is in green. The system considered is a two-layer photonic crystal with  $n_1 = 1, n_2 = 2, a_1 = 2, a_2 = 2$  and  $\Delta(\eta)$  has been computed using Eq. (2.3.25). The impurity is thought concentrated in one period of length  $p = 4$  whose optical properties are parametrized by  $n_1^{imp} = 2, n_2^{imp} = 1, a_1^{imp} = 3$  and  $a_2^{imp} = 0.9$ , while  $a(\eta)w(\eta)\varphi(\eta, p)$  has been calculated by making use of Eq. (2.6.5).

Consequently,

$$\begin{aligned}
 a(\eta)w(\eta)\varphi(\eta, p) &= \frac{1}{2}[N_{11}(\eta) + N_{22}(\eta)]w(\eta)\varphi(\eta, p) - N_{21}(\eta)\varphi(\eta, p) \\
 &\quad + \frac{1}{2}[N_{11}(\eta) - N_{22}(\eta)][\varphi'(\eta, p) - \theta(\eta, p)] - N_{12}(\eta)\theta'(\eta, p),
 \end{aligned}
 \tag{2.6.5}$$

where  $w(\eta)\varphi(\eta, p) = \tau_2(\eta) - \tau_1(\eta)$  has the bands as branch cuts and all other terms on the right-hand side are analytic in  $\eta \in \mathbb{C}$ . Letting  $\eta \rightarrow \ell \pm i0$  for  $\Delta(\ell) \in (-2, 2)$  we get the quasimomentum limit  $k(\eta) \rightarrow \pm\kappa(\ell)$  with  $\kappa(\ell) > 0$

and hence

$$\begin{aligned} \lim_{\eta \rightarrow \ell \pm i0} a(\eta) &= \frac{1}{2}[N_{11}(\ell) + N_{22}(\ell)] \pm \frac{i}{2 \sin(q\kappa(\ell))} \times \\ &\times \left( \frac{1}{2}[N_{11}(\ell) - N_{22}(\ell)][\varphi'(\ell, p) - \theta(\ell, p)] - N_{21}(\ell)\varphi(\ell, p) - N_{12}(\ell)\theta'(\ell, p) \right). \end{aligned} \tag{2.6.6}$$

In the same way, writing  $\tilde{N}(\eta) = M_i(\eta)M(\eta)^{-1}$  and using that this matrix is the cofactor matrix of  $N(\eta)$ , we get (2.6.4) from (2.6.3b).



# Chapter 3

## Inverse Problem for 1D Photonic Crystals

In this chapter we discuss the inverse problem of recovering the refractive index of a 1D photonic crystal from its period map. The solution of this problem allows one to compute the index of refraction  $n(x)$  in the Helmholtz equation

$$-\psi''(\eta, x) = \eta n(x)^2 \psi(\eta, x) \quad (3.0.1)$$

from the period map of one period. For photonic crystals where the impurity is confined to finitely many periods, the solution of this problem allows one to compute a refractive index of the form

$$n(x) = n_0(x) \sqrt{1 + \varepsilon(x)}, \quad (3.0.2)$$

where  $n_0(x)$  is a positive and piecewise continuous function of period  $p$  and  $\varepsilon(x)$  is a piecewise continuous function of compact support satisfying  $\varepsilon(x) > -1$ , from the period map of an interval containing the impurities.

Inversion based on the period map is a difficult problem which does not always have a (unique) solution  $n(x)$ . We present an incomplete solution to this problem which may nevertheless be of practical value. In Subsection 3.1 we indicate how to extract various type of spectral information from the period map. In Subsection 3.2 we convert, for sufficiently smooth  $n(x)$ , the Helmholtz equation 3.0.1 in the position variable  $x$  in the Schrödinger equation in the travel time parameter  $y(x) = \int_0^x dz n(z)$  and compare the two period maps. In subsection 3.3 we discuss various aspects of computing the refractive index from the period map using the travel time parameter. In the final subsection 3.4 we determine  $n(x)$  from the period map in the special case of a piecewise constant refractive index.

### 3.1 Reviewing various inverse problems

The prototypical inverse problem is to compute a periodic refractive index  $n(x)$  from the period map

$$M(\eta) = \begin{pmatrix} \theta(\eta, p) & \varphi(\eta, p) \\ \theta'(\eta, x) & \varphi'(\eta, p) \end{pmatrix}. \quad (3.1.1)$$

This is an inversion problem for the Helmholtz equation on the finite interval  $[0, p]$ . Its solution can be used alternatively to compute a periodic refractive index  $n_0(x)$  from the period map or a refractive index  $n(x)$  as in (3.0.2) from the period map on an interval containing an integer number of periods which contains the impurities (i.e., from the period map on an interval  $J$  of length an integer multiple of  $p$  such that  $\varepsilon = 0$  for  $x \notin J$ ). In Section 2.6 we have explained how to compute the second type of period map from the scattering matrix of an impure 1-D photonic crystal if the impurities are concentrated in a finite number of periods.

The period map (3.1.1) contains a wealth of spectral data on the Helmholtz equation (2.1.1). For instance, letting  $\alpha$  and  $\beta$  be real constants, the zeros  $\eta$  of the scalar function

$$(\cos \beta \quad \sin \beta) M(\eta) \begin{pmatrix} \sin \alpha \\ \cos \alpha \end{pmatrix} = 0 \quad (3.1.2)$$

yield the eigenvalues of the Helmholtz equation (3.0.1) under the mixed boundary conditions

$$(\cos \alpha)\psi(\eta, 0) - (\sin \alpha)\psi'(\eta, 0) = 0, \quad (3.1.3a)$$

$$(\cos \beta)\psi(\eta, p) + (\sin \beta)\psi'(\eta, p) = 0. \quad (3.1.3b)$$

This is easily understood by considering the Helmholtz solution

$$\psi(\eta, x) = (\sin \alpha)\theta(\eta, x) + (\cos \alpha)\varphi(\eta, x),$$

which satisfies  $\psi(\eta, 0) = \sin \alpha$  and  $\psi'(\eta, 0) = \cos \alpha$ . Then  $\psi(\eta, x)$  obviously satisfies (3.1.3a), while

$$(\cos \beta)\psi(\eta, p) + (\sin \beta)\psi'(\eta, p) = (\cos \beta \quad \sin \beta) M(\eta) \begin{pmatrix} \sin \alpha \\ \cos \alpha \end{pmatrix}.$$

Consequently,  $\eta$  is a Helmholtz eigenvalue under the mixed boundary conditions (3.1.3) if and only if (3.1.2) is true. We now get as corollaries the following statements:

- a. The Dirichlet eigenvalues ( $\alpha = \beta = 0$ ) are the zeros of the equation  $\varphi(\eta, p) = 0$ .

- b. The Neumann eigenvalues ( $\alpha = \beta = (\pi/2)$ ) are the zeros of the equation  $\theta'(\eta, p) = 0$ .
- c. The Dirichlet-Neumann eigenvalues, i.e., the eigenvalues under the boundary conditions ( $\alpha = 0, \beta = (\pi/2)$ )

$$\psi(\eta, 0) = 0, \quad \psi'(\eta, p) = 0,$$

are the zeros of the equation  $\varphi'(\eta, p) = 0$ .

- d. The Neumann-Dirichlet eigenvalues, i.e., the eigenvalues under the boundary conditions ( $\alpha = (\pi/2), \beta = 0$ )

$$\psi'(\eta, 0) = 0, \quad \psi(\eta, p) = 0,$$

are the zeros of the equation  $\theta(\eta, p) = 0$ .

Apart from the eigenvalues under any pair of mixed boundary conditions, the period map also yields the eigenvalues under the  $\tau$ -periodic boundary conditions

$$\psi(\eta, p) = \tau\psi(\eta, 0), \quad \psi'(\eta, p) = \tau\psi'(\eta, 0), \quad (3.1.4)$$

where  $\tau$  is a complex constant of modulus 1. In fact, introducing the Hill discriminant

$$\Delta(\eta) = \theta(\eta, p) + \varphi'(\eta, p),$$

the eigenvalues under the  $\tau$ -periodic boundary conditions (3.1.4) are the zeros of the equation

$$\Delta(\eta) = \tau + \tau^{-1}.$$

In particular, the eigenvalues under periodic boundary conditions are the zeros of the equation  $\Delta(\eta) = 2$ , while the eigenvalues under antiperiodic boundary conditions are the zeros of the equation  $\Delta(\eta) = -2$ . Allowing  $\tau$  to vary over the unit circle, the eigenvalues under the  $\tau$ -periodic conditions (3.1.4) together make up the (allowed) energy bands.

In spite of the wealth of spectral information that we can extract from the period map, the inverse problem of computing the refractive index from the period map does not have a straightforward solution. The situation is drastically different for Hill's equation

$$-\psi''(\eta, x) + Q(x)\psi(\eta, x) = \eta\psi(\eta, x), \quad 0 \leq x \leq p, \quad (3.1.5)$$

where  $Q(x)$  is a real function in  $L^2_{\text{loc}}(0, p)$ . As early as 1929, Ambarzumian [36] has proved that  $Q(x) \equiv 0$  and  $p = \pi/\sqrt{c}$  whenever the Neumann eigenvalues of (3.1.6) are given by  $\eta_n = cn^2$  ( $n = 0, 1, 2, \dots$ ). Borg [37, 38] proved that it is possible to find a unique real potential  $Q(x)$  and unique

mixed boundary conditions from the eigenvalues under two sets of boundary conditions, provided the boundary conditions in one endpoint are the same. Unfortunately, Borg did not provide an algorithm for computing  $Q(x)$ . Such an algorithm has been given by Marchenko [39] and, in simplified form, by Trubowitz [40]. Marchenko and Ostrovski [33] have given an algorithm to compute the periodic Schrödinger potential from the energy bands plus either the Dirichlet or the Neumann spectrum. None of these results can be derived in a similar way for the Helmholtz equation (2.1.1).

Let us now indicate how to retrieve the period  $p$  from the period map. The fundamental matrix

$$\Phi(\eta, x) = \begin{pmatrix} \theta(\eta, x) & \varphi(\eta, x) \\ \theta'(\eta, x) & \varphi'(\eta, x) \end{pmatrix}$$

is the unique  $2 \times 2$  matrix solution of the linear system

$$\Phi'(\eta, x) = \begin{pmatrix} 0 & 1 \\ -\eta n(x)^2 & 0 \end{pmatrix} \Phi(\eta, x), \quad \Phi(\eta, 0) = I_2, \quad (3.1.6)$$

where the period map is given by

$$M(\eta) = \Phi(\eta, p). \quad (3.1.7)$$

Since the fundamental matrix  $\Phi(\eta, x)$  is an entire matrix function in  $\eta$ , we can expand it into an absolutely convergent power series as follows:

$$\Phi(\eta, x) = \sum_{j=0}^{\infty} \eta^j \Phi_j(x), \quad (3.1.8)$$

where for  $j = 1, 2, 3, \dots$

$$\Phi'_0(x) = \begin{pmatrix} 0 & 1 \\ 0 & 0 \end{pmatrix}, \quad \Phi_0(0) = I_2, \quad (3.1.9a)$$

$$\Phi'_j(x) = \begin{pmatrix} 0 & 1 \\ 0 & 0 \end{pmatrix} \Phi_j(x) - n(x)^2 \begin{pmatrix} 0 & 0 \\ 1 & 0 \end{pmatrix} \Phi_{j-1}(x), \quad \Phi_j(0) = 0_{2 \times 2}. \quad (3.1.9b)$$

Then

$$\Phi_0(x) = \begin{pmatrix} 1 & x \\ 0 & 1 \end{pmatrix}, \quad (3.1.10a)$$

$$\begin{aligned} \Phi_j(x) &= - \int_0^x n(\hat{x})^2 \begin{pmatrix} 1 & x - \hat{x} \\ 0 & 1 \end{pmatrix} \begin{pmatrix} 0 & 0 \\ 1 & 0 \end{pmatrix} \Phi_{j-1}(\hat{x}) d\hat{x} \\ &= - \int_0^x n(\hat{x})^2 \begin{pmatrix} x - \hat{x} & 0 \\ 1 & 0 \end{pmatrix} \Phi_{j-1}(\hat{x}) d\hat{x}, \end{aligned} \quad (3.1.10b)$$

where  $j = 1, 2, 3, \dots$ . Consequently,

$$M(\eta) = \begin{pmatrix} 1 & p \\ 0 & 1 \end{pmatrix} + O(\eta), \quad \eta \rightarrow 0,$$

and hence

$$p = \left[ \frac{d}{d\eta} M_{12}(\eta) \right]_{\eta=0}. \quad (3.1.11)$$

Equation (3.1.11) allows us to obtain the period  $p$  from the period map.

## 3.2 Conversion to Travel Time

Consider the differential equation (2.1.1)

$$-\psi''(\eta, x) = \eta n(x)^2 \psi(\eta, x),$$

where  $n(x) > 0$  is a real piecewise continuous periodic function of period  $p$  and bounded away from zero. We now define the travel time parameter  $y$  by

$$y(x) = \int_0^x n(\hat{x}) d\hat{x}, \quad q = \int_0^p n(\hat{x}) d\hat{x}, \quad (3.2.1)$$

so that any period function in  $x$  of period  $p$  can be written as a periodic function of  $y$  of period  $q$ . Let prime denote differentiation with respect to  $x$  and overdot differentiation with respect to  $y$ . Then

$$\frac{d\phi}{dx} = n(x(y)) \frac{d\phi}{dy}$$

outside the finitely many (per period) jump discontinuities of  $n(x)$ . Therefore, outside the jump discontinuities we have

$$\frac{d^2\phi}{dx^2} = n(x(y)) \frac{d}{dy} \left( n(x(y)) \frac{d\phi}{dy} \right) = n(x(y))^2 \frac{d^2\phi}{dy^2} + \underbrace{n(x(y)) \dot{n}(x(y))}_{dn/dx} \frac{d\phi}{dy},$$

provided  $n(x)$  is a  $C^1$ -function on each closed interval between consecutive jump discontinuities. From (2.1.1) we now get

$$-\ddot{\psi}(\eta, y) - \frac{\dot{n}(x(y))}{n(x(y))} \dot{\psi}(\eta, y) = \eta \psi(\eta, y), \quad (3.2.2)$$

where overdot denotes differentiation with respect to  $y$ .

For some parameter  $\alpha \in \mathbb{R}$  we put

$$\psi(\eta, y) = n(x(y))^\alpha \Psi(\eta, y).$$

Then

$$\begin{aligned} \dot{\psi} &= n^\alpha \dot{\Psi} + \alpha n^{\alpha-1} \dot{n} \Psi, \\ \ddot{\psi} &= n^\alpha \ddot{\Psi} + 2\alpha n^{\alpha-1} \dot{n} \dot{\Psi} + [\alpha(\alpha-1)n^{\alpha-2}(\dot{n})^2 + \alpha n^{\alpha-1} \ddot{n}] \Psi. \end{aligned}$$

Thus if  $n(x)$  is a  $C^2$ -function on each closed interval between consecutive jump discontinuities, we obtain

$$-\ddot{\Psi} - (2\alpha + 1)\dot{\Psi} + \left[ -\alpha^2 \left( \frac{\dot{n}}{n} \right)^2 - \alpha \frac{\ddot{n}}{n} \right] \Psi = \eta \Psi.$$

Taking  $\alpha = -\frac{1}{2}$  we finally arrive at the periodic (with period  $q$ ) Schrödinger equation

$$-\ddot{\Psi}(\eta, y) + \underbrace{\left[ -\left( \frac{\dot{n}(x(y))}{2n(x(y))} \right)^2 + \frac{\ddot{n}(x(y))}{2n(x(y))} \right]}_{\mathcal{Q}(y)} \Psi(\eta, y) = \eta \Psi(\eta, y), \quad (3.2.3)$$

where  $\mathcal{Q}(y+q) \equiv \mathcal{Q}(y)$ .

If there are no jump discontinuities in  $n(x)$ , then the Hill discriminant  $\Delta(\eta)$  of Eq. (2.1.1) and the Hill discriminant  $\mathbf{\Delta}(\eta)$  of Eq. (3.2.3) coincide and hence these equations have the same band spectrum. Indeed, under this assumption  $C^1$  solutions of (2.1.1) in  $x$  are transformed into  $C^1$  solutions of (3.2.3) in  $y$ . Now put

$$\beta(\eta, y) = n(x(y))^{1/2} \varphi(\eta, x(y)), \quad \gamma(\eta, y) = n(x(y))^{1/2} \theta(\eta, x(y)).$$

Then

$$\begin{aligned} \dot{\beta}(\eta, y) &= n(x(y))^{1/2} \dot{\varphi}(\eta, x(y)) + \frac{1}{2} n(x(y))^{-1/2} \dot{n} \varphi(\eta, x(y)) \\ &= n(x)^{-1/2} \varphi'(\eta, x) + \frac{1}{2} n(x)^{-3/2} n'(x) \varphi(\eta, x), \\ \dot{\gamma}(\eta, y) &= n(x(y))^{1/2} \dot{\theta}(\eta, x(y)) + \frac{1}{2} n(x(y))^{-1/2} \dot{n} \theta(\eta, x(y)) \\ &= n(x)^{-1/2} \theta'(\eta, x) + \frac{1}{2} n(x)^{-3/2} n'(x) \theta(\eta, x). \end{aligned}$$

Hence,

$$\begin{aligned}\beta(\eta, 0) &= 0, & \dot{\beta}(\eta, 0) &= \frac{1}{\sqrt{n(0)}}, \\ \gamma(\eta, 0) &= \sqrt{n(0)}, & \dot{\gamma}(\eta, 0) &= \frac{n'(0)}{2n(0)\sqrt{n(0)}}.\end{aligned}$$

As a result,

$$\begin{aligned}\theta(\eta, y) &= -\frac{n'(0)}{2n(0)\sqrt{n(0)}}\beta(\eta, y) + \frac{1}{\sqrt{n(0)}}\gamma(\eta, y), \\ \varphi(\eta, y) &= \sqrt{n(0)}\beta(\eta, y).\end{aligned}$$

Consequently,

$$\begin{aligned}\Delta(\eta) &= \theta(\eta, q) + \dot{\varphi}(\eta, q) \\ &= -\frac{n'(0)}{2n(0)\sqrt{n(0)}}\beta(\eta, q) + \frac{1}{\sqrt{n(0)}}\gamma(\eta, q) + \sqrt{n(0)}\dot{\beta}(\eta, q) \\ &= -\frac{n'(0)\sqrt{n(p)}}{2n(0)\sqrt{n(0)}}\varphi(\eta, q) + \frac{\sqrt{n(p)}}{\sqrt{n(0)}}\theta(\eta, q) \\ &\quad + \sqrt{\frac{n(0)}{n(p)}}\varphi'(\eta, p) + \sqrt{\frac{n(0)}{n(p)}}\frac{n'(p)}{2n(p)}\varphi(\eta, p) \\ &= \theta(\eta, p) + \varphi'(\eta, p) \\ &= \Delta(\eta),\end{aligned}$$

as claimed. Note that we have used that  $n(0) = n(p)$  and  $n'(0) = n'(p)$ .

Let us now compute the transformed period map. We get

$$\begin{aligned}\mathbf{M}_{11}(\eta) &= \theta(\eta, q) = -\frac{n'(0)}{2n(0)^{3/2}}\beta(\eta, q) + \frac{1}{\sqrt{n(0)}}\gamma(\eta, q) \\ &= \theta(\eta, p) - \frac{n'(0)}{2n(0)}\varphi(\eta, p), \\ \mathbf{M}_{12}(\eta) &= \varphi(\eta, q) = \sqrt{n(0)}\beta(\eta, q) = n(0)\varphi(\eta, p), \\ \mathbf{M}_{21}(\eta) &= -\frac{n'(0)}{2n(0)^{3/2}}\left[\frac{1}{\sqrt{n(p)}}\varphi'(\eta, p) + \frac{n'(p)}{2n(p)^{3/2}}\varphi(\eta, p)\right] \\ &\quad + \frac{1}{\sqrt{n(0)}}\left[\frac{1}{\sqrt{n(p)}}\theta'(\eta, p) + \frac{n'(p)}{2n(p)^{3/2}}\theta(\eta, p)\right]\end{aligned}$$

$$\begin{aligned}
&= \frac{n'(0)}{2n(0)^2} [\theta(\eta, p) - \varphi'(\eta, p)] - \frac{n'(0)^2}{4n(0)^3} \varphi(\eta, p) + \frac{1}{n(0)} \theta'(\eta, p), \\
\mathbf{M}_{22}(\eta) &= \dot{\varphi}(\eta, q) = \sqrt{n(0)} \dot{\beta}(\eta, q) = \varphi'(\eta, p) + \frac{n'(0)}{2n(0)} \varphi(\eta, p),
\end{aligned}$$

where we have used that  $n(0) = n(p)$  and  $n'(0) = n'(p)$ . In other words,

$$\mathbf{M}(\eta) = \begin{pmatrix} 1 & 0 \\ \frac{n'(0)}{2n(0)^2} & \frac{1}{n(0)} \end{pmatrix} M(\eta) \begin{pmatrix} 1 & 0 \\ -\frac{n'(0)}{2n(0)} & n(0) \end{pmatrix}, \quad (3.2.4)$$

which means that  $\mathbf{M}(\eta)$  follows from  $M(\eta)$  by a similarity transformation. As a result, their traces, i.e., the Hill discriminants, coincide. Moreover, since  $M_{12}(\eta)$  and  $\mathbf{M}_{12}(\eta)$  have the same zeros in the complex  $\eta$ -plane, the Dirichlet spectra of the Helmholtz equation in  $x \in [0, p]$  and the Schrödinger equation in  $y \in [0, q]$  coincide.

The Floquet solutions of Eq. (3.2.3) can be expressed in those of Eq. (2.1.1) as follows:

$$\boldsymbol{\psi}_{1,2}(k, y) = n(x(y))^{1/2} \psi_{1,2}(k, x(y)).$$

This is clear by checking their square integrability as  $y \rightarrow \pm\infty$ , using that  $dy = n(x)dx$  and  $n(x)$  is bounded and bounded away from zero. We thus have

$$\boldsymbol{\psi}_{1,2}(k, y) = e^{\pmiky} \boldsymbol{\chi}_{1,2}(k, y),$$

where  $\boldsymbol{\chi}_{1,2}(k, y) = n(x(y))^{1/2} \chi_{1,2}(k, x(y))$  is periodic in  $y$  of period  $q$ . As a result, we have for their Wronskian

$$\begin{aligned}
\mathbf{w}(k) &\stackrel{\text{def}}{=} \mathbf{W}[\boldsymbol{\psi}_1(k, \cdot), \boldsymbol{\psi}_2(k, \cdot)] \\
&= n^{1/2} \psi_1 \left\{ n^{-1/2} \psi_2' + \frac{1}{2} n^{-3/2} n' \psi_2 \right\} - n^{1/2} \psi_2 \left\{ n^{-1/2} \psi_1' + \frac{1}{2} n^{-3/2} n' \psi_1 \right\} \\
&= \psi_1 \psi_2' - \psi_2 \psi_1' = W[\psi_1(k, \cdot), \psi_2(k, \cdot)] = w(k).
\end{aligned}$$

In the same way we see that the Wronskians of  $\psi_j(k, x)$  and  $\psi_l(-k, x)$  ( $j, l = 1, 2$ ) do not change on conversion to travel time coordinates. Finally, from

$$A(k; x, t) = \frac{\psi_2(k, x) \psi_1(k, t) - \psi_1(k, x) \psi_2(k, t)}{w(k)}$$

we get

$$\begin{aligned}
\mathbf{A}(k; y, s) &\stackrel{\text{def}}{=} \frac{\boldsymbol{\psi}_2(k, y) \boldsymbol{\psi}_1(k, s) - \boldsymbol{\psi}_1(k, y) \boldsymbol{\psi}_2(k, s)}{\mathbf{w}(k)} \\
&= n(x(y)) \frac{\psi_1(k, x(y)) \psi_2(k, x(s)) - \psi_2(k, x(y)) \psi_1(k, x(s))}{w(k)} \\
&= n(x(y)) A(k; x(y), x(s)). \quad (3.2.5)
\end{aligned}$$

The Liouville transformation is easily extended to the case in which  $n(x)$  is positive, periodic with period  $p$ , and piecewise  $C^2$ . In other words, there exist points

$$0 = b_0 < b_1 < \dots < b_{m-1} < b_m = p$$

such that, for  $j = 1, \dots, m$ ,  $n(x)$  is positive and  $C^2$  on  $[b_{j-1}, b_j]$ . In each jump the function  $n(x)$  and its first two derivatives may have different left and right limits. Nevertheless nothing stops us from defining the travel time parameter  $y$  and the  $y$ -period  $q$  by (3.2.1). Putting  $d_j = y(b_j)$  we then get the jump points

$$0 = d_0 < d_1 < \dots < d_{m-1} < d_m = q$$

in the  $y$ -variable. The *fundamental solution*  $\Phi(\eta, x)$  of Equation (2.1.1) is the unique solution of the integral equation

$$\Phi(\eta, x) = \begin{pmatrix} 1 & 0 \\ 0 & 1 \end{pmatrix} + \int_0^x d\hat{x} \begin{pmatrix} 0 & 1 \\ -\eta n(\hat{x})^2 & 0 \end{pmatrix} \Phi(\eta, \hat{x}). \quad (3.2.6)$$

Then we define  $\theta(\eta, x)$  and  $\varphi(\eta, x)$  and the period map  $M(\eta)$  by

$$\Phi(\eta, x) = \begin{pmatrix} \theta(\eta, x) & \varphi(\eta, x) \\ \theta'(\eta, x) & \varphi'(\eta, x) \end{pmatrix} \quad (3.2.7)$$

and

$$M(\eta) = \Phi(\eta, p). \quad (3.2.8)$$

If  $n(x)$  has discontinuities, the fundamental matrix  $\Phi(\eta, x)$  remains continuous in  $x \in \mathbb{R}$ , but the derivatives in the second row of (3.2.7) do not exist outside the jump points. We obviously get

$$M(\eta) = M_m(\eta)M_{m-1}(p) \dots M_1(\eta),$$

where  $M_j(\eta)$  is the matrix mapping the solution vector (function value plus  $x$ -derivative) at  $x = b_{j-1}$  into that at  $x = b_j$ .

Unfortunately, the period map before and after Liouville transformation are not easily related if  $n(x)$  has jump discontinuities.

### 3.3 Reconstructing the refractive index

Let us now discuss the various steps involved when recovering  $n(x)$  from  $M(\eta)$ . We shall go through these steps backward.

**1. From  $n(y)$  to  $n(x)$ .** Let us assume that  $n(y)$  is a positive continuous function in  $y \in \mathbb{R}$  that is periodic with period  $q$ . Then the travel time conversion (3.2.1) can be written alternatively in differential form as follows:

$$y'(x) = n(y), \quad y(0) = 0, \quad (3.3.1)$$

which is a separable differential equation. Letting  $H(y)$  be chosen as the  $C^1$ -function such that  $H(0) = 0$  and  $\dot{H}(y) = (1/n(y))$ , we can integrate (3.3.1) to get

$$H(y) = x. \quad (3.3.2)$$

Since  $H : [0, +\infty) \rightarrow [0, +\infty)$  is monotonically increasing, we can invert (3.3.2) to express  $y$  into  $x$  as the following  $C^1$ -function:

$$y(x) = H^{-1}(x). \quad (3.3.3)$$

We then compute the continuous function  $n(x)$  by differentiation with respect to  $x$ . Then  $n(x)$  is periodic with period  $p = H^{-1}(q)$ .

**Example 3.3.1** Consider  $n(y) = 2 + \sin(y)$ . Then for  $0 \leq y \leq \pi$  we have

$$\begin{aligned} H(y) &= \int_0^y \frac{d\hat{y}}{2 + \sin(\hat{y})} = \int_0^{\tan(y/2)} \frac{2 dz}{1 + z^2} \frac{1}{2 + \frac{2z}{1 + z^2}} \\ &= \int_0^{\tan(y/2)} \frac{dz}{z^2 + z + 1} = \left[ \frac{2}{\sqrt{3}} \arctan \left( \frac{2}{\sqrt{3}} \left[ z + \frac{1}{2} \right] \right) \right]_{z=0}^{\tan(y/2)} \\ &= \frac{2}{\sqrt{3}} \left\{ \arctan \left( \frac{2}{\sqrt{3}} \left[ \frac{1}{2} + \tan\left(\frac{y}{2}\right) \right] \right) - \frac{\pi}{6} \right\}, \end{aligned}$$

so that

$$H(\pi) = \int_0^\infty \frac{dz}{z^2 + z + 1} = \frac{2\pi}{3\sqrt{3}}.$$

By inverting  $x = H(y)$  for  $0 \leq y \leq \pi$  we get

$$\frac{x\sqrt{3}}{2} + \frac{\pi}{6} = \arctan \left( \frac{2}{\sqrt{3}} \left[ \frac{1}{2} + \tan\left(\frac{y}{2}\right) \right] \right).$$

Thus for  $0 \leq x < (2\pi/3\sqrt{3})$  we get

$$y(x) = 2 \arctan \left[ -\frac{1}{2} + \frac{\sqrt{3}}{2} \tan \left( \frac{x\sqrt{3}}{2} + \frac{\pi}{6} \right) \right],$$

which tends to  $\pi$  from below as  $x \rightarrow (2\pi/3\sqrt{3})^-$ . By differentiation we get

$$n(x) = \frac{3/2}{\cos^2\left(\frac{x\sqrt{3}}{2} + \frac{\pi}{6}\right) + \left[-\frac{1}{2}\cos\left(\frac{x\sqrt{3}}{2} + \frac{\pi}{6}\right) + \frac{\sqrt{3}}{2}\sin\left(\frac{x\sqrt{3}}{2} + \frac{\pi}{6}\right)\right]^2},$$

where the denominator cannot vanish without producing an angle whose sine and cosine vanish.

For  $\pi \leq y \leq 2\pi$  we have

$$\begin{aligned} H(y) &= \frac{2\pi}{3\sqrt{3}} + \int_{\pi}^y \frac{d\hat{y}}{2 + \sin(\hat{y})} = \frac{2\pi}{3\sqrt{3}} + \int_0^{y-\pi} \frac{d\hat{y}}{2 - \sin(\hat{y})} \\ &= \frac{2\pi}{3\sqrt{3}} + \int_0^{\tan(\frac{y-\pi}{2})} \frac{2 dz}{1+z^2} \frac{1}{2 - \frac{2z}{1+z^2}} \\ &= \frac{2\pi}{3\sqrt{3}} + \int_0^{\tan(\frac{y-\pi}{2})} \frac{dz}{z^2 - z + 1} \\ &= \frac{2\pi}{3\sqrt{3}} + \left[ \frac{2}{\sqrt{3}} \arctan\left(\frac{2}{\sqrt{3}}\left[z - \frac{1}{2}\right]\right) \right]_{z=0}^{\tan(\frac{y-\pi}{2})} \\ &= \frac{\pi}{\sqrt{3}} + \frac{2}{\sqrt{3}} \arctan\left(\frac{2}{\sqrt{3}}\left[-\frac{1}{2} + \tan\left(\frac{y-\pi}{2}\right)\right]\right). \end{aligned}$$

By inverting  $x = H(y)$  for  $\pi \leq y \leq 2\pi$  we get

$$\frac{x\sqrt{3}}{2} - \frac{\pi}{2} = \arctan\left(\frac{2}{\sqrt{3}}\left[-\frac{1}{2} + \tan\left(\frac{y-\pi}{2}\right)\right]\right).$$

Thus for  $(2\pi/3\sqrt{3}) < x \leq (2\pi/\sqrt{3})$  we get

$$y(x) = \pi + 2 \arctan\left[\frac{1}{2} + \frac{\sqrt{3}}{2} \tan\left(\frac{x\sqrt{3}}{2} - \frac{\pi}{2}\right)\right],$$

which tends to  $\pi$  from below as  $x \rightarrow (2\pi/3\sqrt{3})^+$ . As a result,

$$n(x) = \frac{3/2}{\cos^2\left(\frac{x\sqrt{3}}{2} - \frac{\pi}{2}\right) + \left[\frac{1}{2}\cos\left(\frac{x\sqrt{3}}{2} - \frac{\pi}{2}\right) + \frac{\sqrt{3}}{2}\sin\left(\frac{x\sqrt{3}}{2} - \frac{\pi}{2}\right)\right]^2},$$

where the denominator cannot vanish without producing an angle whose sine and cosine vanish. Further,  $n(x)$  is a periodic function with period

$p = (2\pi/\sqrt{3})$ . As a function of  $y$  the period is  $q = 2\pi$ . We easily obtain [3.2.3]

$$\mathbf{Q}(y) = -\frac{\cos^2(y)}{4[2 + \sin(y)]^2} - \frac{\sin(y)}{2[2 + \sin(y)]}.$$

**2. From  $\mathbf{Q}(y)$  and  $q$  to  $n(y)$ , apart from a constant factor.** Starting from  $\mathbf{Q}(y)$ , find a periodic function  $w(y)$  with period  $q$  (as for  $\mathbf{Q}(y)$ ) satisfying the Riccati equation

$$\frac{1}{2}\dot{w}(y) + \frac{1}{4}w(y)^2 = \mathbf{Q}(y). \quad (3.3.4)$$

Given one solution  $w_0$  of (3.3.4) (periodic or not), any other solution  $w$  of (3.3.4) (periodic or not) is given by  $w = w_0 + (1/z)$ , where

$$\dot{z} - w_0 z = \frac{1}{2}. \quad (3.3.5)$$

Suppose that the Riccati equation (3.3.4) has a solution  $w_0$  that is periodic in  $y$  with period  $q$  and satisfies  $\int_0^q d\hat{y} w_0(\hat{y}) = 0$ . Put  $W_0(y) = \int_0^y d\hat{y} w_0(\hat{y})$ . Then (3.3.5) can be written in the form

$$\frac{d}{dy} (e^{-W_0(y)} z(y)) = \frac{1}{2} e^{-W_0(y)},$$

where  $W_0$  is periodic in  $y$  with period  $q$ . Periodicity of  $z$  would imply periodicity of an antiderivative of  $e^{-W_0}$ , which is impossible because  $\int_0^q d\hat{y} e^{-W_0(\hat{y})} \neq 0$ . In other words, for each value of the real parameter  $\eta$ ,  $w_0$  is the only periodic solution of the Riccati equation (3.3.4).

The Riccati equation (3.3.4) can also be written in the form

$$\frac{\partial^2}{\partial y^2} \{n(y)^{1/2}\} = \mathbf{Q}(y)n(y)^{1/2}. \quad (3.3.6)$$

The existence of a unique periodic solution  $n(y)$  (apart from a constant factor) is equivalent to the Hill discriminant condition  $\Delta(0) = 2$  plus the condition that  $\eta = 0$  is not a Dirichlet eigenvalue. Since  $\eta = 0$  is indeed not a Dirichlet eigenvalue of (2.1.1) and at the same time the left endpoint of the first band, there exists a unique solution  $n(y)$  (up to a constant factor) such that  $n(y+q) \equiv n(y)$ . This solution cannot have any zeros and hence can be chosen to be positive, as a result of existing oscillation theorems. This implies the existence and uniqueness of  $w_0(y)$ .

If  $\mathbf{Q}(y)$  is a continuous function of  $y \in \mathbb{R}$ , then  $n(y)^{1/2}$ , and hence also  $n(y)$ , are  $C^2$ -functions. On the other hand, if  $\mathbf{Q}(y)$  is merely locally  $L^2$ , the function  $n(y)$  will be  $C^1$  with absolutely continuous derivative, but not necessarily  $C^2$ . In [33] we can find necessary and sufficient conditions on

the two spectra determining  $\mathbf{Q}(y)$  in order that  $\mathbf{Q}(y)$  belongs to a certain Sobolev space.

**3. Find  $n(x)$  using  $p$  and  $q$  if  $n(y)$  is known up to a constant factor.** Suppose  $n(y)$  is known up to a constant factor, i.e.,  $n(y; c) = cn_0(y)$ , where  $n_0(y)$  is just one of the possible refractive index functions and  $c$  is a positive constant. Then we need to solve the Cauchy problem

$$\dot{H}(y; c) = \frac{1}{cn_0(y)}, \quad H(0; c) = 0,$$

which leads to  $H(y; c) = H_0(y)/c$ , where  $H_0(y) = \int_0^y (d\hat{y}/n_0(\hat{y}))$ . Solving the equation  $x = H(y; c) = (H_0(y)/c)$  we get

$$y(x; c) = y_0(cx),$$

where  $x = H_0(y_0(x))$ . Differentiating with respect to  $x$  we get

$$n(x; c) = cn_0(cx).$$

Using that the period  $p$  in  $x$  is known, we get the following equation:

$$y_0(cp) = q, \tag{3.3.7}$$

which allows us to determine the positive constant  $c$  uniquely.

**4. Find  $\mathbf{Q}(y)$  and  $q$  from the original period map  $M(\eta)$ .** We can certainly construct  $\mathbf{Q}(y)$  uniquely from the transformed period map  $\mathbf{M}(\eta)$ , because this matrix contains two spectra (the Dirichlet spectrum and one of the Dirichlet-Neumann and Neumann-Dirichlet spectra). This inverse problem has in principle been solved [37, 38, 33]. Thus the problem is to determine the period  $q$  and two spectra of (3.2.3) from the original period map  $M(\eta)$ .

One spectrum of (3.2.3) is easily obtained, namely the Dirichlet spectrum, because it consists of the zeros of  $\mathbf{M}_{12}(\eta)$  and hence coincides with the Dirichlet spectrum of (2.1.1). By a well-known result [39], we have for the Dirichlet eigenvalues<sup>1</sup>

$$\eta_n = \left( \frac{n\pi}{q} \right)^2 + O(1/n^2), \quad n \rightarrow +\infty, \tag{3.3.8}$$

so that  $q = \lim_{n \rightarrow \infty} (n\pi/\sqrt{\eta_n})$ . In other words, the Dirichlet spectrum yields the travel time period  $q$ .

---

<sup>1</sup>Equation (3.3.8) is exact if  $\mathbf{Q}(y) \equiv 0$ .

Suppose we know

$$\iota \stackrel{\text{def}}{=} [n'(0)/2n(0)]. \quad (3.3.9)$$

Then we can compute the functions

$$\begin{aligned} \mathbf{M}_{11}(\eta) &= \theta(\eta, p) - \eta\varphi(\eta, p), \\ \mathbf{M}_{22}(\eta) &= \varphi'(\eta, p) + \eta\varphi(\eta, p), \end{aligned}$$

Moreover, the zeros of  $\mathbf{M}_{22}(\eta)$  (i.e., the Dirichlet-Neumann spectrum of (3.2.3)) coincide with the zeros of  $\varphi'(\eta, p) + \eta\varphi(\eta, p)$  (i.e., with the Dirichlet- $\eta$ -mixed spectrum of (2.1.1)), whereas the zeros of  $\mathbf{M}_{11}(\eta)$  coincide with the zeros of  $\theta(\eta, p) - \eta\varphi(\eta, p)$ . Using  $\iota$  as a (real) parameter, we then go on to compute the Schrödinger potential  $\mathbf{Q}(y; \iota)$  by well-known methods [41], especially since the period  $q$  is known. We are thus able to compute  $\mathbf{Q}(y; \iota)$  uniquely from the parameter  $\iota \in \mathbb{R}$ . At the end of the day we have to single out those values of  $\iota$  for which

$$\frac{n'(0; \iota)}{n(0; \iota)} = 2\iota. \quad (3.3.10)$$

Equation (3.3.10) leads to the proper choice of  $\iota$ , but it is not clear if  $\iota$  is found from (3.3.10) uniquely or even exists.

**Example 3.3.2** Consider the trivial example  $n(x) \equiv 1$  with period  $p$ . Then the period map is given by

$$M(\eta) = \begin{pmatrix} \cos(p\sqrt{\eta}) & \frac{\sin(p\sqrt{\eta})}{\sqrt{\eta}} \\ -\sqrt{\eta} \sin(p\sqrt{\eta}) & \cos(p\sqrt{\eta}) \end{pmatrix}.$$

Let us now pretend not to know  $n(x)$ . Then we have the following information on  $\mathbf{M}(\eta)$ :

$$\mathbf{M}(\eta) = \begin{pmatrix} \cos(p\sqrt{\eta}) - \eta \frac{\sin(p\sqrt{\eta})}{\sqrt{\eta}} & \text{const.} \frac{\sin(p\sqrt{\eta})}{\sqrt{\eta}} \\ \dot{\theta}(\eta, p) & \cos(p\sqrt{\eta}) + \eta \frac{\sin(p\sqrt{\eta})}{\sqrt{\eta}} \end{pmatrix},$$

where the constant [=  $n(0)$ ] is positive,  $\eta$  is a real parameter, and  $\dot{\theta}(\eta, p)$  is in principle unknown. The Dirichlet spectrum  $\eta_n = (n\pi/p)^2$  for  $n = 1, 2, 3, \dots$  yields  $q = p$ . We now see that the Dirichlet-Neumann spectrum  $\{\zeta_n(\iota)\}_{n=1}^{\infty}$  of  $\mathbf{Q}(y; \iota)$  is given by the zeros of the function

$$\mathbf{M}_{22}(\eta; \iota) = \cos(p\sqrt{\eta}) + \iota \frac{\sin(p\sqrt{\eta})}{\sqrt{\eta}},$$

i.e., by the positive roots of the equation<sup>2</sup>

$$\tan(p\sqrt{\eta}) = -\frac{\sqrt{\iota}}{\iota}.$$

Using that  $\det \mathbf{M}(\eta) = 1$ , we get

$$\cos^2(p\sqrt{\eta}) - \iota^2 \frac{\sin^2(p\sqrt{\eta})}{\eta} - \text{const.} \dot{\boldsymbol{\theta}}(\eta, p) \frac{\sin(p\sqrt{\eta})}{\sqrt{\eta}} = 1,$$

which implies

$$\left(1 + \frac{\iota^2}{\eta}\right) \sin^2(p\sqrt{\eta}) = -\text{const.} \dot{\boldsymbol{\theta}}(\eta, p) \frac{\sin(p\sqrt{\eta})}{\sqrt{\eta}}.$$

As a result,

$$\dot{\boldsymbol{\theta}}(\eta, p) = -\frac{\eta + \iota^2}{\text{const.}} \frac{\sin(p\sqrt{\eta})}{\sqrt{\eta}}.$$

Thus, the Neumann spectrum of  $\mathbf{Q}(y)$  is  $\{(n\pi/p)^2\}_{n=1}^{\infty}$  for  $\iota \neq 0$  and  $\{([n-1]\pi/p)^2\}_{n=1}^{\infty}$  for  $\iota = 0$ . The former case is excluded, since the  $n$ -th Dirichlet eigenvalue must **strictly** exceed the  $n$ -th Neumann eigenvalue. Thus necessarily  $\iota = 0$ , which leads to the unique solution  $n(x) \equiv 1$ .

Example 3.3.2 suggests proceeding in the same way in general. Using that  $\det M(\eta) = \det \mathbf{M}(\eta) = 1$ , we obtain

$$\begin{aligned} \theta(\eta, p)\varphi'(\eta, p) - \theta'(\eta, p)\varphi(\eta, p) &= [\theta(\eta, p) - \eta\varphi(\eta, p)][\varphi'(\eta, p) + \eta\varphi(\eta, p)] \\ &\quad - \text{const.} \dot{\boldsymbol{\theta}}(\eta, p)\varphi(\eta, p), \end{aligned}$$

and therefore

$$\dot{\boldsymbol{\theta}}(\eta, p) = \frac{\theta'(\eta, p) + \eta\{\theta(\eta, p) - \varphi'(\eta, p)\} - \eta^2\varphi(\eta, p)}{\text{const.}}. \quad (3.3.11)$$

The zeros of the function in (3.3.11) yield the Neumann spectrum of  $\mathbf{Q}(y; \eta)$  and hence determine  $\mathbf{Q}(y; \eta)$  uniquely [36, 26].

---

<sup>2</sup>The case  $\iota = 0$  leads to  $\mathbf{Q}(y) \equiv 0$  and, following the subsequent steps, to  $n(x) \equiv 1$ . We may therefore restrict ourselves to  $\iota \in \mathbb{R} \setminus \{0\}$ .

### 3.4 Recovery of a piecewise constant media

In this subsection we propose a method to determine the refractive indices  $n_j$  and the layer amplitudes  $a_j$  from the period map  $M(\eta)$  when the refractive index is piecewise constant (Example 2.3.3). The piecewise constant case perfectly fits the description of a one-dimensional photonic crystal, i.e. regular arrays of different dielectric materials layered along one spatial direction as displayed in Fig. 3.1. This kind of heterostructure generally consists of

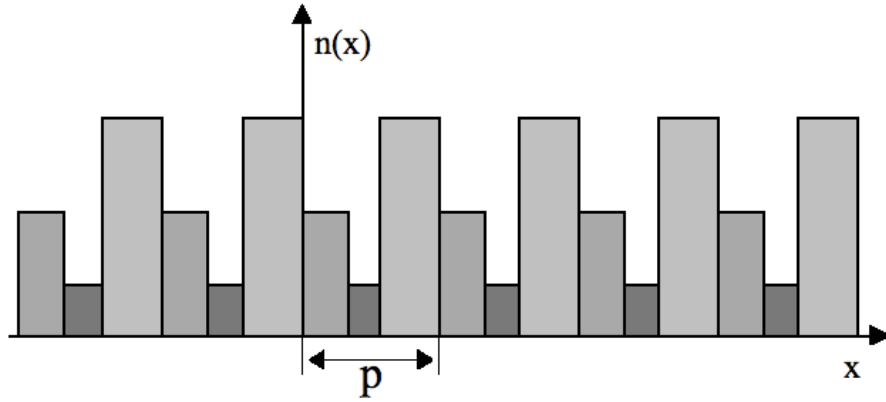


**Figure 3.1:** Example of a periodic structure with period  $p$  in the case of a piecewise constant refractive index. The figure illustrates a 1-D three layer photonic crystal with different layer amplitudes.

no more than three layers per period [5, 42] .

From Example 2.3.3 we know that the period map in the piecewise constant case takes the following form:

$$M(\eta) = \prod_{j=m, m-1, \dots, 1} \begin{pmatrix} \cos(n_j a_j \sqrt{\eta}) & \frac{\sin(n_j a_j \sqrt{\eta})}{n_j \sqrt{\eta}} \\ -n_j \sqrt{\eta} \sin(n_j a_j \sqrt{\eta}) & \cos(n_j a_j \sqrt{\eta}) \end{pmatrix},$$

and we easily see that:

$$\begin{pmatrix} \sqrt{\eta} & 0 \\ 0 & 1 \end{pmatrix} M(\eta) \begin{pmatrix} 1 & 0 \\ \sqrt{\eta} & 1 \end{pmatrix} = \prod_{j=m, m-1, \dots, 1} \begin{pmatrix} \cos(n_j a_j \sqrt{\eta}) & \frac{\sin(n_j a_j \sqrt{\eta})}{n_j} \\ -n_j \sin(n_j a_j \sqrt{\eta}) & \cos(n_j a_j \sqrt{\eta}) \end{pmatrix}, \quad (3.4.1)$$

where the right-hand side is called *modified period map*, has determinant 1 and whose entries are almost periodic polynomials in  $\sqrt{\eta}$ . The diagonal

entries are real even functions of  $\sqrt{\eta}$  and the off-diagonal entries are real odd functions of  $\sqrt{\eta}$  vanishing at  $\sqrt{\eta} = 0$ .

Let us write

$$\mu_j = n_j a_j > 0, \quad z = \sqrt{\eta}, \quad \mathbb{M}(z) = \begin{pmatrix} z & 0 \\ 0 & 1 \end{pmatrix} M(\eta) \begin{pmatrix} z^{-1} & 0 \\ 0 & 1 \end{pmatrix},$$

where  $\mathbb{M}(z)$  is the *modified period map*. Let us write the entries of  $\mathbb{M}(z)$  in the following form:

$$\mathbb{M}_{11}(z) = + \sum c_{\sigma_2, \dots, \sigma_m}^{11} \cos((\mu_1 + \sigma_2 \mu_2 + \dots + \sigma_m \mu_m)z), \quad (3.4.2a)$$

$$\mathbb{M}_{12}(z) = + \sum c_{\sigma_2, \dots, \sigma_m}^{12} \sin((\mu_1 + \sigma_2 \mu_2 + \dots + \sigma_m \mu_m)z), \quad (3.4.2b)$$

$$\mathbb{M}_{21}(z) = - \sum c_{\sigma_2, \dots, \sigma_m}^{21} \sin((\mu_1 + \sigma_2 \mu_2 + \dots + \sigma_m \mu_m)z), \quad (3.4.2c)$$

$$\mathbb{M}_{22}(z) = + \sum c_{\sigma_2, \dots, \sigma_m}^{22} \cos((\mu_1 + \sigma_2 \mu_2 + \dots + \sigma_m \mu_m)z), \quad (3.4.2d)$$

where we sum over all sign patterns  $(\sigma_2, \dots, \sigma_m)$  in the  $2^{m-1}$  element set  $\{-1, +1\}^{m-1}$ . Then the Fourier spectrum of the entries of the modified period map  $\mathbb{M}(z)$  is given by

$$\left\{ \sum_{j=1}^m \sigma_j n_j a_j : \sigma_j = \pm 1 \right\}.$$

Therefore it has at most  $2^m$  points and its maximum is  $\mu_1 + \dots + \mu_m$ . Using the addition formulas of trigonometry, we get the recurrence relations

$$\begin{aligned} c_{\sigma_2, \dots, \sigma_{m-1}, \pm 1}^{11} &= \frac{1}{2} c_{\sigma_2, \dots, \sigma_{m-1}}^{11} \pm \frac{1}{2n_m} c_{\sigma_2, \dots, \sigma_{m-1}}^{21}, \\ c_{\sigma_2, \dots, \sigma_{m-1}, \pm 1}^{22} &= \frac{1}{2} c_{\sigma_2, \dots, \sigma_{m-1}}^{22} \pm \frac{1}{2} n_m c_{\sigma_2, \dots, \sigma_{m-1}}^{12}, \\ c_{\sigma_2, \dots, \sigma_{m-1}, \pm 1}^{12} &= \frac{1}{2} c_{\sigma_2, \dots, \sigma_{m-1}}^{12} \pm \frac{1}{2n_m} c_{\sigma_2, \dots, \sigma_{m-1}}^{22}, \\ c_{\sigma_2, \dots, \sigma_{m-1}, \pm 1}^{21} &= \frac{1}{2} c_{\sigma_2, \dots, \sigma_{m-1}}^{21} \pm \frac{1}{2} n_m c_{\sigma_2, \dots, \sigma_{m-1}}^{11}. \end{aligned}$$

We thus easily recover the expression

$$\mathbf{c}_{1, \dots, 1} \stackrel{\text{def}}{=} \begin{pmatrix} c_{1, \dots, 1}^{11} & c_{1, \dots, 1}^{12} \\ c_{1, \dots, 1}^{21} & c_{1, \dots, 1}^{22} \end{pmatrix} = \frac{1}{2^{m-1}} \begin{pmatrix} 1 & 1/n_m \\ n_m & 1 \end{pmatrix} \cdots \begin{pmatrix} 1 & 1/n_1 \\ n_1 & 1 \end{pmatrix}, \quad (3.4.3)$$

where the subscript  $1, \dots, 1$  have  $m - 1$  entries and the product matrix has

positive entries but zero determinant. More generally,

$$\begin{aligned} \mathbf{c}_{\sigma_2, \dots, \sigma_m} &\stackrel{\text{def}}{=} \begin{pmatrix} c_{\sigma_2, \dots, \sigma_m}^{11} & c_{\sigma_2, \dots, \sigma_m}^{12} \\ c_{\sigma_2, \dots, \sigma_m}^{21} & c_{\sigma_2, \dots, \sigma_m}^{22} \end{pmatrix} \\ &= \frac{1}{2^{m-1}} \begin{pmatrix} 1 & \sigma_m \\ \sigma_m n_m & 1 \end{pmatrix} \dots \begin{pmatrix} 1 & \sigma_2 \\ \sigma_2 n_2 & 1 \end{pmatrix} \begin{pmatrix} 1 & 1 \\ n_1 & 1 \end{pmatrix}. \end{aligned} \quad (3.4.4)$$

By induction on the number of factors we thus easily prove that

$$\left| \frac{c_{\sigma_2, \dots, \sigma_m}^{11}}{c_{\sigma_2, \dots, \sigma_m}^{12}} \right| = \left| \frac{c_{\sigma_2, \dots, \sigma_m}^{21}}{c_{\sigma_2, \dots, \sigma_m}^{22}} \right| = n_1, \quad \frac{c_{\sigma_2, \dots, \sigma_m}^{21}}{c_{\sigma_2, \dots, \sigma_m}^{11}} = \frac{c_{\sigma_2, \dots, \sigma_m}^{22}}{c_{\sigma_2, \dots, \sigma_m}^{12}} = \sigma_m n_m. \quad (3.4.5)$$

### 3.4.1 Two-Layer photonic crystal

Let us consider a crystal where in each period there are two different media with refractive indices  $n_1$  and  $n_2$ , respectively, where  $n_1 \neq n_2$  (Fig. 3.2).

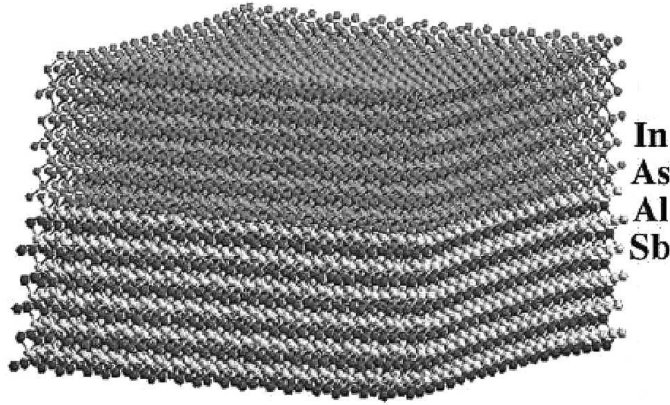


**Figure 3.2:** Example of a heterostructure made of two semiconductor crystals InAs-AlSb with different refractive indices.

- We start from the modified period map  $\mathbb{M}(z)$  and focus on its Fourier spectrum. For a two-layer photonic crystal its Fourier spectrum will be the  $2^2$  element set

$$\{\pm(\mu_1 + \mu_2), \pm(\mu_1 - \mu_2)\} = \{\tilde{\mu}_1, \tilde{\mu}_2, \tilde{\mu}_3, \tilde{\mu}_4\}.$$

- We then consider the maximum of the Fourier spectrum:

$$\tilde{\mu}_i = n_1 a_1 + n_2 a_2 = \mu_1 + \mu_2 , \quad (3.4.6)$$

for some  $i \in \{1, 2, 3, 4\}$ .

- Let  $\mathbf{c}_+$  be the corresponding coefficient matrix. We evaluate  $n_1$  and  $n_2$  from Eqs. (3.4.5):

$$\left| \frac{c_+^{11}}{c_+^{12}} \right| = \left| \frac{c_+^{21}}{c_+^{22}} \right| = n_1, \quad \left| \frac{c_+^{21}}{c_+^{11}} \right| = \left| \frac{c_+^{22}}{c_+^{12}} \right| = n_2. \quad (3.4.7)$$

- We consider the following system

$$\begin{cases} \mu_1 + \mu_2 = \tilde{\mu}_i \\ \mu_1 - \mu_2 = \tilde{\mu}_j \end{cases}$$

for any  $j \in \{1, 2, 3, 4\}$  **different from**  $i$ , so that we get

$$\mu_2^{(j)} = \frac{\tilde{\mu}_i - \tilde{\mu}_j}{2} \quad j \neq i . \quad (3.4.8)$$

- For any computed  $\mu_2^{(j)}$  (for a two-layer photonic crystal there are three of them), we calculate the reduced modified period map  $\mathbb{M}_1^{(j)}(z)$  corresponding to the virtual one-layer photonic crystal

$$\mathbb{M}_1^{(j)}(z) = \begin{pmatrix} \cos(\mu_2^{(j)} z) & -\frac{\sin(\mu_2^{(j)} z)}{n_2} \\ n_2 \sin(\mu_2^{(j)} z) & \cos(\mu_2^{(j)} z) \end{pmatrix} \mathbb{M}_2(z) . \quad (3.4.9)$$

- We select the period map which has a corresponding two-element Fourier spectrum (which is consistent with the one-layer virtual photonic crystal) and whose corresponding coefficient matrix satisfies the following relations:

$$\left| \frac{c^{11}}{c^{12}} \right| = \left| \frac{c^{21}}{c^{22}} \right| = n_1, \quad \left| \frac{c^{21}}{c^{11}} \right| = \left| \frac{c^{22}}{c^{12}} \right| . \quad (3.4.10)$$

Such a period map turns out to be unique and consequently we find the correct  $q \stackrel{\text{def}}{=} \mu_2^{(j)}$ , which corresponds to the uniquely found  $\mathbb{M}_1^{(j)}(z)$ .

- We compute  $a_2 = q/n_2$  and finally we get the value of  $a_1$  from Eq. (3.4.6).

Alternatively one can compute  $a_2$  using the crystal period knowledge (see Eq. (3.1.11) ) and realizing that  $a_1 + a_2 = p$ .

**Example 3.4.1** Consider

$$n_1 = 1, \quad n_2 = 0.5, \quad a_1 = 1, \quad a_2 = 3.$$

Then  $\mu_1 = 1, \mu_2 = 1.5$  and using Eqs. (3.4.2) and (3.4.4), it is straightforward to build the corresponding modified period map:

$$\begin{aligned} \mathbb{M}_{11}(z) &= +\frac{1}{2}[3 \cos(2.5z) - \cos(0.5z)], \\ \mathbb{M}_{12}(z) &= +\frac{1}{2}[3 \sin(2.5z) + \sin(0.5z)], \\ \mathbb{M}_{21}(z) &= -\frac{1}{2}[1.5 \sin(2.5z) - 0.5 \sin(0.5z)], \\ \mathbb{M}_{22}(z) &= +\frac{1}{2}[1.5 \cos(2.5z) + 0.5 \cos(0.5z)]. \end{aligned}$$

The coefficient matrices correspond to the Fourier spectrum as follows:

$$\begin{aligned} +2.5 &\mapsto \frac{1}{2} \begin{pmatrix} 3 & 3 \\ 1.5 & 1.5 \end{pmatrix}, & -2.5 &\mapsto \frac{1}{2} \begin{pmatrix} 3 & -3 \\ -1.5 & 1.5 \end{pmatrix}, \\ +0.5 &\mapsto \frac{1}{2} \begin{pmatrix} -1 & 1 \\ -0.5 & 0.5 \end{pmatrix}, & -0.5 &\mapsto \frac{1}{2} \begin{pmatrix} -1 & -1 \\ 0.5 & 0.5 \end{pmatrix}, \end{aligned}$$

where  $(\mu_1 + \sigma_2 \mu_2) \mapsto \mathbf{c}_{\sigma_2}$ . We now perform the inversion:

- find the Fourier spectrum:  $\{0.5, -0.5, 2.5, -2.5\}$  ;
- focus on its maximum:  $\tilde{\mu}_2 = 2.5$  ;
- evaluate

$$n_1 = \left| \frac{c_+^{11}}{c_+^{12}} \right| = \left| \frac{c_+^{21}}{c_+^{22}} \right| = 1, \quad n_2 = \left| \frac{c_+^{21}}{c_+^{11}} \right| = \left| \frac{c_+^{22}}{c_+^{21}} \right| = 0.5 ;$$

- compute  $\tilde{\mu}_2^j$  for  $j = 1, 2, 4$ :

$$\tilde{\mu}_2^1 = 1, \quad \tilde{\mu}_2^2 = 1.5, \quad \tilde{\mu}_2^4 = 2.5 ;$$

- we calculate  $\mathbb{M}_1^{(j)}(z)$  for  $j = 1, 2, 4$ :

$$\begin{aligned} [\mathbb{M}_1^{(j)}]_{11}(z) &= 6 \cos[(\tilde{\mu}_2^j - 2.5)z] - 2 \cos[(\tilde{\mu}_2^j - 0.5)z], \\ [\mathbb{M}_1^{(j)}]_{12}(z) &= -6 \sin[(\tilde{\mu}_2^j - 2.5)z] - 2 \sin[(\tilde{\mu}_2^j - 0.5)z], \\ [\mathbb{M}_1^{(j)}]_{21}(z) &= 3 \sin[(\tilde{\mu}_2^j - 2.5)z] - \sin[(\tilde{\mu}_2^j - 0.5)z], \\ [\mathbb{M}_1^{(j)}]_{22}(z) &= 3 \cos[(\tilde{\mu}_2^j - 2.5)z] + \cos[(\tilde{\mu}_2^j - 0.5)z], \end{aligned}$$

and it is easy to show that only for  $j = 2$  one gets a one-layer modified period map with a two-point Fourier spectrum and for which relations (3.4.10) are satisfied:

$$\mathbb{M}_1^{(j=2)}(z) = 4 \begin{pmatrix} \cos z & \sin z \\ -\sin z & \cos z \end{pmatrix};$$

- get  $a_2 = \tilde{\mu}_2^2/n_2 = q/n_2 = 1.5/0.5 = 3$  and from  $\mathbb{M}_1^{(j=2)}(z)$  realize that  $\mu_1 = 1$ ;
- finally, obtain  $a_1$  either from  $\mu_1 + q = \tilde{\mu}_2$  or from  $a_1 + a_2 = \lim_{z \rightarrow 0} M^{12}(z) = p$  (see Eq. (3.1.11)) and find  $a_1 = 1$ . Alternatively one gets  $a_1$  straight from  $\mu_1$  using the known  $n_1$  value.

### 3.4.2 General case

The inversion procedure used for the two-layer photonic crystal in Subsection 3.4.1 can easily be generalized to a photonic crystal made of  $m$  layers. In fact, we present the following algorithm [43].

1. Consider the  $2^m$ -element Fourier spectrum corresponding to the modified period map  $\mathbb{M}_m(z)$ ,

$$\left\{ \sum_{j=1}^m \sigma_j \mu_j : \sigma_j = \pm 1 \right\} = \{ \tilde{\mu}_1, \tilde{\mu}_2, \dots, \tilde{\mu}_{2^m} \},$$

where  $\mu_j = n_j a_j$ , and find its maximum

$$\tilde{\mu}_i = \mu_1 + \mu_2 + \dots + \mu_m,$$

where  $i \in \{1, 2, \dots, 2^m\}$ .

2. Evaluate  $n_1$  and  $n_m$  from Eqs. (3.4.5):

$$\left| \frac{c_{+, \dots, +}^{11}}{c_{+, \dots, +}^{12}} \right| = \left| \frac{c_{+, \dots, +}^{21}}{c_{+, \dots, +}^{22}} \right| = n_1, \quad \left| \frac{c_{+, \dots, +}^{21}}{c_{+, \dots, +}^{11}} \right| = \left| \frac{c_{+, \dots, +}^{22}}{c_{+, \dots, +}^{12}} \right| = n_m. \quad (3.4.11)$$

3. Consider the following system

$$\begin{cases} \mu_1 + \dots + \mu_{m-1} + \mu_m = \tilde{\mu}_i \\ \mu_1 + \dots + \mu_{m-1} - \mu_m = \tilde{\mu}_j \end{cases}$$

for any  $j \in \{1, 2, \dots, i-1, i+1, \dots, 2^m\}$  so that

$$\tilde{\mu}_m^{(j)} = \frac{\tilde{\mu}_i - \tilde{\mu}_j}{2}, \quad j \neq i. \quad (3.4.12)$$

4. For any computed  $\tilde{\mu}_m^{(j)}$ , calculate the reduced modified period map  $\mathbb{M}_{m-1}^{(j)}(z)$ :

$$\mathbb{M}_{m-1}^{(j)}(z) = \begin{pmatrix} \cos(\tilde{\mu}_m^{(j)} z) & -\frac{\sin(\tilde{\mu}_m^{(j)} z)}{n_m} \\ n_m \sin(\tilde{\mu}_m^{(j)} z) & \cos(\tilde{\mu}_m^{(j)} z) \end{pmatrix} \mathbb{M}(z). \quad (3.4.13)$$

5. Select the reduced period map whose corresponding spectrum has  $2^{m-1}$  elements and whose coefficient matrix satisfies the following conditions:

$$\left| \frac{c_{m-1}^{11}}{c_{m-1}^{12}} \right| = \left| \frac{c_{m-1}^{21}}{c_{m-1}^{22}} \right| = n_1, \quad \left| \frac{c_{m-1}^{21}}{c_{m-1}^{11}} \right| = \left| \frac{c_{m-1}^{22}}{c_{m-1}^{12}} \right|. \quad (3.4.14)$$

6. This modified period map turns out to be unique and consequently

$$a_m = \frac{q_m}{n_m},$$

where  $q_m$  is the frequency  $\tilde{\mu}_m^{(j)}$  corresponding to the unique  $\mathbb{M}_{m-1}^{(j)}(z)$  computed at step 5.

7. Repeat the same procedure for  $\mathbb{M}_{m-1}(z)$  until the original modified period map has been factorized completely.

After step 3 one can reduce the number of  $\mu_m^{(j)}$  by noticing that

$$\mathbf{c}_{(1, \dots, 1, 1)} + \mathbf{c}_{(1, \dots, 1, -1)} = \mathbf{C}_{m-1}, \quad (3.4.15a)$$

$$\mathbf{c}_{(1, \dots, 1, 1)} - \mathbf{c}_{(1, \dots, 1, -1)} = \begin{pmatrix} 0 & 1 \\ n_m & 0 \end{pmatrix} \mathbf{C}_{m-1}, \quad (3.4.15b)$$

where  $\mathbf{C}_{m-1}$  is the leading coefficient matrix [i.e.,  $\mathbf{c}_{(1, \dots, 1)}$ ] in the modified period map  $\mathbb{M}_{m-1}^{(j)}(z)$  for the first  $m-1$  intervals. Eqs. (3.4.15) thus reduce the number of available  $\mu_m^{(j)}$  so that step 4 is more easily performed.

**Example 3.4.2** Consider

$$n_1 = 1/2, \quad n_2 = 2, \quad n_3 = 10, \quad a_1 = 3/2, \quad a_2 = 2, \quad a_3 = 2/5.$$

Then  $\mu_1 = 0.75$ ,  $\mu_2 = 4$ ,  $\mu_3 = 4$ , and using Eqs. (3.4.2) and (3.4.4), it is straightforward to build the corresponding modified period map:

$$\begin{aligned} \mathbb{M}_{11} &= \frac{1}{4} \left[ \frac{3}{2} \cos(8.75z) + \cos(0.75z) + \frac{3}{5} \cos(0.75z) + \frac{9}{10} \cos(7.25z) \right], \\ \mathbb{M}_{12} &= \frac{1}{4} \left[ 3 \sin(8.75z) + 2 \sin(0.75z) + \frac{6}{5} \sin(0.75z) - \frac{9}{5} \sin(7.25z) \right], \\ \mathbb{M}_{21} &= \frac{1}{4} \left[ 15 \sin(8.75z) - 10 \sin(0.75z) + 6 \sin(0.75z) + 9 \sin(7.25z) \right], \\ \mathbb{M}_{22} &= \frac{1}{4} \left[ 30 \cos(8.75z) - 20 \cos(0.75z) + 12 \cos(0.75z) - 18 \cos(7.25z) \right]. \end{aligned}$$

The coefficient matrices correspond to the Fourier spectrum as follows:

$$\begin{aligned} +8.75 &\mapsto \frac{1}{4} \begin{pmatrix} 3/2 & 3 \\ 15 & 30 \end{pmatrix}, & -8.75 &\mapsto \frac{1}{4} \begin{pmatrix} 3/2 & -3 \\ -15 & 30 \end{pmatrix}, \\ +0.75 &\mapsto \frac{1}{4} \begin{pmatrix} 1 & 2 \\ -10 & 20 \end{pmatrix}, & -0.75 &\mapsto \frac{1}{4} \begin{pmatrix} 1 & -2 \\ 10 & 20 \end{pmatrix}, \\ +0.75 &\mapsto \frac{1}{4} \begin{pmatrix} 3/5 & 6/5 \\ 6 & 12 \end{pmatrix}, & -0.75 &\mapsto \frac{1}{4} \begin{pmatrix} 3/5 & -6/5 \\ -6 & 12 \end{pmatrix}, \\ +7.25 &\mapsto \frac{1}{4} \begin{pmatrix} 9/10 & -9/5 \\ 9 & -18 \end{pmatrix}, & -7.25 &\mapsto \frac{1}{4} \begin{pmatrix} 9/10 & 9/5 \\ -9 & -18 \end{pmatrix}, \end{aligned}$$

where  $(\mu_1 + \sigma_2 \mu_2 + \sigma_3 \mu_3) \mapsto \mathbf{c}_{\sigma_3, \sigma_2}$ .

We now perform the inversion:

- find the Fourier spectrum<sup>3</sup>:  $\{\pm 8.75, \pm 0.75, \pm 0.75, \pm 7.25\}$ ;
- focus on its maximum:  $\tilde{\mu}_3 = 8.75$ ;
- evaluate

$$n_1 = \left| \frac{c_+^{11}}{c_+^{12}} \right| = \left| \frac{c_+^{21}}{c_+^{22}} \right| = \frac{1}{2}, \quad n_3 = \left| \frac{c_+^{21}}{c_+^{11}} \right| = \left| \frac{c_+^{22}}{c_+^{21}} \right| = 10;$$

---

<sup>3</sup>In this example the Fourier spectrum is degenerate.

- compute  $\tilde{\mu}_3^j$  for  $j = 2, 3, 4, 5, 6, 7, 8$ :

$$\tilde{\mu}_3^2 = 8.75, \quad \tilde{\mu}_3^3 = 4, \quad \tilde{\mu}_3^4 = 4.75, \quad \tilde{\mu}_3^5 = 4, \quad \tilde{\mu}_3^6 = 4.75, \quad \tilde{\mu}_3^7 = 0.75, \quad \tilde{\mu}_3^8 = 8;$$

- we calculate  $\mathbb{M}_2^{(j)}(z)$  for  $j = 2, 3, 4, 5, 6, 7, 8$ :

$$\begin{aligned} [\mathbb{M}_2^{(j)}]_{11}(z) &= \frac{1}{8} \left\{ 3 \cos[(\tilde{\mu}_3^j - 8.75)z] + 2 \cos[(\tilde{\mu}_3^j + 0.75)z] \right. \\ &\quad \left. + \frac{6}{5} \cos[(\tilde{\mu}_3^j - 0.75)z] + \frac{9}{5} \cos[(\tilde{\mu}_3^j - 7.25)z] \right\}, \end{aligned}$$

$$\begin{aligned} [\mathbb{M}_2^{(j)}]_{11}(z) &= \frac{1}{8} \left\{ -6 \sin[(\tilde{\mu}_3^j - 8.75)z] + 4 \sin[(\tilde{\mu}_3^j + 0.75)z] \right. \\ &\quad \left. - \frac{12}{5} \sin[(\tilde{\mu}_3^j - 0.75)z] + \frac{18}{5} \sin[(\tilde{\mu}_3^j - 7.25)z] \right\}, \end{aligned}$$

$$\begin{aligned} [\mathbb{M}_2^{(j)}]_{21}(z) &= \frac{1}{8} \left\{ -30 \sin[(\tilde{\mu}_3^j - 8.75)z] - 20 \sin[(\tilde{\mu}_3^j + 0.75)z] \right. \\ &\quad \left. - 12 \sin[(\tilde{\mu}_3^j - 0.75)z] - 18 \sin[(\tilde{\mu}_3^j - 7.25)z] \right\}, \end{aligned}$$

$$\begin{aligned} [\mathbb{M}_2^{(j)}]_{22}(z) &= \frac{1}{8} \left\{ 60 \cos[(\tilde{\mu}_3^j - 8.75)z] - 40 \cos[(\tilde{\mu}_3^j + 0.75)z] \right. \\ &\quad \left. + 24 \cos[(\tilde{\mu}_3^j - 0.75)z] - 36 \cos[(\tilde{\mu}_3^j - 7.25)z] \right\}; \end{aligned}$$

- it is easy to show that for  $j = 3, 5$  (i.e.  $\tilde{\mu}_3^j = 4$ ) one gets a two-layer modified period map with a four-point Fourier spectrum and for which relations (3.4.10) are satisfied:

$$\begin{aligned} [\mathbb{M}_2^{(j=3,5)}]_{11}(z) &= +\frac{1}{2} \left[ \frac{5}{4} \cos(4.75z) + \frac{3}{4} \cos(3.25z) \right], \\ [\mathbb{M}_2^{(j=3,5)}]_{12}(z) &= +\frac{1}{2} \left[ \frac{5}{2} \sin(4.75z) - \frac{3}{2} \sin(3.25z) \right], \\ [\mathbb{M}_2^{(j=3,5)}]_{21}(z) &= +\frac{1}{2} \left[ \frac{5}{2} \sin(4.75z) + \frac{3}{2} \sin(3.25z) \right], \\ [\mathbb{M}_2^{(j=3,5)}]_{22}(z) &= +\frac{1}{2} \left[ 5 \cos(4.75z) - 3 \cos(3.25z) \right]; \end{aligned}$$

- get  $a_3 = \tilde{\mu}_3^{3,4}/n_3 = 2/5$ ;
- find the Fourier spectrum of  $\mathbb{M}_2(z)$ :  $\{4.75, -4.75, 3.25, -3.25\}$ ;

- focus on its maximum:  $\tilde{\mu}_2 = 4.75$ ;
- evaluate

$$n_1 = \left| \frac{c_+^{11}}{c_+^{12}} \right| = \left| \frac{c_+^{21}}{c_+^{22}} \right| = \frac{1}{2}, \quad n_2 = \left| \frac{c_+^{21}}{c_+^{11}} \right| = \left| \frac{c_+^{22}}{c_+^{21}} \right| = 2;$$

- compute  $\tilde{\mu}_2^j$  for  $j = 2, 3, 4$ :

$$\tilde{\mu}_2^2 = 4.75, \quad \tilde{\mu}_2^3 = 0.75, \quad \tilde{\mu}_2^4 = 4;$$

- we calculate  $\mathbb{M}_1^{(j)}(z)$  for  $j = 2, 3, 4$ :

$$\begin{aligned} [\mathbb{M}_1^{(j)}]_{11}(z) &= \frac{1}{4} \left\{ \frac{5}{2} \cos[(\tilde{\mu}_2^j - 4.75)z] + \frac{3}{2} \cos[(\tilde{\mu}_2^j - 3.25)z] \right\}, \\ [\mathbb{M}_1^{(j)}]_{12}(z) &= \frac{1}{4} \left\{ -5 \sin[(\tilde{\mu}_2^j - 4.75)z] + 3 \sin[(\tilde{\mu}_2^j - 3.25)z] \right\}, \\ [\mathbb{M}_1^{(j)}]_{21}(z) &= \frac{1}{4} \left\{ -5 \sin[(\tilde{\mu}_2^j - 4.75)z] - 3 \sin[(\tilde{\mu}_2^j - 3.25)z] \right\}, \\ [\mathbb{M}_1^{(j)}]_{22}(z) &= \frac{1}{4} \left\{ 10 \cos[(\tilde{\mu}_2^j - 4.75)z] - 6 \cos[(\tilde{\mu}_2^j - 3.25)z] \right\}, \end{aligned}$$

and it is easy to show that only for  $j = 4$  one gets a one-layer modified period map with a two-point Fourier spectrum and for which relations (3.4.10) are satisfied:

$$\mathbb{M}_1^{(j=2)}(z) = \begin{pmatrix} \cos(0.75z) & 2 \sin(0.75z) \\ 1/2 \sin(0.75z) & \cos(0.75z) \end{pmatrix};$$

- get  $a_2 = \tilde{\mu}_2^4/n_2 = q/n_2 = 4/2 = 2$  and from  $\mathbb{M}_1^{(j=4)}(z)$  realize that  $\mu_1 = 0.75$ ;
- finally, obtain  $a_1$  either from  $\mu_1 + q = \tilde{\mu}_2$  or from  $a_1 + a_2 = \lim_{z \rightarrow 0} M^{12}(z) = p$  (see Eq. (3.1.11)) and find  $a_1 = 1$ . Alternatively one gets  $a_1$  straight from  $\mu_1$  using the known  $n_1$  value.

### 3.4.3 Recovery from the Hill discriminant

As we saw in the previous Sections, it is possible to implement an inversion procedure for a monodimensional photonic crystal starting from the period

map. It is also well known that a necessary and sufficient condition to get the band structure is to impose that the trace of the period map (Hill discriminant) belongs to the interval  $[-2, 2]$ . But it can be useful trying to answer the following question: what happens if we don't want to start from the period map but from its trace which gives the band structure in a more immediate way? If we start from the period map trace, we are using less information than we'd do if we used the whole period map, and consequently we have to reduce the number of free parameters that characterize the system. Let us then see how to proceed. In the piecewise constant case the Hill discriminant is given by:

$$\begin{aligned} \Delta(z) = \text{Tr}M(z) &= \mathbf{M}_{11}(z) + \mathbf{M}_{22}(z) = \\ &= \sum (c_{\sigma_2, \dots, \sigma_m}^{11} + c_{\sigma_2, \dots, \sigma_m}^{22}) \cos((\mu_1 + \sigma_2 \mu_2 + \dots + \sigma_m \mu_m)z), \end{aligned}$$

where

$$\begin{aligned} \mathbf{c}_{\sigma_2, \dots, \sigma_m} &\stackrel{\text{def}}{=} \begin{pmatrix} c_{\sigma_2, \dots, \sigma_m}^{11} & c_{\sigma_2, \dots, \sigma_m}^{12} \\ c_{\sigma_2, \dots, \sigma_m}^{21} & c_{\sigma_2, \dots, \sigma_m}^{22} \end{pmatrix} \\ &= \frac{1}{2^{m-1}} \begin{pmatrix} 1 & \frac{\sigma_m}{n_m} \\ \sigma_m n_m & 1 \end{pmatrix} \cdots \begin{pmatrix} 1 & \frac{\sigma_2}{n_2} \\ \sigma_2 n_2 & 1 \end{pmatrix} \begin{pmatrix} 1 & \frac{1}{n_1} \\ n_1 & 1 \end{pmatrix}. \end{aligned}$$

If we start from the Hill discriminant, we need to fix another parameter as  $n_1$  (or  $n_m$ ) in order to get the period map and then do the inversion. In fact the knowledge of  $n_1$  makes us get the non-diagonal entries of matrix  $\mathbf{c}$  via the well known formulae:

$$\frac{c_{\sigma_2, \dots, \sigma_m}^{11}}{c_{\sigma_2, \dots, \sigma_m}^{12}} = \frac{c_{\sigma_2, \dots, \sigma_m}^{21}}{c_{\sigma_2, \dots, \sigma_m}^{22}} = n_1,$$

from which one gets:

$$c_{\sigma_2, \dots, \sigma_m}^{12} = \frac{c_{\sigma_2, \dots, \sigma_m}^{11}}{n_1}, \quad c_{\sigma_2, \dots, \sigma_m}^{21} = n_1 c_{\sigma_2, \dots, \sigma_m}^{22}. \quad (3.4.16)$$

Let us see two examples to understand how things work.

**Example 3.4.3** In this example we focus on a three layer photonic crystal.

In this case the Hill discriminant has the following form:

$$\begin{aligned}
\Delta(z) = & \sum_{\sigma_3, \sigma_2 = \pm 1} \left\{ \frac{1}{2^2} \left( 1 + \frac{n_1}{\sigma_2 n_2} + \frac{n_1 + \sigma_2 n_2}{\sigma_3 n_3} \right) + \frac{1}{2^2} \left[ 1 + \frac{\sigma_2 n_2}{n_1} + \sigma_3 n_3 \left( \frac{1}{n_1} + \frac{1}{\sigma_2 n_2} \right) \right] \right\} \\
& \times \cos[(n_1 a_1 + \sigma_2 n_2 a_2 + \sigma_3 n_3 a_3)z] = \left\{ \frac{1}{2^2} \left( 1 + \frac{n_1}{n_2} + \frac{n_1 + n_2}{n_3} \right) \right. \\
& \left. + \frac{1}{2^2} \left[ 1 + \frac{n_2}{n_1} + n_3 \left( \frac{1}{n_1} + \frac{1}{n_2} \right) \right] \right\} \cos[(n_1 a_1 + n_2 a_2 + n_3 a_3)z] + \\
& \left\{ \frac{1}{2^2} \left( 1 - \frac{n_1}{n_2} + \frac{n_1 - n_2}{n_3} \right) + \frac{1}{2^2} \left[ 1 - \frac{n_2}{n_1} + n_3 \left( \frac{1}{n_1} - \frac{1}{n_2} \right) \right] \right\} \\
& \times \cos[(n_1 a_1 - n_2 a_2 + n_3 a_3)z] + \left\{ \frac{1}{2^2} \left( 1 + \frac{n_1}{n_2} - \frac{n_1 + n_2}{n_3} \right) \right. \\
& \left. + \frac{1}{2^2} \left[ 1 + \frac{n_2}{n_1} - n_3 \left( \frac{1}{n_1} + \frac{1}{n_2} \right) \right] \right\} \cos[(n_1 a_1 + n_2 a_2 - n_3 a_3)z] + \\
& \left\{ \frac{1}{2^2} \left( 1 - \frac{n_1}{n_2} - \frac{n_1 - n_2}{n_3} \right) + \frac{1}{2^2} \left[ 1 - \frac{n_2}{n_1} - n_3 \left( \frac{1}{n_1} - \frac{1}{n_2} \right) \right] \right\} \\
& \times \cos[(n_1 a_1 - n_2 a_2 - n_3 a_3)z] ,
\end{aligned}$$

which can be written as follows:

$$\Delta(z) = (\alpha_1 + \beta_1) \cos(\gamma_1 z) + (\alpha_2 + \beta_2) \cos(\gamma_2 z) + (\alpha_3 + \beta_3) \cos(\gamma_3 z) + (\alpha_4 + \beta_4) \cos(\gamma_4 z) ,$$

and it is very easy to get the associated period map as long as either  $n_1$  or  $n_3$  is known. For instance, let's consider the case where we want to find a three layer photonic crystal geometrical characteristics (except of  $n_1 = 1.5$ ) and which has the following band structure (see figure 3.3):

$$\begin{aligned}
\Delta(z) = & \frac{1}{4} [(3.75 + 5) \cos(5.1z) + (1.25 - 1.667) \cos(1.9z) \\
& + (-0.25 - 0.333) \cos(1.1z) + (-0.75 + 1) \cos(-2.1z)] . \quad (3.4.17)
\end{aligned}$$

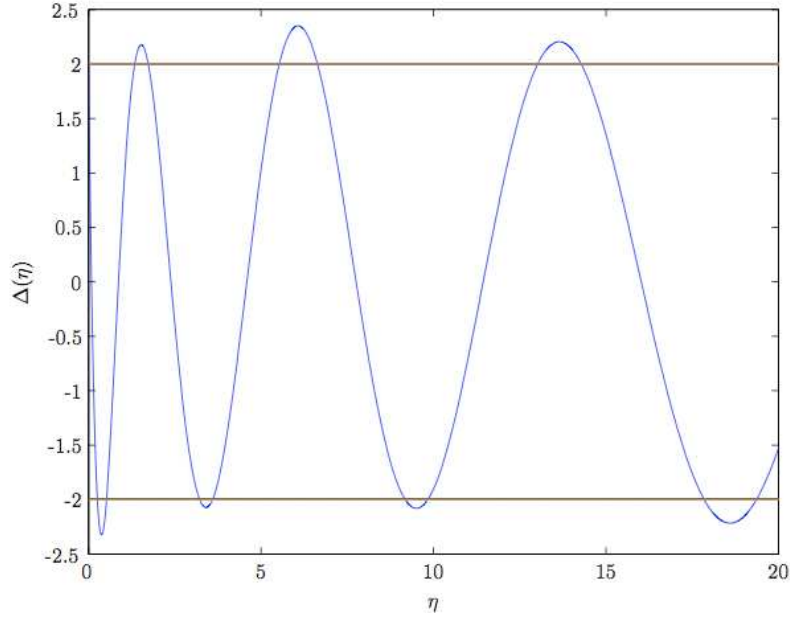


**Figure 3.3:** Band structure of a photonic crystal whose Hill discriminant is given by Eq. 3.4.17.

Thus one builds the period map using the given  $n_1$  value:

$$\begin{aligned}
 M_3^{11}(z) &= \frac{1}{4} [3.75 \cos(5.1z) + 1.25 \cos(1.9z) - 0.25 \cos(1.1z) - 0.75 \cos(2.1z)] , \\
 M_3^{12}(z) &= \frac{1}{4} [2.5 \sin(5.1z) + 0.8333 \sin(1.9z) - 0.1667 \sin(1.1z) + 0.5 \sin(2.1z)] , \\
 M_3^{21}(z) &= -\frac{1}{4} [7.5 \sin(5.1z) - 2.5 \sin(1.9z) - 0.5 \sin(1.1z) - 1.5 \sin(2.1z)] , \\
 M_3^{22}(z) &= \frac{1}{4} [5 \cos(5.1z) - 1.667 \cos(1.9z) - 0.333 \cos(1.1z) - 1.0 \cos(2.1z)] ,
 \end{aligned}$$

and from here the inversion procedure is well known (see Sec. 3.4) and it gives  $n_2 = 1$ ,  $n_3 = 2$ ,  $a_1 = 1$ ,  $a_2 = 2$  and  $a_3 = 0.8$ . We also know that

$$p = \lim_{z \rightarrow 0} M^{12}(z) , \quad (3.4.18)$$

in fact we have ( $n_1 = 1.5$ ):

$$\frac{3.75}{n_1} 5.1 + \frac{1.25}{n_1} 1.9 - \frac{0.25}{n_1} 1.1 + \frac{0.75}{n_1} 2.1 = 3.8 = a_1 + a_2 + a_3 = p .$$

Consequently this fact gives us the way to use give the period  $p$  as inden-

dent parameter instead of  $n_1^4$ . We in fact realize that from the given Hill discriminant, one has:

$$\frac{\alpha_1}{n_1}\gamma_1 + \frac{\alpha_2}{n_1}\gamma_2 + \frac{\alpha_3}{n_1}\gamma_3 + \frac{\alpha_4}{n_1}\gamma_4 = p ,$$

from which

$$n_1 = (\alpha_1\gamma_1 + \alpha_2\gamma_2 + \alpha_3\gamma_3 + \alpha_4\gamma_4)/p . \quad (3.4.19)$$

The generalization of this to an  $m$ -layer photonic crystal is straightforward.

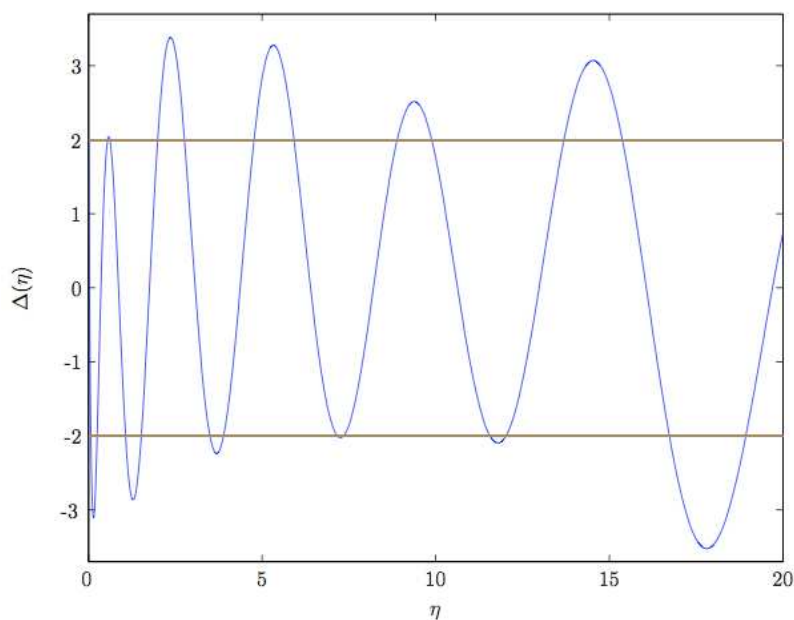


**Figure 3.4:** Band structure of a photonic crystal whose Hill discriminant is given by Eq. 3.4.20.

**Example 3.4.4** We want to find the geometrical features of a four-layer photonic crystal, knowing its band structure  $\Delta(z)$  and its period  $p$ . Then we

---

<sup>4</sup>The corresponding case where one wants to give  $n_m$  is very similar.

have the photonic band structure

$$\begin{aligned}
 \Delta(z) = & \frac{1}{8} [(15.925 + 5.3083) \cos(8.2z) + (-3.675 + 1.225) \cos(6z) \\
 & + (1.575 + 0.525) \cos(3.4z) + (-0.975 - 0.325) \cos(1.8z) \\
 & + (-6.825 + 2.275) \cos(1.2z) + (0.225 - 0.075) \cos(-0.4z) \\
 & + (-0.525 - 0.175) \cos(-3z) + (2.275 - 0.7583) \cos(-5.2z)] ,
 \end{aligned}
 \tag{3.4.20}$$

which is depicted in Fig. 3.4 and we know that the period crystal is  $p = 7.8$ . So we can get  $n_1 = (\alpha_i \gamma_i) / p = 1.5$  and then we can compute the period map exactly as we did in the previous example. From there the inversion is straightforward and it gives  $n_2 = 2$ ,  $n_3 = 0.8$ ,  $n_4 = 0.5$ ,  $a_1 = 1$ ,  $a_2 = 1.6$ ,  $a_3 = 3$  and  $a_4 = 2.2$ .

# Chapter 4

## Two-Dimensional Photonic Crystals

In this chapter we discuss several existing numerical methods to compute the band spectrum of a periodic 2D photonic crystal and develop two, closely related, numerical methods. In the 2D case the harmonic modes can be decomposed into two independent polarizations, the TE mode and the TM mode. Numerical methods will be discussed and developed for either mode. Prior to discussing a method, we shall often dwell on the corresponding 1D problem first.

In a 2D photonic crystal there exists a preferred direction, which we take to be the  $z$ -direction, such that its optical properties do not depend on  $z \in \mathbb{R}$  and hence only depend on  $(x, y) \in \mathbb{R}^2$ . In particular, the dielectric constant only depends on  $(x, y) \in \mathbb{R}^2$ , i.e.,  $\varepsilon = \varepsilon(x, y)$ , so that the refractive index only depends on  $(x, y) \in \mathbb{R}^2$ , i.e.,  $n = n(x, y)$  (see Fig. 4.1). If we then restrict ourselves to a physical situation in which one of the electric or magnetic fields has  $x$  and  $y$  components only depending on  $(x, y)$  and a zero  $z$ -component and the other field has a  $z$ -component only depending on  $(x, y)$  and zero  $x$  and  $y$  components, we obtain the TE and TM modes, depending on which field has a zero  $z$ -component.

The photonic band spectrum can be computed numerically by a method belonging to one of two basic families of methods. A time domain method consists of the numerical solution of a wave equation and an a posteriori Fourier analysis to extract the band spectrum. In this chapter we shall briefly discuss this type of method but avoid using it. On the other hand, a frequency domain method consists of the numerical solution of the Helmholtz equation for a selection of fixed wavevectors  $\mathbf{k}$  to extract the band spectrum. This will be the type of method adopted in this chapter. We adopt two

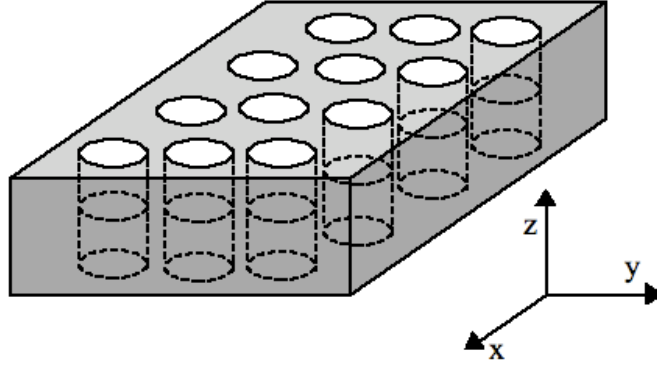


**Figure 4.1:** A two-dimensional photonic crystal of air columns in a dielectric substrate (which we imagine to extend indefinitely in the  $z$  direction). The columns have radius  $r$  and dielectric constant  $\varepsilon = 1$ , whereas the substrate has dielectric constant  $\varepsilon > 1$ .

methods within this family, a finite difference method and a finite element method. We also discuss two other frequency domain methods briefly.

The finite difference and the finite element methods have both been used to compute the photonic band spectrum before. In this chapter we present these methods in such a way that the resulting algebraic systems can be solved numerically by so-called structured matrix codes. This means that we will examine the structure of the matrices resulting from their implementation and exploit it to reduce the computational complexity of our methods.

When discretizing the 2D photonic crystal in such a way that points differing by an integer linear combination of the periodic basis vectors are identified, the resulting linear system is of the type

$$(A - \eta B)\psi = 0,$$

where  $A$  is a two-index circulant matrix (i.e., a circulant matrix whose entries are themselves circulant matrices) and  $B$  is a positive two-index diagonal matrix for the TM mode and a positive two-index circulant matrix for the TE mode. The wavevector dependence is limited to  $A$ . In these cases structured matrix codes can be used with a computational complexity of the order of  $O(n \log(n))$ , where  $n$  is the order of the matrices  $A$  and  $B$  (or the number of discretization points per period parallelogram).

In Sec. 4.1 we present the basic formalism of nD photonic crystals and define the Brillouin zones. This means using the Bloch representation of the Helmholtz solutions to reduce the relevant wavevectors  $\mathbf{k}$  to as small a set

as possible. In Sec. 4.2 we discuss the TM and TE modes. It will turn out to be advantageous to solve the electric eigenvalue problem for the TM mode and the magnetic eigenvalue problem for the TE mode. In Sec. 4.3 we explore solving the Helmholtz equation, for a rectangular crystal, by separation of variables, a method which will turn out to be riddled with technical problems. In Sections 4.4 and 4.5 a variety of numerical methods will be discussed: two time domain methods, namely the finite difference time domain (FDTD) method and plane wave expansion (PWE) method, and four frequency domain methods, namely the multiple scattering (MS), Fourier expansion (FE), finite difference frequency domain (FDFD), and finite element frequency domain (FEFD) methods. Two new frequency domain methods are also introduced in this thesis, that is, the periodic finite difference (PFD) method and the periodic finite element (PFE) method. In both cases the periodicity conditions are automatically satisfied in the algebraic problem obtained by discretizing the spectral problem or by using a finite element technique.

## 4.1 nD crystals and Brillouin zones

Mathematically, an nD periodic crystal can be described as an integer lattice that remains invariant upon translation of a spatial variable  $\mathbf{x} \in \mathbb{R}^n$  by integer linear combinations of the  $n$  linearly independent vectors  $\mathbf{a}_1, \dots, \mathbf{a}_n$ . These vectors generate the so-called *period parallelogram*

$$\mathbf{A} = \{t_1 \vec{\mathbf{a}}_1 + \dots + t_n \vec{\mathbf{a}}_n : t_1, \dots, t_n \in [0, 1)\},$$

also called the *fundamental cell* of the crystal.

To deal with periodicity of the (modified) Helmholtz equation we need to introduce the so-called reciprocal lattice which is invariant under translation of the wave vector  $\mathbf{k} \in \mathbb{R}^n$  by integer linear combinations of the linearly independent vectors  $\mathbf{b}_1, \dots, \mathbf{b}_n$  such that

$$\mathbf{a}_j \cdot \mathbf{b}_l = 2\pi \delta_{j,l}, \quad j, l = 1, \dots, n. \quad (4.1.1)$$

These vectors generate the *reciprocal period parallelogram*

$$\mathbf{B} = \{t_1 \mathbf{b}_1 + \dots + t_n \mathbf{b}_n : t_1, \dots, t_n \in \mathbb{Z}\}.$$

From (4.1.1) it is clear that the matrix  $B$  composed of the  $n$  column vectors  $\mathbf{b}_1, \dots, \mathbf{b}_n$  is given by

$$B \stackrel{\text{def}}{=} \text{col}(\mathbf{b}_1, \dots, \mathbf{b}_n) = 2\pi [\text{col}(\mathbf{a}_1, \dots, \mathbf{a}_n)^T]^{-1} \stackrel{\text{def}}{=} 2\pi (A^T)^{-1}, \quad (4.1.2)$$

where  $A \stackrel{\text{def}}{=} \text{col}(\mathbf{a}_1, \dots, \mathbf{a}_n)$ . In other words,  $\mathbf{b}_1, \dots, \mathbf{b}_n$  are the columns of an  $n \times n$  matrix  $B$  that is  $2\pi$  times the inverse transpose of the  $n \times n$  matrix  $A$  having  $\mathbf{a}_1, \dots, \mathbf{a}_n$  as its columns. As a result, for arbitrary real numbers  $t_1, \dots, t_n$ , we have

$$\begin{aligned} \|t_1 \mathbf{b}_1 + \dots + t_n \mathbf{b}_n\|^2 &= (t_1 \ \dots \ t_n) B^T B \begin{pmatrix} t_1 \\ \vdots \\ t_n \end{pmatrix} \\ &= 4\pi^2 (t_1 \ \dots \ t_n) (A^T A)^{-1} \begin{pmatrix} t_1 \\ \vdots \\ t_n \end{pmatrix}, \end{aligned}$$

where  $A^T A$  is the Gram matrix of the vectors  $\mathbf{a}_1, \dots, \mathbf{a}_n$  and  $B^T B$  is the Gram matrix of the vectors  $\mathbf{b}_1, \dots, \mathbf{b}_n$ . The  $nD$  volumes of  $\mathbf{A}$  and  $\mathbf{B}$  are given by  $m(\mathbf{A}) \stackrel{\text{def}}{=} |\det A|$  and  $m(\mathbf{B}) \stackrel{\text{def}}{=} |\det B|$ , respectively, and hence

$$m(\mathbf{A})m(\mathbf{B}) = |(\det A)(\det B)| = |\det(A^T B)| = |\det(2\pi I_n)| = (2\pi)^n,$$

i.e., the product of the  $nD$  volumes of the period parallelogram and the reciprocal period parallelogram equals  $(2\pi)^n$ .

Consider the Helmholtz equation

$$-\nabla^2 \psi(\mathbf{x}) = \eta n(\mathbf{x})^2 \psi(\mathbf{x}), \quad (4.1.3)$$

where  $\psi(\mathbf{x})$  is a function satisfying the  $\tau$ -periodic boundary conditions  $\psi(\mathbf{x} + \mathbf{a}_j) = \tau_j \psi(\mathbf{x})$ ,  $n(\mathbf{x})$  is a positive function satisfying  $n(\mathbf{x} + \mathbf{a}_j) = n(\mathbf{x})$  ( $j = 1, \dots, n$ ), and  $\eta$  is a spectral parameter. Then the spectrum of (4.1.3), defined as the set of those  $\eta$  for which (4.1.3) has a nontrivial bounded solution  $\psi(\mathbf{x})$ , is known to be the union of the spectra of (4.1.3) under all conceivable  $\tau$ -periodic boundary conditions

$$\psi(\mathbf{x} + \mathbf{a}_j) = \tau_j \psi(\mathbf{x}), \quad j = 1, \dots, n,$$

where  $|\tau_1| = \dots = |\tau_n| = 1$  and  $\tau = (\tau_1, \dots, \tau_n)$ . The proof of this result can be given as for the  $nD$  Schrödinger equation [20].

Let us write

$$\tau_j = e^{i\mathbf{k} \cdot \mathbf{a}_j}, \quad j = 1, \dots, n, \quad (4.1.4)$$

for a suitable wavevector  $\mathbf{k}$  for which (4.1.4) is true. Then any two wavevectors  $\mathbf{k}$  yielding the same  $\tau_j$  differ by an integer linear combination of the reciprocal basis vectors  $\mathbf{b}_1, \dots, \mathbf{b}_n$ . As a result, to describe the band spectrum as the union of the spectra of the Helmholtz equations under all conceivable

$\tau$ -periodic boundary conditions, we can limit ourselves to those vectors  $\mathbf{k}$  which belong to the *Brillouin zone*

$$\mathbf{Z} = \left\{ \mathbf{x} \in \mathbb{R}^n : \|\mathbf{x}\| \leq \left\| \mathbf{x} - \sum_{j=1}^n m_j \mathbf{b}_j \right\| \text{ for every } (m_1, \dots, m_n) \in \mathbb{Z}^n \right\}, \quad (4.1.5)$$

introduced for the first time in [44]. For each wavevector  $\mathbf{k} \in \mathbb{R}^n$  there exists a wavenumber  $\mathbf{k}' \in \mathbf{Z}$  such that  $\mathbf{k} - \mathbf{k}'$  is an integer linear combination of the reciprocal basis vectors and therefore  $\mathbf{k}$  and  $\mathbf{k}'$  generate the same  $\tau$ -values:  $\tau_j = e^{i\mathbf{k} \cdot \mathbf{a}_j} = e^{i\mathbf{k}' \cdot \mathbf{a}_j}$  ( $j = 1, \dots, n$ ).

When computing the band spectrum of the Helmholtz equation, one can often restrict oneself to wavevectors  $\mathbf{k}$  belonging to a proper subset of  $\mathbf{Z}$ , because in some cases different wavevectors in  $\mathbf{Z}$  lead to the same Helmholtz eigenvalues. For instance, by replacing  $\mathbf{k} = t_1 \mathbf{b}_1 + \dots + t_n \mathbf{b}_n$  by  $\sigma_1 t_1 \mathbf{b}_1 + \dots + \sigma_n t_n \mathbf{b}_n$  for any choice of signs  $\sigma_j = \pm 1$ , we replace the  $(\tau_1, \dots, \tau_n)$ -periodic boundary conditions, with  $\tau_j = e^{2\pi i t_j}$ , by  $(\tau_1^{\sigma_1}, \dots, \tau_n^{\sigma_n})$ -periodic boundary conditions. If we then also replace the corresponding Helmholtz solution  $\psi(\mathbf{x})$  by  $\psi(\sigma_1 x_1, \dots, \sigma_n x_n)$ , we see that the eigenvalues remain the same, provided  $n(\sigma_1 x_1, \dots, \sigma_n x_n) = n(\mathbf{x})$ . Thus for constant refractive index, among the various  $\sigma_1 t_1 \mathbf{b}_1 + \dots + \sigma_n t_n \mathbf{b}_n$  in the Brillouin zone  $\mathbf{Z}$ , we may restrict ourselves to just one choice of sign  $\sigma_1, \dots, \sigma_n$ .

More generally, consider an arbitrary isometry  $J$  in  $\mathbb{R}^n$  which maps the reciprocal lattice onto itself. Then  $J$  is an affine transformation in the sense that

$$J(\mathbf{x}) = U_J \mathbf{x} + m_1 \mathbf{b}_1 + \dots + m_n \mathbf{b}_n, \quad \mathbf{x} \in \mathbb{R}^n,$$

where  $U_J$  is an orthogonal  $n \times n$  matrix and  $m_1, \dots, m_n$  are suitable integers which are uniquely determined by  $J$ . In fact, there are unique integers  $m_1, \dots, m_n$  such that a translation of  $J(\mathbf{B})$  by  $m_1 \mathbf{b}_1 + \dots + m_n \mathbf{b}_n$  yields  $\mathbf{B}$ . When defining

$$\tilde{J}(\mathbf{x}) = J(\mathbf{x}) - m_1 \mathbf{b}_1 - \dots - m_n \mathbf{b}_n, \quad \mathbf{x} \in \mathbb{R}^n,$$

each reciprocal lattice invariant isometry  $J$  generates a unique isometry  $\tilde{J}$  which leaves invariant the Brillouin zone  $\mathbf{Z}$ . These isometries  $\tilde{J}$  form a finite group which is completely determined by  $\mathbf{Z}$  and which has at least  $2^n$  elements. We now single out a *restricted Brillouin zone*  $\mathbf{Z}_0$  as such a subset of  $\mathbf{Z}$  that

$$\mathbf{Z} = \bigcup_{\tilde{J}} \tilde{J}[\mathbf{Z}_0].$$

Then for constant refractive index we may restrict ourselves to studying the Helmholtz spectra for the wavenumbers  $\mathbf{k} \in \mathbf{Z}_0$ .

If, in the TM case, the refractive index is a periodic function varying with position, we need to take into account the change in its values when transforming the lattice. In this case we need to restrict ourselves to those isometries  $J$  satisfying

$$n(U_J \mathbf{x}) = n(\mathbf{x}), \quad \mathbf{x} \in \mathbb{R}^n,$$

when determining a restricted Brillouin zone  $\mathbf{Z}$ . When changing the Helmholtz eigenfunctions  $\psi(\mathbf{x})$  by  $\psi(U_J \mathbf{x})$ , we obtain Helmholtz eigenfunctions for exactly the same eigenvalues and hence the Helmholtz spectra do not change. In the TE case, we need to restrict ourselves to those isometries  $J$  such that the dielectric constants  $\varepsilon(\mathbf{x})$  satisfy

$$\varepsilon(U_J \mathbf{x}) = \varepsilon(\mathbf{x}), \quad \mathbf{x} \in \mathbb{R}^n.$$

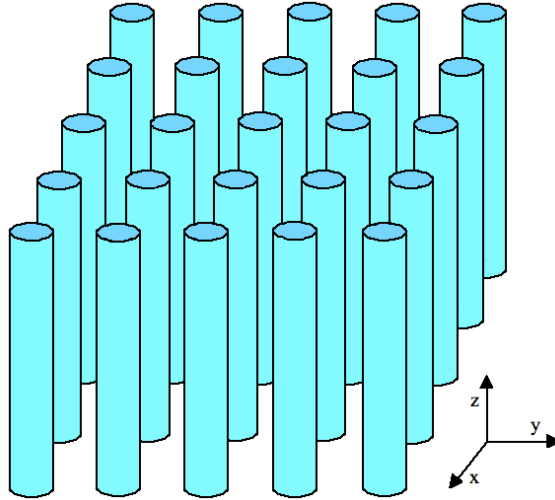


**Figure 4.2:** A two-dimensional photonic crystal made of a square lattice of columns consisting of a material with a different dielectric constant, with radius  $r$  and dielectric constant  $\varepsilon(x, y)$ . The material does not change its physical properties along the  $z$  direction, and periodic along the  $x$  and  $y$  directions.

**Example 4.1.1** If we consider the photonic crystal shown in Fig. 4.2, we realize that its period parallelogram (fundamental cell) is a square. As a

result, the linearly independent vectors  $\mathbf{a}_1$  and  $\mathbf{a}_2$  are:

$$\mathbf{a}_1 = a \begin{pmatrix} 1 \\ 0 \end{pmatrix}, \quad \mathbf{a}_2 = a \begin{pmatrix} 0 \\ 1 \end{pmatrix},$$

where  $a^2$  is the area of the square. Since  $A$  is the matrix having the vectors  $\mathbf{a}_1$  and  $\mathbf{a}_2$  as its columns, we can easily compute the matrix  $B$  using (4.1.2):

$$B = 2\pi(A^T)^{-1} = 2\pi \begin{pmatrix} a & 0 \\ 0 & a \end{pmatrix}^{-1} = \frac{2\pi}{a} \begin{pmatrix} 1 & 0 \\ 0 & 1 \end{pmatrix},$$

and therefore the reciprocal basis vectors are

$$\mathbf{b}_1 = \frac{2\pi}{a} \begin{pmatrix} 1 \\ 0 \end{pmatrix}, \quad \mathbf{b}_2 = \frac{2\pi}{a} \begin{pmatrix} 0 \\ 1 \end{pmatrix}.$$

In general, if the period parallelogram is spanned by orthogonal basis vectors, the reciprocal period parallelogram is spanned by orthogonal basis vectors too (Fig. 4.3). Indeed, if  $A^T A = D = \text{diag}(D_1, \dots, D_n)$  is a diagonal matrix, then  $B = 2\pi A D^{-1}$  and hence  $\mathbf{b}_j = (2\pi/D_j)\mathbf{a}_j$  ( $j = 1, \dots, n$ ). The Brillouin zone  $\mathbf{Z}$  defined by (4.1.5) can be constructed as follows (see Fig. 4.3). Take its center point as the origin and draw the perpendicular bisectors (blue) of all segments connecting the origin to any other lattice point (red). Then the bisectors divide the euclidean plane into polygons. The Brillouin zone  $\mathbf{Z}$  (yellow) then coincides with the polygon having the origin as its interior points. In the case of a square lattice with constant refractive index, the restricted Brillouin zone  $\mathbf{Z}_0$  is given by one eighth of the Brillouin zone and therefore is given by the blue triangle shown in Fig. 4.3.

**Example 4.1.2** If we consider the photonic crystal shown in Fig. 4.4, we realize that its period parallelogram (fundamental cell) has four edges of the same length  $a$  and two  $60^\circ$  angles. In this case the linearly independent vectors  $\mathbf{a}_1$  and  $\mathbf{a}_2$  are as follows:

$$\mathbf{a}_1 = \frac{a}{2} \begin{pmatrix} 1 \\ \sqrt{3} \end{pmatrix}, \quad \mathbf{a}_2 = \frac{a}{2} \begin{pmatrix} 1 \\ -\sqrt{3} \end{pmatrix},$$

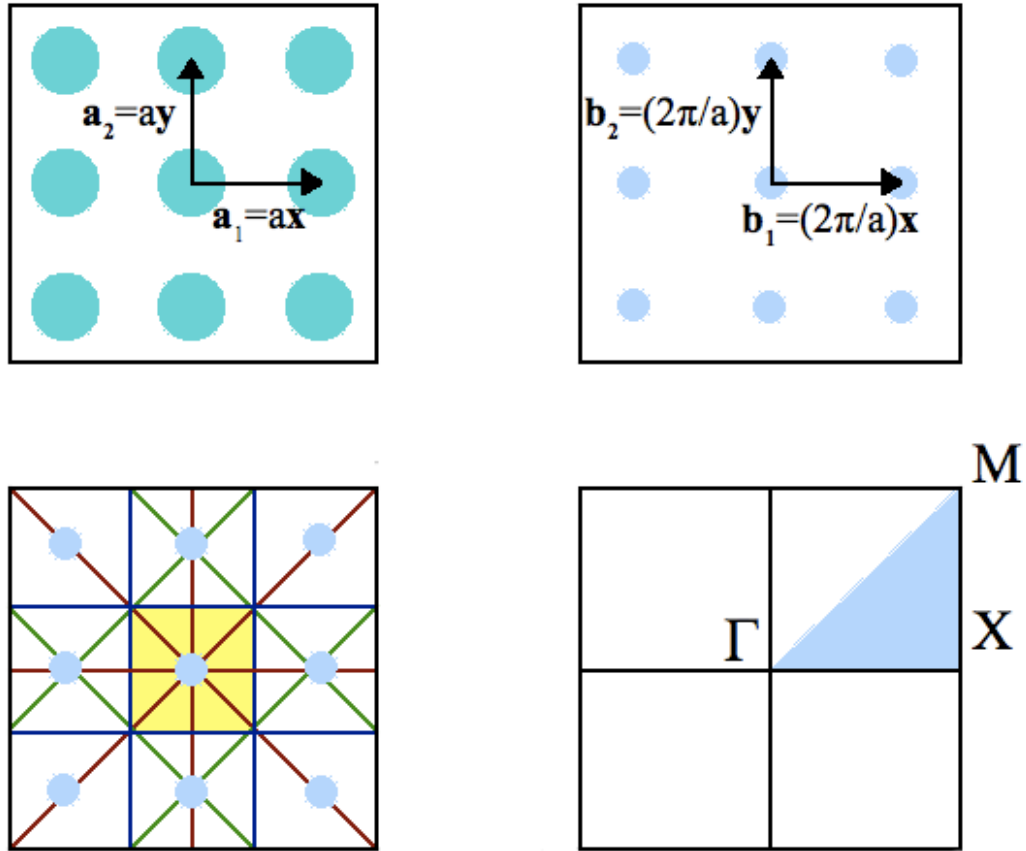


**Figure 4.3:** The top half of the figure shows a square lattice. On the left the lattice points of the period parallelogram are depicted while the lattice points of the reciprocal period parallelogram are depicted on the right. The bottom half of the figure shows its Brillouin zone and (in blue) the restricted Brillouin zone  $\mathbf{Z}_0$  to be considered when computing the spectrum.

Using (4.1.2) we have

$$\frac{B}{2\pi} = (A^T)^{-1} = \left[ \frac{a}{2} \begin{pmatrix} 1 & \sqrt{3} \\ 1 & -\sqrt{3} \end{pmatrix} \right]^{-1} = \frac{1}{a} \begin{pmatrix} 1 & 1 \\ 1/\sqrt{3} & -1/\sqrt{3} \end{pmatrix},$$

and therefore the reciprocal vectors are (Fig. 4.4)

$$\mathbf{b}_1 = \frac{2\pi}{a} \begin{pmatrix} 1 \\ 1/\sqrt{3} \end{pmatrix}, \quad \mathbf{b}_2 = \frac{2\pi}{a} \begin{pmatrix} 1 \\ -1/\sqrt{3} \end{pmatrix}.$$

Considering (4.1.5), the construction of the Brillouin zone is the same as for the previous example (see Fig. 4.4), and in this case the restricted Brillouin zone  $\mathbf{Z}_0$  to be considered to get the photonic crystal spectrum for a constant refractive index, is given by one twelfth of the Brillouin zone and therefore is given by the blue triangle highlighted in Fig. 4.4.

## 4.2 TM and TE eigenvalue problems

In 2D photonic crystals we can choose the cartesian coordinates in such a way that its dielectric properties only depend on  $(x, y) \in \mathbb{R}^2$  and not on  $z \in \mathbb{R}$ . In this case the electric and magnetic fields can be decomposed in a natural way into **two distinct polarizations** (see Fig. 4.5):

- **transverse electric (TE) modes** where  $\mathbf{H} = (0, 0, H(x, y))^T$  and  $\mathbf{E} = (E_1(x, y), E_2(x, y), 0)^T$ ,
- **transverse magnetic (TM) modes** where  $\mathbf{E} = (0, 0, E(x, y))^T$  and  $\mathbf{H} = (H_1(x, y), H_2(x, y), 0)^T$ .

Let's start discussing the eigenvalue problem for the magnetic field (1.3.11):

$$\begin{cases} \nabla \times \left( \frac{1}{\varepsilon(\mathbf{r})} \nabla \times \mathbf{H}(\mathbf{r}) \right) = \eta \mathbf{H}(\mathbf{r}), \\ \nabla \cdot [\mathbf{H}(\mathbf{r})] = 0, \end{cases} \quad (4.2.1)$$

where  $\varepsilon(\mathbf{r})$  depends only on  $(x, y) \in \mathbb{R}^2$ . Writing the components of the left-hand side of the eigenvalue equation, we get:

$$\epsilon_{ijk} \partial_j \left( \frac{1}{\varepsilon(x, y)} \epsilon_{klm} \partial_l H_m(x, y) \right) = \epsilon_{ijk} \epsilon_{klm} \partial_j \left( \frac{\partial_l H_m(x, y)}{\varepsilon(x, y)} \right) =$$

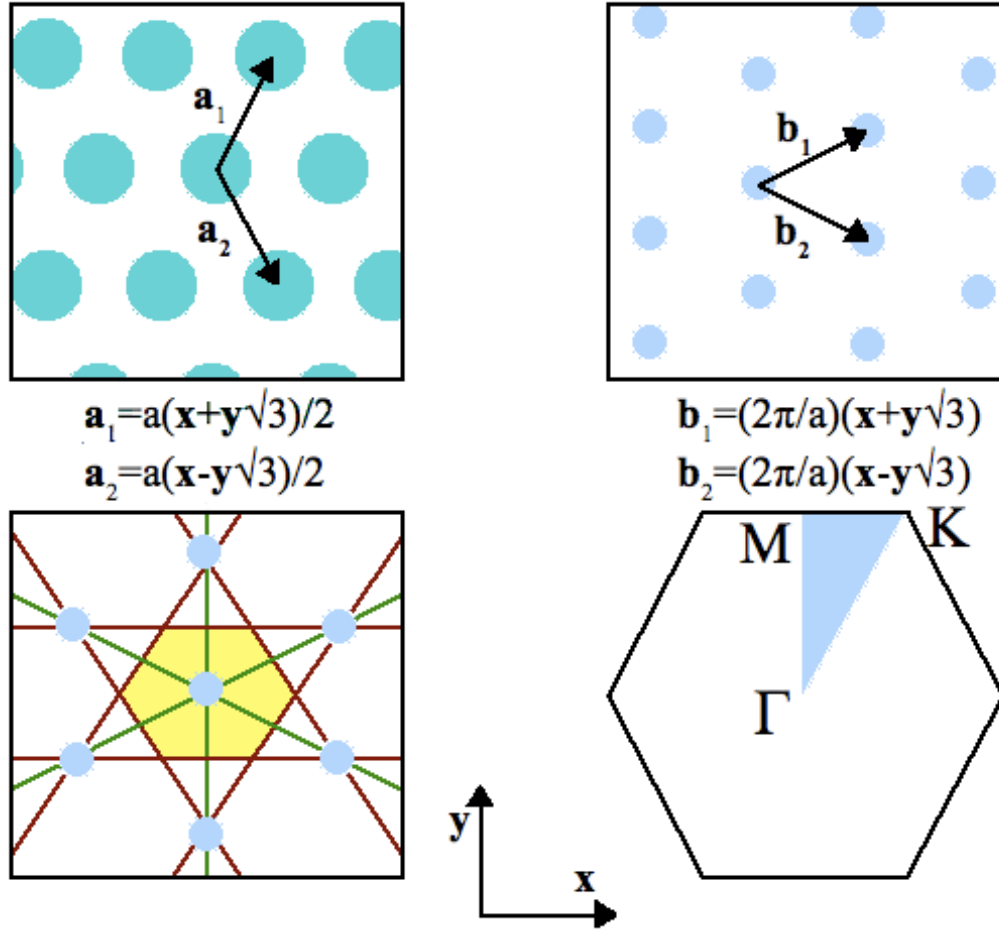


**Figure 4.4:** The top half of figure shows a parallelogram lattice. On the left the lattice points of the period parallelogram are depicted while the lattice points of the reciprocal period parallelogram are depicted on the right. In this case the reciprocal vectors  $\mathbf{b}_1$  and  $\mathbf{b}_2$  are a rotated version of the vectors  $\mathbf{a}_1$  and  $\mathbf{a}_2$ . The bottom half of figure shows its Brillouin zone, which is given by a hexagon centered around the origin, and (in blue) the restricted Brillouin zone  $\mathbf{Z}_0$  to be considered for computing the spectrum.

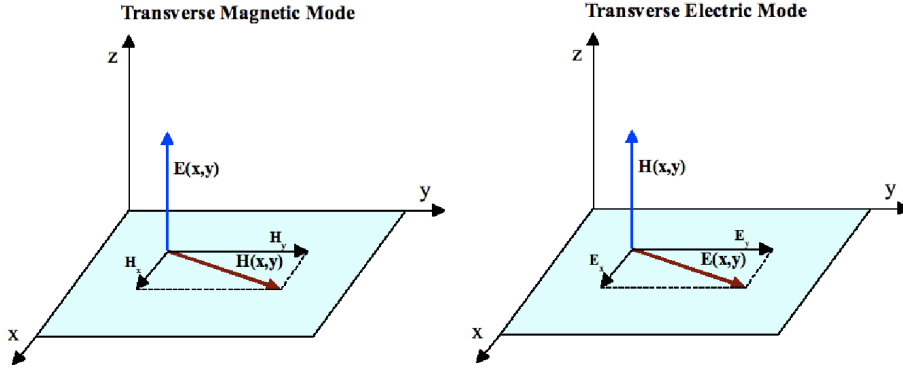


**Figure 4.5:** In the TM mode the magnetic field is confined to the  $xy$  plane and the electric field is aligned along the  $z$ -axis, whereas in the TE mode the electric field is confined to the  $xy$  plane and the magnetic field is aligned along the  $z$ -axis.

$$(\delta_{il}\delta_{jm} - \delta_{im}\delta_{jl})\partial_j \left( \frac{\partial_l H_m(x, y)}{\varepsilon(x, y)} \right) = \partial_j \left( \frac{\partial_i H_j(x, y)}{\varepsilon(x, y)} \right) - \partial_j \left( \frac{\partial_j H_i(x, y)}{\varepsilon(x, y)} \right),$$

where  $\epsilon_{ijk}$  is the Levi-Civita tensor. In the **transverse electric** configuration we have  $i = 3$  and it's straightforward to see that the eigenvalue problem (1.3.11) takes the following form:

$$\begin{cases} -\partial_j \left( \frac{1}{\varepsilon(x,y)} \partial_j H_3(x, y) \right) = \eta H_3(x, y), & j = 1, 2, \\ \partial_3 [H_3(x, y)] = 0, \end{cases} \quad (4.2.2)$$

where the divergence condition is automatically satisfied. On the other hand, in the **transverse magnetic** configuration we have  $i = 1, 2$  and it's easy to see that the eigenvalue problem (1.3.11) becomes:

$$\begin{cases} \begin{pmatrix} \partial_2 \left( \frac{1}{\varepsilon(x,y)} [\partial_1 H_2(x, y) - \partial_2 H_1(x, y)] \right) \\ \partial_1 \left( \frac{1}{\varepsilon(x,y)} [\partial_2 H_1(x, y) - \partial_1 H_2(x, y)] \right) \end{pmatrix} = \eta \begin{pmatrix} H_1(x, y) \\ H_2(x, y) \end{pmatrix}, \\ \partial_1 [H_1(x, y)] + \partial_2 [H_2(x, y)] = 0, \end{cases} \quad (4.2.3)$$

Let's now consider the electric eigenvalue problem (1.3.12):

$$\begin{cases} \nabla \times (\nabla \times \mathbf{E}(\mathbf{r})) = \eta \varepsilon(\mathbf{r}) \mathbf{E}(\mathbf{r}), \\ \nabla \cdot [\varepsilon(\mathbf{r}) \mathbf{E}(\mathbf{r})] = 0, \end{cases} \quad (4.2.4)$$

where  $\varepsilon(\mathbf{r})$  depends on  $(x, y) \in \mathbb{R}^2$ . Equation (4.2.4) reads in components:

$$\begin{cases} \left( \partial_j \partial_i E_j(x, y) - \partial_j \partial_j E_i(x, y) \right) = \eta \varepsilon(x, y) E_i(x, y), \\ \partial_i \left( \varepsilon(x, y) E_i(x, y) \right) = 0. \end{cases} \quad (4.2.5)$$

In the **transverse electric configuration** we have  $i = 1, 2$  so that the eigenvalue problem takes the following form:

$$\begin{cases} \begin{pmatrix} [\partial_2 \partial_1 E_2(x, y) - \partial_2^2 E_1(x, y)] \\ [\partial_1 \partial_2 E_1(x, y) - \partial_1^2 E_2(x, y)] \end{pmatrix} = \eta \varepsilon(x, y) \begin{pmatrix} E_1(x, y) \\ E_2(x, y) \end{pmatrix}, \\ \partial_1 \left[ \varepsilon(x, y) E_1(x, y) \right] + \partial_2 \left[ \varepsilon(x, y) E_2(x, y) \right] = 0. \end{cases} \quad (4.2.6)$$

In the **transverse magnetic configuration** we have  $i = 3$  and consequently the eigenvalue problem takes the following form:

$$\begin{cases} -(\partial_1^2 + \partial_2^2) E_3(x, y) = -\Delta E_3(x, y) = \eta \varepsilon(x, y) E_3(x, y), \\ \partial_3 \left( \varepsilon(x, y) E_3(x, y) \right) = 0, \end{cases} \quad (4.2.7)$$

where the divergence condition is automatically satisfied.

It is clear from (4.2.2) and (4.2.7) that it is more convenient to solve the electric eigenvalue problem for TM modes and the magnetic eigenvalue problem for TE modes, especially because we only need to solve one of the electric or magnetic eigenvalue problems to compute the energy bands. Hence from now on we solve the Helmholtz equation

$$-\left( \frac{\partial^2 \psi}{\partial^2 x} + \frac{\partial^2 \psi}{\partial^2 y} \right) = \eta n^2(x, y) \psi \quad (4.2.8)$$

in the TM mode (where as usual in this context  $\varepsilon = n^2$ ) and the Helmholtz equation

$$-\nabla \cdot \left( \frac{1}{\varepsilon(x, y)} \nabla \psi \right) = \eta \psi \quad (4.2.9)$$

in the TE mode. In (4.2.8) the electric field is given by  $(0, 0, \psi(x, y))^T$ , whereas in (4.2.9) the magnetic field is given by  $(0, 0, \psi(x, y))^T$ .

### 4.3 Separation of variable method

In this section we'll be dealing with the case of TM modes where the refractive index function is piecewise constant, applying the separation of variable method to the two-dimensional Helmholtz equation (4.2.8). Such a separation exists only if the photonic crystal is rectangular.

We assume that  $n = 2$ ,<sup>1</sup>  $\mathbf{a}_1 = (a, 0)$  with  $a > 0$ ,  $\mathbf{a}_2 = (0, b)$  with  $b > 0$ , and

$$\varepsilon(x, y) = \varepsilon_{pq}, \quad A_{p-1} < x < A_p, B_{q-1} < y < B_q .$$

Here

$$\begin{cases} 0 = A_0 < A_1 < A_2 < \dots < A_m = a, & A_p = a_1 + \dots + a_p, \\ 0 = B_0 < B_1 < B_2 < \dots < B_l = b, & B_q = b_1 + \dots + b_q. \end{cases}$$

Separation of variables under  $\tau$ -periodic boundary conditions, where  $\tau = (\tau_1, \tau_2)$  with  $|\tau_1| = |\tau_2| = 1$ , amounts to substituting

$$E_z(x, y) = X_p(x)Y_q(y)$$

into (4.2.8) for  $p = 1, \dots, m$  and  $q = 1, \dots, l$  under the following conditions:

$$X_p(A_p^-) = X_{p+1}(A_p^+), \quad X'_p(A_p^-) = X'_{p+1}(A_p^+), \quad p = 1, \dots, m-1, \quad (4.3.1a)$$

$$Y_q(B_q^-) = Y_{q+1}(B_q^+), \quad Y'_q(B_q^-) = Y'_{q+1}(B_q^+), \quad q = 1, \dots, l-1, \quad (4.3.1b)$$

$$X_m(a^-) = \tau_1 X_1(0^+), \quad X'_m(a^-) = \tau_1 X'_1(0^+), \quad (4.3.1c)$$

$$Y_l(b^-) = \tau_2 Y_1(0^+), \quad Y'_l(b^-) = \tau_2 Y'_1(0^+). \quad (4.3.1d)$$

The one-variable functions  $X_p(x)$  and  $Y_q(y)$  satisfy the partial differential equation

$$\frac{X_p''(x)}{X_p(x)} + \frac{Y_q''(y)}{Y_q(y)} + \eta \varepsilon_{pq} = 0, \quad (4.3.2)$$

where  $p = 1, \dots, m$  and  $q = 1, \dots, l$ .

It is clear that the two fractions in the left-hand side of (4.3.2) are constants adding up to  $-\eta \varepsilon_{pq}$ . Let us therefore define  $\alpha_p$  and  $\beta_q$  ( $p = 1, \dots, m$  and  $q = 1, \dots, l$ ) such that

$$\frac{X_p''(x)}{X_p(x)} = -(\alpha_p)^2, \quad \frac{Y_q''(y)}{Y_q(y)} = -(\beta_q)^2, \quad (4.3.3)$$

where

$$\eta = \frac{(\alpha_p)^2 + (\beta_q)^2}{\varepsilon_{pq}}. \quad (4.3.4)$$

---

<sup>1</sup>The generalization to the case  $n \geq 3$  with orthogonal vectors  $\mathbf{a}_1, \dots, \mathbf{a}_n$  is straightforward.

From the physics of photonic crystals we know that the eigenvalue  $\eta$  is the squared frequency of light propagating in the crystal:  $\eta = \omega^2/c^2 = k^2/n^2 = k^2/\varepsilon$  for linear media. Therefore in the piecewise constant case

$$\eta = \frac{\alpha_p^2 + \beta_q^2}{\varepsilon_{pq}} = \frac{(k_p^x)^2 + (k_q^y)^2}{\varepsilon_{pq}}, \quad (4.3.5)$$

and from Eq. (4.3.4) we see the physical meaning of  $\alpha_p^2$  and  $\beta_q^2$ : they represent the  $x$  and  $y$  components of the wavevector in each subcell, respectively.

$$\begin{aligned} \alpha_1 &\rightarrow k_1^x, & \beta_1 &\rightarrow k_1^y, \\ \alpha_2 &\rightarrow k_2^x, & \beta_2 &\rightarrow k_2^y. \end{aligned} \quad (4.3.6)$$

As a result,  $\eta$  is the squared frequency of light propagating in the  $(p, q)$  cell (Fig. 4.6):

$$\eta^{(p,q)} = \frac{\alpha_p^2 + \beta_q^2}{\varepsilon_{pq}} = \frac{(k_p^x)^2 + (k_q^y)^2}{\varepsilon_{pq}}. \quad (4.3.7)$$

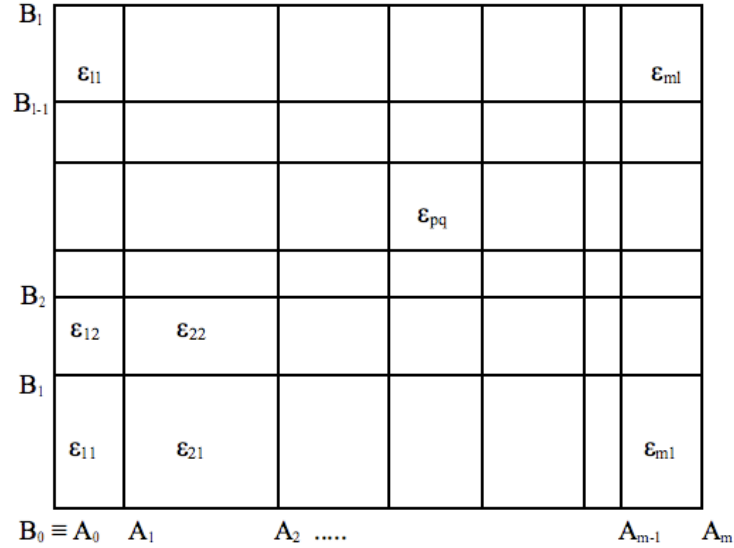


**Figure 4.6:** Example of a two-dimensional photonic crystal in the case of a piecewise constant dielectric constant.

It is helpful to depict these wavevector components for a photonic crystal composed of four different materials as shown in Fig. 4.7. Since we are dealing with lossless photonic crystals, the wavevector is always real. Solving

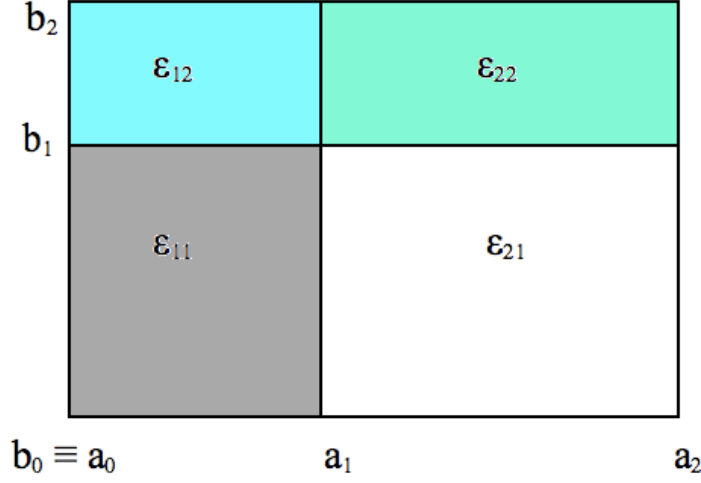


**Figure 4.7:** Example of a two-dimensional photonic crystal composed of four different media in the case of a piecewise constant dielectric constant.

the differential equations (4.3.3) under the coupling condition (4.3.1) implies that

$$X_p(x) = c_{p1} \cos(k_p^x(x - A_{p-1})) + c_{p2} \frac{\sin(k_p^x(x - A_{p-1}))}{k_p^x}, \quad A_{p-1} < x < A_p, \quad (4.3.8a)$$

$$Y_q(y) = d_{q1} \cos(k_q^y(y - B_{q-1})) + d_{q2} \frac{\sin(k_q^y(y - B_{q-1}))}{k_q^y}, \quad B_{q-1} < y < B_q, \quad (4.3.8b)$$

$$\begin{pmatrix} c_{p+1,1} \\ c_{p+1,2} \end{pmatrix} = M(k_p^x; a_p) \begin{pmatrix} c_{p1} \\ c_{p2} \end{pmatrix}, \quad p = 1, \dots, m-1, \quad (4.3.8c)$$

$$\begin{pmatrix} d_{q+1,1} \\ d_{q+1,2} \end{pmatrix} = M(k_p^y; b_q) \begin{pmatrix} d_{q1} \\ d_{q2} \end{pmatrix}, \quad q = 1, \dots, l-1, \quad (4.3.8d)$$

$$\begin{pmatrix} c_{m1} \\ c_{m2} \end{pmatrix} = \tau_1 \begin{pmatrix} c_{11} \\ c_{12} \end{pmatrix}, \quad (4.3.8e)$$

$$\begin{pmatrix} d_{l1} \\ d_{l2} \end{pmatrix} = \tau_2 \begin{pmatrix} d_{11} \\ d_{12} \end{pmatrix}, \quad (4.3.8f)$$

where

$$M(k_p^x; a_p) = \begin{pmatrix} \cos(k_p^x a_p) & \frac{\sin(k_p^x a_p)}{k_p^x} \\ -k_p^x \sin(k_p^x a_p) & \cos(k_p^x a_p) \end{pmatrix}, \quad (4.3.9a)$$

$$M(k_p^y; b_q) = \begin{pmatrix} \cos(k_q^y b_q) & \frac{\sin(k_q^y b_q)}{k_q^y} \\ -k_q^y \sin(k_q^y b_q) & \cos(k_q^y b_q) \end{pmatrix}. \quad (4.3.9b)$$

Equations (4.3.8) imply that

$$\underbrace{M(k_m^x; a_m) \dots M(k_2^x; a_2) M(k_1^x; a_1)}_{\stackrel{\text{def}}{=} M(k_m^x; a_m | \dots | k_2^x; a_2 | k_1^x; a_1)} \begin{pmatrix} c_{11} \\ c_{12} \end{pmatrix} = \tau_1 \begin{pmatrix} c_{11} \\ c_{12} \end{pmatrix}, \quad (4.3.10a)$$

$$\underbrace{M(k_l^y; b_l) \dots M(k_2^y; b_2) M(k_1^y; b_1)}_{\stackrel{\text{def}}{=} M(k_l^y; b_l | \dots | k_2^y; b_2 | k_1^y; b_1)} \begin{pmatrix} d_{11} \\ d_{12} \end{pmatrix} = \tau_2 \begin{pmatrix} d_{11} \\ d_{12} \end{pmatrix}. \quad (4.3.10b)$$

We get nontrivial solutions provided:

$$\begin{cases} \det(M(k_m^x; a_m | \dots | k_2^x; a_2 | k_1^x; a_1) - \tau_1 I_2) = 0, \\ \det(M(k_l^y; b_l | \dots | k_2^y; b_2 | k_1^y; b_1) - \tau_2 I_2) = 0, \end{cases} \quad (4.3.11)$$

where  $\tau_j = \exp(i\phi_j) = \exp(2\pi i\varphi_j)$  for  $\varphi_j \in [0, 1)$  ( $j = 1, 2$ ). If we let  $\tau$  run through  $\mathbb{T}^2$  and hence  $(\varphi_1, \varphi_2)$  run through  $[0, 1)^2$ , in principle the system (4.3.11) allows us to find  $k_p^x$  and  $k_q^y$  ( $p = 1, \dots, m$ ,  $q = 1, \dots, l$ ) which in turn allows to get the band structure of the crystal (see condition (4.3.7)).

It's straightforward to see that the conservation of the tangential component of  $\mathbf{k}$  is fulfilled as Fig. 4.8 shows. In the case of a  $2 \times 2$  grid as

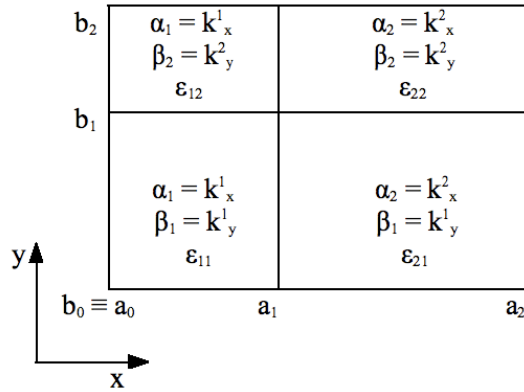


**Figure 4.8:** Wavevector components in a two-dimensional photonic crystal composed of four different media in the case of a piecewise constant dielectric constant. As one can see, the conservation of  $k_{\parallel}$  parallel to the interface is preserved.

that one shown in Fig. 4.7, the eigenvalue formula (4.3.7) gives the following expressions (see Fig. 4.9):

$$\eta^{(1,1)} = \frac{(k_x^1)^2 + (k_y^1)^2}{\varepsilon_{11}}, \quad \eta^{(2,1)} = \frac{(k_x^2)^2 + (k_y^1)^2}{\varepsilon_{21}}, \quad (4.3.12)$$

$$\eta^{(1,2)} = \frac{(k_x^1)^2 + (k_y^2)^2}{\varepsilon_{12}}, \quad \eta^{(2,2)} = \frac{(k_x^2)^2 + (k_y^2)^2}{\varepsilon_{11}}. \quad (4.3.13)$$

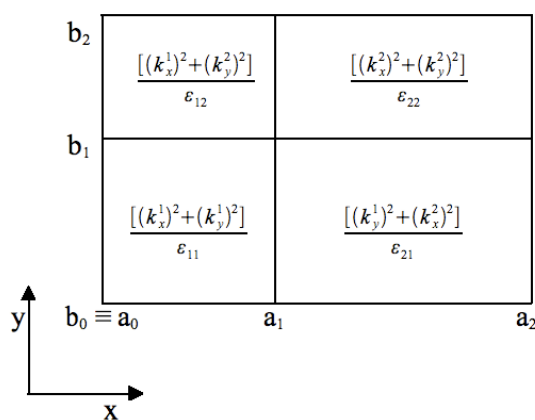


**Figure 4.9:** Eigenvalues for each subcell of a two-dimensional photonic crystal composed of four different media in the case of a piecewise constant dielectric constant.

**Example 4.3.1** We consider a  $2 \times 2$  grid where  $a_1 = 2$ ,  $a_2 = 1$ ,  $b_1 = 0.5$ ,  $b_2 = 1.5$ , and the dielectric constant is given by

$$\begin{aligned} \varepsilon_{11} &= 6, & \varepsilon_{12} &= 1, \\ \varepsilon_{21} &= 7, & \varepsilon_{22} &= 2. \end{aligned}$$

Using (4.3.11) we get:

$$\begin{cases} \det(M(k_2^x; a_2 | k_1^x; a_1) - \tau_1 I_2) = 0, \\ \det(M(k_2^y; b_2 | k_1^y; b_1) - \tau_2 I_2) = 0, \end{cases} \quad (4.3.14)$$

where  $\tau_j = \exp(i\phi_j) = \exp(2\pi i\varphi_j)$  for  $\varphi_j \in [0, 1)$  ( $j = 1, 2$ ) and

$$M(k_2^x; a_2 | k_1^x; a_1) = \begin{pmatrix} \cos(k_2^x a_2) & \frac{\sin(k_2^x a_2)}{k_2^x} \\ -k_2^x \sin(k_2^x a_2) & \cos(k_2^x a_2) \end{pmatrix} \begin{pmatrix} \cos(k_1^x a_1) & \frac{\sin(k_1^x a_1)}{k_1^x} \\ -k_1^x \sin(k_1^x a_1) & \cos(k_1^x a_1) \end{pmatrix}, \quad (4.3.15)$$

$$M(k_2^y; b_2 | k_1^y; b_1) = \begin{pmatrix} \cos(k_2^y b_2) & \frac{\sin(k_2^y b_2)}{k_2^y} \\ -k_2^y \sin(k_2^y b_2) & \cos(k_2^y b_2) \end{pmatrix} \begin{pmatrix} \cos(k_1^y b_1) & \frac{\sin(k_1^y b_1)}{k_1^y} \\ -k_1^y \sin(k_1^y b_1) & \cos(k_1^y b_1) \end{pmatrix}. \quad (4.3.16)$$

From condition (4.3.14) it's easy to see the following:

$$\begin{cases} \left| \begin{pmatrix} m^{11}(k_2^x; a_2 | k_1^x; a_1) & m^{12}(k_2^x; a_2 | k_1^x; a_1) \\ m^{21}(k_2^x; a_2 | k_1^x; a_1) & m^{22}(k_2^x; a_2 | k_1^x; a_1) \end{pmatrix} - \tau_1 \begin{pmatrix} 1 & 0 \\ 0 & 1 \end{pmatrix} \right| = 0 \\ \left| \begin{pmatrix} m^{11}(k_2^y; b_2 | k_1^y; b_1) & m^{12}(k_2^y; b_2 | k_1^y; b_1) \\ m^{21}(k_2^y; b_2 | k_1^y; b_1) & m^{22}(k_2^y; b_2 | k_1^y; b_1) \end{pmatrix} - \tau_2 \begin{pmatrix} 1 & 0 \\ 0 & 1 \end{pmatrix} \right| = 0 \\ \left\{ \begin{array}{l} \left| \begin{array}{cc} m^{11}(k_2^x; a_2 | k_1^x; a_1) - \tau_1 & m^{12}(k_2^x; a_2 | k_1^x; a_1) \\ m^{21}(k_2^x; a_2 | k_1^x; a_1) & m^{22}(k_2^x; a_2 | k_1^x; a_1) - \tau_1 \end{array} \right| = 0 \\ \left| \begin{array}{cc} m^{11}(k_2^y; b_2 | k_1^y; b_1) - \tau_2 & m^{12}(k_2^y; b_2 | k_1^y; b_1) \\ m^{21}(k_2^y; b_2 | k_1^y; b_1) & m^{22}(k_2^y; b_2 | k_1^y; b_1) - \tau_2 \end{array} \right| = 0 \end{array} \right. \\ \left\{ \begin{array}{l} (m_\alpha^{11} - \tau_1)(m_\alpha^{22} - \tau_1) - m_\alpha^{12} m_\alpha^{21} = 0, \\ (m_\beta^{11} - \tau_2)(m_\beta^{22} - \tau_2) - m_\beta^{12} m_\beta^{21} = 0, \end{array} \right. \end{cases}$$

where  $m_\alpha^{ij} = m^{ij}(k_2^x; a_2 | k_1^x; a_1)$  and  $m_\beta^{ij} = m^{ij}(k_2^y; b_2 | k_1^y; b_1)$  for  $i, j = 1, 2$ .

After some algebra we get

$$\begin{cases} \tau_1^2 - (m_\alpha^{11} + m_\alpha^{22})\tau_1 + m_\alpha^{11}m_\alpha^{22} - m_\alpha^{12}m_\alpha^{21} = 0, \\ \tau_2^2 - (m_\beta^{11} + m_\beta^{22})\tau_2 + m_\beta^{11}m_\beta^{22} - m_\beta^{12}m_\beta^{21} = 0, \end{cases}$$

but

$$m_\alpha^{11}m_\alpha^{22} - m_\alpha^{12}m_\alpha^{21} = \det [M(\alpha_2; a_2 | \alpha_1; a_1)] = 1,$$

$$m_\beta^{11}m_\beta^{22} - m_\beta^{12}m_\beta^{21} = \det [M(\beta_2; b_2 | \beta_1; b_1)] = 1,$$

and therefore

$$\begin{cases} \tau_1^2 - \text{Tr}[M(k_2^x; a_2|k_1^x; a_1)]\tau_1 = -1, \\ \tau_2^2 - \text{Tr}[M(k_2^y; b_2|k_1^y; b_1)]\tau_2 = -1, \\ \text{Tr}[M(k_2^x; a_2|k_1^x; a_1)] = \tau_1 + \tau_1^{-1}, \\ \text{Tr}[M(k_2^y; b_2|k_1^y; b_1)] = \tau_2 + \tau_2^{-1}. \end{cases}$$

Using the fact that  $\tau_j = \exp(i\phi_j) = \exp(2\pi i\varphi_j)$  for  $\varphi_j \in [0, 1)$  ( $j = 1, 2$ ), we get

$$\begin{cases} \text{Tr}[M(k_2^x; a_2|k_1^x; a_1)] = 2 \cos(2\pi\varphi_1) \in [-2, 2], \\ \text{Tr}[M(k_2^y; b_2|k_1^y; b_1)] = 2 \cos(2\pi\varphi_2) \in [-2, 2]. \end{cases}$$

Therefore we get the points  $(k_1^x, k_2^x)$  and  $(k_1^y, k_2^y)$  from imposing the surfaces  $\text{Tr}[M(k_2^x; a_2|k_1^x; a_1)]$  and  $\text{Tr}[M(k_2^y; b_2|k_1^y; b_1)]$  to stay between the planes  $z = 2$  and  $z = -2$  (Figs. 4.10- 4.13). Some calculations show that

$$\begin{aligned} \text{Tr}[M(k_2^x; a_2|k_1^x; a_1)] &= 2 \cos(a_1 k_1^x) \cos(a_2 k_2^x) - \frac{(k_1^x)^2 + (k_2^x)^2}{k_1^x k_2^x} \sin(a_1 k_1^x) \sin(a_2 k_2^x), \\ \text{Tr}[M(k_2^y; b_2|k_1^y; b_1)] &= 2 \cos(b_1 k_1^y) \cos(b_2 k_2^y) - \frac{(k_1^y)^2 + (k_2^y)^2}{k_1^y k_2^y} \sin(b_1 k_1^y) \sin(b_2 k_2^y). \end{aligned}$$

In order to get the spectrum, we compute the values of  $(k_1^x, k_2^x)$  and  $(k_1^y, k_2^y)$  such that  $\text{Tr}[M(k_2^x; a_2|k_1^x; a_1)] \in [-2, 2]$  and  $\text{Tr}[M(k_2^y; b_2|k_1^y; b_1)] \in [-2, 2]$ , respectively. Therefore we depict the level set of surfaces  $\text{Tr}[M(k_2^x; a_2|k_1^x; a_1)]$  and  $\text{Tr}[M(k_2^y; b_2|k_1^y; b_1)]$  at  $z = \pm 2$  (Figs. 4.14 and 4.15). As we can see from Figs. 4.14 and 4.15 the level sets show a symmetry which implies that the eigenvalues don't change when inverting the sign of the wavevector  $\mathbf{k}$ :

$$\begin{aligned} \eta^{(p,q)}(k_p^x, k_q^y; \varepsilon_{p,q}) &= \eta^{(p,q)}(-k_p^x, k_q^y; \varepsilon_{p,q}) = \eta^{(p,q)}(k_p^x, -k_q^y; \varepsilon_{p,q}) \\ &= \eta^{(p,q)}(-k_p^x, -k_q^y; \varepsilon_{p,q}), \quad p, q = 1, 2, \end{aligned}$$

and therefore one can focus only on points in the first quadrant both in Figs. 4.14 and 4.15. Since it's a bit complicated checking all  $(k_1^x, k_2^x)$  and  $(k_1^y, k_2^y)$  for which  $|\text{Tr}[M(k_2^x; a_2|k_1^x; a_1)]| < 2$  and  $|\text{Tr}[M(k_2^y; b_2|k_1^y; b_1)]| < 2$ ,

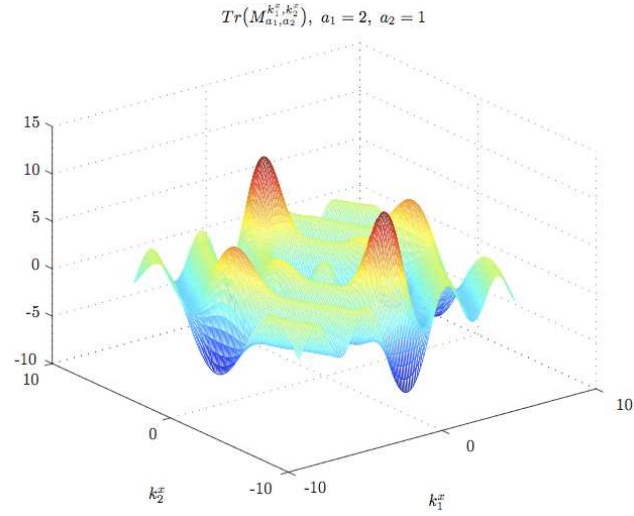


**Figure 4.10:** The figure displays the surface  $\text{Tr}[M(k_2^x; a_2 | k_1^x; a_1)]$  with respect to  $k_1^x$  and  $k_2^x$ .

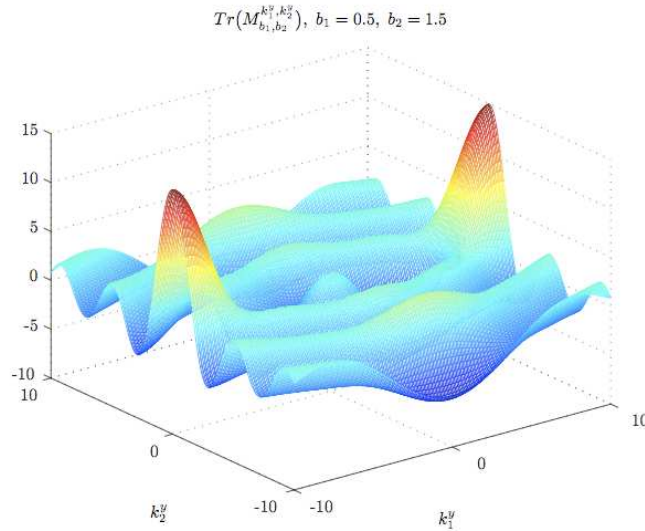


**Figure 4.11:** The figure displays the surface  $\text{Tr}[M(k_2^y; b_2 | k_1^y; b_1)]$  with respect to  $k_1^y$  and  $k_2^y$ .

we considered the easier situation when  $k_2^x = (a_1/a_2)k_1^x$  and  $k_2^y = (b_1/b_2)k_1^y$ , as Fig 4.16 shows.

Roughly speaking, we only pay attention to the light which propagates

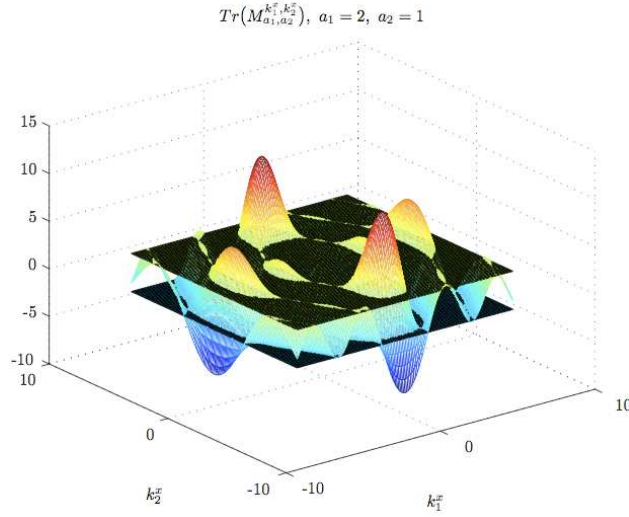


**Figure 4.12:** The figure displays the surface  $\text{Tr}[M(k_2^x; a_2 | k_1^x; a_1)]$  and the planes  $z = \pm 2$ . The values of  $(k_1^x, k_2^x)$  for which the surface lies between the two planes ( $\text{Tr}[M(k_2^x; a_2 | k_1^x; a_1)] \in [-2, 2]$ ) are necessary to compute the spectrum.

with correlated normal wavevector components at the interface. For instance, if the light coming from the subcell filled with  $\varepsilon_{11}$  medium, is directed towards the subcell filled with  $\varepsilon_{21}$  medium, its normal wavevector component changes by a constant ( $a_1/a_2$ ), while its parallel component remains the same. As a result, we have to examine the  $(k_1^x, k_2^x)$  and  $(k_1^y, k_2^y)$  values on the oblique line in Figs. 4.14 and 4.15, respectively. Those values for which  $|\text{Tr}[M(k_2^x; a_2 | k_1^x; a_1)]| < 2$  and  $|\text{Tr}[M(k_2^y; b_2 | k_1^y; b_1)]| < 2$  have to be used to build up the allowed frequencies. Let  $\sigma_{k_1^x, k_2^x}$  be the set of  $(k_1^x, k_2^x)$  such that  $|\text{Tr}[M(k_2^x; a_2 | k_1^x; a_1)]| < 2$  and  $\sigma_{k_1^y, k_2^y}$  be the set of  $(k_1^y, k_2^y)$  such that  $|\text{Tr}[M(k_2^y; b_2 | k_1^y; b_1)]| < 2$ . From Fig. 4.14 we find:

$$\begin{aligned} \sigma_{k_1^x, k_2^x} = & \left\{ k_1^x \in [0, 0.6008] : k_2^x = \frac{a_1}{a_2} \alpha_1 \right\} \cup \left\{ k_1^x \in [0.9627, 2.1788] : k_2^x = \frac{a_1}{a_2} k_1^x \right\} \\ & \cup \left\{ k_1^x \in [2.5118, 2\pi/a_1] : k_2^x = \frac{a_1}{a_2} k_1^x \right\}, \end{aligned} \quad (4.3.17)$$

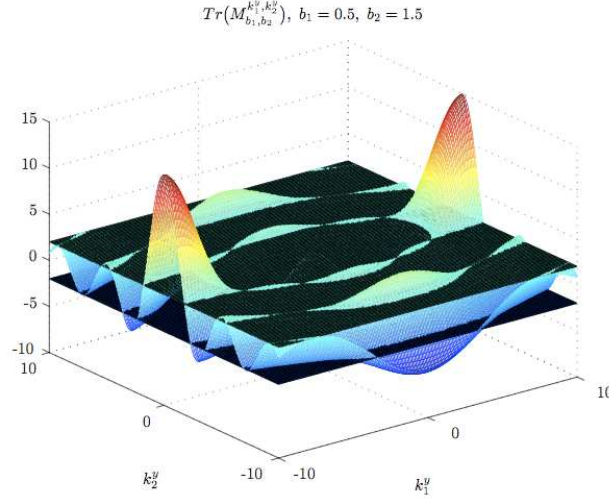


**Figure 4.13:** The figure displays the surface  $\text{Tr}[M(k_2^y; b_2 | k_1^y; b_1)]$  and the planes  $z = \pm 2$ . The values of  $(k_1^y, k_2^y)$  for which the surface lies between the two planes ( $\text{Tr}[M(k_2^y; b_2 | k_1^y; b_1)] \in [-2, 2]$ ) are necessary to compute the spectrum.

and from Fig. 4.15 we read:

$$\begin{aligned} \sigma_{k_1^y, k_2^y} = & \left\{ k_1^y \in [0, 2.0558] : k_2^y = \frac{b_1}{b_2} k_1^y \right\} \cup \left\{ k_1^y \in [4.1405, 8.3100] : k_2^y = \frac{b_1}{b_2} k_1^y \right\} \\ & \cup \left\{ k_1^y \in [10.4527, 2\pi/b_1] : k_2^y = \frac{b_1}{b_2} k_1^y \right\}. \end{aligned} \quad (4.3.18)$$

From the sets  $\sigma_{k_1^x, k_2^x}$  and  $\sigma_{k_1^y, k_2^y}$  we are able to compute the allowed frequencies **in each subcell** making use of the relation

$$\eta^{(p,q)} = \frac{(k_x^p)^2 + (k_y^q)^2}{\varepsilon_{pq}} = \frac{(k_p^x)^2 + (k_q^y)^2}{\varepsilon_{pq}}, \quad p, q = 1, 2.$$

**First Allowed Band** We have:

$$\begin{aligned} \eta^{(1,1)} &= \frac{(k_1^x)^2 + (k_1^y)^2}{\varepsilon_{11}} = \frac{(k_1^x)^2 + (k_1^y)^2}{\varepsilon_{11}}, \\ \eta^{(2,1)} &= \frac{(k_2^x)^2 + (k_1^y)^2}{\varepsilon_{21}} = \frac{(k_2^x)^2 + (k_1^y)^2}{\varepsilon_{21}} = \frac{[(a_1/a_2)k_1^x]^2 + (k_1^y)^2}{\varepsilon_{21}}, \\ \eta^{(1,2)} &= \frac{(k_1^x)^2 + (k_2^y)^2}{\varepsilon_{12}} = \frac{(k_1^x)^2 + (k_2^y)^2}{\varepsilon_{12}} = \frac{(k_1^x)^2 + [(b_1/b_2)k_1^y]^2}{\varepsilon_{12}}, \\ \eta^{(2,2)} &= \frac{(k_2^x)^2 + (k_2^y)^2}{\varepsilon_{22}} = \frac{(k_2^x)^2 + (k_2^y)^2}{\varepsilon_{22}} = \frac{[(a_1/a_2)k_1^x]^2 + [(b_1/b_2)k_1^y]^2}{\varepsilon_{22}}, \end{aligned}$$

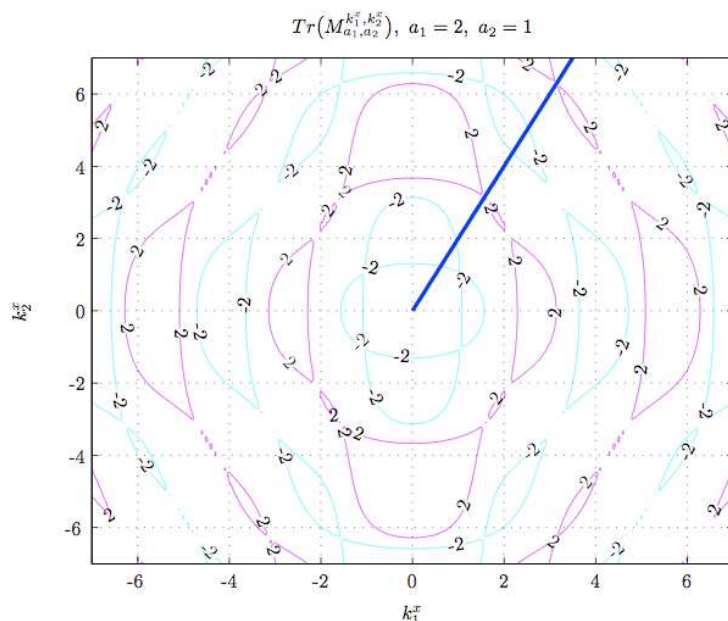


**Figure 4.14:** The figure displays the set level of surface  $\text{Tr}[M(k_2^x; a_2 | k_1^x; a_1)]$  at  $z = \pm 2$ . The values of  $(k_1^x, k_2^x)$  necessary to compute the spectrum lie inside the piecewise regular curves given by the intersection of  $\text{Tr}[M(k_2^x; a_2 | k_1^x; a_1)]$  and the planes  $z = \pm 2$ . Since it's a bit tricky getting these  $(k_1^x, k_2^x)$  values altogether, we calculated the band structure for the particular case when  $k_2^x = (a_1/a_2)k_1^x$ .

where  $k_1^x \in [0, 0.6008]$  and  $k_1^y \in [0, 2.0558]$ . Therefore in the subcell (1, 1) light is allowed to travel, provided its squared frequency  $\eta^{(1,1)} \in \{0, 0.7645\}$ , whereas in the subcell (2, 1) light is allowed to travel, provided its squared frequency  $\eta^{(2,1)} \in \{0, 0.8100\}$ . Since the frequency is preserved when it passes through the interface between the  $\varepsilon_{11}$  medium and the  $\varepsilon_{21}$  medium, we understand that light with a squared frequency of up to 0.7645 can propagate from subcell (1, 1) to subcell (2, 1), and that light coming from subcell (2, 1) with squared frequency of 0.8100 will not enter subcell (1, 1).

In subcells (1, 2) and (2, 2) light can propagate with squared frequencies  $\eta^{(1,2)} \in \{0, 0.8306\}$  and  $\eta^{(2,2)} \in \{0, 0.9567\}$ , respectively. The above considerations lead us to conclude that the first allowed band is for  $\eta \in [0, 0.7645]$ ,

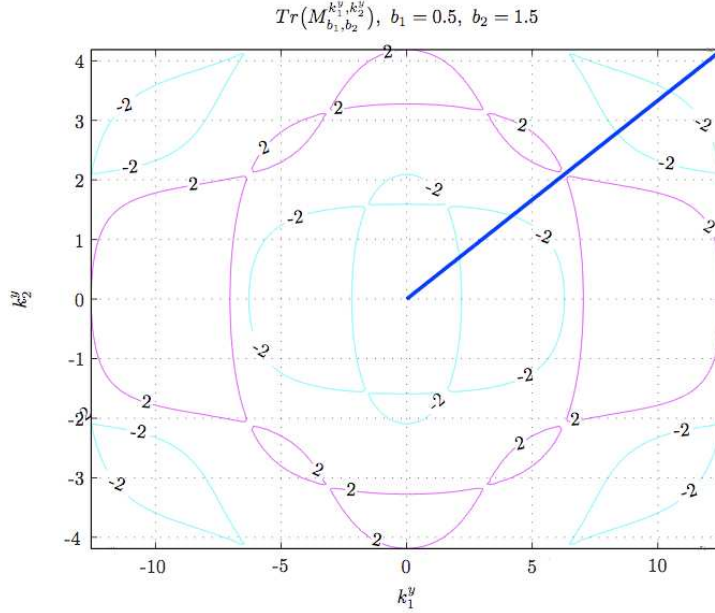


**Figure 4.15:** The figure displays the set level of surface  $\text{Tr}[M(k_2^y; b_2 | k_1^y; b_1)]$  at  $z = \pm 2$ . The values of  $(k_1^y, k_2^y)$  necessary to compute the spectrum lie inside the piecewise regular curves given by the intersection of  $\text{Tr}[M(k_2^y; b_2 | k_1^y; b_1)]$  and the planes  $z = \pm 2$ . Since it's a bit tricky getting these  $(k_1^y, k_2^y)$  values altogether, we calculated the band structure for the particular case when  $k_2^y = (b_1/b_2)k_1^y$ .

where

$$0.7645 = \min_{p,q=1,2} \eta_{\max}^{(p,q)}.$$

**Second Allowed Band** We have:

$$\begin{aligned} \eta^{(1,1)} &= \frac{(k_1^x)^2 + (k_1^y)^2}{\varepsilon_{11}} = \frac{(k_1^x)^2 + (k_1^y)^2}{\varepsilon_{11}}, \\ \eta^{(2,1)} &= \frac{(k_2^x)^2 + (k_1^y)^2}{\varepsilon_{21}} = \frac{(k_2^x)^2 + (k_1^y)^2}{\varepsilon_{21}} = \frac{[(a_1/a_2)k_1^x]^2 + (k_1^y)^2}{\varepsilon_{21}}, \\ \eta^{(1,2)} &= \frac{(k_1^x)^2 + (k_2^y)^2}{\varepsilon_{12}} = \frac{(k_1^x)^2 + (k_2^y)^2}{\varepsilon_{12}} = \frac{(k_1^x)^2 + [(b_1/b_2)k_1^y]^2}{\varepsilon_{12}}, \\ \eta^{(2,2)} &= \frac{(k_2^x)^2 + (k_2^y)^2}{\varepsilon_{22}} = \frac{(k_2^x)^2 + (k_2^y)^2}{\varepsilon_{22}} = \frac{[(a_1/a_2)k_1^x]^2 + [(b_1/b_2)k_1^y]^2}{\varepsilon_{22}}, \end{aligned}$$

where this time  $k_1^x \in [0.9627, 2.1788]$  and  $k_1^y \in [4.1405, 8.3100]$ . As before, we have:

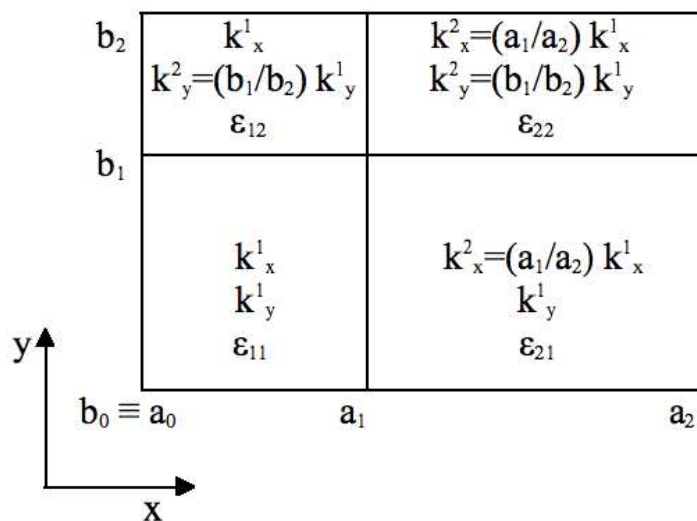


**Figure 4.16:** Wavevector components in a two-dimensional photonic crystal made of four different media in the case of a piecewise constant dielectric constant. For the sake of numerical complexity, we focus on the case where the normal components of the wavevector at the interface are related by a constant factor.

subcell	squared frequency range
(1, 1)	$\eta^{(1,1)} \in [3.0118, 12.3005]$
(2, 1)	$\eta^{(2,1)} \in [2.9787, 12.5778]$
(1, 2)	$\eta^{(1,2)} \in [2.8317, 12.4201]$
(2, 2)	$\eta^{(2,2)} \in [2.8060, 13.3308]$

and therefore we expect the second allowed band to be

$$\eta \in [\max_{p,q=1,2} \eta_{\min}^{(p,q)}, \min_{p,q=1,2} \eta_{\max}^{(p,q)}],$$

where in this case  $\max_{p,q=1,2} \eta_{\min}^{(p,q)} = 3.0118$  and  $\min_{p,q=1,2} \eta_{\max}^{(p,q)} = 12.3005$ . As a result we get the first two allowed bands and band gaps (Fig. 4.17).

Example 4.3.1 was an effort to extend the Hill discriminant formalism to two dimensions and it shows how tricky it can be finding the photonic crystal spectrum by using the separation of variables method applied to Eq. (4.2.8)

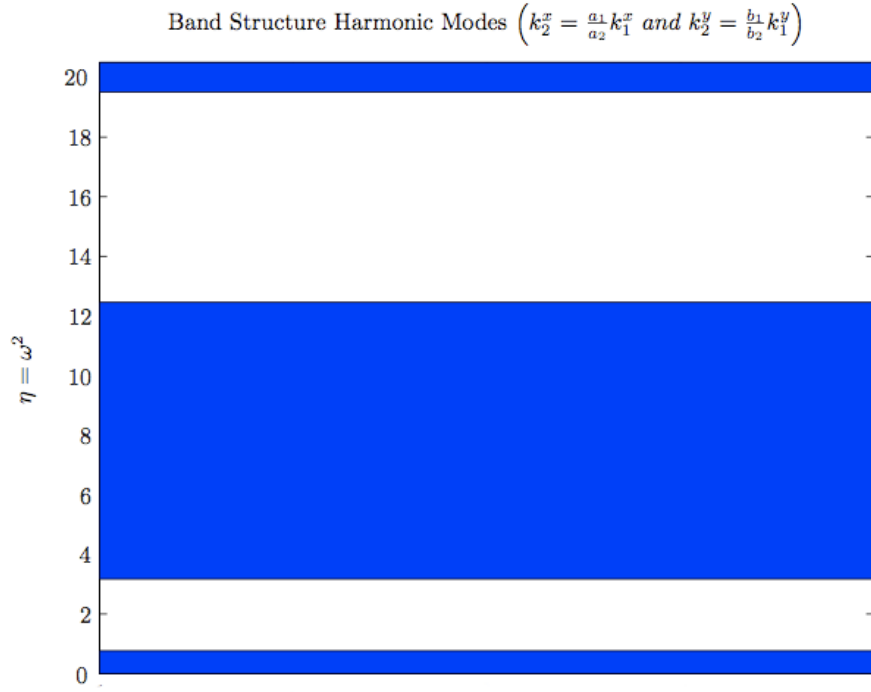


**Figure 4.17:** The figure depicts the band structure for a two-dimensional photonic crystal made of a  $2 \times 2$  grid in the piecewise constant case when the wavevector components are all real (TM Harmonic Modes). The spectrum concerns the light that at the interface changes its normal wavevector component by a constant factor ( $k_2^x = (a_1/a_2)k_1^x$ ,  $k_2^y = (b_1/b_2)k_1^y$ ). In blue the allowed bands are displayed, while in white the band gaps are displayed.

(TM modes) for square lattices. Therefore this technique has been discarded in favor of the numerical approaches of the subsequent sections.

## 4.4 Prevailing Numerical Methods

Several numerical methods have been proposed for the solution of Maxwell's equations for the case of  $1D$ ,  $2D$  and  $3D$  periodic dielectric media. Depending on the problem, algorithms working either in the time or frequency domain or algorithms working in real or reciprocal space can be employed.

### 4.4.1 Time Domain Methods

A time domain method consists of two steps: the numerical solution of the wave equation generated by Maxwell equations in a periodic medium with position dependent dielectric properties and an a posteriori Fourier analysis of the discretized solution obtained to extract the photonic band spectrum. It is widely disseminated, in spite of its high computational complexity and memory requirements pertaining to the additional variable (time  $t$ ) in the PDE that must be solved.

#### *a) Plane wave expansion (PWE) method*

One way to solve the Maxwell equations is to expand the electric and/or magnetic fields into plane waves. This comparatively simple method has been applied to  $3D$  photonic crystals composed of a face centered cubic (FCC) [45, 46, 47] and a diamond [47] array of spheres and a periodic array of Gaussian spheres [48] having a dielectric constant differing from that of the background material. It has also been applied to  $2D$  photonic crystals composed of parallel rods immersed in a background material with centers forming a triangular [49] array and to a  $2D$  photonic crystal composed of an hexagonal array of airholes imbedded in a nonvacuum background material [50]. Even though the first two bands can be computed, the convergence problems inherent in applying a plane wave expansion in a medium with interfaces may lead to considerable inaccuracies.

#### *b) Finite difference time domain (FDTD) method*

In the (FDTD) method space and time are both divided into a proper uniform grid of discrete points and the derivatives of the Maxwell equations are approximated by finite differences. When propagating in time the so called leap-frog scheme [51] is used which means that the electric fields at time  $t$  are computed from the electric fields at time  $t - \Delta t$  along with the magnetic fields at time  $t - \Delta t/2$ , and one has the opposite computing the magnetic fields at time  $t + \Delta t/2$ , i.e., the magnetic fields at time  $t + \Delta t/2$  are computed

from the magnetic fields at time  $t - \Delta t/2$  along with the electric fields at time  $t - \Delta t$  (Fig. 4.18).

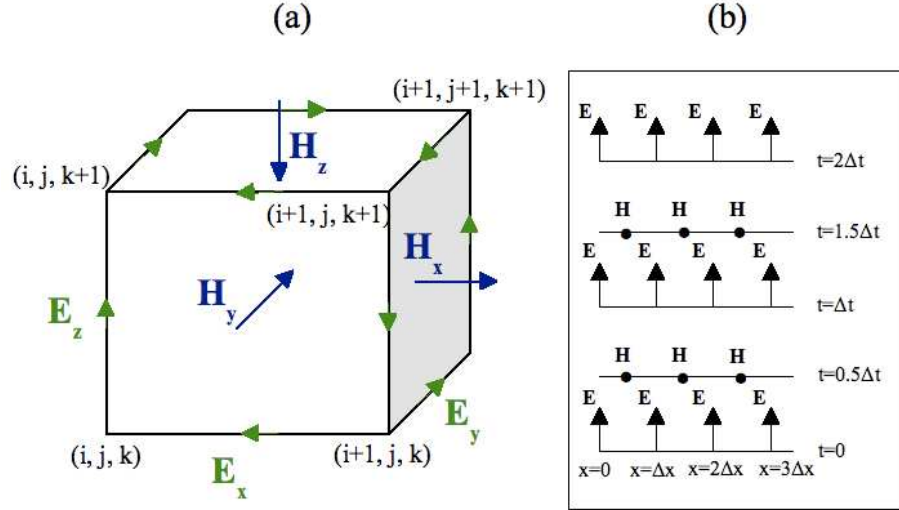


**Figure 4.18:** Finite Difference Time Domain (FDTD) algorithm. (a) Schematic of the Yee cell. (b) Illustration of the leap-frog method.

In the case of two-dimensional photonic crystals, one can separate the field components and obtain two groups (TM and TE modes) of equations that describe the evolution of the electrical and magnetic fields, respectively:

$$\begin{cases} H_x|_{l,m}^{\tau+1} = H_x|_{l,m}^{\tau+1/2} - \frac{\Delta t}{2\Delta y} (E_z|_{l,m+1/2}^{\tau+1/2} - E_z|_{l,m-1/2}^{\tau+1/2}) \\ H_y|_{l,m}^{\tau+1} = H_y|_{l,m}^{\tau+1/2} + \frac{\Delta t}{2\Delta x} (E_z|_{l+1/2,m}^{\tau+1/2} - E_z|_{l-1/2,m}^{\tau+1/2}) \\ E_z|_{l,m}^{\tau+1} = E_z|_{l,m}^{\tau+1/2} + \frac{\Delta t}{\varepsilon_{l,m}} \left[ \frac{H_y|_{l+1/2,m}^{\tau+1/2} - H_y|_{l-1/2,m}^{\tau+1/2}}{2\Delta x} - \frac{H_x|_{l,m+1/2}^{\tau+1/2} - H_x|_{l,m-1/2}^{\tau+1/2}}{2\Delta y} \right], \\ \begin{cases} E_x|_{l,m}^{\tau+1} = E_x|_{l,m}^{\tau+1/2} - \frac{1}{\varepsilon_{l,m}} \frac{\Delta t}{2\Delta y} (H_z|_{l,m+1/2}^{\tau+1/2} - H_z|_{l,m-1/2}^{\tau+1/2}) \\ E_y|_{l,m}^{\tau+1} = E_y|_{l,m}^{\tau+1/2} + \frac{1}{\varepsilon_{l,m}} \frac{\Delta t}{2\Delta x} (H_z|_{l+1/2,m}^{\tau+1/2} - H_z|_{l-1/2,m}^{\tau+1/2}) \\ H_z|_{l,m}^{\tau+1} = H_z|_{l,m}^{\tau+1/2} + \left[ \frac{E_y|_{l+1/2,m}^{\tau+1/2} - E_y|_{l-1/2,m}^{\tau+1/2}}{2\Delta x} - \frac{E_x|_{l,m+1/2}^{\tau+1/2} - E_x|_{l,m-1/2}^{\tau+1/2}}{2\Delta y} \right], \end{cases} \end{cases}$$

where  $\mathbf{H}|_{l,m}^{\tau} = \mathbf{H}(l\Delta x, m\Delta y, \tau\Delta t)$  and  $\mathbf{E}|_{l,m}^{\tau} = \mathbf{E}(l\Delta x, m\Delta y, \tau\Delta t)$  with

$$\begin{aligned} \tau &= 0, 1, \dots, T+1, \\ l &= 0, 1, \dots, L+1, \\ m &= 0, 1, \dots, M+1. \end{aligned}$$

To compute the band structure one has to take the Fourier transform of the computed fields. The position of the peaks obtained in the frequency domain gives the eigenvalues. In fact, if  $\omega_0$  is an eigenvalue, then the fields can be written as

$$\mathbf{E}(\mathbf{r}, t) = \tilde{\mathbf{E}}(\mathbf{r})e^{-i\omega_0 t}, \quad \mathbf{H}(\mathbf{r}, t) = \tilde{\mathbf{H}}(\mathbf{r})e^{-i\omega_0 t},$$

and therefore the Fourier transform of a field is a Delta function:

$$\int_{-\infty}^{+\infty} \mathbf{E}(\mathbf{r}, t)e^{-i\omega t} dt = 2\pi \tilde{\mathbf{E}}(\mathbf{r})\delta(\omega - \omega_0),$$

$$\int_{-\infty}^{+\infty} \mathbf{H}(\mathbf{r}, t)e^{-i\omega t} dt = 2\pi \tilde{\mathbf{H}}(\mathbf{r})\delta(\omega - \omega_0).$$

Finite difference time domain (FDTD) methods have been introduced to determine photonic band spectra by Chan et al. [52], the so-called order- $N$  method. Further results were obtained for  $2D$  diamond [53, 54] and triangular [55, 56] photonic lattices, and  $2D$  lattices of square rods in a background material [57, 55, 58].

## 4.4.2 Frequency Domain Methods

A frequency domain method consists of the numerical solution of the eigenvalue problem for the Helmholtz equation in a periodic medium whose dielectric properties vary with respect to the solution.

### *a) Finite difference frequency domain (FDFD) method*

The FDFD method has been used to compute TM and TE photonic band spectra for  $2D$  crystals with various geometric configurations. Some numerical results concerning the effectiveness of this method can be found in Hermann et al. [59, 60, 61]. In Sec. 4.5 we shall implement this method in a novel way, aimed at greatly reducing the computational complexity and also at obtaining linear systems with structured matrices.

### *b) Multiple scattering (MS) method*

In the MS method the Green's function corresponding to the Helmholtz equation with  $\varepsilon = 1$ , is used to convert the Helmholtz equation into a Fredholm integral equation of the second kind which can be solved by various numerical methods, one of which is iteration (see [62, 63] for the formalism). Several variants of the so-called Korringa-Kohn-Rostoker (KKR) code for electronic

band calculations by the MS method have been used to compute photonic band spectra, namely for 2D honeycomb dielectric structures [45], 3D HCP and FCC spheres in a vacuum background [64], and 2D triangular lattices of parallel rods in a vacuum background [65, 66].

*c) Fourier expansion (FE) method*

Let's see how this method works for the case of TM modes in two-dimensional photonic crystals. Generalizations to higher dimensions and the extension to TE modes are straightforward.

For TM modes one has to study the 2D Helmholtz equation (see (4.2.8))

$$-\nabla^2\psi(\mathbf{x}) = \eta n(\mathbf{x})^2\psi(\mathbf{x}), \quad \mathbf{x} \in \mathbb{R}^2, \quad (4.4.1)$$

where  $\eta$  is a spectral parameter and the refractive index  $n(\mathbf{x})$  is a continuous positive function satisfying the periodicity conditions

$$n(\mathbf{x} + m_1\mathbf{a}_1 + m_2\mathbf{a}_2) = n(\mathbf{x}), \quad \mathbf{x} \in \mathbb{R}^2, \quad m_1, m_2 \in \mathbb{Z}. \quad (4.4.2)$$

We seek nontrivial bounded solutions  $\psi$  of the Helmholtz equation (4.4.1) whose distributional Laplacian  $\nabla^2\psi$  is also bounded in  $\mathbb{R}^2$ . Such solutions have the Bloch representation

$$\psi(\mathbf{x}) = e^{i\mathbf{k}\cdot\mathbf{x}}\phi(\mathbf{x}), \quad (4.4.3)$$

where  $\phi$  satisfies the periodicity condition

$$\phi(\mathbf{x} + m_1\mathbf{a}_1 + m_2\mathbf{a}_2) = \phi(\mathbf{x}), \quad \mathbf{x} \in \mathbb{R}^2, \quad m_1, m_2 \in \mathbb{Z},$$

and the vector  $\mathbf{k} = t_1\mathbf{b}_1 + t_2\mathbf{b}_2$  for certain integers  $t_1, t_2$ ,  $\mathbf{b}_1$  and  $\mathbf{b}_2$  being the reciprocal vectors basis. Substituting (4.4.3) into (4.4.1) we get

$$-\nabla^2\phi(\mathbf{x}) - 2i\mathbf{k} \cdot \nabla\phi(\mathbf{x}) + \|\mathbf{k}\|^2\phi(\mathbf{x}) = \eta n(\mathbf{x})^2\phi(\mathbf{x}). \quad (4.4.4)$$

Let us now construct an orthonormal basis of the complex Hilbert space  $\mathcal{H}$  consisting of those functions in  $L^2(\mathbf{A})$  that satisfy the above periodicity condition. Writing  $\mathbf{B} = \{t_1\mathbf{b}_1 + t_2\mathbf{b}_2 : (t_1, t_2) \in \mathbb{Z}^2\}$ , we get the orthonormal basis

$$\{m(\mathbf{A})^{-1/2}\varphi_t : t \in \mathbb{Z}^2\},$$

where

$$\varphi_t(\mathbf{x}) = e^{i(t_1\mathbf{b}_1 + t_2\mathbf{b}_2)\cdot\mathbf{x}}, \quad t = (t_1, t_2) \in \mathbb{Z}^2, \quad m(\mathbf{A}) = \det A.$$

Note that each basis function satisfies the periodicity condition

$$\varphi_t(\mathbf{x} + m_1\mathbf{a}_1 + m_2\mathbf{a}_2) = \varphi_t(\mathbf{x}), \quad (m_1, m_2) \in \mathbb{Z}^2, \quad t \in \mathbb{Z}^2,$$

as well as the conjugation symmetry

$$\overline{\varphi_t(\mathbf{x})} = \varphi_{-t}(x), \quad t \in \mathbb{Z}^2.$$

The expansion coefficients  $\phi_t$  in

$$\phi(\mathbf{x}) = \sum_{t \in \mathbb{Z}^2} \phi_t \varphi_t(\mathbf{x})$$

are computed as follows:

$$\phi_t = m(\mathbf{A})^{-1} \int_{\mathbf{A}} d\mathbf{x} \phi(x) \overline{\varphi_t(\mathbf{x})} = m(\mathbf{A})^{-1} \int_{\mathbf{A}} d\mathbf{x} \phi(x) \varphi_{-t}(\mathbf{x}). \quad (4.4.5)$$

Observe that

$$-\nabla^2 \varphi_t(\mathbf{x}) = \|t_1 \mathbf{b}_1 + t_2 \mathbf{b}_2\|^2 \varphi_t(\mathbf{x}) = 4\pi^2 \mathbf{t}^T (A^T A)^{-1} \mathbf{t} \varphi_t(\mathbf{x}),$$

where  $\mathbf{t}$  is the column vector with integer elements  $t_1, t_2$ . Expanding the squared refractive index  $n(\mathbf{x})$  and an arbitrary  $\phi$  in  $\mathcal{H}$  as follows

$$n(\mathbf{x})^2 = \sum_{t \in \mathbb{Z}^2} n_t \varphi_t(\mathbf{x}), \quad \phi(\mathbf{x}) = \sum_{t \in \mathbb{Z}^2} \phi_t \varphi_t(\mathbf{x}),$$

where

$$\int_{\mathbf{A}} d\mathbf{x} n(\mathbf{x})^4 = m(\mathbf{A}) \sum_{t \in \mathbb{Z}^2} |n_t|^2, \quad \int_{\mathbf{A}} d\mathbf{x} |\phi(\mathbf{x})|^2 = m(\mathbf{A}) \sum_{t \in \mathbb{Z}^2} |\phi_t|^2, \quad (4.4.6)$$

we get, by using  $\varphi_t(\mathbf{x}) \varphi_s(\mathbf{x}) = \varphi_{t+s}(\mathbf{x})$  for  $t, s \in \mathbb{Z}^n$  while considering  $\mathbb{Z}^2$  to be an additive group,

$$n(\mathbf{x})^2 \phi(\mathbf{x}) = \sum_{t \in \mathbb{Z}^2} \left( \sum_{s \in \mathbb{Z}^2} n_{t-s} \phi_s \right) \varphi_t(\mathbf{x}).$$

As a result, the Helmholtz equation (4.4.1) with  $\psi(\mathbf{x}) = e^{i\mathbf{k} \cdot \mathbf{x}} \phi(\mathbf{x})$  for some given  $\mathbf{k} = \tau_1 \mathbf{b}_1 + \tau_2 \mathbf{b}_2 \in \mathbf{B}$  (with  $\tau = (\tau_1, \tau_2) \in \mathbb{Z}^2$ ) can be written as the linear system

$$4\pi^2 \mathbf{t}^T (A^T A)^{-1} \mathbf{t} \phi_{t-\tau} = \|t_1 \mathbf{b}_1 + t_2 \mathbf{b}_2\|^2 \phi_{t-\tau} = \lambda \sum_{s \in \mathbb{R}^2} n_{t-s} \phi_s, \quad (4.4.7)$$

where  $t \in \mathbb{Z}^2$ . Equation (4.4.7) has to be solved for  $\{\phi_t\}_{t \in \mathbb{Z}^2}$  in the complex Hilbert space  $\ell^2(\mathbb{Z}^2)$ . This system can also be written in the form

$$\begin{aligned} 4\pi^2 (\mathbf{t} + \boldsymbol{\tau})^T (A^T A)^{-1} (\mathbf{t} + \boldsymbol{\tau}) \phi_t &= \|(t_1 + \tau_1) \mathbf{b}_1 + (t_2 + \tau_2) \mathbf{b}_2\|^2 \phi_t \\ &= \lambda \sum_{s \in \mathbb{R}^2} n_{t+\tau-s} \phi_s, \end{aligned} \quad (4.4.8)$$

where  $t \in \mathbb{Z}^2$  and  $\boldsymbol{\tau}$  is the column vector with entries  $\tau_1, \tau_2$ . Equation (4.4.8) has the abstract form

$$(M - \eta T)\boldsymbol{\phi} = 0, \quad (4.4.9)$$

where  $M = 4\pi^2 \text{diag}([\mathbf{t} + \boldsymbol{\tau}]^T (A^T A)^{-1} [\mathbf{t} + \boldsymbol{\tau}])_{t \in \mathbb{Z}^2}$  is an unbounded diagonal matrix with nonnegative entries and  $T$  is a multiindex Toeplitz matrix whose spectrum is given by  $\{n(\mathbf{x})^2 : \mathbf{x} \in \mathbf{A}\}$ , a compact subset of  $(0, +\infty)$ , provided  $n(\mathbf{x})$  is a continuous function of  $\mathbf{x} \in \mathbf{A}$ .

Fourier expansion methods have a major drawback. Since the speed of convergence of a Fourier series of a function on the unit circle is intimately connected to its smoothness, the convergence of Fourier series is exceedingly slow if we expand piecewise continuous functions. Since piecewise constant refractive indices constitute our major application, the Fourier expansion method will invariably lead to slow convergence of Fourier series and high demands on computer time and speed. Nevertheless, the FE method has been used by Sakoda [67, 68] to determine the specular and Bragg reflectivity and the optical transmittance of a slab of a 2D photonic crystal composed of triangular array of cylindrical rods and among the others, by the Joannopolous et al group at the MIT in Boston [1], where they studied photonic crystals extensively. In this group the refractive index function is regularized to speed up the convergence of the Fourier series.

#### d) Finite element frequency domain (FEFD) method

Let's first discuss how one can set the variational formulation of Eq. (4.2.8) (TM modes) in two variables under  $\tau$ -periodic boundary conditions, where  $\tau = (\tau_1, \tau_2)$  is pair of complex numbers of modulus 1. The extension of the procedure to higher dimensions is straightforward.

Letting  $\mathbf{k}$  be a wavevector satisfying

$$e^{i\mathbf{k} \cdot \mathbf{a}_j} = \tau_j, \quad j = 1, 2, \quad (4.4.10)$$

we substitute (4.4.3) into (4.4.1) and arrive at the modified Helmholtz equation (4.4.4). Obviously, there is a unique vector  $\mathbf{k} \in \mathbf{B}$  satisfying (4.4.10).

Using complex scalar products in  $L^2(\mathbf{A})$  and choosing an appropriate test function  $v(\mathbf{x})$ , we take the scalar product of (4.4.4) with  $v$  and apply Green's identity to simplify the resulting equation. Suppressing the  $\mathbf{x}$ -variable under

the integral signs, we get

$$\begin{aligned}
0 &= \int_{\mathbf{A}} d\mathbf{x} \{ \nabla^2 \psi + 2i\mathbf{k} \cdot \nabla \psi - \|\mathbf{k}\|^2 \psi + \eta n^2 \phi \} v^* \\
&= \int_{\mathbf{A}} d\mathbf{x} \{ \nabla \cdot (v^* \nabla \psi) - \nabla \psi \cdot \nabla v^* + 2i[\mathbf{k} \cdot \nabla \psi]v^* - \|\mathbf{k}\|^2 \psi v^* + \eta n^2 \psi v^* \} \\
&= \int_{\partial \mathbf{A}} d\sigma(\mathbf{x}) \frac{\partial \psi}{\partial n} v^* - \int_{\mathbf{A}} d\mathbf{x} \{ \nabla \psi \cdot \nabla v^* - 2i[\mathbf{k} \cdot \nabla \psi]v^* + \|\mathbf{k}\|^2 \psi v^* - \eta n^2 \psi v^* \}.
\end{aligned}$$

Obviously, we wish to choose the test functions in such a way that the integral over the boundary  $\partial \mathbf{A}$  vanishes and the integral over  $\mathbf{A}$  can be written as the sum of six scalar products in  $L^2(\mathbf{A})$ .

In order to do so, we choose both  $\psi(\mathbf{x})$  and  $v(\mathbf{x})$  in the Sobolev space  $H^1(\mathbf{A})$  of those functions in  $L^2(\mathbf{A})$  whose first weak partial derivatives belong to  $L^2(\mathbf{A})$  as well. Since  $n^2$  is a bounded function, the multiplication by  $n^2$  is a bounded linear operator on  $L^2(\mathbf{A})$ . As a result, the integral over  $\mathbf{A}$  is the sum of six (complex) scalar products in  $L^2(\mathbf{A})$ . Next, we observe that the trace map  $\psi \mapsto (\partial \psi / \partial n)$  maps the Sobolev space  $H^1(\mathbf{A})$  into the Sobolev space  $H^{1/2}(\partial \mathbf{A})$  and that the latter Sobolev space consists of functions that are continuous on the closure  $\overline{\mathbf{A}}$  of  $\mathbf{A}$ . This trace map is the restriction of functions defined on  $\mathbf{A}$  to the boundary  $\partial \mathbf{A}$  if these functions are in  $C^1(\overline{\mathbf{A}})$ . Defining  $H_{\text{per}}^1(\mathbf{A})$  as the closed linear subspace of  $H^1(\mathbf{A})$  consisting of those  $\phi \in H^1(\mathbf{A})$  whose trace is periodic in the sense that

$$\psi \left( \sum_{j \neq r} t_j \mathbf{a}_j + \mathbf{a}_r \right) = \psi \left( \sum_{j \neq r} t_j \mathbf{a}_j \right), \quad 0 \leq t_j < 1, \quad r = 1, \dots, n, \tag{4.4.11}$$

we get for  $\psi, v \in H_{\text{per}}^1(\mathbf{A})$

$$\int_{\mathbf{A}} d\mathbf{x} \{ \nabla \psi \cdot \nabla v^* - 2i[\mathbf{k} \cdot \nabla \psi]v^* + \|\mathbf{k}\|^2 \psi v^* \} = \eta \int_{\mathbf{A}} d\mathbf{x} n^2 \psi v^*. \tag{4.4.12}$$

In terms of two sesquilinear forms  $a(u, v)$  and  $b(u, v)$  on  $H_{\text{per}}^1(\mathbf{A})$  we get the following weak formulation:

Find  $\psi \in H_{\text{per}}^1(\mathbf{A})$  such that  $a(\psi, v) = \eta b(\psi, v)$  for all  $v \in H_{\text{per}}^1(\mathbf{A})$ .

(4.4.13)

Here the sesquilinear forms are defined by

$$a(u, v) = \int_{\mathbf{A}} d\mathbf{x} \{ \nabla u \cdot \nabla v^* - 2i[\mathbf{k} \cdot \nabla u]v^* + \|\mathbf{k}\|^2 uv^* \}, \tag{4.4.14a}$$

$$b(u, v) = \int_{\mathbf{A}} d\mathbf{x} n^2 uv^*. \tag{4.4.14b}$$

Thanks to the periodicity condition (4.4.11) we get

$$\int_{\mathbf{A}} d\mathbf{x} [\mathbf{k} \cdot \nabla u] v^* = \underbrace{\int_{\partial \mathbf{A}} d\sigma(\mathbf{x}) u v^* \mathbf{k} \cdot \mathbf{n}}_{=0} - \int_{\mathbf{A}} d\mathbf{x} u [\mathbf{k} \cdot \nabla v]^*,$$

so that

$$a(u, v) = \int_{\mathbf{A}} d\mathbf{x} \left\{ \nabla u \cdot \nabla v^* - i[\mathbf{k} \cdot \nabla u] v^* + iu[\mathbf{k} \cdot \nabla v]^* + \|\mathbf{k}\|^2 u v^* \right\}. \quad (4.4.15)$$

Consequently,  $a(u, v)$  and  $b(u, v)$  are hermitian sesquilinear forms.

The variational formulation of Eq. (4.2.8) for TE modes is as follows. Consider

$$-\nabla \cdot \left( \frac{1}{\varepsilon} \nabla \psi \right) = \eta \psi,$$

where relation (4.4.10) holds. As before we apply Bloch's Theorem putting

$$\psi(\mathbf{x}) = e^{i\mathbf{k} \cdot \mathbf{x}} \tilde{\psi}(\mathbf{x}).$$

We now consider an arbitrary test function  $u(\mathbf{x})$  with sufficient smoothness which satisfies

$$u(\mathbf{x} + \mathbf{a}_j) = \tau_j u(\mathbf{x}), \quad \mathbf{x} \in \mathbb{R}^2, \quad j = 1, 2.$$

Let us now assume

$$u(\mathbf{x}) = e^{i\mathbf{k} \cdot \mathbf{x}} v(\mathbf{x}),$$

where  $v(\mathbf{x})$  is periodic. Then  $\psi$  is a solution to the  $\tau$ -periodic TE Helmholtz equation if for every eligible test function  $u(\mathbf{x})$  we have

$$\iint_A \left\{ -\nabla \cdot \left( \frac{1}{\varepsilon} \nabla \psi \right) - \eta \psi \right\} u^* d\mathbf{x} = 0.$$

Here  $A = \{t_1 \mathbf{a}_1 + t_2 \mathbf{a}_2 : t_1, t_2 \in [0, 1]\}$ .

Let us now transform the integral in the definition of a TE solution. We get

$$\iint_A \left\{ -\nabla \cdot \left( \frac{u^*}{\varepsilon} \nabla \psi \right) + \frac{1}{\varepsilon} \nabla \psi \cdot \nabla u^* - \eta \psi u^* \right\} d\mathbf{x} = 0,$$

or:

$$- \oint_{\partial A} \frac{u^*}{\varepsilon} \frac{\partial \psi}{\partial n} d\sigma + \iint_A \left\{ \frac{1}{\varepsilon} \nabla \psi \cdot \nabla u^* - \eta \psi u^* \right\} d\mathbf{x} = 0.$$

Let us now consider each term of the integrand separately. We have

$$\begin{aligned} \frac{u^*}{\varepsilon} \frac{\partial \psi}{\partial n} &= \frac{e^{-i\mathbf{k}\cdot\mathbf{x}} v^*}{\varepsilon} e^{i\mathbf{k}\cdot\mathbf{x}} \left[ \frac{\partial \tilde{\psi}}{\partial n} + i\mathbf{k} \cdot \hat{\mathbf{n}} \right] = \frac{v^*}{\varepsilon} \left[ \frac{\partial \tilde{\psi}}{\partial n} + i\mathbf{k} \cdot \hat{\mathbf{n}} \right], \\ \frac{1}{\varepsilon} \nabla \psi \cdot \nabla u^* &= \frac{1}{\varepsilon} e^{i\mathbf{k}\cdot\mathbf{x}} \left[ \nabla \tilde{\psi} + i\tilde{\psi} \mathbf{k} \right] \cdot e^{-i\mathbf{k}\cdot\mathbf{x}} \left[ \nabla v^* - i v^* \mathbf{k} \right] \\ &= \frac{1}{\varepsilon} \left[ \nabla \tilde{\psi} + i\tilde{\psi} \mathbf{k} \right] \cdot \left[ \nabla v^* - i v^* \mathbf{k} \right], \\ \eta \psi u^* &= \eta e^{i\mathbf{k}\cdot\mathbf{x}} \tilde{\psi} e^{-i\mathbf{k}\cdot\mathbf{x}} v^* = \eta \tilde{\psi} v^*, \end{aligned}$$

all three of them being periodic. In other words,  $\tilde{\psi} \in H_{\text{per}}^1(\mathbf{A})$  is a TE solution with  $\tau$ -periodic boundary conditions if for every suitable periodic test function  $v^* \in H_{\text{per}}^1(\mathbf{A})$  we have

$$\iint_{\mathbf{A}} \left\{ \frac{1}{\varepsilon} \left[ \nabla \tilde{\psi} + i\tilde{\psi} \mathbf{k} \right] \cdot \left[ \nabla v^* - i v^* \mathbf{k} \right] - \eta \tilde{\psi} v^* \right\} d\mathbf{x} = 0. \quad (4.4.16)$$

Using the FEFD method, photonic band spectra have been computed for  $2D$  circular cylinders embedded in a vacuum background [69, 70],  $2D$  photonic crystals consisting of cylindrical air holes embedded in a nonvacuum background material [71], and  $2D$  photonic crystals consisting of cylindrical [72, 73, 74, 75, 76] or square [72, 73, 74] rods imbedded in a background material. In [77] a variational approach using convenient basis functions has been given to compute the eigenvalues of a  $2D$  photonic crystal in the TM case. In [77] upper and lower estimates for the eigenvalues were derived.

## 4.5 Periodic Finite Element Method

In this section we present a periodic finite element (PFE) method, whose name is due the fact that the finite elements are periodic functions, as well as the test functions considered. Let us now explain this method in more detail [78]. Taking, in the  $1D$  case,

$$\varphi(x) = \begin{cases} 1 - |x|, & -1 \leq x \leq 1, \\ 0, & x \leq -1 \text{ or } x \geq 1, \end{cases} \quad (4.5.1)$$

with  $n$  discretization points per period  $p = nh$  ( $h$  being the step size), we define, for  $j \in \mathbb{Z}$ ,  $x_j = jh = (j/n)p$ , the translates

$$\phi_j(x) = \varphi\left(\frac{x - x_{ns+j}}{h}\right), \quad s \in \mathbb{Z}, \quad (4.5.2)$$

that we extend periodically to  $x \in \mathbb{R}$ . We then expand  $\tilde{\psi}(x)$  in (4.4.16) as follows:

$$\tilde{\psi}(x) = \sum_{j=0}^{n-1} \psi_j \phi_j(x),$$

and take  $v = \phi_l$  for some  $l \in \{0, 1, \dots, n-1\}$ . As a result we get the linear system

$$\sum_{j=0}^{n-1} \psi_j \langle \phi'_j - ik\phi_j, \phi'_l + ik\phi_l \rangle = \eta \sum_{j=0}^{n-1} \psi_j \int_0^p dx n^2(x) \phi_j(x) \phi_l(x), \quad (4.5.3)$$

where the angular brackets stand for the complex scalar product in  $L^2(0, p)$ .

In the 2D rectangular case we introduce the bivariate functions

$$\phi_{j_1, j_2}(x, y) = \varphi\left(\frac{x - x_{ns+j_1}}{h_1}\right) \varphi\left(\frac{y - y_{mt+j_2}}{h_2}\right), \quad (s, t) \in \mathbb{Z}^2,$$

extended periodically to  $(x, y) \in \mathbb{R}^2$ . Here, for  $(j, l) \in \mathbb{Z}^2$ , we have  $x_j = j_1 h_1 = (j_1/n) a_1$  and  $y_l = j_2 h_2 = (j_2/m) a_2$ . As before, we expand  $\psi(x, y)$  in (4.4.16) as follows:

$$\psi(x, y) = \sum_{j_1=0}^{n-1} \sum_{j_2=0}^{m-1} \psi_{j_1, j_2} \phi_{j_1, j_2}(x, y)$$

and take  $v = \phi_{l_1, l_2}$  for every  $l_1 \in \{0, 1, \dots, n-1\}$  and  $l_2 \in \{0, 1, \dots, m-1\}$ . In the TM case, from Eq. (4.4.12), we get

$$\begin{aligned} & \sum_{j_1=0}^{n-1} \sum_{j_2=0}^{m-1} \psi_{j_1, j_2} \int_0^{a_1} \int_0^{a_2} dx dy \{(\nabla \phi_{j_1, j_2} - i\phi_{j_1, j_2} \mathbf{k}) \cdot (\nabla \phi_{l_1, l_2} + i\phi_{l_1, l_2} \mathbf{k})\} \\ &= \eta \sum_{j_1=0}^{n-1} \sum_{j_2=0}^{m-1} \psi_{j_1, j_2} \int_0^{a_1} \int_0^{a_2} dx dy n^2(x, y) \phi_{j_1, j_2} \phi_{l_1, l_2}. \end{aligned}$$

In the TE case we get

$$\begin{aligned} & \sum_{j_1=0}^{n-1} \sum_{j_2=0}^{m-1} \psi_{j_1, j_2} \int_0^{a_1} \int_0^{a_2} \frac{dx dy}{\varepsilon(x, y)} \{(\nabla \phi_{j_1, j_2} - i\phi_{j_1, j_2} \mathbf{k}) \cdot (\nabla \phi_{l_1, l_2} + i\phi_{l_1, l_2} \mathbf{k})\} \\ &= \eta \sum_{j_1=0}^{n-1} \sum_{j_2=0}^{m-1} \psi_{j_1, j_2} \int_0^{a_1} \int_0^{a_2} dx dy \phi_{j_1, j_2} \phi_{l_1, l_2}. \end{aligned}$$

In the **nonrectangular** 2D case we use the basis vectors  $\mathbf{a}_1$  and  $\mathbf{a}_2$  to convert the Helmholtz equation to cartesian coordinates (as we'll show in Subsec. 4.6.4) before applying the PFE method.

### 4.5.1 1D Case

Let us now write the linear system we obtained by applying the 1D PFE method. From relations (4.5.1) and (4.5.2) consider

$$\phi_j(x) = 1 - \frac{|x - x_j|}{h},$$

with support  $[x_{j-1}, x_{j+1}]$ . Then

$$\phi'_j(x) = \text{sign}(x - x_j) \frac{1}{h},$$

where

$$\text{sign}(x - x_j) = \begin{cases} 1 & \text{if } x > x_j, \\ -1 & \text{if } x < x_j. \end{cases}$$

Let us now write the linear system (4.5.3) as

$$\sum_{j=0}^{n-1} \psi_j a(\phi_j, \phi_l) = \eta \sum_{j=0}^{n-1} \psi_j b(\phi_j, \phi_l), \quad (4.5.4)$$

where

$$a(\phi_j, \phi_l) = \int_0^p dx [\phi'_j(x) - ik\phi_j(x)] [\phi'_l(x) + ik\phi_l(x)], \quad (4.5.5)$$

and

$$b(\phi_j, \phi_l) = \int_0^p dx \phi_j(x) \phi_l(x), \quad (4.5.6)$$

In order to get the algebraic form of the linear system (4.5.4), we have to compute some scalar products of functions in  $L^2(0, p)$  for  $n(x) = 1$  (homogeneous medium).

$$\begin{aligned} \langle \phi_j, \phi_j \rangle &= \int_0^p dx \phi_j(x)^2 = \int_{x_{j-1}}^{x_{j+1}} dx \left(1 - \frac{|x - x_j|}{h}\right)^2 = \frac{2}{3}h, \\ \langle \phi_j, \phi_{j+1} \rangle &= \\ \int_0^p dx \phi_j(x) \phi_{j+1}(x) &= \int_{x_j}^{x_{j+1}} dx \left(1 - \frac{x - x_j}{h}\right) \left(1 + \frac{x - x_{j+1}}{h}\right) = \frac{1}{6}h, \\ \langle \phi'_j, \phi'_j \rangle &= \int_0^p dx \phi'_j(x)^2 = \frac{2}{h}, \\ \langle \phi'_j, \phi'_{j+1} \rangle &= \int_0^p dx \phi'_j(x) \phi'_{j+1}(x) = -\frac{1}{h}, \end{aligned}$$



$$\operatorname{Im}\{a(\phi_j, \phi_l)\} = k \begin{pmatrix} 0 & 1 & 0 & 0 & 0 & 0 & 0 & 0 & 0 & -1 \\ -1 & 0 & 1 & 0 & 0 & 0 & 0 & 0 & 0 & 0 \\ 0 & -1 & 0 & 1 & 0 & 0 & 0 & 0 & 0 & 0 \\ 0 & 0 & -1 & 0 & 1 & 0 & 0 & 0 & 0 & 0 \\ 0 & 0 & 0 & -1 & 0 & 1 & 0 & 0 & 0 & 0 \\ 0 & 0 & 0 & 0 & -1 & 0 & 1 & 0 & 0 & 0 \\ 0 & 0 & 0 & 0 & 0 & -1 & 0 & 1 & 0 & 0 \\ 0 & 0 & 0 & 0 & 0 & 0 & -1 & 0 & 1 & 0 \\ 0 & 0 & 0 & 0 & 0 & 0 & 0 & -1 & 0 & 1 \\ 1 & 0 & 0 & 0 & 0 & 0 & 0 & 0 & 0 & -1 \end{pmatrix}.$$

Therefore<sup>2</sup>

$$a(\phi_j, \phi_l) = \operatorname{circ} \left( \frac{2}{h} + \frac{2}{3}hk^2, -\frac{1}{h} + \frac{h}{6}k^2 + ik, 0, \dots, 0, -\frac{1}{h} + \frac{h}{6}k^2 - ik \right),$$

$$b(\phi_j, \phi_l) = \operatorname{circ} \left( \frac{2}{3}h, \frac{1}{6}h, 0, \dots, 0, \frac{1}{6}h \right).$$

It is immediate that  $b(\phi_j, \phi_l)$  is a diagonally strictly dominant symmetric matrix and hence is positive symmetric.

Putting  $\theta_j = (2\pi j/n)$ , the eigenvalues of  $a(\phi_j, \phi_l)b^{-1}(\phi_j, \phi_l)$  are given by

$$\hat{c}(z; k) = \frac{\frac{2}{h} + \frac{2}{3}hk^2 + \left(-\frac{1}{h} + \frac{h}{6}k^2 + ik\right)e^{i\theta_j} + \left(-\frac{1}{h} + \frac{h}{6}k^2 - ik\right)e^{-i\theta_j}}{\frac{2}{3}h + \frac{h}{3}\cos\theta_j}$$

$$= \frac{\frac{6}{h^2} + 2k^2 + \left[-\frac{6}{h^2} + k^2\right]\cos\theta_j - 6\frac{k}{h}\sin\theta_j}{2 + \cos\theta_j},$$

where  $j = 0, 1, \dots, n-1$ . Since

$$\hat{c}(e^{i\theta_j}; k) = \frac{\frac{6}{h^2} + 2k^2 + \left[-\frac{6}{h^2} + k^2\right]\cos\theta_j - 6\frac{k}{h}\sin\theta_j}{2 + \cos\theta_j}$$

$$\stackrel{n \rightarrow +\infty}{\simeq} k^2 + \frac{2n^2}{a^2} \frac{1}{2} \left(\frac{2\pi j}{n}\right)^2 + \frac{2kn}{a} \frac{2\pi j}{n} = \left(k + \frac{2\pi j}{a}\right)^2,$$

we see that, as  $n \rightarrow +\infty$ , the eigenvalues of the circulant matrix  $C$  converge

---

<sup>2</sup>We write  $\operatorname{circ}(q_0, q_1, \dots, q_{n-1})$  for the circulant matrix having  $(q_0 \ q_1 \ \dots \ q_{n-1})$  as its first row.

to the eigenvalues of the boundary value problem

$$\begin{cases} -\psi''(x) - 2ik\psi'(x) + k^2\psi(x) = \eta\psi(x), \\ \psi(0) = \psi(a), \\ \psi'(0) = \psi'(a). \end{cases}$$

In other words, the eigenvalues of the discretized model converge to those of the continuous model as the step length goes to zero whenever the refractive index  $n(x)$  is constant. Further, the absolute error (as  $n \rightarrow +\infty$ ) equals  $O(1/n^2)$ . In fact, using that  $h = a/n$ , we get

$$\begin{aligned} E_{\text{abs}} &= \frac{\frac{6}{h^2} + 2k^2 + \left[-\frac{6}{h^2} + k^2\right] \cos \theta_j - 6\frac{k}{h} \sin \theta_j}{2 + \cos \theta_j} - \left(k + \frac{2\pi j}{a}\right)^2 \\ &= -\left[\frac{2n^2}{a^2} \frac{1}{24} \left(\frac{2\pi j}{n}\right)^4 + \frac{2kn}{a} \frac{1}{6} \left(\frac{2\pi j}{n}\right)^3\right] \left\{1 + O\left(\left(\frac{1}{n}\right)^2\right)\right\} \\ &= -\frac{1}{3} \left(\frac{\pi j}{n}\right)^2 \left[\left(\frac{2\pi j}{a} + k\right)^2 - k^2\right] \left\{1 + O\left(\left(\frac{1}{n}\right)^2\right)\right\}, \quad (4.5.7) \end{aligned}$$

where we have used that as  $x \rightarrow 0$

$$1 - \cos(x) = \frac{1}{2}x^2 - \frac{1}{24}x^4 + O(x^6), \quad \sin(x) = x - \frac{1}{3}x^3 + O(x^5).$$

Thus for  $j = 0, 1, 2, \dots$  the relative error is bounded above by

$$E_{\text{rel}} = -\frac{1}{3} \left(\frac{\pi j}{n}\right)^2 \left\{1 + O\left(\left(\frac{1}{n}\right)^2\right)\right\}, \quad (4.5.8)$$

where the expression is exact for  $k = 0$ . Here  $n \rightarrow +\infty$  for fixed  $j$ .

## 4.6 Periodic Finite Difference Method

In this section we propose a new frequency domain method based on a finite difference scheme applied to Eqs. (4.2.8) and (4.2.9) in order to get the band structure of both one-dimensional and two-dimensional photonic crystals for the TM and TE modes, and to compare them to the literature results. We called this method periodic finite difference (PFD) method since the linear system generated by the finite difference scheme includes the periodicity conditions.

### 4.6.1 1D Case

Consider the one-dimensional Helmholtz equation

$$-E_z''(x) = \eta n^2(x)E_z(x). \quad (4.6.1)$$

Recalling that a photonic crystal is a periodic structure, we apply Bloch's Theorem writing

$$E_z(x) = e^{ikx}\psi(x), \quad (4.6.2)$$

where  $\psi(x+p) = \psi(x)$ ,  $p$  being the crystal period. Substituting (4.6.2) into (4.6.1) we get the modified Helmholtz equation

$$-\psi''(x) - 2ik\psi'(x) + k^2\psi(x) = \eta n(x)^2\psi(x), \quad (4.6.3)$$

under the periodic boundary conditions

$$\psi(0) = \psi(p), \quad \psi'(0) = \psi'(p). \quad (4.6.4)$$

Let us now introduce the division points

$$x_j = \frac{jP}{n}, \quad j = -1, 0, 1, \dots, n, n+1.$$

Finite differencing (4.6.3) yields, for  $h = p/n$ ,

$$-\frac{\psi_{j+1} - 2\psi_j + \psi_{j-1}}{h^2} - 2ik\frac{\psi_{j+1} - \psi_{j-1}}{2h} + k^2\psi_j = \eta N_j^2\psi_j,$$

where  $\psi_j = \psi(\mathbf{x}_j)$ ,  $N_j = n(\mathbf{x}_j)$ , and  $j = 0, 1, \dots, n$ . The periodic boundary conditions take the form

$$\psi_{-1} = \psi_{n-1}, \quad \psi_0 = \psi_n, \quad \psi_1 = \psi_{n+1}, \quad \psi_1 - \psi_{-1} = \psi_{n+1} - \psi_{n-1}.$$

We assume that  $n(x)$  is periodic in the sense that  $n(0) = n(a)$ , so that  $N_{-1} = N_{n-1}$ ,  $N_0 = N_n$ , and  $N_1 = N_{n+1}$ . To remove redundancies in the above formulation, we use the periodic boundary conditions to find a linear system in the variables  $\psi_0, \psi_1, \dots, \psi_{n-1}$ . We then get the circulant-diagonal system (see Appendix B)

$$(C - \eta D)\Psi = 0, \quad (4.6.5)$$

where  $\Psi$  is the column vector with entries  $\psi_0, \psi_1, \dots, \psi_{n-1}$ ,  $D$  is the diagonal matrix with diagonal entries  $N_0^2, N_1^2, \dots, N_{n-1}^2$ , and  $C$  is the circulant matrix with entries

$$C_{j',j} = c_{j'-j} = \begin{cases} \frac{2}{h^2} + k^2, & j = j', \\ -\frac{1}{h^2} - \frac{ik}{h}, & j' - j = 1, \\ -\frac{1}{h^2} - \frac{ik}{h}, & j' - j = 1 - n, \\ -\frac{1}{h^2} + \frac{ik}{h}, & j' - j = -1, \\ -\frac{1}{h^2} + \frac{ik}{h}, & j' - j = n - 1, \\ 0, & \text{otherwise.} \end{cases}$$

Using another notation, the circulant matrix  $C$  has the following form:

$$C = \begin{pmatrix} c & c^+ & 0 & 0 & 0 & 0 & 0 & 0 & 0 & 0 & 0 & c^- \\ c^- & c & c^+ & 0 & 0 & 0 & 0 & 0 & 0 & 0 & 0 & 0 \\ 0 & c^- & c & c^+ & 0 & 0 & 0 & 0 & 0 & 0 & 0 & 0 \\ 0 & 0 & c^- & c & c^+ & 0 & 0 & 0 & 0 & 0 & 0 & 0 \\ 0 & 0 & 0 & c^- & c & c^+ & 0 & 0 & 0 & 0 & 0 & 0 \\ 0 & 0 & 0 & 0 & c^- & c & c^+ & 0 & 0 & 0 & 0 & 0 \\ 0 & 0 & 0 & 0 & 0 & c^- & c & c^+ & 0 & 0 & 0 & 0 \\ 0 & 0 & 0 & 0 & 0 & 0 & c^- & c & c^+ & 0 & 0 & 0 \\ 0 & 0 & 0 & 0 & 0 & 0 & 0 & c^- & c & c^+ & 0 & 0 \\ 0 & 0 & 0 & 0 & 0 & 0 & 0 & 0 & c^- & c & c^+ & 0 \\ 0 & 0 & 0 & 0 & 0 & 0 & 0 & 0 & 0 & c^- & c & c^+ \\ c^+ & 0 & 0 & 0 & 0 & 0 & 0 & 0 & 0 & 0 & c^- & c \end{pmatrix},$$

where  $c = (\frac{1}{h^2} + k^2)$ ,  $c^+ = (-\frac{1}{h^2} + i\frac{k}{h})$  and  $c^- = (-\frac{1}{h^2} - i\frac{k}{h})$ . For each fixed  $k$ -value, the eigenvalues of  $C$  are the values of the function

$$\hat{c}(z; k) = \frac{2}{h^2} + k^2 + \left(-\frac{1}{h^2} - \frac{ik}{h}\right)z + \left(-\frac{1}{h^2} + \frac{ik}{h}\right)z^{-1},$$

where  $z^n = 1$  (see Appendix B). The corresponding eigenvectors are  $(1, z, z^2, \dots, z^{n-1})^T$ , where  $z^n = 1$ . Writing  $z = e^{i\theta_j}$  with  $\theta_j = \frac{2\pi j}{n}$  for  $j = 0, 1, \dots, n-1$ , we get for the eigenvalues, corresponding to  $k$ ,

$$\hat{c}(e^{i\theta_j}; k) = k^2 + \frac{2}{h^2}(1 - \cos \theta_j) + \frac{2k}{h} \sin \theta_j.$$

Putting  $\tan \alpha = hk(1 + h^2k^2)^{-1/2}$  we can write the eigenvalues as follows:

$$\hat{c}(e^{i\theta_j}; k) = k^2 + \frac{2}{h^2} - \frac{2}{h^2} \sqrt{1 + k^2h^2} \cos(\theta_j + \alpha),$$

which is nonnegative (and equals zero iff  $k = 0$  and  $j = 0$ ). Thus  $k^2$  is a simple eigenvalue ( $j = 0$ ), while

$$\hat{c}(e^{i\theta_{n-j}}; k) = \hat{c}(e^{i\theta_j}; -k).$$

For even  $n$  (and  $j = \frac{n}{2}$ ), the number  $k^2 + [4/h^2]$  is another simple eigenvalue. For  $k = 0$  the remaining eigenvalues are between zero and  $4/h^2$  and have multiplicity two. As in Subsec. 4.5.1

$$\begin{aligned} \hat{c}(e^{i\theta_j}; k) &= k^2 + \frac{2n^2}{a^2} \left(1 - \cos \frac{2\pi j}{n}\right) + \frac{2kn}{a} \sin \frac{2\pi j}{n} \\ &\stackrel{n \rightarrow +\infty}{\simeq} k^2 + \frac{2n^2}{a^2} \frac{1}{2} \left(\frac{2\pi j}{n}\right)^2 + \frac{2kn}{a} \frac{2\pi j}{n} = \left(k + \frac{2\pi j}{a}\right)^2, \end{aligned}$$

we see that, as  $n \rightarrow +\infty$ , the eigenvalues of the circulant matrix  $C$  converge to the eigenvalues of the boundary value problem

$$\begin{cases} -\psi''(x) - 2ik\psi'(x) + k^2\psi(x) = \eta\psi(x), \\ \psi(0) = \psi(a), \\ \psi'(0) = \psi'(a). \end{cases}$$

We get the same formula (4.5.7) and (4.5.8) for the the absolute and relative errors, respectively.

When studying the system (4.6.5) for two choices of the refractive index,  $n^{(1)}(\mathbf{x})$  and  $n^{(2)}(\mathbf{x})$ , where  $n^{(1)}(\mathbf{x}) \geq n^{(2)}(\mathbf{x})$ , the corresponding diagonal matrices,  $D^{(1)}$  and  $D^{(2)}$ , satisfy

$$[D^{(1)}]_{jj} \geq [D^{(2)}]_{jj}, \quad j = 1, \dots, n;$$

whereas the circulant matrix  $C$  remains invariant. The corresponding eigenvalues  $\eta$  are those of the nonnegative hermitian matrices  $[D^{(1)}]^{-1/2}C[D^{(1)}]^{-1/2}$  and  $[D^{(2)}]^{-1/2}C[D^{(2)}]^{-1/2}$ . These matrices satisfy

$$[D^{(1)}]^{-1/2}C[D^{(1)}]^{-1/2}\mathbf{h} \cdot \mathbf{h} \leq [D^{(2)}]^{-1/2}C[D^{(2)}]^{-1/2}\mathbf{h} \cdot \mathbf{h},$$

for each  $\mathbf{h} \in \mathbb{R}^n$ . According to [79, Thm. 1 of Sec. 8.7], the eigenvalues  $\eta_1^{(1)} \leq \dots \leq \eta_n^{(1)}$  of  $[D^{(1)}]^{-1/2}C[D^{(1)}]^{-1/2}$  and  $\eta_1^{(2)} \leq \dots \leq \eta_n^{(2)}$  of  $[D^{(2)}]^{-1/2}C[D^{(2)}]^{-1/2}$  satisfy

$$\eta_j^{(1)} \leq \eta_j^{(2)}, \quad j = 1, \dots, n. \quad (4.6.6)$$

The monotonicity condition (4.6.6) can be used to obtain error estimates for the eigenvalues  $\eta$  computed. Suppose we know the eigenvalues  $\eta$  of the system (4.6.5) with refractive indices  $n^{(d)}(\mathbf{x})$  and  $n^{(e)}(\mathbf{x})$  such that

$$n^{(d)}(\mathbf{x}) \leq n(\mathbf{x}) \leq n^{(e)}(\mathbf{x}),$$

while we want to compute the eigenvalues of (4.6.5) with refractive index  $n(\mathbf{x})$ , knowing the eigenvalues  $\eta^{(e)}$  and  $\eta^{(d)}$  associated to the defect and excess refractive indices  $n^{(e)}$  and  $n^{(d)}$ . As a result, the corresponding eigenvalues satisfy the following monotonicity relation

$$\eta_j^{(e)} \leq \eta_j \leq \eta_j^{(d)}, \quad j = 1, \dots, n.$$

Hence, the error in computing  $\eta_j$  is bounded above by  $\eta_j^{(e)} - \eta_j^{(d)}$ .

### 4.6.2 2D Case: TM Modes

In this subsection we discuss the application of the PFD scheme to the study of two-dimensional photonic crystals for TM modes. We therefore consider a periodic rectangular 2D crystal, where the primitive cell is  $[0, a] \times [0, b]$ . To study Transverse Magnetic light propagation in a two-dimensional photonic crystal, one has to consider the two-dimensional Helmholtz equation

$$-\nabla^2 E_z(x, y) = \eta n^2(x, y) E_z(x, y). \quad (4.6.7)$$

Applying Bloch's Theorem  $E_z(x, y) = e^{i\mathbf{k}\cdot\mathbf{x}}\psi(x, y)$  to (4.6.7) one gets the two-dimensional modified Helmholtz equation:

$$-\nabla^2\psi(x, y) - 2i\mathbf{k}\cdot\nabla\psi(x) + \|\mathbf{k}\|^2\psi(x) = \eta n(x, y)^2\psi(x, y), \quad (4.6.8)$$

under the periodicity conditions

$$\begin{aligned} \psi(x, 0) &= \psi(x, b), \\ \psi(0, y) &= \psi(a, y), \\ \frac{\partial\psi}{\partial y}(x, 0) &= \frac{\partial\psi}{\partial y}(x, b), \\ \frac{\partial\psi}{\partial x}(0, y) &= \frac{\partial\psi}{\partial x}(a, y), \end{aligned}$$

where  $x \in \mathbb{R}^2$ .

Let us now introduce the division points

$$x_{j,l} = \left( \frac{ja}{n}, \frac{lb}{m} \right),$$

where  $j = -1, 0, 1, \dots, n, n+1$  and  $l = -1, 0, 1, \dots, m, m+1$ . Finite differencing yields, for  $h_x = a/n$  and  $h_y = b/m$ ,

$$\begin{aligned} & -\frac{\psi_{j+1,l} - 2\psi_{j,l} + \psi_{j-1,l}}{h_x^2} - \frac{\psi_{j,l+1} - 2\psi_{j,l} + \psi_{j,l-1}}{h_y^2} \\ & + 2ik_x \frac{\psi_{j+1,l} - \psi_{j-1,l}}{2h_x} + 2ik_y \frac{\psi_{j,l+1} - \psi_{j,l-1}}{2h_y} + [k_x^2 + k_y^2]\psi_{j,l} \\ & = \eta N_{j,l}^2 \psi_{j,l}, \end{aligned}$$

where  $\psi_{j,l} = \psi(x_{j,l})$  and  $N_{j,l} = n(x_{j,l})$ . The subscripts  $j, l$  range over  $j = 0, 1, \dots, n$  and  $l = 0, 1, \dots, m$ . The periodic boundary conditions take the form

$$\begin{aligned} \psi_{j,-1} &= \psi_{j,m-1}, & \psi_{j,0} &= \psi_{j,m}, \\ \psi_{j,1} &= \psi_{j,m+1}, & \psi_{-1,l} &= \psi_{n-1,l}, \\ \psi_{0,l} &= \psi_{n,l}, & \psi_{1,l} &= \psi_{n+1,l}, \\ \psi_{j,1} - \psi_{j,-1} &= \psi_{j,m+1} - \psi_{j,m-1}, & \psi_{1,l} - \psi_{-1,l} &= \psi_{n+1,l} - \psi_{n-1,l}. \end{aligned}$$

The above formulation of the finite differencing scheme for the (modified) Helmholtz equation contains many redundancies. These are caused by the fact that it is sufficient to compute  $\psi_{j,l}$  for the following  $(j, l)$ :

$$\begin{cases} (j, l), & j = 1, \dots, n-1, l = 1, \dots, m-1, \\ (0, l), & l = 1, \dots, m-1, \\ (j, 0), & j = 1, \dots, n-1, \\ (0, 0), & \end{cases}$$

a total of  $(n-1)(m-1) + (m-1) + (n-1) + 1 = nm$  values. Moreover,  $\psi_{j,l}$  and  $\psi_{j',l'}$  are to coincide whenever  $j - j'$  is a multiple of  $n$  and  $l - l'$  is a multiple of  $m$ . Further,  $N_{j,l} = N_{j',l'}$  whenever  $j - j'$  is a multiple of  $n$  and  $l - l'$  is a multiple of  $m$ . We can therefore restrict ourselves to these  $nm$  values of  $\psi$  and restate the finite differencing scheme as an  $nm \times nm$  systems in the variable  $\psi_{j,l}$  with  $(j, l)$  as above.

We now get the following circulant-diagonal system:

$$(C - \eta D)\Psi = 0, \quad (4.6.9)$$

where  $\Psi$  is the column vector with entries  $\psi_{j,l}$ ,  $\eta$  is the spectral parameter, and  $C$  is, for  $G = \mathbb{Z}[n] \times \mathbb{Z}[m]$ , the  $G$ -circulant matrix with entries

$$C_{(j',l'),(j,l)} = c_{j'-j, l'-l} = \begin{cases} \frac{2}{h_x^2} + \frac{2}{h_y^2} + k_x^2 + k_y^2, & j = j', l = l', \\ -\frac{1}{h_x^2} - \frac{ih_x}{k_x}, & j' - j = 1, l = l', \\ -\frac{1}{h_x^2} - \frac{ih_x}{k_x}, & j' - j = 1 - n, l = l', \\ -\frac{1}{h_y^2} - \frac{ih_y}{k_y}, & j' = j, l' - l = 1, \\ -\frac{1}{h_y^2} - \frac{ih_y}{k_y}, & j' = j, l' - l = 1 - m, \\ -\frac{1}{h_x^2} + \frac{ih_x}{k_x}, & j' - j = -1, l = l', \\ -\frac{1}{h_x^2} + \frac{ih_x}{k_x}, & j' - j = -1 + n, l = l', \\ -\frac{1}{h_y^2} + \frac{ih_y}{k_y}, & j' = j, l' - l = -1, \\ -\frac{1}{h_y^2} + \frac{ih_y}{k_y}, & j' = j, l' - l = -1 + m, \\ 0, & \text{otherwise.} \end{cases}$$

Thus the entry  $c_{j,l}$  only depends on the remainders of  $j$  and  $l$  on dividing by  $n$  and  $m$ , respectively. Using another notation, the circulant matrix  $C$  takes

the form of a circulant matrix where each entry is itself a circulant matrix:

$$C = \left( \begin{array}{cccc|cccc|cccc|cccc} \alpha & \beta & 0 & \bar{\beta} & \gamma & 0 & 0 & 0 & 0 & 0 & 0 & 0 & \bar{\gamma} & 0 & 0 & 0 \\ \bar{\beta} & \alpha & \beta & 0 & 0 & \gamma & 0 & 0 & 0 & 0 & 0 & 0 & 0 & \bar{\gamma} & 0 & 0 \\ 0 & \bar{\beta} & \alpha & \beta & 0 & 0 & \gamma & 0 & 0 & 0 & 0 & 0 & 0 & 0 & \bar{\gamma} & 0 \\ \beta & 0 & \bar{\beta} & \alpha & 0 & 0 & 0 & \gamma & 0 & 0 & 0 & 0 & 0 & 0 & 0 & \bar{\gamma} \\ \hline \bar{\gamma} & 0 & 0 & 0 & \alpha & \beta & 0 & \beta & \gamma & 0 & 0 & 0 & 0 & 0 & 0 & 0 \\ 0 & \bar{\gamma} & 0 & 0 & \bar{\beta} & \alpha & \beta & 0 & 0 & \gamma & 0 & 0 & 0 & 0 & 0 & 0 \\ 0 & 0 & \bar{\gamma} & 0 & 0 & \bar{\beta} & \alpha & \beta & 0 & 0 & \gamma & 0 & 0 & 0 & 0 & 0 \\ 0 & 0 & 0 & \bar{\gamma} & \beta & 0 & \bar{\beta} & \alpha & 0 & 0 & 0 & \gamma & 0 & 0 & 0 & 0 \\ \hline 0 & 0 & 0 & 0 & \bar{\gamma} & 0 & 0 & 0 & \alpha & \beta & 0 & \beta & \gamma & 0 & 0 & 0 \\ 0 & 0 & 0 & 0 & 0 & \bar{\gamma} & 0 & 0 & \bar{\beta} & \alpha & \beta & 0 & 0 & \gamma & 0 & 0 \\ 0 & 0 & 0 & 0 & 0 & 0 & \bar{\gamma} & 0 & 0 & \bar{\beta} & \alpha & \beta & 0 & 0 & \gamma & 0 \\ 0 & 0 & 0 & 0 & 0 & 0 & 0 & \bar{\gamma} & \beta & 0 & \bar{\beta} & \alpha & 0 & 0 & 0 & \gamma \\ \hline \gamma & 0 & 0 & 0 & 0 & 0 & 0 & 0 & \bar{\gamma} & 0 & 0 & 0 & \alpha & \beta & 0 & \beta \\ 0 & \gamma & 0 & 0 & 0 & 0 & 0 & 0 & 0 & \bar{\gamma} & 0 & 0 & \bar{\beta} & \alpha & \beta & 0 \\ 0 & 0 & \gamma & 0 & 0 & 0 & 0 & 0 & 0 & 0 & \bar{\gamma} & 0 & 0 & \bar{\beta} & \alpha & \beta \\ 0 & 0 & 0 & \gamma & 0 & 0 & 0 & 0 & 0 & 0 & 0 & \bar{\gamma} & \beta & 0 & \bar{\beta} & \alpha \end{array} \right),$$

where

$$\alpha = \left( \frac{2}{h_x^2} + \frac{2}{h_y^2} + k^2 \right),$$

$$\beta = \left( -\frac{1}{h_x^2} + i\frac{k_x}{h_x} \right), \quad \bar{\beta} = \left( -\frac{1}{h_x^2} - i\frac{k_x}{h_x} \right),$$

$$\gamma = \left( -\frac{1}{h_y^2} + i\frac{k_y}{h_y} \right), \quad \bar{\gamma} = \left( -\frac{1}{h_y^2} - i\frac{k_y}{h_y} \right).$$

The eigenvalues of  $C$  are the numbers

$$\hat{c}(z, w; \mathbf{k}) = \frac{2}{h_x^2} + k_x^2 + k_y^2 + \left( -\frac{1}{h_x^2} + \frac{ik_x}{h_x} \right) z + \left( -\frac{1}{h_x^2} - \frac{ik_x}{h_x} \right) z^{-1}$$

$$+ \frac{2}{h_y^2} + \left( -\frac{1}{h_y^2} + \frac{ik_y}{h_y} \right) w + \left( -\frac{1}{h_y^2} - \frac{ik_y}{h_y} \right) w^{-1},$$

where  $z^n = 1$  and  $w^m = 1$ . Writing  $z = e^{i\theta_j}$  with  $\theta_j = \frac{2\pi j}{n}$  and  $w = e^{i\varphi_l}$  with  $\varphi_l = \frac{2\pi l}{m}$ , we can write the eigenvalues in the form

$$\hat{c}(z, w; \mathbf{k}) = k_x^2 + k_y^2 + \frac{2}{h_x^2} (1 - \cos \theta_j) - \frac{2k_x}{h_x} \sin \theta_j + \frac{2}{h_y^2} (1 - \cos \varphi_l) - \frac{2k_y}{h_y} \sin \varphi_l,$$

where  $j = 0, 1, \dots, n-1$  and  $l = 0, 1, \dots, m-1$ . Further, all eigenvalues are nonnegative (and equal to zero iff  $k = 0$  and  $j = l = 0$ ). To estimate

the error in computing the eigenvalue  $\hat{c}(z, w; \mathbf{k})$  in orders of magnitude of  $j/n$  and  $l/m$  in the 2D case, we have to add two almost copies of the same absolute error formula (4.5.7), which results in

$$E_{\text{abs}} = -\frac{1}{3} \left( \frac{\pi j}{n} \right)^2 \left[ \left( \frac{2\pi j}{a} + k_x \right)^2 - k_x^2 \right] \left\{ 1 + O \left( \left( \frac{1}{n} \right)^2 \right) \right\} \\ - \frac{1}{3} \left( \frac{\pi l}{m} \right)^2 \left[ \left( \frac{2\pi l}{b} + k_y \right)^2 - k_y^2 \right] \left\{ 1 + O \left( \left( \frac{1}{m} \right)^2 \right) \right\},$$

while the exact expression for the  $(j, l)$ -th eigenvalue is as follows:

$$\eta_{(j,l)}(\mathbf{k}) = \left( \frac{2\pi j}{a} + k_x \right)^2 + \left( \frac{2\pi l}{b} + k_y \right)^2,$$

and for the relative error we then get the following upper bound:

$$E_{\text{rel}} = -\max \left[ \frac{1}{3} \left( \frac{\pi j}{n} \right)^2 \left\{ 1 + O \left( \left( \frac{1}{n} \right)^2 \right) \right\}, \frac{1}{3} \left( \frac{\pi l}{m} \right)^2 \left\{ 1 + O \left( \left( \frac{1}{m} \right)^2 \right) \right\} \right],$$

where  $n$  and  $m$  go to  $+\infty$  for fixed  $j$  and  $l$ . Hence, for each fixed  $j$ -value, both the absolute and the relative errors go to zero as  $\frac{1}{n^2} + \frac{1}{m^2}$ .

For the monotonicity of the eigenvalues of the system (4.6.9) in terms of the refractive index, the same considerations hold as in the 1D case: the  $j$ -th eigenvalue of the system (4.6.9) decreases monotonically as the refractive index increases. As said before, this monotonicity property can be used to get error estimates for the eigenvalues.

### 4.6.3 1D and 2D Cases: TE Modes

Now consider the TE Helmholtz equation (4.2.2)

$$-\nabla \cdot \left( \frac{1}{\varepsilon} \nabla E_z(x, y) \right) = \eta E_z(x, y),$$

where  $\varepsilon$  has periodicity properties and  $\phi$  has  $\tau$ -periodic boundary conditions. Write

$$E_z(x, y) = e^{i\mathbf{k} \cdot \mathbf{x}} \psi,$$

where  $\psi$  is periodic. Then

$$-\nabla \cdot \left( \frac{1}{\varepsilon} \nabla \psi \right) - i\mathbf{k} \cdot \nabla \left( \frac{1}{\varepsilon} \psi \right) - i\mathbf{k} \cdot \frac{1}{\varepsilon} \nabla \psi + |\mathbf{k}|^2 \psi = \eta \psi \quad (4.6.10)$$

under periodic boundary conditions. Assuming a rectangular crystal with step sizes  $h_x$  in the  $x$ -direction and  $h_y$  in the  $y$ -direction, we get

$$\begin{aligned}
& - \frac{\frac{1}{\varepsilon_{j+1,l}} \frac{\psi_{j+2,l} - \psi_{j,l}}{2h_x} - \frac{1}{\varepsilon_{j-1,l}} \frac{\psi_{j,l} - \psi_{j-2,l}}{2h_x}}{2h_x} - \frac{\frac{1}{\varepsilon_{j,l+1}} \frac{\psi_{j,l+2} - \psi_{j,l}}{2h_y} - \frac{1}{\varepsilon_{j,l-1}} \frac{\psi_{j,l} - \psi_{j,l-2}}{2h_y}}{2h_y} \\
& - ik_x \frac{\frac{1}{\varepsilon_{j+2,l}} \psi_{j+2,l} - \frac{1}{\varepsilon_{j-2,l}} \psi_{j-2,l}}{4h_x} - ik_y \frac{\frac{1}{\varepsilon_{j,l+2}} \psi_{j,l+2} - \frac{1}{\varepsilon_{j,l-2}} \psi_{j,l-2}}{4h_y} \\
& - ik_x \frac{\frac{1}{\varepsilon_{j,l}} \psi_{j+2,l} - \frac{1}{\varepsilon_{j,l}} \psi_{j-2,l}}{4h_x} - ik_y \frac{\frac{1}{\varepsilon_{j,l}} \psi_{j,l+2} - \frac{1}{\varepsilon_{j,l}} \psi_{j,l-2}}{4h_y} + k^2 \psi_{j,l} = \eta \psi_{j,l},
\end{aligned}$$

where  $j = 0, 1, \dots, n$  and  $l = 0, 1, \dots, m$  and the grid is turned into a grid on the torus  $\mathbf{T}^2$  by identifying  $\psi_{j_1, l_1}$  and  $\psi_{j_2, l_2}$  if  $j_1 - j_2$  is divisible by  $n$  and  $l_1 - l_2$  is divisible by  $m$ . Written in this way, we have only used ‘‘even’’ grid points and interpolation values of  $1/\varepsilon$ . We can therefore cut the number of grid points in half and write the finite difference scheme as follows:

$$\begin{aligned}
& - \frac{\frac{1}{2} \left( \frac{1}{\varepsilon_{j+1,l}} + \frac{1}{\varepsilon_{j,l}} \right) \frac{\psi_{j+1,l} - \psi_{j,l}}{h_x} - \frac{1}{2} \left( \frac{1}{\varepsilon_{j,l}} + \frac{1}{\varepsilon_{j-1,l}} \right) \frac{\psi_{j,l} - \psi_{j-1,l}}{h_x}}{h_x} \\
& - \frac{\frac{1}{2} \left( \frac{1}{\varepsilon_{j,l+1}} + \frac{1}{\varepsilon_{j,l}} \right) \frac{\psi_{j,l+1} - \psi_{j,l}}{h_y} - \frac{1}{2} \left( \frac{1}{\varepsilon_{j,l}} + \frac{1}{\varepsilon_{j,l-1}} \right) \frac{\psi_{j,l} - \psi_{j,l-1}}{h_y}}{h_y} \\
& - ik_x \frac{\frac{1}{\varepsilon_{j+1,l}} \psi_{j+1,l} - \frac{1}{\varepsilon_{j-1,l}} \psi_{j-1,l}}{2h_x} - ik_y \frac{\frac{1}{\varepsilon_{j,l+1}} \psi_{j,l+1} - \frac{1}{\varepsilon_{j,l-1}} \psi_{j,l-1}}{2h_y} \\
& - ik_x \frac{\frac{1}{\varepsilon_{j,l}} \psi_{j+1,l} - \frac{1}{\varepsilon_{j,l}} \psi_{j-1,l}}{2h_x} - ik_y \frac{\frac{1}{\varepsilon_{j,l}} \psi_{j,l+1} - \frac{1}{\varepsilon_{j,l}} \psi_{j,l-1}}{2h_y} + k^2 \psi_{j,l} = \eta \psi_{j,l},
\end{aligned}$$

where  $j = 0, 1, \dots, n$  and  $l = 0, 1, \dots, m$ . The latter difference scheme can be written as follows:

$$\begin{aligned}
& \frac{1}{2} \left( \frac{1}{\varepsilon_{j+1,l}} + \frac{1}{\varepsilon_{j,l}} \right) \left[ -\frac{1}{h_x^2} - \frac{ik_x}{h_x} \right] \psi_{j+1,l} + \frac{1}{2} \left( \frac{1}{\varepsilon_{j-1,l}} + \frac{1}{\varepsilon_{j,l}} \right) \left[ -\frac{1}{h_x^2} + \frac{ik_x}{h_x} \right] \psi_{j-1,l} \\
& + \frac{1}{2} \left( \frac{1}{\varepsilon_{j,l+1}} + \frac{1}{\varepsilon_{j,l}} \right) \left[ -\frac{1}{h_y^2} - \frac{ik_y}{h_y} \right] \psi_{j,l+1} + \frac{1}{2} \left( \frac{1}{\varepsilon_{j,l-1}} + \frac{1}{\varepsilon_{j,l}} \right) \left[ -\frac{1}{h_y^2} + \frac{ik_y}{h_y} \right] \psi_{j,l-1} \\
& + \left[ \frac{1}{2} \left( \frac{1}{\varepsilon_{j+1,l}} + \frac{1}{\varepsilon_{j-1,l}} + \frac{2}{\varepsilon_{j,l}} \right) \frac{1}{h_x^2} + \frac{1}{2} \left( \frac{1}{\varepsilon_{j,l+1}} + \frac{1}{\varepsilon_{j,l-1}} + \frac{2}{\varepsilon_{j,l}} \right) \frac{1}{h_y^2} + k^2 \right] \psi_{j,l} \\
& = \eta \psi_{j,l},
\end{aligned}$$

where  $j = 0, 1, \dots, n-1$  and  $l = 0, 1, \dots, m-1$ . Here  $\psi_{j,l}$  and  $\varepsilon_{j,l}$  only depend on the remainders that  $j$  and  $l$  have on division by  $n$  and  $m$ , respectively.

Let us consider the corresponding 1D system

$$\begin{aligned} & \frac{1}{2} \left( \frac{1}{\varepsilon_{j+1}} + \frac{1}{\varepsilon_j} \right) \left[ -\frac{1}{h^2} - \frac{ik}{h} \right] \psi_{j+1} + \frac{1}{2} \left( \frac{1}{\varepsilon_{j-1}} + \frac{1}{\varepsilon_j} \right) \left[ -\frac{1}{h^2} + \frac{ik}{h} \right] \psi_{j-1} \\ & + \left[ \frac{1}{2} \left( \frac{1}{\varepsilon_{j+1}} + \frac{1}{\varepsilon_{j-1}} + \frac{2}{\varepsilon_j} \right) \frac{1}{h^2} + k^2 \right] \psi_j = \eta \psi_j, \end{aligned}$$

where  $j = 0, 1, \dots, n-1$ . Here  $\psi_j$  and  $\varepsilon_j$  only depend on the remainder that  $j$  has on division by  $n$ . Then

$$\begin{aligned} \eta h^2 \sum_j |\psi_j|^2 &= \sum_j \frac{1}{2} \left( \frac{1}{\varepsilon_{j+1}} + \frac{1}{\varepsilon_j} \right) [-1 - i h k] \psi_{j+1} \overline{\psi_j} \\ &+ \sum_j \frac{1}{2} \left( \frac{1}{\varepsilon_{j-1}} + \frac{1}{\varepsilon_j} \right) [-1 + i h k] \psi_{j-1} \overline{\psi_j} \\ &+ \sum_j \left[ \frac{1}{2} \left( \frac{1}{\varepsilon_{j+1}} + \frac{1}{\varepsilon_{j-1}} + \frac{2}{\varepsilon_j} \right) + h^2 k^2 \right] |\psi_j|^2, \end{aligned}$$

which is supposed to be nonnegative. Using that

$$\sum_j \frac{1}{2} \left( \frac{1}{\varepsilon_{j-1}} + \frac{1}{\varepsilon_j} \right) [1 - i h k] \psi_{j-1} \overline{\psi_j} = \sum_j \frac{1}{2} \left( \frac{1}{\varepsilon_j} + \frac{1}{\varepsilon_{j+1}} \right) [1 - i h k] \psi_j \overline{\psi_{j+1}};$$

$$\sum_j \frac{1}{2} \left( \frac{1}{\varepsilon_{j-1}} + \frac{1}{\varepsilon_j} \right) |\psi_j|^2 = \sum_j \frac{1}{2} \left( \frac{1}{\varepsilon_j} + \frac{1}{\varepsilon_{j+1}} \right) |\psi_{j+1}|^2,$$

we can write this identity in the form

$$\begin{aligned} \eta h^2 \sum_j |\psi_j|^2 &= \sum_j \frac{1}{2} \left( \frac{1}{\varepsilon_{j+1}} + \frac{1}{\varepsilon_j} \right) [-1 - i h k] \psi_{j+1} \overline{\psi_j} \\ &+ \sum_j \frac{1}{2} \left( \frac{1}{\varepsilon_j} + \frac{1}{\varepsilon_{j+1}} \right) [-1 + i h k] \psi_j \overline{\psi_{j+1}} \\ &+ \frac{1}{2} \sum_j \left[ \left( \frac{1}{\varepsilon_{j+1}} + \frac{1}{\varepsilon_j} \right) + h^2 k^2 \right] (|\psi_j|^2 + |\psi_{j+1}|^2) \\ &= \frac{1}{2} \sum_j \left( \frac{1}{\varepsilon_j} + \frac{1}{\varepsilon_{j+1}} \right) |(1 - i h k) \psi_j - \psi_{j+1}|^2 \geq 0. \end{aligned}$$

In the 2D case we write  $k^2 = k_x^2 + k_y^2$  and derive the nonnegativity by a dual

application of the 1D result. More precisely,

$$\begin{aligned}
\eta \sum_{j,l} |\psi_{j,l}|^2 &= \frac{1}{2h_x^2} \sum_{j,l} \left( \frac{1}{\varepsilon_{j+1,l}} + \frac{1}{\varepsilon_{j,l}} \right) [-1 - ih_x k_x] \psi_{j+1,l} \overline{\psi_{j,l}} \\
&+ \frac{1}{2h_x^2} \sum_{j,l} \left( \frac{1}{\varepsilon_{j,l}} + \frac{1}{\varepsilon_{j+1,l}} \right) [-1 + ih_x k_x] \psi_{j,l} \overline{\psi_{j+1,l}} \\
&+ \frac{1}{2h_x^2} \sum_{j,l} \left[ \left( \frac{1}{\varepsilon_{j+1,l}} + \frac{1}{\varepsilon_{j,l}} \right) + h_x^2 k_x^2 \right] (|\psi_{j,l}|^2 + |\psi_{j+1,l}|^2) \\
&+ \frac{1}{2h_y^2} \sum_{j,l} \left( \frac{1}{\varepsilon_{j,l+1}} + \frac{1}{\varepsilon_{j,l}} \right) [-1 - ih_y k_y] \psi_{j,l+1} \overline{\psi_{j,l}} \\
&+ \frac{1}{2h_y^2} \sum_{j,l} \left( \frac{1}{\varepsilon_{j,l}} + \frac{1}{\varepsilon_{j,l+1}} \right) [-1 + ih_y k_y] \psi_{j,l} \overline{\psi_{j,l+1}} \\
&+ \frac{1}{2h_y^2} \sum_{j,l} \left[ \left( \frac{1}{\varepsilon_{j,l+1}} + \frac{1}{\varepsilon_{j,l}} \right) + h_y^2 k_y^2 \right] (|\psi_{j,l}|^2 + |\psi_{j,l+1}|^2) \\
&= \frac{1}{2h_x^2} \sum_{j,l} \left( \frac{1}{\varepsilon_{j,l}} + \frac{1}{\varepsilon_{j+1,l}} \right) |(1 - ih_x k_x) \psi_{j,l} - \psi_{j+1,l}|^2 \\
&+ \frac{1}{2h_y^2} \sum_{j,l} \left( \frac{1}{\varepsilon_{j,l}} + \frac{1}{\varepsilon_{j,l+1}} \right) |(1 - ih_y k_y) \psi_{j,l} - \psi_{j,l+1}|^2 \geq 0.
\end{aligned}$$

Consequently, the matrix at the basis of the finite difference scheme is non-negative. The zero eigenvalue only occurs if  $\vec{k} = 0$  and  $\psi_{j,l}$  does not depend on  $(j, l)$ . Using the same arguments as in Subsection 4.5.1, we can also prove that the  $s$ -th eigenvalue  $\eta$  (from) below increases as  $\varepsilon(x, y)$  decreases.

We have generated a finite difference scheme in which  $1/\varepsilon$  has been replaced by the arithmetic means of two of its values at neighboring division points. Instead a different averaging scheme for the values of  $1/\varepsilon$  could be obtained, provided the average is periodic in  $(j, l)$ , which also leads to a linear system with a nonnegative hermitian matrix. One alternative way to do so is to interpolate the  $1/\varepsilon$  by a surface and to take the interpolating value at the intermediate points  $(j + \frac{1}{2}, l)$  and  $(j, l + \frac{1}{2})$ .

#### 4.6.4 Nonrectangular lattices

In this subsection we'll see how the PFD technique works when one deals with nonrectangular lattices as a triangular lattice, which are very common in photonic crystal structures. The description of the method for both the TM and the TE modes is provided below.

**TM modes**

Consider the 2D modified Helmholtz equation (4.6.8)

$$-\nabla^2\psi(x, y) - 2i\mathbf{k} \cdot \nabla\psi(x) + \|\mathbf{k}\|^2\psi(x) = \eta n(x, y)^2\psi(x, y),$$

under the boundary conditions

$$\psi(\mathbf{x} + m_1\mathbf{a}_1 + m_2\mathbf{a}_2) = \psi(\mathbf{x}), \quad \mathbf{x} \in \mathbb{R}^2, \quad m_1, m_2 \in \mathbb{Z},$$

where we assume  $\mathbf{a}_1$  and  $\mathbf{a}_2$  to be two linearly independent vectors in  $\mathbb{R}^2$ .

We also assume that

$$n(\mathbf{x} + m_1\mathbf{a}_1 + m_2\mathbf{a}_2) = n(\mathbf{x}), \quad \mathbf{x} \in \mathbb{R}^2, \quad m_1, m_2 \in \mathbb{Z}.$$

Let us now write

$$\mathbf{x} = A\boldsymbol{\xi}, \quad \text{OR} \quad \begin{pmatrix} x \\ y \end{pmatrix} = \begin{pmatrix} a_{11} & a_{21} \\ a_{12} & a_{22} \end{pmatrix} \begin{pmatrix} \xi \\ \zeta \end{pmatrix},$$

where  $A$  is the nonsingular  $2 \times 2$  matrix with columns  $\mathbf{a}_1$  and  $\mathbf{a}_2$  and  $\xi$  and  $\zeta$  are the orthogonal coordinates corresponding to  $x$  and  $y$ . Letting  $\mathbf{b}_1$  and  $\mathbf{b}_2$  be the column vectors spanning the reciprocal lattice (so that the matrix  $B$  having  $\mathbf{b}_1$  and  $\mathbf{b}_2$  as its columns equals  $2\pi(A^T)^{-1}$ ), we get

$$\begin{pmatrix} \xi \\ \zeta \end{pmatrix} = \frac{1}{2\pi} B^T \mathbf{x} = \frac{1}{2\pi} \begin{pmatrix} b_{11} & b_{12} \\ b_{21} & b_{22} \end{pmatrix} \begin{pmatrix} x \\ y \end{pmatrix}.$$

Using that

$$\frac{\partial\psi}{\partial x} = \frac{1}{2\pi} \left( b_{11} \frac{\partial\psi}{\partial\xi} + b_{21} \frac{\partial\psi}{\partial\zeta} \right), \quad \frac{\partial\psi}{\partial y} = \frac{1}{2\pi} \left( b_{12} \frac{\partial\psi}{\partial\xi} + b_{22} \frac{\partial\psi}{\partial\zeta} \right), \quad (4.6.11)$$

we obtain

$$\begin{aligned} \mathbf{k} \cdot \nabla\psi &= \frac{1}{2\pi} (B^T \vec{k}) \cdot \nabla_{\boldsymbol{\xi}}\psi; \\ \nabla^2\psi &= \frac{1}{4\pi^2} \left( \|\mathbf{b}_1\|^2 \frac{\partial^2\psi}{\partial\xi^2} + \|\mathbf{b}_2\|^2 \frac{\partial^2\psi}{\partial\zeta^2} + 2\mathbf{b}_1 \cdot \mathbf{b}_2 \frac{\partial^2\psi}{\partial\xi\partial\zeta} \right). \end{aligned} \quad (4.6.12)$$

Putting

$$\tilde{\psi}(\boldsymbol{\xi}) = \psi(A^{-1}\mathbf{x})$$

we get for the 2D Helmholtz equation

$$\begin{aligned} & - \frac{1}{4\pi^2} \left( \|\mathbf{b}_1\|^2 \frac{\partial^2\tilde{\psi}}{\partial\xi^2} + \|\mathbf{b}_2\|^2 \frac{\partial^2\tilde{\psi}}{\partial\zeta^2} + 2\mathbf{b}_1 \cdot \mathbf{b}_2 \frac{\partial^2\tilde{\psi}}{\partial\xi\partial\zeta} \right) \\ & - \frac{i}{\pi} (B^T \mathbf{k}) \cdot \nabla_{\boldsymbol{\xi}}\tilde{\psi} + k^2\tilde{\psi}(\boldsymbol{\xi}) = \eta n(A^{-1}\boldsymbol{\xi})^2\tilde{\psi} \end{aligned}$$

with the periodic boundary conditions

$$\tilde{\psi}(\xi + m_1, \zeta + m_2) = \tilde{\psi}(\xi, \zeta), \quad m_1, m_2 \in \mathbb{Z},$$

where  $\boldsymbol{\xi} = (\xi, \zeta)$ .

Let us now discretize as before, using the step sizes  $h_\xi = (1/n)$  and  $h_\zeta = (1/m)$ . We get

$$\begin{aligned} & -\frac{1}{4\pi^2} \left( \|\mathbf{b}_1\|^2 \frac{\psi_{j+1,l} - 2\psi_{j,l} + \psi_{j-1,l}}{h_\xi^2} + \|\mathbf{b}_2\|^2 \frac{\psi_{j,l+1} - 2\psi_{j,l} + \psi_{j,l-1}}{h_\zeta^2} \right. \\ & \left. + 2 \mathbf{b}_1 \cdot \mathbf{b}_2 \frac{\psi_{j+1,l+1} + \psi_{j-1,l-1} - \psi_{j+1,l-1} - \psi_{j-1,l+1}}{4h_\xi h_\zeta} \right) \\ & - \frac{i}{\pi} \left( [B^T \mathbf{k}]_1 \frac{\psi_{j+1,l} - \psi_{j-1,l}}{2h_\xi} + [B^T \mathbf{k}]_2 \frac{\psi_{j,l+1} - \psi_{j,l-1}}{2h_\zeta} \right) + \|\mathbf{k}\|^2 \psi_{j,l} = \eta N_{j,l}^2 \psi_{j,l}, \end{aligned} \quad (4.6.13)$$

where the subscripts range over  $j = 0, 1, \dots, n$  and  $l = 0, 1, \dots, m$  and periodic boundary conditions in discretized form are imposed. Let us implement the previous reduction to a biindex circulant-diagonal system. The eigenvalues of the biindex circulant matrix now are the numbers

$$\begin{aligned} \hat{c}(z, w) &= -\frac{1}{4\pi^2} \left( \|\mathbf{b}_1\|^2 \frac{z - 2 + z^{-1}}{h_\xi^2} + \|\mathbf{b}_2\|^2 \frac{w - 2 + w^{-1}}{h_\zeta^2} \right. \\ & \left. + 2 \mathbf{b}_1 \cdot \mathbf{b}_2 \frac{(z - z^{-1})(w - w^{-1})}{4h_\xi h_\zeta} \right) \\ & - \frac{i}{\pi} \left( [B^T \mathbf{k}]_1 \frac{z - z^{-1}}{2h_\xi} + [B^T \mathbf{k}]_2 \frac{w - w^{-1}}{2h_\zeta} \right) + \|\mathbf{k}\|^2, \end{aligned}$$

where  $z^n = 1$  and  $w^m = 1$ . Writing  $z = e^{i\theta_j}$  with  $\theta_j = \frac{2\pi j}{n}$  and  $w = e^{i\varphi_l}$  with  $\varphi_l = \frac{2\pi l}{m}$ , we can write the eigenvalues in the form

$$\begin{aligned} \hat{c}(z, w; \mathbf{k}) &= \frac{1}{2\pi^2} \left( \frac{\|\mathbf{b}_1\|^2}{h_\xi^2} (1 - \cos \theta_j) + \frac{\|\mathbf{b}_2\|^2}{h_\zeta^2} (1 - \cos \varphi_l) + \frac{\mathbf{b}_1 \cdot \mathbf{b}_2}{h_\xi h_\zeta} \sin \theta_j \sin \varphi_l \right) \\ & + \frac{1}{\pi} \left( \frac{\mathbf{b}_1 \cdot \mathbf{k}}{h_\xi} \sin \theta_j + \frac{\mathbf{b}_2 \cdot \vec{k}}{h_\zeta} \sin \varphi_l \right) + \|\mathbf{k}\|^2, \end{aligned}$$

where  $j = 0, 1, \dots, n-1$  and  $l = 0, 1, \dots, m-1$ . These eigenvalues are all nonnegative, because

$$\begin{aligned} \hat{c}(z, w; \mathbf{k}) &= \left\| \mathbf{k} + \frac{\sin \theta_j}{2\pi h_\xi} \mathbf{b}_1 + \frac{\sin \varphi_l}{2\pi h_\zeta} \mathbf{b}_2 \right\|^2 \\ & + \frac{1}{\pi^2} \left( \frac{\|\mathbf{b}_1\|^2}{h_\xi^2} \sin^4(\tfrac{1}{2}\theta_j) + \frac{\|\mathbf{b}_2\|^2}{h_\zeta^2} \sin^4(\tfrac{1}{2}\varphi_l) \right). \end{aligned}$$

The zero eigenvalue only occurs if  $\mathbf{k} = 0$ ,  $j = 0$ , and  $l = 0$ . As  $n, m \rightarrow +\infty$ , we obtain as a limit

$$\|\mathbf{k} + j\mathbf{b}_1 + l\mathbf{b}_2\|^2,$$

where the relative error is of the order of  $O(\frac{1}{n^2}) + O(\frac{1}{m^2})$ .

### TE modes

Consider the 2D Helmholtz-like equation (4.6.10)

$$-\nabla \cdot \left( \frac{1}{\varepsilon} \nabla \psi \right) - i\mathbf{k} \cdot \nabla \left( \frac{1}{\varepsilon} \psi \right) - i\mathbf{k} \cdot \frac{1}{\varepsilon} \nabla \psi + |\mathbf{k}|^2 \psi = \eta \psi$$

under the boundary conditions

$$\psi(\mathbf{x} + m_1 \mathbf{a}_1 + \mathbf{a}_2) = \psi(\mathbf{x}), \quad \mathbf{x} \in \mathbb{R}^2, \quad m_1, m_2 \in \mathbb{Z},$$

and  $\mathbf{a}_1$  and  $\mathbf{a}_2$  are linearly independent vectors in  $\mathbb{R}^2$ .

Using (4.6.11) and (4.6.12), we obtain

$$\begin{aligned} \mathbf{k} \cdot \nabla_x \psi &= \frac{1}{2\pi} (B^T \vec{k}) \cdot \nabla_\xi \psi; \\ \nabla_x \cdot \left( \frac{1}{\varepsilon} \nabla_x \psi \right) &= \frac{1}{4\pi^2} \left[ \|\mathbf{b}_1\|^2 \frac{\partial}{\partial \xi} \left( \frac{1}{\varepsilon} \frac{\partial \psi}{\partial \xi} \right) + \|\mathbf{b}_2\|^2 \frac{\partial}{\partial \zeta} \left( \frac{1}{\varepsilon} \frac{\partial \psi}{\partial \zeta} \right) \right. \\ &\quad \left. + \mathbf{b}_1 \cdot \mathbf{b}_2 \frac{\partial}{\partial \zeta} \left( \frac{1}{\varepsilon} \frac{\partial \psi}{\partial \xi} \right) + \mathbf{b}_1 \cdot \mathbf{b}_2 \frac{\partial}{\partial \xi} \left( \frac{1}{\varepsilon} \frac{\partial \psi}{\partial \zeta} \right) \right]. \end{aligned}$$

Putting

$$\tilde{\psi}(\boldsymbol{\xi}) = \psi(A^{-1}\mathbf{x}), \quad \tilde{\varepsilon}(\boldsymbol{\xi}) = \varepsilon(A^{-1}\mathbf{x})$$

we get for the 2D Helmholtz-like equation

$$\begin{aligned} &-\frac{1}{4\pi^2} \left[ \|\mathbf{b}_1\|^2 \frac{\partial}{\partial \xi} \left( \frac{1}{\tilde{\varepsilon}} \frac{\partial \tilde{\psi}}{\partial \xi} \right) + \|\mathbf{b}_2\|^2 \frac{\partial}{\partial \zeta} \left( \frac{1}{\tilde{\varepsilon}} \frac{\partial \tilde{\psi}}{\partial \zeta} \right) \right. \\ &\quad \left. + \mathbf{b}_1 \cdot \mathbf{b}_2 \frac{\partial}{\partial \zeta} \left( \frac{1}{\tilde{\varepsilon}} \frac{\partial \tilde{\psi}}{\partial \xi} \right) + \mathbf{b}_1 \cdot \mathbf{b}_2 \frac{\partial}{\partial \xi} \left( \frac{1}{\tilde{\varepsilon}} \frac{\partial \tilde{\psi}}{\partial \zeta} \right) \right] \\ &+ \frac{1}{2\pi i} (B^T \mathbf{k}) \cdot \nabla_\xi \left( \frac{1}{\tilde{\varepsilon}} \tilde{\psi} \right) + \frac{1}{2\pi i} \frac{1}{\tilde{\varepsilon}} (B^T \mathbf{k}) \cdot \nabla_\xi \tilde{\psi} + |\mathbf{k}|^2 \tilde{\psi}(\boldsymbol{\xi}) = \eta \tilde{\psi}(\boldsymbol{\xi}) \end{aligned}$$

with the periodic boundary conditions

$$\tilde{\psi}(\xi + m_1, \zeta + m_2) = \tilde{\psi}(\xi, \zeta), \quad m_1, m_2 \in \mathbb{Z},$$

where  $\boldsymbol{\xi} = (\xi, \zeta)$ .

Let us now discretize as before, using the step sizes  $h_\xi = (1/n)$  and  $h_\zeta = (1/m)$ . We get

$$\begin{aligned}
& \frac{1}{2} \left[ \frac{1}{\tilde{\varepsilon}_{j+1,l}} + \frac{1}{\tilde{\varepsilon}_{j,l}} \right] \left[ -\frac{\|\mathbf{b}_1\|^2}{4\pi^2 h_\xi^2} + \frac{[B^T \mathbf{k}]_1}{2\pi i h_\xi} \right] \tilde{\psi}_{j+1,l} + \frac{1}{2} \left[ \frac{1}{\tilde{\varepsilon}_{j,l}} + \frac{1}{\tilde{\varepsilon}_{j-1,l}} \right] \left[ -\frac{\|\mathbf{b}_1\|^2}{4\pi^2 h_\xi^2} - \frac{[B^T \mathbf{k}]_1}{2\pi i h_\xi} \right] \tilde{\psi}_{j-1,l} \\
& + \frac{1}{2} \left[ \frac{1}{\tilde{\varepsilon}_{j,l+1}} + \frac{1}{\tilde{\varepsilon}_{j,l}} \right] \left[ -\frac{\|\mathbf{b}_2\|^2}{4\pi^2 h_\zeta^2} + \frac{[B^T \mathbf{k}]_2}{2\pi i h_\zeta} \right] \tilde{\psi}_{j,l+1} + \frac{1}{2} \left[ \frac{1}{\tilde{\varepsilon}_{j,l-1}} + \frac{1}{\tilde{\varepsilon}_{j,l}} \right] \left[ -\frac{\|\mathbf{b}_2\|^2}{4\pi^2 h_\zeta^2} - \frac{[B^T \mathbf{k}]_2}{2\pi i h_\zeta} \right] \tilde{\psi}_{j,l-1} \\
& - \frac{\mathbf{b}_1 \cdot \mathbf{b}_2}{16\pi^2 h_\xi h_\zeta} \left[ \left( \frac{1}{\tilde{\varepsilon}_{j,l+1}} + \frac{1}{\tilde{\varepsilon}_{j+1,l}} \right) \tilde{\psi}_{j+1,l+1} + \left( \frac{1}{\tilde{\varepsilon}_{j,l-1}} + \frac{1}{\tilde{\varepsilon}_{j-1,l}} \right) \tilde{\psi}_{j-1,l-1} \right. \\
& \left. - \left( \frac{1}{\tilde{\varepsilon}_{j,l+1}} + \frac{1}{\tilde{\varepsilon}_{j-1,l}} \right) \tilde{\psi}_{j-1,l+1} - \left( \frac{1}{\tilde{\varepsilon}_{j,l-1}} + \frac{1}{\tilde{\varepsilon}_{j+1,l}} \right) \tilde{\psi}_{j+1,l-1} \right] \\
& + \left[ \frac{1}{2} \left[ \frac{1}{\tilde{\varepsilon}_{j+1,l}} + \frac{1}{\tilde{\varepsilon}_{j-1,l}} + \frac{2}{\tilde{\varepsilon}_{j,l}} \right] \frac{\|\mathbf{b}_1\|^2}{4\pi^2 h_\xi^2} + \frac{1}{2} \left[ \frac{1}{\tilde{\varepsilon}_{j,l+1}} + \frac{1}{\tilde{\varepsilon}_{j,l-1}} + \frac{2}{\tilde{\varepsilon}_{j,l}} \right] \frac{\|\mathbf{b}_2\|^2}{4\pi^2 h_\zeta^2} + \mathbf{k}^2 \right] \tilde{\psi}_{j,l} \\
& = \eta \tilde{\psi}_{j,l},
\end{aligned}$$

where  $j = 0, 1, \dots, n-1$  and  $l = 0, 1, \dots, m-1$ . Here  $\tilde{\psi}_{j,l}$  and  $\tilde{\varepsilon}_{j,l}$  only depend on the remainders that  $j$  and  $l$  have on division by  $n$  and  $m$ , respectively.

# Chapter 5

## Numerical Results

In this Chapter we present some numerical results of band structure calculations using the PFE and PFD methods for one-dimensional photonic crystals and the PFD method for two-dimensional photonic crystals and compare the results to those found in the literature. In the  $2D$  case, the photonic crystal configurations considered in this section are those depicted in Fig. 5.3 in the case of a rectangular lattice and in Fig. 5.12 in the case of a nonrectangular lattice. In these case the band structure for both the TM and the TE modes will be given.

All numerical results in this Ph.D. thesis have been obtained using MatLab (version 7.4.0) on a MacBook equipped with an Intel Core 2 Duo processor with a speed of 2.2 GHz.

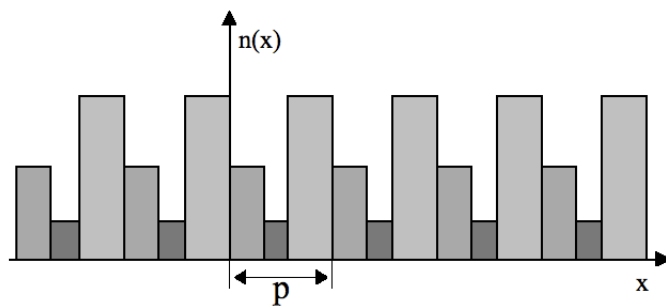


**Figure 5.1:** Example of a periodic structure with period  $p$  in the case of a piecewise constant refractive index. The figure illustrates a  $1D$  three layer photonic crystal with different layer amplitudes.

**Table 5.1:** The first two columns show the periodic ( $k = 0$ ) and antiperiodic ( $k = \pi/p$ ) eigenvalues for a two-layer photonic crystal ( $a_1 = 1, n_1 = 1, a_2 = 3, n_2 = 2$ ), whereas the last two columns show that the periodic ( $k = 0$ ) and antiperiodic ( $k = \pi/p$ ) eigenvalues for a three-layer photonic crystal ( $a_1 = 1, n_1 = 1.5, a_2 = 3, n_2 = 1, a_3 = 0.8, n_3 = 2$ ).

$k = 0$	$k = \pi/p$	$k = 0$	$k = \pi/p$
0.0000	0.1570	0.0000	0.2555
0.2330	0.6574	0.5226	1.3462
0.9258	1.5593	1.7318	3.2200
2.0541	2.9132	3.6086	5.5404
3.5775	4.7380	6.6503	9.1831
5.4212	7.0470	9.8367	13.0079
7.5175	9.8207	14.2923	17.8273
9.8275	12.4493	19.2987	23.4142
13.0583	15.4995	25.0186	29.5911
16.7057	19.0993	31.6193	37.1683

## 5.1 1D spectrum

In the case of one-dimensional photonic crystals (Fig. 5.1) we considered both a two-layer and a three-layer crystal and compared our numerical results to the analytical counterpart given by the Hill discriminant formalism. In fact, from the Oscillation Theorem 2.3.1, to get the 1D spectrum it is sufficient to find the zeros of  $\Delta(\eta) = 2$  (periodic eigenvalues) and the zeros of  $\Delta(\eta) = -2$  (antiperiodic eigenvalues). Therefore, by using the 1D PFE and PFD techniques one finds the periodic and antiperiodic eigenvalues by putting the wavenumber in the circulant systems (4.5.4) and (4.6.5), equal to zero ( $k = 0$ ) and to  $\pi/p$  ( $k = \pi/p$ ), respectively. From Subsecs. 4.5.1 and 4.6.1 we know that both the absolute and relative errors in the homogeneous case (constant refractive index) are of the order of  $1/n^2$ ,  $n$  being the number of grid points. We therefore tested the code numerically by considering 1000 grid points and checked that the error for a constant index of refraction was of the order of  $10^{-6}$ , as expected. This gives us a good indication of the accuracy of the PFE and PFD techniques, also when the refractive index

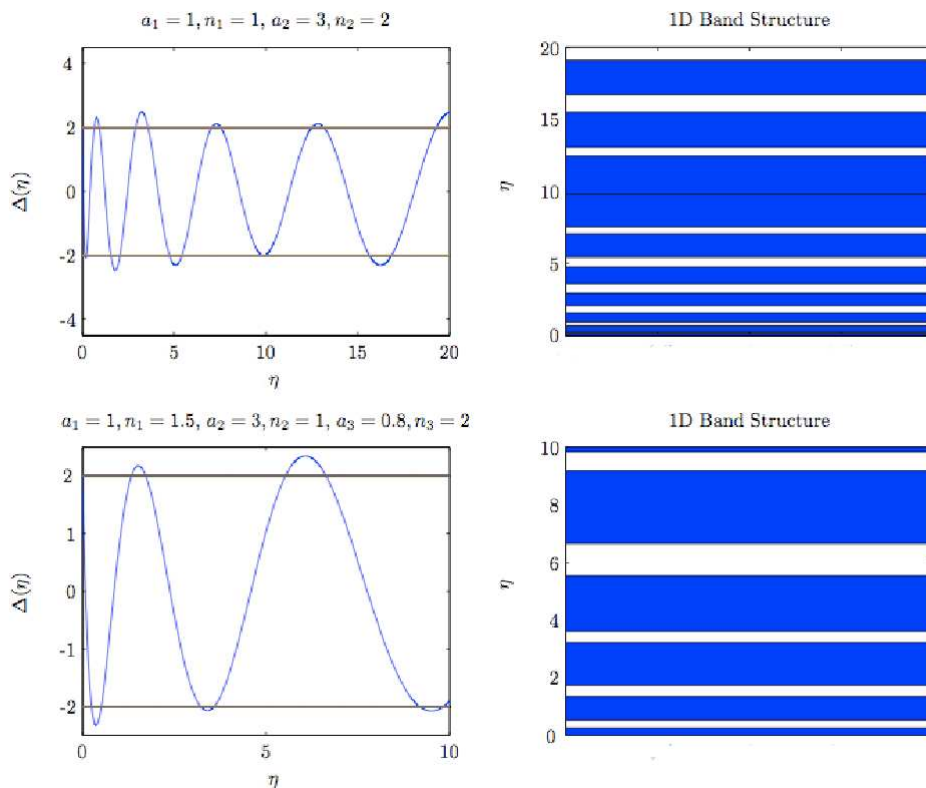


**Figure 5.2:** The left hand-side of the figure shows the Hill discriminant of both a two-layer ( $a_1 = 1, n_1 = 1, a_2 = 3, n_2 = 2$ ) and a three-layer ( $a_1 = 1, n_1 = 1.5, a_2 = 3, n_2 = 1, a_3 = 0.8, n_3 = 2$ ) photonic crystal. On the right hand-side the allowed bands are depicted in blue and the band gaps in white. The PFD algorithm finds the zeros of  $\Delta(\eta) = 2$  (periodic eigenvalues) and of  $\Delta(\eta) = -2$  (antiperiodic eigenvalues), respectively. The accuracy of the algorithm depends on the number of grid points as shown in Subsecs. 4.5.1 and 4.6.1.

varies with respect to the  $x$  variable, as it happens in 1D photonic crystals. In fact, Fig. 5.2 shows that the numerical results of both the PFE and the PFD band structure calculations are in good agreement with the analytical results given by the Hill discriminant formalism (see Sec. 2.3). Tables 5.1 show the numerical results obtained, i.e., the zeros of  $\Delta(\eta) = 2$  (periodic eigenvalues) and the zeros of  $\Delta(\eta) = -2$  (antiperiodic eigenvalues), which are in perfect accordance with those derived from Hill's discriminant.

## 5.2 TM spectrum in rectangular lattices

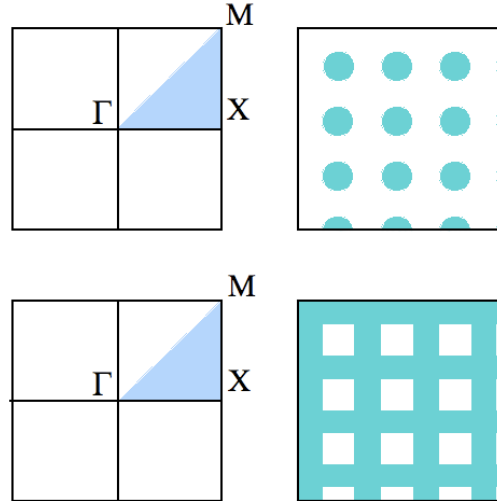


**Figure 5.3:** The top half of the figure shows a photonic crystal composed of a square distribution of dielectric rods embedded in air and the corresponding Brillouin zone. The  $\Gamma$ -point corresponds to  $k_x = k_y = 0$ , the  $X$ -point to  $k_x = \pi/a$  and  $k_y = 0$  and finally at the  $M$ -point one has  $k_x = k_y = \pi/a$ ,  $a$  being either period. The bottom of the figure shows a photonic crystal composed of a square distribution of dielectric veins in air and the corresponding Brillouin zone.

When dealing with TM modes in rectangular lattices, we first consider the case where the photonic crystal is composed of a square distribution of dielectric rods embedded in air (Fig. 5.3) and then the case where the photonic crystal is composed of a rectangular distribution of dielectric veins in air (Fig. 5.3). In either case the dielectric constant has the value of 8.9 and the rods have radius  $r = 0.2a$  and the thickness of the veins is  $0.165a$ ,  $a$  being the side of the period parallelogram (a square in these cases).

By the PFD technique we computed the spectrum solving the circulant-diagonal eigenvalue problem (4.6.9) for fixed  $\mathbf{k}$  values. Since we are dealing with square lattices where  $n(\mathbf{x})$  is invariant under the group of automorphisms of the square, it is sufficient to consider one eighth of the Brillouin zone (Fig. 5.3) as explained in Sec. 4.1. Therefore we solved the circulant-diagonal system each time for different wavevector values varying, as specified below, on the boundary of the blue region shown in Fig. 5.3:

1.  $k_x \in [0, \pi/a], \quad k_y = 0,$
2.  $k_x = \pi/a, \quad k_y \in [0, \pi/a],$
3.  $k_x \in [0, \pi/a], \quad k_y \in [0, \pi/a].$

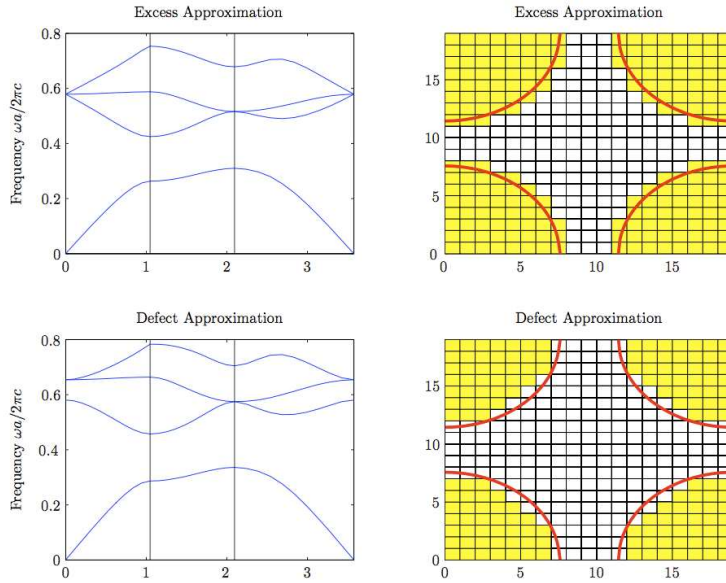


**Figure 5.4:** The left-hand side of the Figure shows the band structure corresponding the the defect and excess grid approximation for TM modes. On the right-hand side the  $20 \times 20$  corresponding grids are shown.

Since the PFD technique uses a regular grid, the dielectric constant  $\varepsilon(x, y)$  has been sampled first in a defect approximation where the dielectric values different from one have been taken when the grid points are only inside the circles with radius  $r = 0.2a$ , and then in an excess approximation where the dielectric values different from one have been taken for both the inside grid points and the grid point closest to the circles with radius  $r = 0.2a$ . The right-hand side of Fig. 5.4 shows the dielectric constant distribution on a  $20 \times 20$  regular grid both in the defect and the excess approximation and the left-hand side shows the corresponding band structure.

As explained at the end of Secs. 4.6.1 and 4.6.2, taking a finer grid, the band structure in the excess and defect approximations converge to each other and yield results ready to be compared with those in the literature. In our case it has been sufficient to take a  $40 \times 40$  grid for this to happen. The outcome is shown in Fig. 5.5.

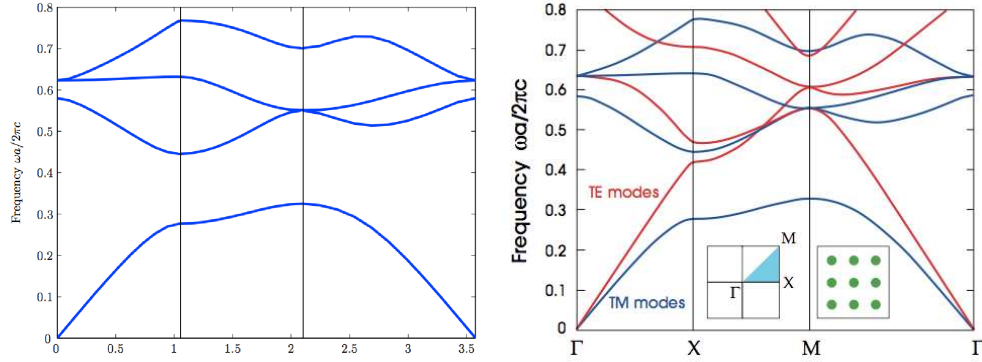


**Figure 5.5:** The left-hand side of the figure shows the result obtained by the PFD technique and the right-hand side the results compared obtained by the Joannopoulos et al. group using the Fourier expansion (FE) method. The PFD results have been achieved using a  $40 \times 40$  grid where the excess and defect approximation give basically the same band structure figure.

The procedure followed to compute the band structure for the configuration of dielectric veins shown in Fig. 5.3 is the same as the one described above. Numerical results and comparisons with the literature are shown in Figs. 5.6 and 5.7.

The considerations for the error shown in Sec. 5.1 are still valid. In fact, from Subsec. 4.6.2 it follows that the absolute and relative errors behave like  $n^{-2} + m^{-2}$  (where  $n$  and  $m$  are the number of grid points in the  $x$  and  $y$  axis, respectively) when the refractive index is constant (homogeneous case), and therefore we first tested our code in this situation taking a  $40 \times 40$  grid and obtaining a  $10^{-3}$  error as expected. In the inhomogeneous case the error should be of the same order and in fact Figs. 5.5 and 5.7 show that there is a perfect geometrical matching between our results and those obtained by Joannopoulos et al. ones [1] using the Fourier expansion (FE) method.

### 5.3 TE spectrum in rectangular lattices

As we did in Sec. 5.2 for the TM modes, to deal with the TE modes in rectangular lattices, we first consider the case where the photonic crystal representation is given in Fig. 5.3 (dielectric rods embedded in air) and then the case where the photonic crystal representation is depicted in Fig. 5.3 (dielectric veins in air). Once again in either case the dielectric constant has the value of 8.9, the rods have radius  $r = 0.2a$  and the thickness of the veins is

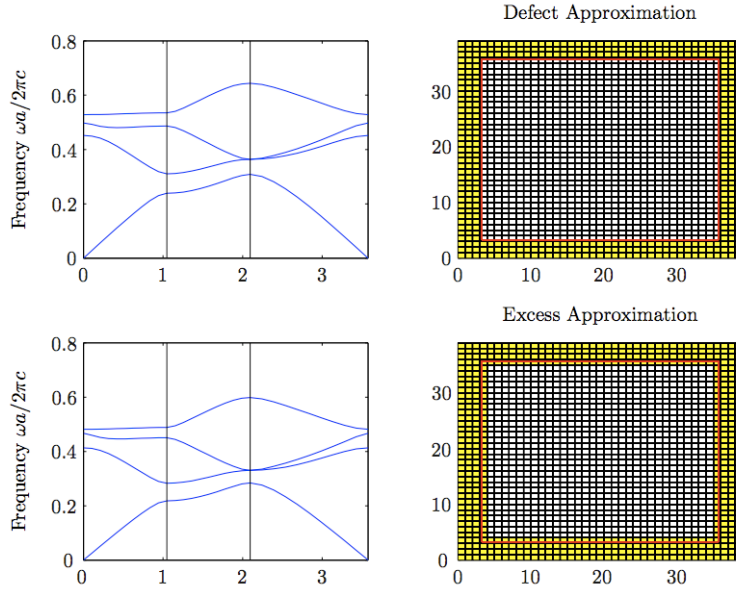


**Figure 5.6:** The left-hand side of the Figure shows the band structure corresponding to the defect and excess grid approximation for TM modes. On the right-hand side the  $40 \times 40$  corresponding grids are shown.

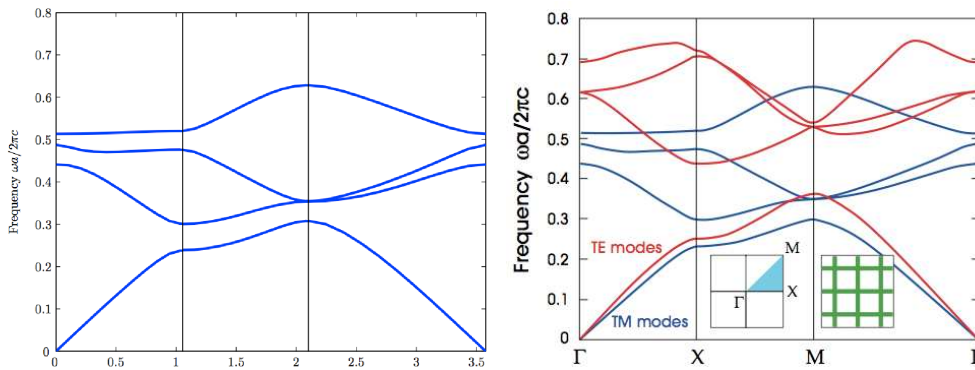


**Figure 5.7:** The left-hand side of the figure shows the result obtained by the PFD technique and the right-hand side the results compared obtained by the Joannopoulos et al. group [1] using the Fourier expansion (FE) method. The PFD results have been achieved using a  $60 \times 60$  grid where the excess and defect approximation give basically the same band structure figure.

$0.165a$ ,  $a$  being the side of the square lattice. Since the period parallelogram

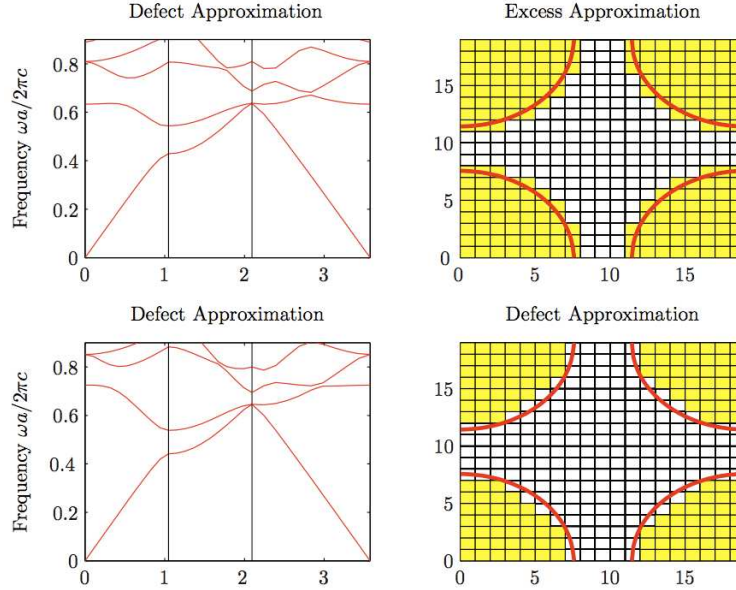


**Figure 5.8:** The left-hand side of the Figure shows the band structure corresponding to the defect and excess grid approximation for TE modes. On the right-hand side the  $20 \times 20$  corresponding grids are shown.

is given by a square, the considerations for the choice of the values of the wavevector  $\mathbf{k}$  and the procedure to compute the band structure are the same as in Sec. 5.2. In fact, we computed the photonic band structure with an excess and a defect approximation of the dielectric constant in a regular grid (Fig. 5.8 and Fig. 5.9). Therefore we took a finer grid, in order to get a band structure ready to be compared with the results in the literature. As before we considered a  $40 \times 40$  grid for the dielectric rods embedded in air configuration (Fig. 5.3) and a  $60 \times 60$  grid for the dielectric veins configuration (Fig. 5.3). The corresponding band structures are shown on the left-hand side of Fig. 5.10 for the dielectric rods embedded in air, and on the left-hand side of Fig. 5.11 for the dielectric veins in air. On the right-hand side of either Figure we displayed the results by Joannopoulos et al. [1]. As we can see, our band structure calculations don't fully agree with those given in [1]. Nevertheless, in the TM case we have perfect agreement (Figs. 5.5 and 5.7). This contrast is caused by the greater difficulty we have encountered in treating TE modes, especially when using finite differences. In fact, in the TE case, the Helmholtz equation (4.2.2) contains the dielectric constant inside the differential operator and therefore the finite difference approximation has poor accuracy whenever the dielectric constant is a  $2D$  piecewise constant function, though the error analysis doesn't differ substantially in the two

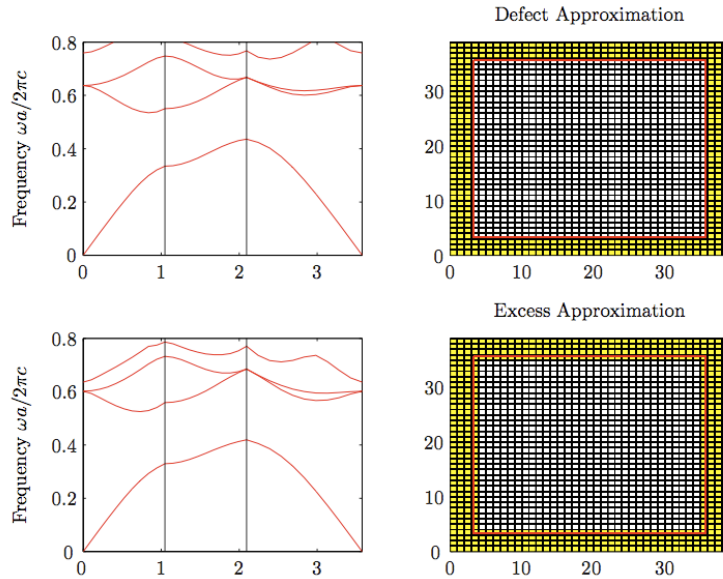


**Figure 5.9:** The left-hand side of the Figure shows the band structure corresponding to the defect and excess grid approximation for TE modes. On the right-hand side the  $40 \times 40$  corresponding grids are shown.

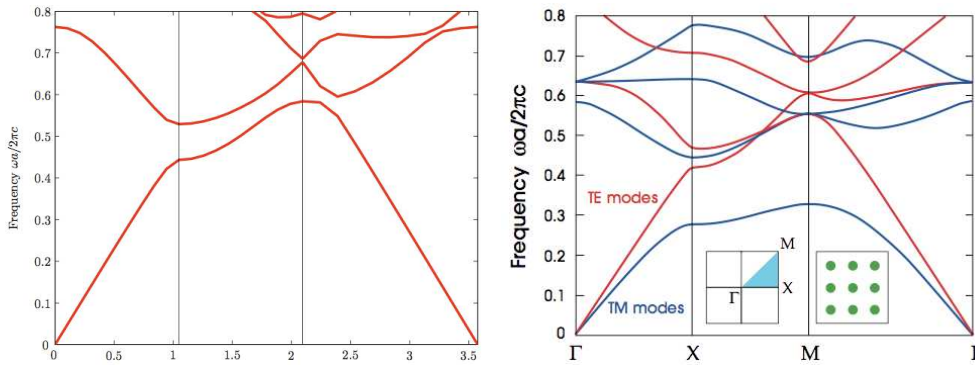


**Figure 5.10:** The left-hand side of the figure shows the result obtained by the PFD technique and the right-hand side the results compared obtained by the Joannopoulos et al. group [1] using the Fourier expansion (FE) method. The PFD results have been obtained using a  $40 \times 40$  grid where the excess and defect approximations give basically the same band structure figure.

cases.

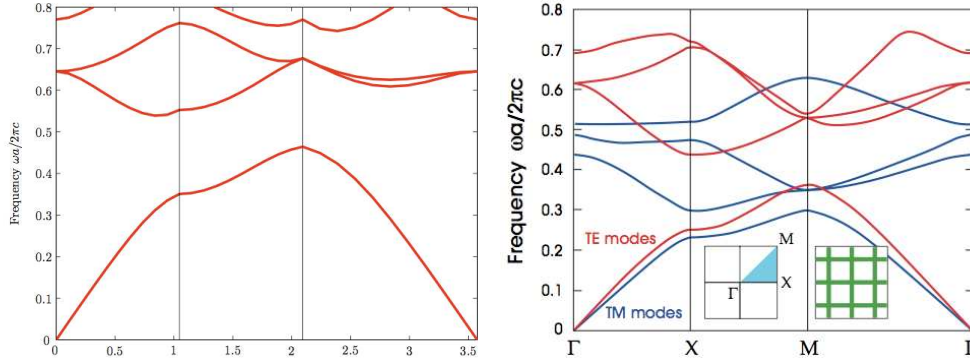


**Figure 5.11:** The left-hand side of the figure shows the result obtained by the PFD technique and the right-hand side the results compared obtained by the Joannopoulos et al. [1] group using the Fourier expansion (FE) method. The PFD results have been achieved using a  $40 \times 40$  grid where the excess and defect approximations give basically the same band structure figure.

## 5.4 Nonrectangular lattice

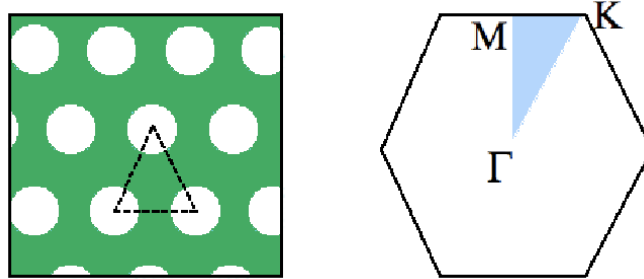


**Figure 5.12:** The figure shows a photonic crystal made of a triangular distribution of rods embedded in a dielectric medium and the corresponding Brillouin zone. The  $\Gamma$ -point corresponds to  $k_x = k_y = 0$ , the  $M$ -point to  $k_x = 0$  and  $k_y = 2\pi/(\sqrt{3}a)$  and finally at the  $K$ -point one has  $k_x = 2\pi/(3a)$  and  $k_y = 2\pi/(\sqrt{3}a)$ , where the period parallelogram is a rhombus with sides  $a$ .

In this section we study the band structure of  $2D$  photonic crystals when its lattice is a parallelogram. In order to make comparisons with the literature, we choose the configuration depicted in Fig. 5.12 where the crystal

is composed of a triangular distribution of rods embedded in a dielectric medium ( $\varepsilon = 13$ ) whose radius is  $r = 0.48a$ ,  $a$  being the identical sides of the period parallelogram. As before, we give and discuss the band structure for both TM and TE modes.

### 5.4.1 TM and TE spectra

By the PFD technique we computed the spectrum solving the circulant-diagonal eigenvalue problem (4.6.13) for fixed  $\mathbf{k}$  values. This time we are dealing with a nonrectangular lattice. From Sec. 4.1 we know that it is sufficient to consider the restricted Brillouin zone  $\mathbf{Z}_0$  (Fig. 5.12). Therefore we solved the circulant-diagonal system each time for different wavevector values varying them, on the boundary of the blue region shown in Fig. 5.12 as follows:

1.  $k_x = 0, \quad k_y \in [0, 2\pi/(\sqrt{3}a)],$
2.  $k_x \in [0, 2\pi/(3a)], \quad k_y = 2\pi/(\sqrt{3}a),$
3.  $k_x \in [2\pi/(3a), 0], \quad k_y \in [2\pi/(\sqrt{3}a), 0].$

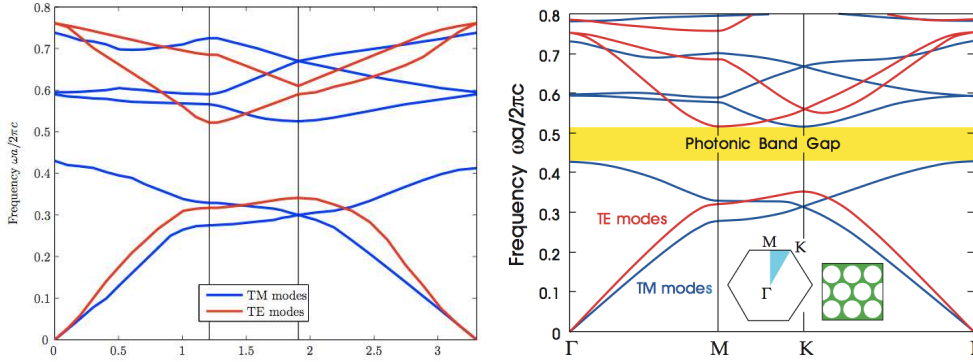


**Figure 5.13:** The left-hand side of the figure shows the result obtained by the PFD technique and the right-hand side the results compared obtained by the Joannopoulos et al. [1] group using the Fourier expansion (FE) method. The PFD results have been achieved using a  $40 \times 40$  grid where the excess and defect approximations give basically the same band structure figure.

As in Secs. 5.2 and 5.3, the dielectric function  $\varepsilon(x, y)$  has been sampled first in a defect approximation and then in an excess approximation. More precisely, in the first case, the dielectric values different from one have been

taken when the grid points are only inside the circles with radius  $r = 0.48a$ , while in the excess approximation they have been taken for both the inside grid points and the grid point closest to the circles with radius  $r = 0.48a$ . Then we took a finer grid, in order to get a band structure ready to be compared with the results in the literature. We considered a  $40 \times 40$  grid. The corresponding band structures for both the TM and the TE modes are shown on the left-hand side of Fig. 5.13, while the right-hand side shows the results by Joannopoulos et al. [1]. As we saw in the preceding Sections the TM band spectrum matches the results in the literature unlike in the case of TE band spectrum. The reason is that the Helmholtz equation (4.2.2) for TE modes contains the dielectric constant inside the differential operator. Therefore the finite difference approximation has poor accuracy when the dielectric constant is a  $2D$  piecewise constant function.

## 5.5 Conclusions

In this PhD thesis we studied the mathematical properties of  $1D$  and  $2D$  pure photonic crystals with the purpose of finding a satisfactory analytical or numerical method to get their band spectrum.

In Chapter 2 we focused on the mathematical study of properties of  $1D$  photonic crystals. This part of the thesis relies upon the master thesis of Paolo Pintus, who is finishing his PhD thesis at the Scuola Superiore Sant'Anna in Pisa, Italy. In Chapter 3 we considered  $1D$  photonic crystals and tried to solve a design problem, i.e., given the allowed frequencies and the photonic path at each allowed frequency we want to identify the corresponding refractive index as a function of the position in the crystal. We managed to give a satisfactory answer in the case where the refractive index is a piecewise constant function, which is the situation that best fits  $1D$  crystals. We published our results in [43], where basically Chapters 2 and 3 of this thesis are summarized.

The main subject of Chapters 4 and 5 is a numerical approach to find the band structure of two-dimensional photonic crystals. With this purpose we first focused on a periodic finite difference (PFD) method which led to a successful computation of the spectrum for TM modes. When dealing with TE modes, however, the numerical results did not correspond in a satisfactory way with those in the literature. In the  $1D$  case we succeeded in obtaining satisfactory results by using the PFE method.

On the basis of the numerical results obtained by either method, we consider the periodic finite element (PFE) method more suitable than the PFD method to compute the band structures in the TE mode case. In fact,

we are confident that the PFE method will give us satisfactory results in the  $2D$  case, as it did in the  $1D$  case. Research is going on in this direction and a paper on the subject is in preparation.



# Appendix A

## Extreme values of Hill's discriminant

In this appendix we prove that, for the Helmholtz-Schrödinger equation having a potential and refractive index of period  $p$ , Hill's discriminant  $\Delta(\eta)$  has exactly one extreme value in each nonempty bounded band gap. This result has been established in the Schrödinger case by Kramers [29]. It is crucial to constructing the quasimomentum  $k(\eta)$ . Here we apply Kramers' methods in the Helmholtz-Schrödinger case.

Let us start with two linearly independent real solutions  $\phi_1(\eta, x)$  and  $\phi_2(\eta, x)$  of the Helmholtz-Schrödinger equation

$$-\psi''(\eta, x) + Q(x)\psi(\eta, x) = \eta n(x)^2\psi(\eta, x), \quad (\text{A.0.1})$$

where  $Q(x+p) \equiv Q(x)$  is real-valued and  $n(x+p) \equiv n(x)$  is positive. Let us assume that the initial conditions of these two solutions do not depend on  $\eta$ . In other words, let the matrix

$$\Phi = \begin{pmatrix} \phi_1(\eta, 0) & \phi_2(\eta, 0) \\ \phi_1'(\eta, 0) & \phi_2'(\eta, 0) \end{pmatrix}$$

be nonsingular and not depend on  $\eta$ . We write  $c = \det \Phi \neq 0$  and omit the argument  $\eta$  in the entries of  $\Phi$ . It is then clear that

$$\phi_1(\eta, x) = \phi_1(0)\theta(\eta, x) + \phi_1'(0)\varphi(\eta, x), \quad (\text{A.0.2a})$$

$$\phi_2(\eta, x) = \phi_2(0)\theta(\eta, x) + \phi_2'(0)\varphi(\eta, x), \quad (\text{A.0.2b})$$

where  $\theta(\eta, x)$  and  $\varphi(\eta, x)$  are defined by (2.1.3).

In analogy with the period map we define the real numbers  $\beta_{jl}$  ( $j, l = 1, 2$ ) as follows:

$$\begin{pmatrix} \phi_1(\eta, x+p) & \phi_2(\eta, x+p) \\ \phi'_1(\eta, x+p) & \phi'_2(\eta, x+p) \end{pmatrix} = \begin{pmatrix} \phi_1(\eta, x) & \phi_2(\eta, x) \\ \phi'_1(\eta, x) & \phi'_2(\eta, x) \end{pmatrix} \begin{pmatrix} \beta_{11} & \beta_{12} \\ \beta_{21} & \beta_{22} \end{pmatrix}. \quad (\text{A.0.3})$$

Substituting  $x = 0$  and using (A.0.2) we get

$$\begin{aligned} \begin{pmatrix} \theta(\eta, p) & \varphi(\eta, p) \\ \theta'(\eta, p) & \varphi'(\eta, p) \end{pmatrix} \begin{pmatrix} \phi_1(0) & \phi_2(0) \\ \phi'_1(0) & \phi'_2(0) \end{pmatrix} &= \begin{pmatrix} \phi_1(\eta, p) & \phi_2(\eta, p) \\ \phi'_1(\eta, p) & \phi'_2(\eta, p) \end{pmatrix} \\ &= \begin{pmatrix} \phi_1(0) & \phi_2(0) \\ \phi'_1(0) & \phi'_2(0) \end{pmatrix} \begin{pmatrix} \beta_{11} & \beta_{12} \\ \beta_{21} & \beta_{22} \end{pmatrix}. \end{aligned}$$

Hence,

$$\begin{pmatrix} \beta_{11} & \beta_{12} \\ \beta_{21} & \beta_{22} \end{pmatrix} = \Phi^{-1} \begin{pmatrix} \theta(\eta, p) & \varphi(\eta, p) \\ \theta'(\eta, p) & \varphi'(\eta, p) \end{pmatrix} \Phi,$$

i.e., the  $\beta$ -matrix is similar to the period map. As a result, these two matrices have the same trace and determinant:

$$\Delta(\eta) = \beta_{11} + \beta_{22}, \quad (\text{A.0.4a})$$

$$1 = \beta_{11}\beta_{22} - \beta_{12}\beta_{21}. \quad (\text{A.0.4b})$$

Let us now apply Cramer's rule to solve the linear system obtained from (A.0.3) by substituting  $x = 0$  for  $\beta_{jl}$  ( $j, l = 1, 2$ ). We get

$$\beta_{11} = \frac{1}{c} \begin{vmatrix} \varphi_1(\eta, p) & \varphi_2(0) \\ \varphi'_1(\eta, p) & \varphi'_2(0) \end{vmatrix}, \quad \beta_{12} = \frac{1}{c} \begin{vmatrix} \varphi_2(\eta, p) & \varphi_2(0) \\ \varphi'_2(\eta, p) & \varphi'_2(0) \end{vmatrix}, \quad (\text{A.0.5a})$$

$$\beta_{21} = \frac{1}{c} \begin{vmatrix} \varphi_1(0) & \varphi_1(\eta, p) \\ \varphi'_1(0) & \varphi'_1(\eta, p) \end{vmatrix}, \quad \beta_{22} = \frac{1}{c} \begin{vmatrix} \varphi_1(0) & \varphi_2(\eta, p) \\ \varphi'_1(0) & \varphi'_2(\eta, p) \end{vmatrix}. \quad (\text{A.0.5b})$$

Let us denote the  $\eta$ -derivative of  $\psi$  by  $\dot{\psi}$ . Differentiating (A.0.1) by  $\eta$  we get

$$-\dot{\psi}(\eta, x) + Q(x)\dot{\psi}(\eta, x) = \eta n(x)^2 \dot{\psi}(\eta, x) + n(x)^2 \psi(\eta, x).$$

By the method of variation of parameters we easily get

$$\begin{aligned} \dot{\psi}(\eta, x) &= c_1(\eta, 0)\phi_1(\eta, x) + c_2(\eta, 0)\phi_2(\eta, x) \\ &+ \frac{1}{c} \int_0^x dy n(y)^2 \begin{vmatrix} \phi_1(\eta, x) & \phi_2(\eta, x) \\ \phi_1(\eta, y) & \phi_2(\eta, y) \end{vmatrix} \psi(\eta, y), \end{aligned} \quad (\text{A.0.6})$$

where

$$\begin{pmatrix} c_1(\eta, 0) \\ c_2(\eta, 0) \end{pmatrix} = \Phi^{-1} \begin{pmatrix} \dot{\psi}(\eta, 0) \\ \dot{\psi}'(\eta, 0) \end{pmatrix}.$$

By differentiation with respect to  $x$  we get

$$\begin{aligned} \dot{\psi}'(\eta, x) &= c_1(\eta, 0)\phi_1'(\eta, x) + c_2(\eta, 0)\phi_2'(\eta, x) \\ &+ \frac{1}{c} \int_0^x dy n(y)^2 \begin{vmatrix} \phi_1'(\eta, x) & \phi_2'(\eta, x) \\ \phi_1(\eta, y) & \phi_2(\eta, y) \end{vmatrix} \psi(\eta, y). \end{aligned} \quad (\text{A.0.7})$$

Thus if the initial conditions  $\psi(\eta, 0)$  and  $\psi'(\eta, 0)$  do not depend on  $\eta$ , (A.0.6) and (A.0.7) simplify to

$$\dot{\psi}(\eta, x) = \frac{1}{c} \int_0^x dy n(y)^2 \begin{vmatrix} \phi_1(\eta, x) & \phi_2(\eta, x) \\ \phi_1(\eta, y) & \phi_2(\eta, y) \end{vmatrix} \psi(\eta, y), \quad (\text{A.0.8a})$$

$$\dot{\psi}'(\eta, x) = \frac{1}{c} \int_0^x dy n(y)^2 \begin{vmatrix} \phi_1'(\eta, x) & \phi_2'(\eta, x) \\ \phi_1(\eta, y) & \phi_2(\eta, y) \end{vmatrix} \psi(\eta, y). \quad (\text{A.0.8b})$$

Putting

$$I_{jl}(\eta) = \frac{1}{c} \int_0^p dy n(y)^2 \phi_j(\eta, y)\phi_l(\eta, y),$$

we apply (A.0.7) to  $\psi \in \{\phi_1, \phi_2\}$  and obtain

$$\dot{\phi}_1(\eta, p) = -\phi_2(\eta, p)I_{11}(\eta) + \phi_1(\eta, p)I_{12}(\eta), \quad (\text{A.0.9a})$$

$$\dot{\phi}_1'(\eta, p) = -\phi_2'(\eta, p)I_{11}(\eta) + \phi_1'(\eta, p)I_{12}(\eta), \quad (\text{A.0.9b})$$

$$\dot{\phi}_2(\eta, p) = -\phi_2(\eta, p)I_{12}(\eta) + \phi_1(\eta, p)I_{22}(\eta), \quad (\text{A.0.9c})$$

$$\dot{\phi}_2'(\eta, p) = -\phi_2'(\eta, p)I_{12}(\eta) + \phi_1'(\eta, p)I_{22}(\eta). \quad (\text{A.0.9d})$$

Differentiating (A.0.5) with respect to  $\eta$  and using (A.0.9) we get

$$\dot{\beta}_{11} = -\beta_{12}I_{11}(\eta) + \beta_{11}I_{12}(\eta), \quad (\text{A.0.10a})$$

$$\dot{\beta}_{12} = -\beta_{12}I_{12}(\eta) + \beta_{11}I_{22}(\eta), \quad (\text{A.0.10b})$$

$$\dot{\beta}_{21} = -\beta_{22}I_{11}(\eta) + \beta_{21}I_{12}(\eta), \quad (\text{A.0.10c})$$

$$\dot{\beta}_{22} = -\beta_{22}I_{12}(\eta) + \beta_{21}I_{22}(\eta). \quad (\text{A.0.10d})$$

Equations (A.0.4a), (A.0.10a), and (A.0.10d) imply that

$$\dot{\Delta}(\eta) = -\beta_{12}I_{11}(\eta) + \beta_{21}I_{22}(\eta) + (\beta_{11} - \beta_{22})I_{12}(\eta). \quad (\text{A.0.11})$$

Differentiating (A.0.11) with respect to  $\eta$  and using (A.0.10) we obtain after some simplifications

$$\begin{aligned} \ddot{\Delta}(\eta) &= -\Delta(\eta)\{I_{11}(\eta)I_{22}(\eta) - I_{12}(\eta)^2\} \\ &- \beta_{12}\dot{I}_{11}(\eta) + \beta_{21}\dot{I}_{22}(\eta) + (\beta_{11} - \beta_{22})\dot{I}_{12}(\eta). \end{aligned} \quad (\text{A.0.12})$$

Now suppose  $\Delta(\eta) > 2$  or  $\Delta(\eta) < -2$ , while  $\Delta'(\eta) = 0$ . For this particular value of  $\eta$ , the period map and hence also the  $\beta$ -matrix has two distinct real eigenvalues with product 1. Hence there exists a matrix  $\Phi$  of initial conditions of the solutions  $\phi_1$  and  $\phi_2$  which diagonalizes the period map and creates a diagonal  $\beta$ -matrix. We note that this diagonalization only occurs for this particular  $\eta$  value, since we need to avoid any  $\eta$ -dependence of  $\Phi$ . Hence, for this  $\eta$  we have  $\beta_{12} = \beta_{21} = 0$ . Then for this  $\eta$

$$\begin{aligned} 0 < \Delta(\eta)^2 - 4 &= (\beta_{11} + \beta_{22})^2 - 4\{\beta_{11}\beta_{22} - \beta_{12}\beta_{21}\} \\ &= (\beta_{11} - \beta_{22})^2 + 4\beta_{12}\beta_{21} = (\beta_{11} - \beta_{22})^2, \end{aligned}$$

so that

$$0 < |\beta_{11} - \beta_{22}| < |\Delta(\eta)|. \quad (\text{A.0.13})$$

For this  $\eta$  we have according to (A.0.11)

$$0 = \dot{\Delta}(\eta) = (\beta_{11} - \beta_{22})I_{12}(\eta),$$

and hence  $I_{12}(\eta) = 0$ . Using (A.0.12) we then get for this  $\eta$

$$\ddot{\Delta}(\eta) = -\Delta(\eta)I_{11}(\eta)I_{22}(\eta) + (\beta_{11} - \beta_{22})\dot{I}_{12}(\eta), \quad (\text{A.0.14})$$

where  $I_{11}(\eta) > 0$  and  $I_{22}(\eta) > 0$ . Now

$$\begin{aligned} \dot{I}_{12}(\eta) &= \frac{1}{c} \int_0^p dy n(y)^2 \{\phi_1(\eta, y)\dot{\phi}_2(\eta, y) + \dot{\phi}_1(\eta, y)\phi_2(\eta, y)\} \\ &= \frac{1}{c^2} \int_0^p dy \int_0^y dz n(y)^2 n(z)^2 \begin{vmatrix} \phi_1(\eta, y) & \phi_2(\eta, y) \\ \phi_1(\eta, z) & \phi_2(\eta, z) \end{vmatrix} \times \\ &\quad \times \{\phi_1(\eta, y)\phi_2(\eta, z) + \phi_2(\eta, y)\phi_1(\eta, z)\} \\ &= \frac{1}{c^2} \int_0^p dy \int_0^y dz n(y)^2 n(z)^2 \{\phi_1(\eta, y)^2 \phi_2(\eta, z)^2 - \phi_2(\eta, y)^2 \phi_1(\eta, z)^2\}. \end{aligned}$$

A change of variables yields

$$\dot{I}_{12}(\eta) = \frac{1}{c^2} \int_0^p dy \int_y^p dz n(y)^2 n(z)^2 \{\phi_2(\eta, y)^2 \phi_1(\eta, z)^2 - \phi_1(\eta, y)^2 \phi_2(\eta, z)^2\}.$$

Taking half the sum of the two expressions for  $\dot{I}_{12}(\eta)$ , we get by easy estimation

$$\begin{aligned} |\dot{I}_{12}(\eta)| &< \frac{1}{2c^2} \int_0^p dy \int_0^p dz n(y)^2 n(z)^2 \{\phi_1(\eta, y)^2 \phi_2(\eta, z)^2 + \phi_2(\eta, y)^2 \phi_1(\eta, z)^2\} \\ &= I_{11}(\eta)I_{22}(\eta). \end{aligned} \quad (\text{A.0.15})$$

Consequently, from (A.0.13)-(A.0.15) we see that  $\ddot{\Delta}(\eta)$  is positive if  $\Delta(\eta) > 2$  and  $\dot{\Delta}(\eta) = 0$ , and negative if  $\Delta(\eta) < -2$  and  $\dot{\Delta}(\eta) = 0$ . As a net result, the Hill discriminant has exactly one extreme value in the interior of each nonempty bounded band gap, as claimed.

# Appendix B

## Circulant Matrices

Let  $C = (C_{j,l})_{j,l=1}^n$  be a real or complex  $n \times n$  matrix. Then  $C$  is called a *circulant matrix* [80] if  $C_{j,l}$  only depends on the remainder of  $j - l$  on division on  $n$ . This means that a circulant matrix depends on only  $n$  real or complex parameters  $c_0, c_1, \dots, c_{n-1}$ , where

$$C_{j,l} = \begin{cases} c_{l-j}, & l \geq j, \\ c_{l-j+n}, & l < j. \end{cases}$$

In other words,

$$C = \begin{pmatrix} c_0 & c_1 & c_2 & \dots & \dots & \dots & c_{n-1} \\ c_{n-1} & c_0 & c_1 & \dots & \dots & \dots & c_{n-2} \\ & \ddots & \ddots & & & & \\ & & & \ddots & & & \\ \vdots & & & & & \ddots & \vdots \\ c_1 & c_2 & c_3 & \dots & \dots & \dots & c_0 \end{pmatrix}.$$

It is then easily verified that the column vector  $(1, z, z^2, \dots, z^{n-1})^T$  is an eigenvector of  $C$  whenever  $z^n = 1$ . The corresponding eigenvalue is

$$\hat{c}(z) = c_0 + zc_1 + c_2z^2 + \dots + c_{n-1}z^{n-1}, \quad z^n = 1.$$

Introducing, apart from the factor  $1/\sqrt{n}$ , the Vandermonde matrix

$$U = \frac{1}{\sqrt{n}} \begin{pmatrix} 1 & 1 & \dots & 1 \\ z_1 & z_2 & \dots & z_n \\ z_1^2 & z_2^2 & \dots & z_n^2 \\ \vdots & \vdots & & \vdots \\ z_1^{n-1} & z_2^{n-1} & \dots & z_n^{n-1} \end{pmatrix},$$

where  $z_1, \dots, z_n$  are the distinct  $n$ -th roots of unity, we obtain

$$CU = UD,$$

where  $U$  is a unitary matrix and

$$D = \text{diag}(\hat{c}(z_1), \dots, \hat{c}(z_n))$$

is a diagonal matrix. Hence circulant matrices allow for an orthonormal basis of eigenvectors and are hence diagonalizable. The diagonalizing unitary transformation does not depend on the circular  $n \times n$  matrix.

Before generalizing the notion of a circulant matrix, we introduce the additive group  $\mathbb{Z}[n]$  of remainders of the integers on division by  $n$ . In factor,  $\mathbb{Z}[n]$  is obtained from the additive group  $\mathbb{Z}$  of the integers by identifying any pair of integers which differ by an integer multiple of  $n$ . Then a circulant matrix  $C$  is a Toeplitz matrix whose entries are numbered using  $\mathbb{Z}[n]$ . In other words,  $C_{j,l} = c_{l-j}$ , where the difference  $l - j$  is to be intended in  $\mathbb{Z}[n]$ .

Now let  $G$  be an arbitrary finite abelian group. By a  $G$ -circulant matrix [81] we mean a matrix whose entries  $j, l$  are indexed by  $G$  and only depend on the difference  $l - j$  in  $G$ :  $C_{j,l} = c_{l-j}$ . Let us now restrict ourselves to the case

$$G = \mathbb{Z}[n] \times \mathbb{Z}[m],$$

where  $n, m \geq 2$ . Then the entries of the  $G$ -circulant matrices  $C$  are indexed by pairs

$$(j, l) \in \{1, 2, \dots, n\} \times \{1, 2, \dots, m\},$$

where

$$C_{(j_1, j_2), (l_1, l_2)} = \begin{cases} c_{(l_1 - j_1, l_2 - j_2)}, & l_1 \geq j_1, l_2 \geq j_2, \\ c_{(l_1 - j_1 + n, l_2 - j_2)}, & l_1 < j_1, l_2 \geq j_2, \\ c_{(l_1 - j_1, l_2 - j_2 + m)}, & l_1 \geq j_1, l_2 < j_2, \\ c_{(l_1 - j_1 + n, l_2 - j_2 + m)}, & l_1 < j_1, l_2 < j_2. \end{cases}$$

So the eigenvectors of  $C$  are the column vectors with  $(j, l)$ -th entry  $z^{j-1}w^{l-1}$ , where  $z^n = 1$  and  $w^m = 1$ . When aligned as columns of an  $nm \times nm$  matrix, we get a matrix which becomes unitary on division by  $\sqrt{nm}$ . We then get

$$CU = UD,$$

where  $D$  is the diagonal matrix with  $(j, l)$ -th entry

$$\hat{c}(z^{j-1}, w^{l-1}) = \sum_{r=0}^{n-1} \sum_{s=0}^{m-1} c_{(r,s)} [z^{j-1}]^r [w^{l-1}]^s,$$

for any  $(z, w)$  satisfying  $z^n = 1$  and  $w^m = 1$ . Here,  $\hat{c}(\zeta, \omega)$  is a bivariate polynomial of the variables  $\zeta$  and  $\omega$ .

# Bibliography

- [1] John D. Joannopoulos, Robert D. Meade, and Juhua N. Winn, *Photonic Crystals, Molding the flow of light*, Princeton University Press, (2006).
- [2] Kazuaki Sakoda, *Optical Properties of Photonic Crystals*, Springer-Verlag, (2001).
- [3] Natural Photonic Crystals: <http://www.viewsfromscience.com/>.
- [4] S.Wickham, M.Large, L.Poladian, and L.Jermiin, *Exaggeration and Suppression of Iridescence: the evolution of two-dimensional butterfly structural colours*, Journal of the Royal Society Interface, Volume 3, No. 6, pp. 99–108 (2006).
- [5] Emanuel Istrate and Edward H. Sargent, *Photonic crystal heterostructures and interfaces*, Rev. Mod. Phys. **78**, 455–481 (2006).
- [6] S.J. Osher and F. Santosa, *Level set methods for optimization problems involving geometry and constraints*, J. Comp. Phys., **171**, 272–288 (2001).
- [7] C. Y. Kao, S. Osher, and E. Yablonovitch, *Maximizing Band Gaps in Two-Dimensional Photonic Crystals, using Level Set Methods*, Appl. Phys. B, **81**, 235–244 (2005).
- [8] Max Born and Emil Wolf, *Principles of Optics. Electromagnetic theory of propagation, interference and diffraction of light*, Cambridge University Press, 6th Edition, (1999).
- [9] Viktor G Veselago, *The electrodynamics of substances with simultaneously negative values of  $\epsilon$  and  $\mu$* , Sov. Phys. Usp. **10** 509–514 (1968).
- [10] H. Kosaka, T. Kawashima, A. Tomita, M. Notomi, T. Tamamura, T. Sato, and S. Kawakami, *Superprism phenomena in photonic crystals*:

- toward microscale lightwave circuits, *J. Lightwave Technol.* **17**, 2032–2038 (1999).
- [11] A. M. Malvezzi, G. Vecchi, M. Patrini, G. Guizzetti, L. C. Andreani, F. Romanato, L. Businaro, E. Di Fabrizio, A. Passaseo, and M. De Vittorio, *Resonant second-harmonic generation in a GaAs photonic crystal waveguide*, *Phys. Rev. B* **68**, 161306(R), (2003).
- [12] P. P. Markowicz, H. Tiryaki, P. N. Prasad, V. P. Tondiglia, L. V. Natarajan, T. J. Bunning, and J. W. Haus, *Electrically switchable third-harmonic generation in photonic crystals*, *J. Appl. Phys.* **97**, 083512 (2005).
- [13] P. Weinberger, *John Kerr and his effects found in 1877 and 1878*, *Philosophical Magazine Letters* **88**, 897–907 (2008).
- [14] Agostino Giorgio, Decio Pasqua, and Anna Gina Perri, *Cristalli fotonici: principi di funzionamento ed applicazioni - prima parte*, *La comunicazione - note, recensioni e notizie, numero unico*, 173–185 (2003).
- [15] Agostino Giorgio, Decio Pasqua, and Anna Gina Perri, *Cristalli fotonici: principi di funzionamento ed applicazioni - seconda parte*, *La comunicazione - note, recensioni e notizie, numero unico*, 165–182 (2004).
- [16] Jes Broeng, Dmitri Mogilevstev, Stig E. Barkou, and Anders Bjarklev, *Photonic Crystal Fibers: a new class of optical waveguides*, *Optical Fiber Technology* **5**, 305–330 (1999).
- [17] Babak Momeni, Jiandong Huang, Mohammad Soltani, Murtaza Askari, Saeed Mohammadi, Mohammad Rakhshandehroo, and Ali Adibi, *Compact wavelength demultiplexing using focusing negative index photonic crystal superprisms*, *Optics Express*, **14**, 2413–2422 (2006).
- [18] Mehmet Fatih Yanik, Shanhui Fan, Marin Soljačić, and J.D. Joannopoulos, *All-optical transistor action with bistable switching in a photonic crystal cross-waveguide geometry*, *Optics Letters*, Vol. 28, No. 24, 2506–2508 (2003).
- [19] John Jackson, *Classical Electrodynamics*, New York: Wiley, (1999).
- [20] M.S.P. Eastham, *The Spectral Theory of Periodic Differential Equations*, Scottish Academic Press, Edinburgh and London, (1973).
- [21] W. Magnus and S. Winkler, *Hill's Equation*, Dover Publ., New York, (1979).

- [22] E.C. Titchmarsh, *Eigenfunction Expansions associated with Second-order Differential Equations*, Vol. II, Clarendon Press, Oxford, (1958).
- [23] E. Korotyaev, *Lattice dislocations in a 1-dimensional model*, Commun. Math. Phys. **213**, 471–489 (2000).
- [24] N.E. Firsova, *The direct and inverse scattering problems for the one-dimensional perturbed Hill operator*, Math. USSR Sbornik **58**(2), 351–388 (1987).
- [25] J. Weidmann, *Lineare Operatoren in Hilberträumen, Teil II: Anwendungen*, Teubner, Stuttgart, (2003).
- [26] E.M. Harrel II, *On the extension of Ambarzumian's inverse spectral theorem to compact symmetric spaces*, Amer. J. Math. **109**, 787–795 (1987).
- [27] I. B. Conway, *Functions of One Complex Variable*, Graduate Texts in Mathematics II, Springer, New York, (1973).
- [28] B.Ja. Levin, *Distribution of Zeros of Entire Functions*, Transl. Math. Monographs **5**, Amer. Math. Soc., Providence, RI, (1972).
- [29] H.A. Kramers, *Das Eigenwertproblem im eindimensionalen periodischen Kraftfelde*, Physica **2**, 483–490 (1935).
- [30] L.D. Faddeev, *Properties of the S-matrix of the one-dimensional Schrödinger equation*, Amer. Math. Soc. Transl. **2**, 139–166 (1964); also: Trudy Mat. Inst. Steklova **73**, 314–336 (1964) [Russian].
- [31] P. Deift and E. Trubowitz, *Inverse scattering on the line*, Commun. Pure Appl. Math. **32**, 121–251 (1979).
- [32] N.E. Firsova, *Riemann surface of quasimomentum and scattering theory for the perturbed Hill operator*, J. Math. Sci. **11**, no. 3, 487–497 (1979); also: Zapiski Nauchnykh Seminarov Leningrad. Otdel. Matem. Inst. im. V.A. Steklova, Akad. Nauk SSSR, **51**, 183–196, (1975) [Russian].
- [33] V.A. Marchenko and I.V. Ostrovski, *A characterization of the spectrum of the Hill operator*, Math. USSR Sbornik **26**, 493–554 (1975).
- [34] K. Chadan and P. Sabatier, *Inverse Problems in Quantum Scattering Theory*, 2nd ed., Springer, New York, (1989).

- [35] N.E. Firsova, *Levinson formula for perturbed Hill operator*, Theor. Math. Phys. **62**(2), 130–140 (1985); also: Teor. Matem. Fiz. **62**(2), 196–209 (1985) [Russian].
- [36] V.A. Ambarzumian, *Über eine Frage der Eigenwerttheorie*, Zeitschrift für Physik **53**, 690–695 (1929).
- [37] G. Borg, *Eine Umkehrung der Sturm-Liouvilleschen Eigenwertaufgabe. Bestimmung der Differenzialgleichung durch die Eigenwerte*, Acta Math. **78**, 1–96 (1946).
- [38] G. Borg, *Uniqueness theorems in the spectral theory of  $y'' + (\lambda - q(x))y = 0$* . In: *Proceedings of the 11th Scandinavian Congress of Mathematicians*, Johan Grundt Tanums Forlag, Oslo, pp. 276–287 (1952).
- [39] V.A. Marchenko, *Sturm-Liouville Operators and Applications*, Birkhäuser OT **22**, Basel and Boston, (1986); also: Naukova Dumka, Kiev, (1977) [Russian].
- [40] E. Trubowitz, *The inverse problem for periodic potentials*, Commun. Pure Appl. Math. **30**, 321–337 (1977).
- [41] B.M. Levitan and M.G. Gasymov, *Determination of a differential equation by two spectra*, Uspehi Mat. Nauk **19**(2), 3–63 (1964) [Russian].
- [42] S.M. Sze, *Physics of semiconductor devices, second edition*, Wiley, New York, (1981).
- [43] Cornelis van der Mee, Pietro Contu, and Paolo Pintus, *One-dimensional Photonic Crystal Design*, Journal of Quantitative Spectroscopy and Radiative Transfer **111**, 214–225 (2010).
- [44] L. Brillouin, *Wave Propagation in Periodic Structures*, Dover Publ., New York, (1953).
- [45] K.M. Leung and Y. Qiu, *Multiple-scattering calculation of the two-dimensional photonic band structure*, Phys. Rev. B **48**, 7767–7771 (1993).
- [46] Ze Zhang and S. Satpathy, *Electromagnetic wave propagation in periodic structures: Bloch wave solution of Maxwell's equations*, Phys. Rev. Lett. **65**, 2650–2653 (1990).
- [47] K.M. Ho, C.T. Chan, and C.M. Soukoulis, *Existence of a photonic gap in periodic dielectric structures*, Phys. Rev. Lett. **65**, 3152–3155 (1990).

- [48] H.S. Sözüer and J.W. Haus, *Photonic bands: Convergence problems with the planewave method*, Phys. Rev. B **45**, 13962–13972 (1992).
- [49] M. Philal and A.A. Maradudin, *Photonic band structure of two-dimensional systems: The triangular lattice*, Phys. Rev. B **44**, 8565–8571 (1991).
- [50] P.P. Villeneuve and M. Piché, *Photonic band gaps in two-dimensional square and hexagonal lattices*, Phys. Rev. B **46**, 4969–4972 (1992).
- [51] Kane Yee, *Numerical solution of initial boundary value problems involving Maxwell's equations in isotropic media*, IEEE Transactions on Antennas and Propagation, **14**, 302–317 (1966).
- [52] C.T. Chan, Q.L. Yu, and K.M. Ho, *Order- $N$  spectral method for electromagnetic waves*, Phys. Rev. B **51**, 16635–16642 (1995).
- [53] A.J. Ward and J.B. Pendry, *Refraction and geometry in Maxwell's equations*, J. Mod. Opt. **43**, 773–793 (1996).
- [54] A.J. Ward and J.B. Pendry, *Calculating photonic Green's functions using a nonorthogonal finite-difference time-domain method*, Phys. Rev. B **58**, 7252–7259 (1998).
- [55] Min Qiu and Sailing He, *A nonorthogonal finite-difference time-domain method for computing the band structure of a two-dimensional photonic crystal with dielectric and metallic inclusions*, J. Appl. Phys. **87**, 8268–8275 (2000).
- [56] B. Cowan, *FDTD modeling of photonic crystal fibers*, ARDB Technical Notes **4**, ARDB-339, 7 pp., (2003).
- [57] J. Arriaga, A.J. Ward, and J.B. Pendry, *Order- $N$  photonic band structures for metals and other dispersive materials*, Phys. Rev. B **59**, 1874–1877 (1999).
- [58] Sailing He, Sanshui Xiao, Linfang Shen, Jiangping He, and Jian Fu, *A new finite-difference time-domain method for photonic crystals consisting of nearly-free-electron metals*, J. Phys A **34**, 9713–9721 (2001).
- [59] Hung Yu David Yang, *Finite difference analysis of 2-D photonic crystals*, IEEE Trans. on Microwave Theory and Techniques **44**, 2688–2695 (1996).
- [60] J.B. Pendry and A. MacKinnon, *Calculation of photon dispersion relations*, Phys. Rev. Lett. **69**, 2772–2775 (1992).

- [61] D. Hermann, M. Frank, K. Busch, and P. Wölffe, *Photonic band structure computations*, Opt. Express **8**, 167–172 (2000).
- [62] Xindong Wang, X.-G. Zhang, Qingliang Yu, and B.N. Harmon, *Multiple-scattering theory for electromagnetic waves*, Phys. Rev. B **47**, 4161–4167 (1993).
- [63] R.C. McPhedran, L.C. Botten, J. McOrist, A.A. Asatryan, C.M. de Sterke, and N.A. Nicorovici, *Density of states function for photonic crystals*, Phys. Rev. E **69**, 016609, 16 pp. (2004).
- [64] Weiyi Zhang, C.T. Chan, and Ping Sheng, *Multiple scattering theory and its application to photonic band gap systems consisting of coated spheres*, Opt. Express **8**, 203–208 (2000).
- [65] O.J.F. Martin and C. Girard, *Generalized field propagator for arbitrary finite-size photonic band gap structures*, Phys. Rev. Lett. **82**, 315–318 (1999).
- [66] E. Moreno, D. Erni, and C. Hafner, *Band structure computations of metallic photonic crystals with the multiple multipole method*, Phys. Rev. B **65**, 155120, 10 pp. (2002).
- [67] K. Sakoda, *Optical transmittance of a two-dimensional triangular photonic lattice*, Phys. Rev. B **51**, 4672–4675 (1995).
- [68] K. Sakoda, *Transmittance and Bragg reflectivity of two-dimensional photonic lattices*, Phys. Rev. B **52**, 8992–9002 (1995).
- [69] Jeong-Ki Hwang, Seok-Bong Hyun, Han-Youl Ryu, and Yong-Hee Lee, *Resonant modes of two-dimensional photonic bandgap cavities determined by the finite-element method and by use of the anisotropic perfectly matched layer boundary condition*, J. Opt. Soc. Am. B **15**, 2316–2324 (1998).
- [70] G. Pelosi, *A hybrid FEM-based procedure for the scattering from photonic crystals illuminated by a gaussian beam*, IEEE Trans. on Antennas and Propagation **48**, 973–980 (2000).
- [71] B.P. Hiett, J.M. Generowicz, S.J. Cox, M. Molinari, D.H. Beckett, and K.S. Thomas, *Application of finite element methods to photonic crystal modelling*, IEE Proc.-Sci. Meas. Technol. **149**, 293–296 (2002).
- [72] D.C. Dobson, *An efficient method for band structure calculations in 2D photonic crystals*, J. Comp. Phys. **149**, 363–376 (1999).

- [73] W. Axmann and P. Kuchment, *An efficient finite element method for computing spectra of photonic and acoustic band-gap materials*, J. Comp. Phys. **150**, 468–481 (1999).
- [74] D.C. Dobson, J. Gopalakrishnan, and J.E. Pasciak, *An efficient method for band structure calculations in 3D photonic crystals*, J. Comp. Phys. **161**, 668–679 (2000).
- [75] Woo Jun Kim and J. O’Brien, *Optimization of a two-dimensional photonic-crystal waveguide branch by simulated annealing and the finite-element method*, J. Opt. Soc. Am. B **21**, 289–295 (2004).
- [76] M. Koshiya, *Time-domain beam propagation method and its application to photonic crystal circuits*, J. Lightwave Technology **18**, 102–110 (2000).
- [77] Vu Hoang, Micheal Plum, and Christian Wieners, *A computer assisted proof for photonic band gaps*, Z. angew. Math. Phys. **60** 1035–1052 (2009).
- [78] M.S. Gockenbach, *Understanding and Implementing the Finite Element Method*, SIAM, Philadelphia (2006).
- [79] Peter Lancaster and Miron Tismenetsky, *The Theory of Matrices*, Academic Press, Orlando etc., (1985).
- [80] Ph. I. Davis, *Circulant Matrices*, Wiley-Interscience, New York, (1979).
- [81] C. van der Mee, G. Rodriguez, and S. Seatzu, *Fast superoptimal preconditioning of multiindex Toeplitz matrices*, Linear Algebra and its Applications, **418**, 576–590 (2006).